The University Of Sheffield.

Department of Chemical and Biological Engineering

Metabolic engineering for increased electrogenic activity and bioenergy production

Stephen Robert Paul Jaffé (BSc (Hons), MRes)
April 2014

Supervisor: Prof. P. C. Wright

Thesis submitted to the University of Sheffield for the degree of Doctor of Philosophy (PhD)

Declaration

This is a declaration to state that this thesis is an account of the author's work which was conducted at the University of Sheffield, U.K. This work has not been submitted for any other degree or qualification.

Acknowledgements

Without question the first people I would like to extend my deepest thanks are to Professor Phillip Wright and Dr Greg Fowler. They were the people who interviewed me and chose to give me the opportunity to do something that I was very excited about. Without their consistent help, guidance, support and friendship throughout the years, I would not be submitting this thesis. I am sincerely grateful and indebted for the chance I was given and can only hope that I have in some way repaid their faith in me.

At the inception of this project, a person, who would go on to become a dear friend, took me under her wing. She did whatever she could to ensure that I settled in, made friends and managed the task at hand often at her expense. To Ana Gabriela Pereira-Medrano-O'Callaghan, I am incredibly thankful to have had someone so kind, generous and understanding so closely linked to my life over those early years.

Although these people have been here with me on a day to day basis I cannot and have not forgotten the love, support and laughter that my family has given me over the years. Their persistent good wishes and desire for me to be the best I can be has helped to spur me along. To Mum, Dad, David, Nonna, Grandma, Bill, uncles Julian, Jeremy and Neil, aunties Amanda and Fiona, cousins Olivia, Daniel, Benji, Ruby, Mia, Josh, Fleur, Zio Reno, Vito, Zia Irma and Bertilla I thank you and love you all. For my relatives that have sadly passed away but are still often in my thoughts; Joey, Simone, Nonno and in this instance perhaps a genetic advantage gained from Werner Paul Jaffé (5 Nature and 1 Science paper to aim towards – I know I never met you but I'm trying my best to emulate you. I'm trying!).

To my girlfriend, Katie, I thank you for the great times we've had together, for your love, trust and understanding throughout, especially through the tough times. It's finally (hopefully) over! Thanks to Pebble, the miniature waste disposal unit.

To my friends, without you, I would surely have gone mad. Thank you for being there and either having no clue what I was doing or just plain not caring about it and just having fun. I thank you for your understanding and hope to be able to be to return the favour and look forward to many more good times. To my friends that have experienced that have gone through the same ordeal, Xavier Mesnier (Moroccan skeletor), Joseph Longworth, Josselin Noirel (Dear Fellow), Nathan West, Leon Pybus, Pratik Desai (Dear Fellow), James Osborne (Beans and Fishcakes), Steve Hible, Rob Whitfield, Faith Robert (Professor Swag), Mahendra Raut (Tom Cruise), Yimin Chen (James Bond), Rahul Kapoore, Kirubhakaran Krishnanathan (Krish), Sakharam Waghmare (Rat Killer), Helen Phillips, Esther Karunakaran, Jenn Dick thank you for being a part of this journey and for making the good times great and the bad times much more bearable. To Martin Benefer, Khanita Kamwilaisak, Matt Martinkovic, Liam Hennesey, Dan Scott, Alexandra Ion and Zdeno Levarski, you're sorely missed from Sheffield.

To the mass spec guru's, Saw Ow Yen, Caroline Evans, Narciso Couto, Phil Jackson, Mark Dickman, Jagroop Pandhal and Trong Khoa Pham thank you for your time, patience and understanding.

To the next cohort of PhD's and the remainder of ChELSI, you are too numerous to mention and I apologise for not including every name but a special mention to the G4b team consisting of the dedicated students Simon Hall, Benjamin Strutton and Juliano Bertozzi-Silva.

None of this could have been possible without the support of the University of Sheffield, the Engineering and Physical Science Research Council (EPSRC) (EP/E036252/1) and Ortus Energy for funding this research project. Special thanks go to Dr. Neville Hargreaves and Dr. Andrew Bennett for their support and guidance throughout.

Thanks to collaborators, advisors and generous donators of materials. Thank you to Dr Ioannis Ieropoulous, Dr Pablo Ledezma for MFC work on the *Shewanella* iTRAQ study, Dr Liang Shi for the kind gifted gift of multiple Mtr antibodies, Dr Robert Kranz for the

cytochrome maturation gene plasmids, Dr David Richardson for the initial OmcA and MtrA plasmids and finally to Dr Jeffrey Gralnick for the charitable donation of *Shewanella oneidensis* MR-1.

It is at this point, when the finishing touches are being made to my thesis before submission that the truly collaborative effort of the work becomes apparent. As much as I may like to assume that the achievements, however limited, are my own, I realise more than ever that without the people mentioned above, I would not be in this position today. I thank you all for the part you have played in this, for being there through the ups and downs. I wish you all the very best for the future.

Contents

List of Figures

List of Tables

Abbreviations

1DE	one-dimensional electrophoresis
2DE	two-dimensional electrophoresis
AB	Applied Biosystems
AD	anaerobic digester
Amp	ampicillin
ATP	adenosine triphosphate
BES	Bioelectrochemical system
BLAST	Basic Local Alignment Search Tool
bp	base pairs
CE	coulombic efficiency
CID	collision induced dissociation
CIP	calf intestinal phosphatase
Cm	chloramphenicol
COD	chemical oxygen demand
Da	Dalton
DMRB	dissimilatory metal reducing bacteria
dNTPs	deoxyribonucleotide mixture
dsDNA	double stranded DNA
DTT	dithiothreitol
EBI	European Bioinformatics institute
EMBL	European Molecular Biology Laboratory
EPS	extracellular polymeric substance
FLP	flippase
FRT	flippase recognition target
HPLC	high performance liquid chromatography

IME	inverse metabolic engineering
iTRAQ	isobaric tags for relative and absolute quantitation
JGI	Joint Genome Institute
Kan	Kanamycin
kb	kilo base pairs
KEGG	Kyoto Encyclopedia of Genes and Genomes
LB	Luria-Bertani media
M	Molar
MALDI	matrix assisted laser desorption ionisation
MEC	microbial electrolysis cell
MFC	microbial fuel cell
min	minute
mL	millilitres
mM	millimolar
MS	mass spectrometry
MS/MS	tandem mass spectrometry
mW	molecular weight
NCBI	National Centre for Biotechnology Information
OD	optical density
ORF	open reading frame
PAGE	polyacrylamide gel electrophoresis
PCR	polymerase chain reaction
PEM	proton exchange membrane
PIC	protease inhibitor cocktail
PMF	peptide mass fingerprinting
ppm	parts per million
PTM	post translational modification

rpm	revolutions per minute
RT-qPCR	real-time quantitative polymerase chain reaction
SCX	strong cation exchange
SDS	sodium dodecyl sulphate
SEM	scanning electron microscopy
ssDNA	single stranded DNA
TAE	tris acetate ethylenediaminetetraacetic acid
TEA	terminal electron acceptor
Tris	tris(hydroxymethyl)aminomethane
UV	ultraviolet
v/v	volume per volume
w/v	weight per volume

Summary

Microbial fuel cells (MFCs) are a fascinating green technology with potential to simultaneously degrade waste organic material, reducing the chemical oxygen demand (COD) of the effluent and generate harvestable energy in the form of electrons. A key element in the function of this potentially powerful technology is the microorganisms that make this all possible – dissimilatory metal reducing bacteria (DMRB). These ancient organisms are able to generate their energy through interactions with insoluble terminal electron acceptors such as Iron (III), Manganese (IV) and Uranium (VI) but are also able to interact with anodes within MFCs. These interactions occur due to the ability of the cells to transfer electrons extracellularly through complex protein pathways. Understanding the mechanisms by which they are able to do this presents opportunities to further tune or enhance this capability in order to generate greater power outputs. This thesis aims to make use of the engineering paradigm of "measure, model, manipulate , make" in order to generate obtain and generate results.

- Through the use of modern molecular biology techniques, the mechanisms of extracellular electron transfer have been transferred into an organism previously incapable of this activity (manipulate and make – being based heavily upon previous research detailing previous electrochemical measurements and models). Through these methods a 60% increase in power generation was noted compared to the wild type host organism. This was also a 64% power output of the model, naturally electrogenic organism.
- A proteomic analysis was carried out in order to try and elucidate the underlying proteomic profile of a dissimilatory metal reducing bacterium (DMRB) within an MFC compared to controlled aerobic growth (measure and model – with the intention to manipulate and make). The study found differential regulation of several proteins outside the "classical Mtr pathway", including upregulation of TolC within anode bound cells.
- In order to try and reduce the metabolic burden of the exoelectrogenic system and increase the potential power density, it was attempted to be based on the

chromosome of *E. coli* (manipulate and make). A variety of techniques were applied to attempt this, and although the transfer of the genetic constructs onto the genome was unsuccessful, a wide range of important things to avoid are noted. In the second part of this chapter, an attempt to try and understand the native cellular components the recombinant system was interacting with a tandem affinity purification study was attempted (measure and model).

This thesis therefore hopes to demonstrate comprehensive use of the engineering paradigm to help develop understanding of current generation by a biological organism, and the functional transfer of this activity to from a model organism to *E. coli*.

Chapter 1: Introduction

"Water and air, the two essential fluids on which all life depends, have become global garbage cans"

Jacques Yves Cousteau

Although my view of the world may not be quite as bleak as Monsieur Cousteau's statement, I felt that in order to set the scene for this project it was apt to start not only with a quote but with some startling figures of the state of things as they currently stand.

The Earth is in bad shape:

- Currently roughly 7.2 billion people are on the planet and we are racing towards a total of approximately 10 billion in 2050 (1).
- With increasing populations and development of economies come increasing demands for food, water and energy.
- People are using increasingly desperate ways of harvesting fossil fuels using techniques such as the highly controversial fracking technique to the incredibly toxic harvesting of hydrocarbons from tar sands.
- In 2009, the UN estimated the number of undernourished people to be roughly 1 billion (2). This is all at a time when between 30-40% of food is approximately wasted in both the developed and developing world, albeit due to very different reasons (3) (4).
- More food requires more water and around 1.8 billion people were estimated to have used unsafe drinking water in 2010 (5).
- Although the world is two thirds covered in water, only 3% of the water on the planet is freshwater, with only 0.3% of that 3% being surface water (6) as shown in Figure 1.1:

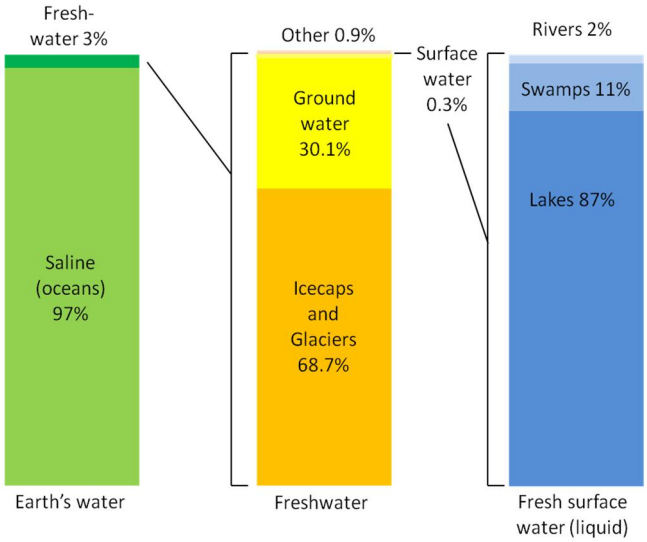

Figure 1.1 Distribution of the Earth's water, showing the minute amount of easily accessible fresh water on the planet

In order to be able to deal with the increasing global demands there are many issues, such as the ones stated above that need to be tackled. Being able to develop technology that is able to deal with any of these is a great challenge.

A technology that is able to effectively detoxify and or desalinate water, degrade waste organic material, generate energy in a variety of forms and potentially produce high value products, all simultaneously is highly desirable. This technology exists, albeit in a relatively immature form, in bioelectrochemical systems (BES). These systems are able to harness the capabilities of metabolically diverse microorganisms known as dissimilatory metal reducing bacteria (DMRB) to degrade organic material and transfer the released electrons to an extracellular acceptor for desired use elsewhere (7–9).

As with a great many biological systems, the discovery of the organism producing the desired chemical molecule or trait is not the one that is economically viable for further use due (often) to inabilities to meet demands. This may be due to growth limitations, cost issues or potentially due to a lack of tools for simple and timely genetic manipulation. As previously inferred, the ability of BES to degrade waste organic material and generate energy or high value products is currently very limited (10). The

systems suffer from a range of multi-disciplinary issues that encompass the biological and engineering aspects. Relatively low power density (11) and incomplete degradation of waste organics (12), all within currently lengthy timeframes (13) are some of the factors currently preventing this technology from gaining wider acceptance.

Gaining an understanding of the mechanisms by which DMRB are able to perform these actions, provides a great opportunity to tune and further enhance their abilities. As argued in this thesis, discovering the genetic basis behind these traits requires the use of techniques such as genetic manipulation, transcriptomics analysis and quantitative proteomics. Although a relatively new field, a great deal of research has been put into this type of experimentation with a significant increase in the level of knowledge.

In an attempt to try and alleviate some of the biological issues, a favoured microbiology workhorse, *Escherichia coli*, was employed in this thesis as a suitable host for genetic manipulation. This was done not only to help determine the basic genetic elements required for extracellular electron transfer, but also to be able to transfer this ability to a non DMRB – in this case referring specifically to the inability of *E. coli* to perform extracellular electron transfer. All of this was done with a view to transferring released electrons to a bioelectrochemical system (BES), with the potential for further manipulation to enhance the maximum power density.

1.1 Chapter breakdown and Aims

The main aims of this thesis, divided into each of the research chapters (4, 5 and 6) were therefore:

- The focus of chapter 4 is the use of modern genetic and protein analysis techniques to integrate a functional extracellular electron transfer pathway into *E. coli* and test the success of the heterologous pathway within a BES, with the centre of attention being microbial fuel cells (MFCs).

- The focus of chapter 5 was to gain a proteomic understanding of the model DMRB organism, *Shewanella oneidensis* MR-1 under current generating conditions within an MFC.
- Chapter 6 is broken down into two subsections with distinct aims:
    - The first section is directed towards streamlining the recombinant exoelectrogenic system and alleviating the metabolic burden by shifting away from large multi plasmid systems by incorporating the required genes into the host genome.
    - The second part is focussed on determining the interacting partners of this heterologous pathway within a non native system with an intended aim of forward engineering for further enhancement of power output.

Chapter 2: General Background and Review

2. Introduction

The increasing demand for energy in a world with diminishing supplies requires not only more efficient energy usage but also the development of renewable energy technology. The water sector consumes a vast amount of energy yet possesses huge, largely untapped energy resources that could be utilised by emerging technologies such as BESs including, MFCs. In order to be able to make full use of this synergy between biology and engineering technology, there are a great deal of biological challenges that must be tackled. The literature review in this chapter provides an overview of the available technologies, discussion about the challenges at hand and some ideas about potential ways for these to be overcome.

2.1 Background and Literature Review

2.1.1 End of fossil fuels, beginning of a new renewable age

The use of fossil fuels, especially gas and oil has accelerated due to the economic development of countries such as China, India and Brazil and the increased energy demand that has come with it (14–17). The natural stores of fossil fuels compounds are being rapidly depleted throughout the world, leading to high prices due to demand that is soon expected to go beyond peak production levels (18,19)**.** The price of oil increased from a long steady period of around $20/barrel in the 1980's and early 90's to around $50/barrel in 2007 and then shot up to $150/barrel in spring 2008 (20). This did not last but there have been (admittedly difficult) predictions that the price of oil per barrel could reach as high as $270 by 2020 (21,22). The increase in requirement has led to more drastic and dangerous ways of extracting these compounds. This deep drilling for oil and gas has led to events such as that recently seen with BP in the Gulf of Mexico.

Even without disasters like this, the age of fossil fuels has caused immense damage to the environment as seen with the advent of global warming due to the highest CO_2 levels in human existence (23). This has led to the decision to reduce global CO_2 emissions significantly by 2050 with the UK aiming for a 60% decrease and Germany, France and the Netherlands aiming for 80%, 75% and 80% reduction respectively (24).

These reductions in carbon emissions aim to be achieved when there will be the highest energy demand in history as the world population is expected to be around 9 billion by 2050 (25). This energy demand must therefore come from the development of clean, renewable sources with the largest focus on renewable energies seen in solar, tidal and wind energy. All of these energies are intermittent and in order for the energy produced to be efficiently harnessed requires the development of a more advanced smart grid (26). This would be one which is capable of handling sporadically high levels of energy production that can be stored away for further use and be able to regulate the flow of energy.

In order to be able to provide a westernised country with enough energy, it must come from a variety of different sources (Table 2.1).

Table 2.1 – Comparison of different potential energy sources

Energy source	**Renewable**	**Pros**	**Cons**
Nuclear	Potentially	No CO_2, Cheap	Very dangerous, Toxic waste (27)
Wind	Yes	No CO_2, Low siting costs, Take place alongside farming	Unpredictable energy, Eye sore (28)

Solar	Yes	No CO_2, Remote usage, Suited for developing countries, Integrate with buildings, More efficient than biofuel	Weather dependent, Reliant on storage, DC to AC conversion losses (29,30)
Tidal	Yes	Reliable, No CO_2	Environmental impact (31,32), transmission lines
Biomass	Yes	Burn organic by-products, Carbon neutral, Abundant	Possible net energy loss in production, Competition with food use. Unable to replace current gasoline and diesel levels (33) (34)
Geothermal	Yes	Low deployment costs, Continuous energy, No CO_2	Very location dependent (35)
Hydroelectric	Yes	Constant energy, No primary pollution, Relies on gravity	Serious environmental impact, Long transmission lines (36)

Apart from nuclear power, none of these energy sources are likely to be able to individually power an entire nation and must instead be combined in order to deal with demand.

A large proportion of a developed country's energy expenditure comes from the water industry (37) where there is a constant demand for clean, fresh water that must be treated and transported. In the USA, the treatment of wastewater to a safe level through the removal of toxic compounds is believed to require 1.5% of the total

energy produced, with the whole industry being responsible for between 4-5% (37). The high levels of organic compounds present in the wastewater are believed to hold 9.3 times the energy currently required for the operation of this sector (37). According to Logan's calculations (24), if even 50% of the energy stated by Logan could be harnessed it has the potential to provide around 20% of the country's energy requirements. Methods for simultaneous energy production and degradation of organic compounds in wastewater can be seen with anaerobic digesters, and the development of microbial fuel cells (MFCs).

2.1.1.1 Anaerobic digesters – This system makes use of different types of microorganisms to degrade organic material under anaerobic conditions to produce methane. This is done through 4 different steps (38,39):

I. Hydrolysis – Degradation of matter into its constituents compounds such as long chain carbohydrates like starch down to sugars, and proteins to amino acids.
II. Acidogenesis – The sugars and amino acids are then converted into the desired organic acids but by products such as ammonia, hydrogen and carbon dioxide are also produced. This is all done by acidogenic bacteria.
III. Acetogenesis – The organic acids are converted into acetic acid along with the limited amounts of ammonia, hydrogen and carbon dioxide by acetogenic bacteria.
IV. Methanogenesis – The organic acids and the derivatives such as acetic acid are converted into methane and carbon dioxide at roughly 60% and 40%, respectively.

The methane can then be used to heat water, peoples' homes or even used as a replacement fuel in transportation (40). However the conversion of this methane into electricity that can be used to power a wide range of appliances is highly inefficient with more than 60% of the energy being lost in the process (41). There are further limitations to this technology as the containers must be kept under certain conditions in order to efficiently produce methane. The most common example being the

requirement to keep the tanks at a temperature of either 35°C (mesophilic) or 55°C (thermophilic) (41) in order to provide the required environment for the microbial species to be most effective. There are many different steps that occur throughout this procedure where energy is expended and which require the transportation of the media through different containment tanks to provide the desired conditions. The methane that is produced needs to be burned in order for the energy to be released as heat or used in a combustion engine and is therefore limited by the Carnot cycle (42).

The anaerobic digester system is instead more reliant on heating and proper mixing of the feedstock to ensure an even distribution within the container and provide optimal conditions for methane production.

An alternative to this technology can be seen in MFCs, which are the focus of this study.

2.1.2 Microbial fuel cells – Principles, potential and drawbacks

MFCs provide an alternative to anaerobic digesters and present several advantages. They are in essence living batteries in which organic material is degraded to its smallest constituent compounds in the anode so that the energy stored in the chemical bonds within the compounds is released when they are oxidised (43). This is an exploitation of all organisms' requirement to dispose of high energy electrons released following the catabolism of a substrate to create a proton gradient (44). Instead of utilising a standard terminal electron acceptor (TEA) such as oxygen to pass these electrons to, the bacteria make use of the anode. These electrons are then harnessed and can be used to power electrical equipment (45) (46). This was first discovered to be possible by Potter (47) although the power output achieved was incredibly small due to a number of limiting factors: (I) An inability to effectively transfer the electrons produced by the bacteria to the anode and (II) The use of a strain that lacked metabolic versatility, preventing the complete oxidation of the organic compounds leading to a loss in the number of electrons that could be extracted (48).

Potter's discovery was unnoticed until the 1980's when interest in the use of MFCs for the degradation of organic material and electricity production drew attention. At this point there was no knowledge of the ability of dissimilatory metal reducing bacteria (DMRB) to transfer electrons to an anode within an MFC and so strains incapable of extracellular electron transfer such as *Escherichia coli* were used in association with artificial electron mediators like methyl viologen and neutral red (49). These soluble mediators were able to greatly accelerate the transfer of electrons from the cells to the anode (50). There are however many problems with the use of such mediators. They are often expensive, toxic compounds that degrade over time and therefore require continual replenishment for effective activity (51). This makes them highly unfavourable for long term use within a MFC used to treat water that will later go on to be used for human consumption as it would require further treatment to remove these compounds.

An example of a two chamber MFC can be seen in Figure 2.1. Recent developments in MFCs have made use of metabolically versatile dissimilatory metal reducing bacteria that are able to degrade a wide range of organic materials under a large variety of conditions.

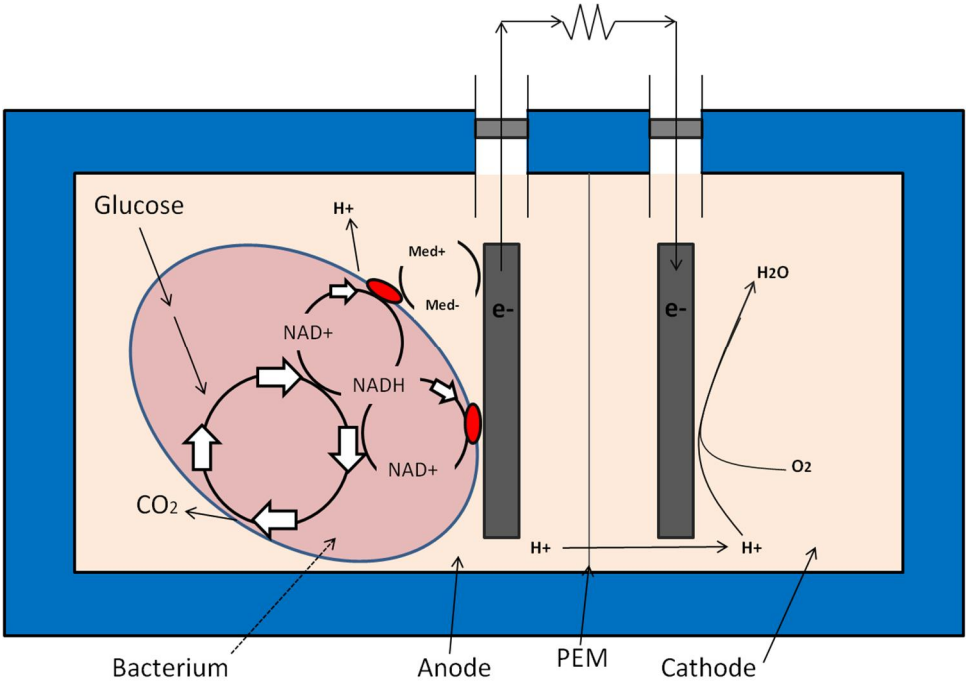

Figure 2.1 – Example of a two chamber MFC

Figure 2.1 illustrates the setup of a two chamber MFC. The microbes and organic material are stored in the anaerobic anode chamber, where the biological oxidation is allowed to take place and the electrons are transferred to the anode electrode (52):

$$\text{Anode:} \quad \text{Starch} \rightarrow C_6H_{12}O_6 + 6H_2O \rightarrow 6CO_2 + 24H^+ + 24e^- \qquad (1)$$

The polysaccharide is enzymatically degraded to its monomer, glucose and is then oxidised to CO_2 yielding 24 protons and 24 electrons. The thin line that can be seen in the middle of Figure 2.1 that divides the two chambers is known as the proton exchange membrane (PEM). This selectively permeable membrane limits the transfer of oxygen present in the water in the cathode from transferring into the anode and acting as a terminal electron acceptor (TEA). It also permits the transfer of protons released from the oxidation of the organic material from the anode to the cathode where they can then be used to reduce oxygen to water.

$$\text{Cathode:} \quad 24H^+ + 24e^- + 6O_2 \rightarrow 12H_2O \qquad (2)$$

The electrons that are released must travel through the anode and along the circuit where they can be harvested for use in electrical circuits. The organisms must be kept under anaerobic conditions so that the only available TEA is the anode.

The combination of the reactions (1) and (2) can be seen in reaction (3), theoretically yielding a high power output.

$$C_6H_{12}O_6 + 6O_2 \rightarrow 6CO_2 + 6H_2O + \text{electrical energy} \qquad (3)$$

(theoretically approaching – 2840 kJ/mol) (53)

The example MFC shown in Figure 2.1 presents the use of an added soluble mediator such as methyl viologen to the anode chamber to allow for electron transfer. This setup is now considered obsolete due to the number of issues that arise from their use such as the need to be frequently replenished, their cost and their toxicity. This lead to a search for organisms that were capable of transferring their electrons to the anode without the need for mediators. These were eventually found in the form of DMRB such as *Geobacter* and *Shewanella* as discussed in section 2.1.4.

2.1.3 Advantages over anaerobic digesters

There are several advantages of using MFCs over anaerobic digesters (AD) and other methods of organic waste to energy conversion. Unlike anaerobic digesters, MFCs are not greatly inhibited by limited substrate concentrations and are still able to produce electricity at temperatures below 20°C (53). The limited heating required provides an opportunity to save significant amounts of energy compared to AD. The other major consideration is the further combustion of the methane that is required, which limits the achievable efficiency (54). This is not necessary for MFCs as the electricity produced is available for usage without conversion. The methane that is produced from AD requires drying to remove the steam and purification from other gases that are also expelled. Although ADs are able to use a wide range of substrates in order to be able to produce methane, they are still not able to utilise quite as many energy sources as MFCs. MFCs are able to use complex polysaccharides such as starch and cellulose and have even shown potential with light (55,56). With the theoretical maximum conversion rate of 100% coulombic efficiency, an MFC can produce 3kWh for every kg of organic matter compared to the 1 kWh of electricity and 2 kWh of heat produced during biomethanation (57).

There are many different types of MFCs that have been developed, but there is currently a large amount of work that must be done in order for the technology to be able to be applied on a realistic scale for wastewater treatment (an example of a Pilot scale MFC has been demonstrated at Foster's brewer in Queensland, Australia). There are obviously other opportunities in which MFCs can be utilised, but there is no standard model that can be applied to all situations, as no one setup will likely be able to provide the greatest output and efficiency under a variety of environments. Not all of these issues are specifically to do with the engineering side of the MFC.

The most obvious disadvantage of this technology at present is the inability to upscale. It is not simply a task of increasing the size of each of the chambers as this brings with it a wide range of problems such as increasing resistance and proton transfer issues (58,59). One possible option can be seen with stacking technology as shown in Figure 2.2. The energy output that can be achieved from a single MFC is not particularly

useful but the voltage that can be obtained through stacking MFCs can allow for a yield of over 100 V (53). The use of single chamber and continuous flow MFCs for wastewater treatment can remove up to 80% COD meaning much less energy is then needed to remove the rest. This is all proposed to be done at a CE of ~80% (59,60).

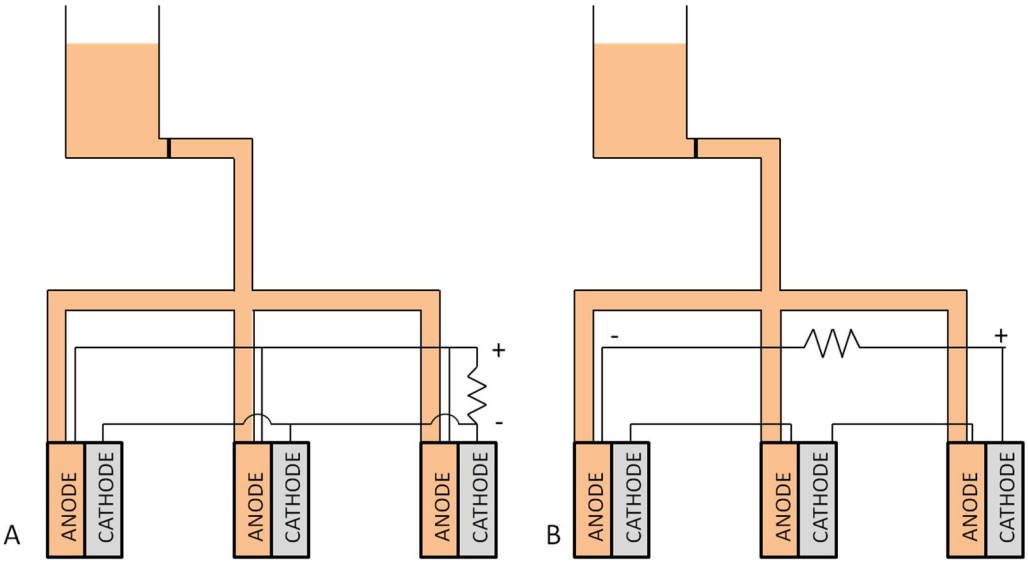

Figure 2.2 – Example of potential MFC stacking for increased power output (modified from Ieropoulos et al* (61)*) A) Demonstrates a parallel setup B) Demonstrates series

The use of PEMs within MFCs creates a wide range of problems such as increasing the internal resistance due to the difficulty that protons often have diffusing through the membrane. This is further complicated by the direct competition that is seen between the protons and other cations present in the media.

This is not the only issue to be noted with the MFCs as there are significant problems with slow kinetics of electrochemical reactions occurring at the electrode surface that can be a limiting step (62). This can be affected by the ability of the bacterial culture to adhere not only to the electrode but also in the formation of biofilms. The macro and microstructure of the electrode can play a large role as this needs to provide a large surface area for the cells, with high reaction kinetics and also be designed for adsorption of the cells (63). The inability of the cells to transfer their electrons through the cell membrane is often a major cause of poor power output. All of these are often

referred to as activation polarisation, where the activation energy must be overcome by the cellular components in order for the reaction to occur (63). With non electrogenic strains used in the past, this was overcome through the use of added mediators (49). Rare metals such as platinum are added to the electrodes to provide an efficient electrocatalyst (64) and redox reagents such as ferricyanide can be added to the cathode. Graphite is poorly suited for use as a catalyst for oxygen reduction in the cathode as the saturation value for dissolved oxygen is more than 6.6 mg/l (65). In air-saturated water this value is approximately 80% of the oxygen present. This is very often the rate limiting step in the reaction, as the oxygen content can quickly reduce below 6.6 mg/l. The reaction in the cathode may then become suppressed. This can be aided by the addition of catalysts such as platinum that can reduce the oxygen level required down to 2.0 mg/l (65) as platinum has a lower energy barrier. The change from graphite to platinum cathode has also been shown to permit a maximum current three to four times higher than a standard carbon electrode (49). Potassium ferricyanide is often used in the cathode chamber to increase the reducing potential (compared to oxygen) and therefore the power output (66). This however is not a standard catalyst as although it can reduce oxygen, over time this occurs less frequently resulting in the need for replenishment of ferricyanide, making it expensive and infeasible for long term runs. The need to increase the dissolved oxygen content through the use of inexpensive means could possibly be accomplished through the use of microbubble technology which is capable of transferring gases at a greater rate (67).

The power output that is achieved can vary due to a vast number of influences. In the context of this study these can be seen in the complex nature of the respiratory chain of the organism, which varies between organisms and also under differing conditions due to regulated metabolism and protein expression levels (62). It is the reduced potential of the terminal cytochrome transferring the electrons to the terminal electron accepting anode that determines the power achieved from the anode compartment. There are also always losses that occur within the system that in certain setups can cause a significant decrease in the power output achieved (61). These

losses can occur through internal resistances encountered within certain areas of the fuel cell, such as in the electrolyte and the electrode.

There are a wide number of sources in which losses can occur as shown in Figure 2.3. This study is concerned with the first two stages in the process and the issues with bacterial metabolism and the transport of electrons to electrodes. The transfer of electrons through the electrolyte can also be impeded due to internal resistances. This can be overcome through reducing the distance between the two electrodes and also increasing the ionic conductivity of the electrolytes (68). This however produces its own problems as reducing the spacing distance between the electrodes too far can itself reduce the power output achieved (68) whilst the natural occurrence of salts within the media for proton transfer can also interfere with the PEM (due to blocking).

The PEMs used are designed for use within standard chemical fuel cells and are therefore unsuited for use within MFCs. The use of salts within the growth media of the bacteria causes high levels of interference with the current PEMs (65). Up to 74% of the sulfonated residues on the PEM can be occupied by Na^+ or K^+ instead of being free for the transportation of protons. This then disrupts the conditions within the MFC as the anode chamber can become more acidic due to inefficient transfer of protons and the cathode become alkaline which limits oxygen reduction (65) (69). The decrease of pH within the anode means that the enzymes required for oxidation of the organic compounds are not able to operate under optimum condition, which in turn limits electron flow and power output (65) (69).

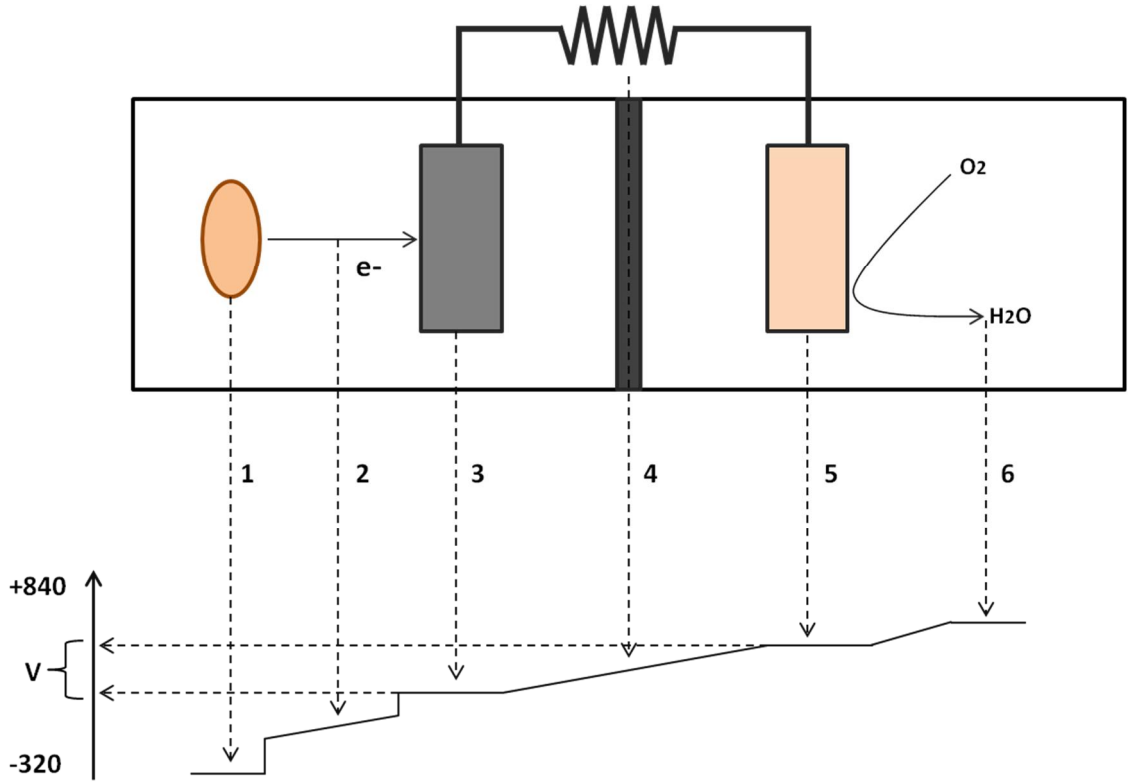

Figure 2.3 – The potential losses during electron transfer within an MFC – 1) Losses due to bacterial metabolism 2) Losses due to bacterial electron transfer 3) Losses at the anode. 4) Losses due to MFC resistance including membrane resistance. 5) Losses at the cathode. 6) Losses owing to electron acceptor reduction.

As shown in Figure 2.3, the potential gradient between the two chambers in the MFC allows for the transfer between the anode and the cathode. The greater the difference, the higher the voltage achieved is.

Whilst MFC technology is still being developed, there is potential for the use of MFCs alongside AD. The effluent that is released from the digested organic material passed through the AD following methane production, could then be transferred to an MFC setup, once the concentration of organic material has potentially dropped. As the oxidation of the organic compounds is still incomplete this provides an opportunity for electricity production. The typical chemical oxygen demand (COD) of the wastewater released from an AD is a few kg/m^3 and this still provides ample opportunity for highly efficient electricity production (57).

There have also been developments in other types of BESs such as microbial electrolysis cells (MEC) (70,71), microbial desalination cell (MDC) (72,73) and microbial electrolysis desalination cell (MEDC) (74). All of these are variants of the regular MFC that provide different advantages depending on the situation. The MEC for example, is instead capable of producing hydrogen as a final product in order to keep up with the proposed hydrogen economy of the future. This is apparently a more efficient method of hydrogen production than that achieved from fermentation or from the electrolysis of water (70). The production of hydrogen within a standard MFC is thermodynamically unfavourable, but with the application of an external voltage of only 110 mV (75) this was possible to achieve. The application of this small external voltage to the cathode chamber of the MEC meant that instead of oxygen being reduced to water, hydrogen gas is produced (70). This is a much lower energy input than that required for standard electrolysis, which needs 1210 mV (75), and also provides the potential to yield 8-9 mol H_2/ mol glucose compared to the 4 mol H_2/ mol glucose yielded from fermentation (75).

Compared to other forms of renewable energy, there is a constant stream of wastewater production with the highest levels of wastewater occurring during times of the highest human activity. The energy produced from the degradation of organic compounds can then be fed to the national grid where it can be used to power electrical appliances, power transportation or with sufficient infrastructure development, stored for later use. The use of this directly converted electricity has already been used to power autonomous robotic experiments (76,77). The use of MFCs over anaerobic digesters allows for higher energy levels to be produced alongside a more useful energy product in the form of electricity over methane. This can then be used to power turbines required for the distribution of clean water to the consumer, making the water industry self sufficient.

There is still a substantial amount of research that must be carried out in MFC technology as there is uncertainty with respect to engineering, electrochemistry and biology of MFCs. Research into all of these areas is required due to the lack of

understanding of how the different microbial electron transfer mechanisms affect current output and hence, MFC performance (78).

The type of MFC that is used can determine the type of environment within the chambers and therefore the organisms best suited to growth under those conditions. The use of a system that is highly anoxic, has been shown to result in the enrichment of *Geobacter* species within the anode, whereas an MFC type that permits oxygen leakage into the anode, allows for facultative anaerobic organisms to excel (45).

The bacterial culture that is present within the anodic chamber can have a vast impact on the achievable power output. In general, the use of pure bacterial cultures within the anode for the degradation of waste organic material, limits the rate at which this can occur (79). This is due to the complex mix of compounds present within the mixture that requires metabolic versatility for efficient catabolic activity. Using a mixed microbial culture, provides a wide range of metabolic pathways that can allow for faster breakdown of compounds and may encourage the development of symbiotic relationships, whereby electrons are transferred from a non electrogenic strain to an electrogenic one which is then capable of transferring the electrons to the anode (80)**.** The use of a mixed culture also appears to reduce the internal resistance within the MFC (81) and has also demonstrated the ability that mixed cultures are capable of producing between 68 and 480% more power than pure *S. oneidensis* MR-1 (81). For the greatest power output, the microbial community would need to be tailored in for the conditions in which it would be used i.e. pH, temperature and compound concentrations within the waste matter. The mixed microbial community would be more capable of withstanding and adapting to changes in conditions. Over a period of time, the bacteria best suited to the specific conditions imposed upon them, would dominate the community. When assessing the bacteria within a MFC following the inoculation with a wide range of waste sources, there is one class of bacteria that tend to prevail. Proteobacteria are the most commonly found bacteria within analysed MFC communities, although no single species has been found to be ubiquitous (41). The

fact that proteobacteria are seen throughout is not that surprising considering that *Shewanella, Geobacter, Arcobacter* and even *Escherichia* are found within this phylum.

2.1.4 Dissimilatory Metal Reducing Bacteria

Dissimilatory metal reducing bacteria (DMRB) such as *Geobacter* and *Shewanella* have been studied closely since the discovery of the first *Geobacter* strain GS-15 (82,83). This is due to the fact that these bacteria are highly metabolically versatile with the ability to degrade a wide range of organic compounds (84,85) decontaminate oil polluted soils and waters (86,87) and oxidise toxic uranium to a less soluble form (88). However, it is the capacity of these bacteria to reduce Fe (III) extracellularly that has been the subject of most attention.

The discovery of these bacteria revolutionised MFC technology, as devices were able to be operated without the use of expensive and toxic additional mediators as the bacteria were able to produce their own extracellular transport mechanisms. These bacteria are far from sparsely distributed throughout the planet. Rich sources of these DMRB and electrogenic organisms can be seen in marine sediment, soil, wastewater, fresh water sediment and activated sludge (62). Several publications have called for the production of a genetic library containing the chromosomal information of known electrogenic species (62,89).

The choice of substrate available within the anodic chamber can have a vast impact upon the strains that develop there and can therefore greatly affect the achievable power output. Electrochemically active microorganisms are able to out compete methanogens when non fermentable substrates such as acetate are used (44). This is however a different case when fermentable substrates such as glucose and ethanol are used, as they can lead to notable amounts of methane production. This is due to the inability of many DMRB such as *Geobacter* and *Shewanella* to fully oxidise glucose and ethanol (44). The use of a strain capable of doing this would out compete the methanogens due to the higher redox potential capable through the use of the anode. If this was infeasible, then the methanogens convert the glucose and ethanol to compounds that can then be oxidised by the DMRB and there would still be

harvestable methane produced. There is a significant decrease in the power output achieved when using complex organic substrates such as those seen in wastewater when compared to pure substrates such as acetate. This has been shown to decrease the power output to as little as 10 % of the value seen with pure substrate (57). This is not particularly surprising considering that the wastewater will contain complex organic molecules that will need a variety of enzymes in order to fully oxidise them. The effect that the variety of the substrate has upon the microbial community has yet to be elucidated, but the ability of an organism to fully oxidise a substrate can determine how successful it is within an MFC. Although *Shewanella* species are DMRB and able to transfer their electrons to a variety of electron acceptors including the anode, they cannot fully oxidise a variety of substrates to CO_2. So, although they are classified as electrogenic bacteria due to their ability to generate current, they are not classed as electricigens under the criteria established by Lovley and colleagues (whereby full oxidation of substrates to CO_2 is required) (45). These criteria state that electricigens must be able to fully oxidise organic compounds to CO_2 and transfer the released electrons to the anode (45). *Shewanella* is only capable of converting lactate to acetate, but is incapable of full oxidation to CO_2 meaning that only a third of the electrons available are converted to electricity (90). This is, however, a hazy definition as *Geobacter* is itself, alongside *Shewanella,* unable to reduce glucose as stated above (44). The bacteria rely on more oxidised substrates such as acetate, produced by fermentative organisms (52).

The most widely used method of expressing the efficiency of a MFC is to describe its coulombic efficiency (CE). This is the percentage of the electrons released from the oxidation of a substrate that are collected as current (91). This value does not relate solely to any particular part of the MFC as it can be affected by the design, such as increased leakage of oxygen into the anode chamber, which could lead to the use of oxygen as the TEA and reduce the number of electrons moving to the anode. It has been shown to be resistance dependant, whereby applying an increased load upon the circuit decreases the achievable CE (92). In order to decipher the coulombic efficiency of the system (both BES and culture setup combined), the amount of substrate added

must be known. The choice of substrate and the metabolic versatility of the anodic organisms which provide higher CE values are obtained from the use of non fermentable substrates such as acetate compared to fermentable substrates, such as glucose. In general, the more complex the organic matter, the lower the CE due to the energy required in the construction of enzymes for its degradation (7,62). This again leads back to the fact that, to this date, mixed cultures provide a significant number of advantages over single strains as they are as a community much more metabolically versatile and therefore able to degrade a wide range of compounds. Versatility within the culture provides them with the ability to survive under changing conditions within the anode, where the substrate concentration and makeup may alter. Overall, this leads to a greater power output and greater CE (7). This demonstrates that alongside the electrogenic activities of an organism, its metabolic capabilities must also be considered, as this can have a great impact upon the energy conversion percentage.

The electrons released from the degradation of the organic material are not directly used by respiring bacteria and are instead used to create a proton gradient and therefore regenerate ATP supplies (93). The bacteria are searching for a TEA with the highest potential difference between their electron donor redox protein and the acceptor, as this will provide the greatest energy return. An acceptor that is able to provide the greatest return will be preferentially used where possible and is the main reason why oxygen must be kept out of the anode chamber. The anode potential can determine the electron transport pathway that is used by the bacterium, but this is also very dependent on the strain (7).

The ideal conditions within an MFC would be for a highly negative redox potential compound such as glucose to be completely oxidised in the anode and a highly positive compound such as oxygen to be reduced in the cathode (94). A setup such as this would provide the greatest power output due to the large difference in potential, but this is not easily achieved as although these compounds are easily obtained, there are very slow reaction kinetics when used with pure carbon electrodes (95). It is for this reason that compounds such as platinum and ferricyanide are used to speed the

reaction up. The final amount of voltage that is generated within the MFC is dependent on the difference between redox potential of the substrate and the redox couple within the bacterial metabolism. The potential difference between the host metabolism and the terminal electron acceptor then determines how much potential is utilised within the system (124).

In order for the anodic electrode to be used as the TEA, the bacteria must not only be capable of interacting with it, but it must also have a sufficiently high positive redox potential. This is to ensure that in the absence of oxygen this is the TEA that provides the greatest energetic gain (7). Any minimal amounts of oxygen that are able to diffuse through the PEM will be used up very quickly by facultative anaerobes but will kill strict anaerobes and must therefore be limited (96). The electron transfer of NADH to NAD+ using oxygen as a terminal electron acceptor provides a high potential difference as shown by using the values stated in Table 2.2 and the calculations in reaction 4:

$$\Delta E = O2/H2O\ (+0.820V) - NAD+/NADH\ (-0.320V) = 1.14\ V \quad (4)$$

1.14 V is obviously a very high redox potential, meaning that oxygen will be used by facultative anaerobes if it is present. The anode potential needs to be high enough to prevent the bacteria from using alternative sources of TEAs or even resort to fermentation.

The use of sulphate for example provides a very low potential difference (although SO_4 can be used as an effective mediator):

$$\Delta E = SO_4^{2-}\ (-0.220V) - NAD+/NADH\ (-0.320V) = 0.1\ V \quad (5)$$

The comparison between the energy released from the complete oxidation of glucose to CO_2 compared to that achieved through its fermentation to high energy compounds such as butyrate and acetate can be seen in reaction 6 to 8 (44,97)

Glucose fully oxidised to CO_2 provides a high energetic gain:

$$C_6H_{12}O_6 + 6\ O_2 \longrightarrow 6\ H_2O + 6\ CO_2 \quad \Delta G = 2895\ kJ\ mol \quad (6)$$

Glucose to butyrate provides a low energy gain due to the vast majority of the energy being contained within the end product:

$$C_6H_{12}O_6 \longrightarrow C_3H_7COOH + 2\ CO_2 + 2\ H_2 \qquad \Delta G^0 = 225\ kJ\ mol \quad (7)$$

Glucose to acetate provides an even lower energy gain

$$C_6H_{12}O_6 + 2\ H_2O \longrightarrow 2CH_3COOH + 2\ CO_2 + 4\ H_2 \quad \Delta G^0 = 206\ kJ\ mol \quad (8)$$

Table 2.2 also demonstrates the major advantage of being able to reduce Fe (III), as this has a redox potential second only to oxygen.

$$\Delta E = Fe^3/Fe^2\ (+771) - NAD+/NADH\ (-0.320V) = 1.09\ V \qquad (9)$$

The energy gain provided from this is much greater than that seen with the reduction of sulphate or even nitrate.

Table 2.2 – MFC electrode reactions and corresponding redox potentials (Modified from Fan et al (46))

Oxidation/reduction pairs	**E^0 (mV)**
H^+/H_2	-420
NAD^+/NADH	-320
S^0/HS^-	-270
$SO^{2-}{}_4/H_2S$	-220
$Pyruvate^{2-}/Lactate^{2-}$	-185
2,6-AQDS/2,6-AHQDS	-184
$FAD/FADH_2$	-180
Menaquinone ox/red	-75

Pyocyanin ox/red	-34
Humic substances ox/red	-200 to +300
Methylene blue ox/red	+11
$Fumarate^{2-}/Succinate^{2-}$	+31
Thionine ox/red	+64
Cytochrome b(Fe^{3+})/Cytochrome b(Fe^{2+})	+75
Fe(III) EDTA/Fe(II) EDTA	+96
Ubiquinone ox/red	+113
Cytochrome c(Fe^{3+})/Cytochrome c (Fe^{2+})	+254
O_2/H_2O_2	+275
Fe(III) citrate/Fe(II) citrate	+372
Fe(III)NTA/Fe(II) NTA	+385
NO_3^-/NO_2^-	+421
$Fe(CN)^{3-}_6$/ $Fe(CN)^{4-}_6$	+430
NO_2/NH_4^+	+440
Fe^3/Fe^2	+771
O_2/H_2O	+820

If the substrate is fermented, then a much lower energy output may be generated within the MFC. This is highly inefficient as the substrate is a long way from being fully oxidised, leaving the vast majority of the energy stored in the fermentation compound

(97). This will depend upon the microbial community present on the anode and whether there are organisms that are able to further break down these compounds.

As shown above, the anode must have a higher redox potential than other TEAs present within the media otherwise the electrons will not be transferred to it. The bacteria must however also be able to interact with the anode. This interaction is currently one of many rate limiting steps within MFCs. If it is to be resolved, then a deeper understanding of how extracellular electron transfer occurs in nature must be gained.

2.1.5 Understanding of mechanisms of electrogenicity and synthetic biology's potential role in increasing activity.

Most bacterial strains are unable to directly transfer their electrons to the anode due to the lack of conductivity seen in the lipid membrane, peptidoglycans and lipopolysaccharides (62). They therefore require soluble TEAs such as oxygen or nitrate that are able to permeate the outer membrane and move into the cytoplasm where it is enzymatically reduced to provide a high energy return (98)**.** DMRB do not require soluble electron acceptors in order to be able to respire; they are capable of reducing insoluble extracellular compounds such as Mn(IV),U(VI) and Fe(III) (88,99).

The rise of synthetic biology within recent years holds significant potential in this field. Synthetic biology is not simply the development of molecular biology into the 21st century, but also encompasses engineering and design of novel biological systems. The ability to chemically synthesise genomes (100) now allows for the production of completely unique organisms that have been designed to serve a specific purpose.

In order to be able to develop a highly electrogenic bacterium using modern synthetic biology techniques, a better understanding of the proposed methods in which this occurs in naturally electrogenic bacteria must first be obtained. The exact method in which this occurs is yet to be deciphered, although there are 3 known ways in which the electrons are transferred:

- Direct contact – The bacteria make use of a series of *c*-type cytochromes such as MtrA and OmcA in *Shewanella oneidensis* MR-1 (101) or OmcS and OmcE in *Geobacter sulferreducens* (102). These cytochromes provide a connection between the cells inner membrane through the periplasm to the outer membrane.
- Nanowires – These are electrically conductive appendages that do not require direct contact of the cell body with the extracellular acceptor (103). They instead use pili like structures to transfer electrons to the TEA. These appendages are normally seen in conjunction with the direct contact method.
- Endogenous mediators – Some DMRB such as *Shewanella* excrete mediators that are able to accept electrons and can then pass them to a TEA outside of the cell (78). This has been shown to be the dominant method of extracellular electron transport in *Shewanella* species (104). Within this category, synthetic/artificial mediators can also be considered, as they perform the same function as the naturally occurring molecules.

The uppermost cluster of cells in Figure 2.4 present the most well documented method of electron transfer. The cells adhere directly to the anode and transfer their electrons through the cell membrane and straight to the electrode using multi haem *c*-type cytochromes (37,44). The expression of these cytochromes in *S. oneidensis* MR-1 is dependent on anaerobic growth, where they provide a route for extracellular reduction of metals such as Fe (III) oxide Mn (IV) (105). This regulated expression limits the metabolic load on the cells when the cytochromes are not necessary. The *c*-type cytochromes believed to be responsible for this are found widely within DMRB, with *G. sulferreducens* and *S. oneidensis* thought to possess roughly 100 and 42 of these proteins respectively (45,85,106). Analysis of the literature only indicates the predicted use of around 7 of these to be required for metal reduction or current production (107,108). This is shown here by the comparison of the predicted extracellular electron transfer pathways of two of the most highly documented DMRB, *S. oneidensis* MR-1 and *G. sulferreducens* shown in Figure 2.5**.** The high level of potential redundancy seen within the system has meant that the exact method in which the electrons are

transferred had until recently remained elusive (109). The elucidation of the structure of the *Shewanella* outer membrane cytochrome, MtrF (110) provided the first insight into a proposed electron transfer pathway through the 10 haems spread across the protein in a cross conformation (111).

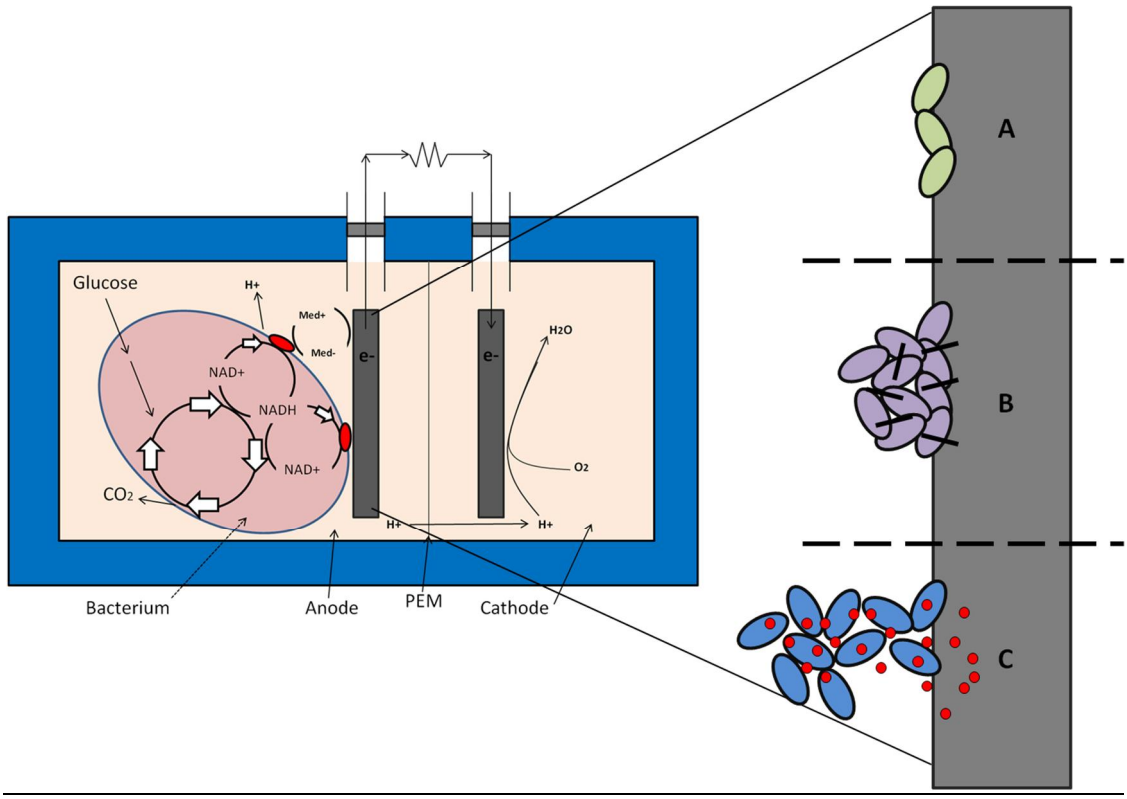

Figure 2.4 - Method of electron transfer to the anode. A) Direct contact of bacterial cells with the anode. Electrons transferred through the use of proteins such as those contained within the S. oneidensis* MTR pathway. *B) Electrons are transferred through the use of electrically conductive appendages known as nanowires. C) Mediators, either generated by the cells or added to the media are used to transfer electrons to the anode.

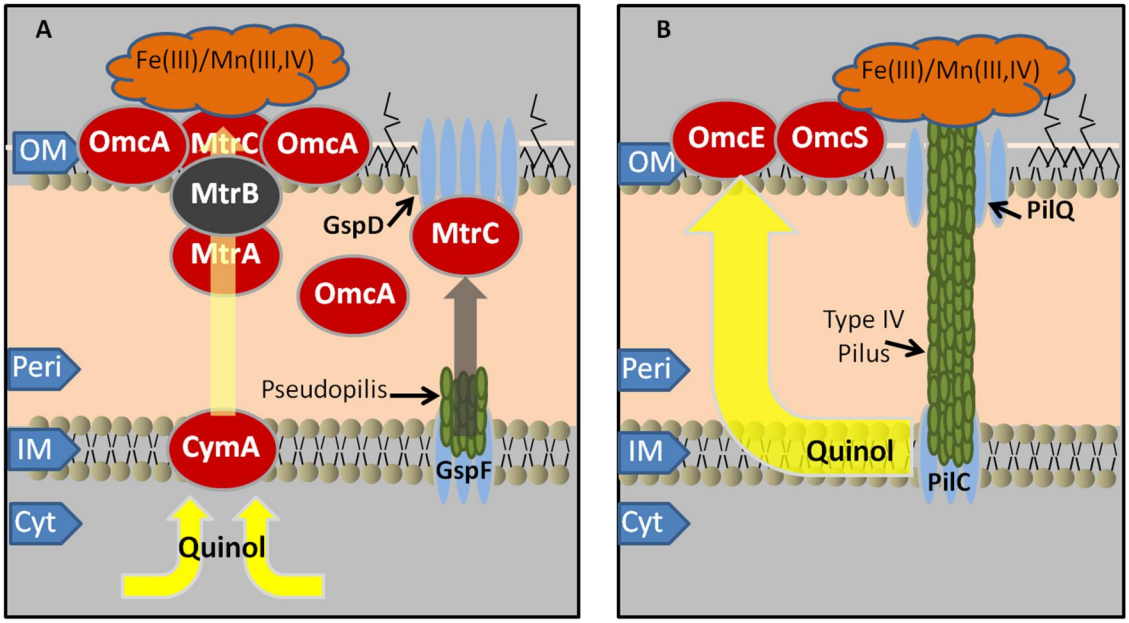

Figure 2.5 – Predicted extracellular electron transport pathways in two DMRB strains. OM – Outer membrane, Peri – Periplasm, IM – Inner membrane, Cyt – Cytoplasm. A) S. oneidensis MR-1, demonstrating the transfer of electrons from quinol to CymA, through MtrCAB an OmcA complex to a terminal electron acceptor. Pseudopilus from the type II secretion pathway (GspF involvement) transfers OmcA and MtrC through the periplasm and through GspD to cellular surface. B) G. sulferreducens, demonstrating transfer of electrons from quinol to OmcE/OmcS in the OM.

This redundancy is also further documented in an analysis of a variety of strains from the *Shewanella* species carried out by Fredrickson et al. (108). This revealed that a number of strains such as *S. frigidimarina* were capable of metal reduction with only 4 *c*-type cytochromes compared to the 7 (plus 2 iron binding proteins) *S. oneidensis* is believed to use and were all contained within a single locus. This can be seen in Figure 2.6 along with the even greater numbers seen by strains such as *S. halifaxensis*. Analysis of the genomes of both *S. oneidensis* MR-1 and *G. sulferreducens* allowed the determination of the position of the genes encoding these *c*-type cytochromes within the organisms' chromosome. From the data available through the National Centre for

Biotechnology Information (NCBI) (http://www.ncbi.nlm.nih.gov/) it was noted that the predicted genes required for metal reduction within *S. oneidensis* MR-1 were within a single locus (Figure 2.6), whereas the genes in *G. sulfurreducens* were distributed throughout its genome.

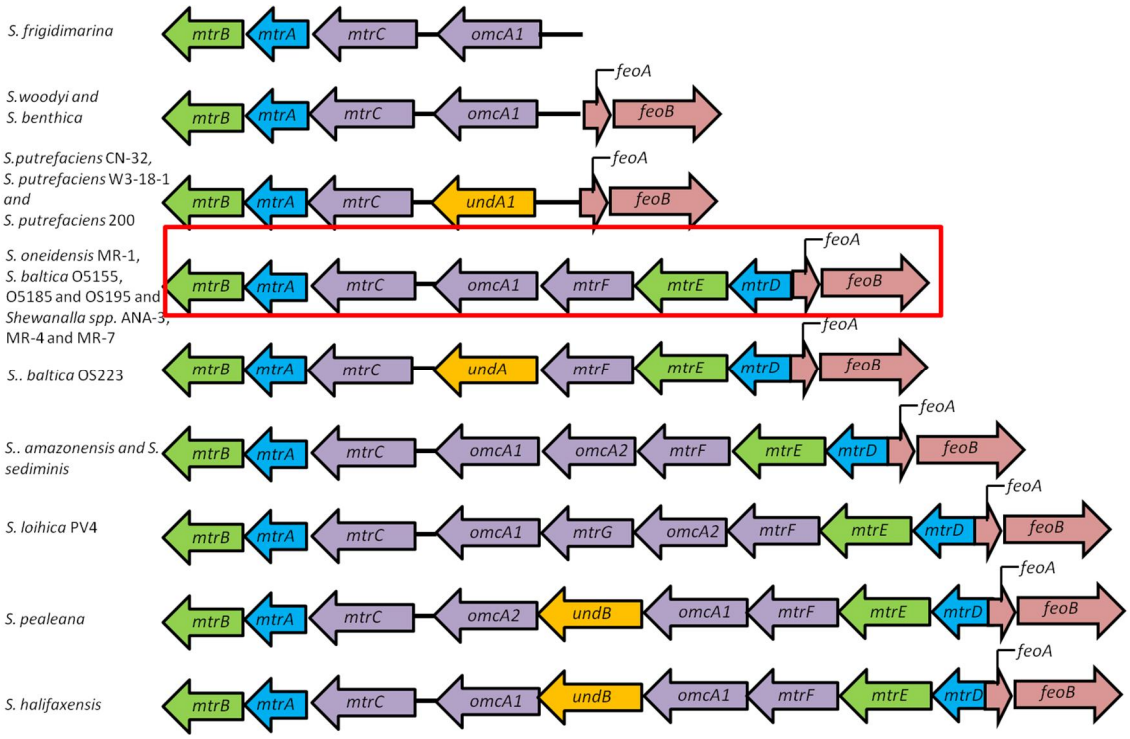

Figure 2.6 – Predicted metal reducing c-type cytochromes from a variety of Shewanella species including S. oneidensis MR-1 (Highlighted). Different colours are used to represent different components of the Mtr pathway (and extension to Feo components). Green arrows represent beta barrels, blue denotes periplasmic c-type cytochromes, purple and yellow are outer membrane cytochromes (yellow are lesser known). Red arrows relate to genes involved in ferrous iron transport.

This then raises the question as to whether all of these proteins are necessary for full activity or if some are presenting an unrequired metabolic burden. This has led to many studies conducted to try to determine the exact genes, or at least the most essentially required for activity (48,109,112,113).This type of analysis was first conducted by Holmes et al. (48) on *G. sulfurreducens* presenting the difference in the

regulation of transcript levels for a wide range of genes following growth on electrodes compared to using Fe (III) as the TEA. The greatest upregulation seen was 19-fold, 7-fold and 2-fold increase in the transcript levels of the genes coding for the outer membrane proteins OmcS, OmcT and OmcE, respectively (48). These were not the only changes noted, as there were a total of 474 genes with significantly different transcript levels when grown on an electrode compared to Fe (III) (48). Mutant strains deficient in each of the most highly upregulated cytochromes were made, with unsurprisingly the biggest decrease in current production of more than 50%, seen with the removal of *OmcS* (48).

A further *Geobacter* study (114) was carried out in which a pure culture of *Geobacter sulfurreducens DL-1* was added to a MFC with a poised anode potential of -400 mV, thereby making the transfer of electrons from it much harder. Through the challenge of surviving within this environment within a 5 month period, the strain adapted to the situation, resulting in a substantial increase in the achievable power output. The adapted strain named KN400 had a power density of 3.9 W/m^2 compared to 0.5 W/ m^2 achieved by the WT strain (114).

An example of potential redundancy within the genome of *S. oneidensis* MR-1 can be seen with the deletion of MtrB, the beta-barrel sheath protein. Removal of this protein is known to knock out dissimilatory iron reduction (115) but in this case, complementation with two *S. oneidensis* genes *SO4359* and *SO4360* was enough to restore activity. This suggests a level of genomic plasticity which confers the ability to replace the function of one protein for another. This study was however, conducted using ferric citrate which is capable of permeating the cell membrane, allowing for reduction at locations other than the outer membrane (107).

A more in depth study into the functional involvement of certain genes was carried out by Bretschger et al (109) with the use of wild type *S. oneidensis* MR-1 and a wide variety of single gene knockout mutants (apart from *OmcA* and *MtrC* which was studied as a complex). This study provided a real insight into the genes required for current production and the reduction of Fe (III) and Mn (IV). There were a number of

these mutants in which the removal had caused a significant impact on the cells ability to produce current. The most evident of these could be seen in the deletions shown in Table 2.3.

Table 2.3 – S. oneidensis MR-1 mutants that showed severe decrease in current production (Produced using data from Bretschger et al. (109))

MR-1 Strain/Mutant	**Current output (µA/cm^2) with 10 Ω resistor**	**Percentage of Wild Type**
Wild Type	13.8	N/A
ΔMtrA	0.35	2.5
ΔMtrB	0.35	2.5
ΔOmcA/MtrC	2.3	16.7
ΔCymA	0.4	2.9
ΔPilD	0.68	4.9
ΔGspD	0.7	5.1
ΔGspG	0.35	2.5

It is evident from Table 2.3 that only the top 4 mutants are deficient in the cytochromes that are typically shown to have a predicted involvement in metal reduction (The use of *CymA* is shown in Figure 2.5). Each of these genes is believed to play a pivotal role in extracellular electron transfer, as *MtrB* is required for proper localisation and incorporation of *OmcA* and *MtrC* into the outer membrane in the highly similar strain *Shewanella putrefaciens* MR-1 (112). The deletion of *CymA* has been shown to inhibit the ability of *S. oneidensis* MR-1 to reduce Fe (III), Manganese (IV) and nitrate demonstrating the necessity of this inner membrane periplasmic

cytochrome (116). Mutants in other *c*-type cytochromes that were predicted to have an involvement in activity such as *MtrD* and *MtrF* did not have any negative effect in activity. There was even a slight increase in activity noted with the removal of *MtrF.* This further demonstrates the redundancy within the *c*-type cytochromes within these defined conditions, as these genes may well be required for electron transfer to other insoluble metals. The bottom 3 mutants in Table 3 have other functions within the protein secretion ability of the cell and come into effect with the expression of nanowires (109).

There were a number of gene deletions that caused significant increases in activity as shown in Table 2.4. The highest power increase was seen in the removal of *NrfA*, a gene involved in the nitrate reduction function of the cell as is *NapB.* The other genes are believed to play a role in redox reactions involving suphur.

Table 2.4 – S. oneidensis MR-1 mutants that showed significant increase in activity (produced using data from Bretschger, et al. (109))

MR-1 Strain/Mutant	**Current output (µA/cm^2)**	**Percentage of Wild Type**
Wild Type	13.8	N/A
ΔNrfA	31.2	226.1
ΔSO0717	24.3	176.1
ΔSorB	24.0	173.9
ΔNapB	24.2	175.4
ΔDmsC	23.1	167.4

During the course of Bretschger et al's study an attempt to increase the expression of *MtrC* resulted in a significant increase in the activity but not as much as the removal of *NrfA.* The other complement strains were made through firstly deleting the noted gene

and then reintroducing it and determining its activity. The results from this can be seen in Table 2.5.

Table 2.5 - S. oneidensis MR-1 complement mutants and their activities (produced using data from (Bretschger et al. (109))

MR-1 Strain/Mutant	**Current output (µA/cm^2)**	**Percentage of Wild Type**
Wild Type	13.8	N/A
WT + *MtrC*	21.3	154.3
ΔMtrB complement	16.9	122.5
ΔMtrA complement	13.9	100.7
ΔMtrC complement	14.8	107.2
ΔOmcA complement	10.8	78.3

Although the experiment provided information on the changes seen by the removal of individual cytochromes, it also highlighted the highly complex nature of electron flow through MR-1 cytochromes.

All of this demonstrates potential for the development of a genetically modified strain in which a combination of different genes could be knocked out in order to reduce the metabolic load and increase electron transfer to the anode. This is however all conducted within the bacterial strain that these proteins are native to and therefore does not show how the use of a combination of these proteins would act if transferred into a foreign strain such as *E. coli*.

2.1.6 Transfer of iron reduction capability into *E. coli* using cytochromes

From the predicted activities of some of these *c*-type cytochromes there have been attempts made to transfer the extracellular iron reduction capabilities of *S. oneidensis* MR-1 into various *E. coli* strains. This was first seen through the introduction of the periplasmic cytochrome MtrA into *E. coli* JM109 (DE3) by Pitts et al. (105). This gene

was inserted into the host organism along with cytochrome maturation genes required for proper insertion of the haem groups into the protein and correct protein localisation (shown in Figure 2.7) (117). Through this the *E. coli* strain was shown to be able to reduce Fe (III) EDTA, Fe (III) Maltol and Fe (III) benzohydroxamic acid through the pathway proposed in Figure 2.7. There are however several issues with this as all of these forms of iron are soluble and therefore able to pass into the periplasmic space where MtrA is being expressed.

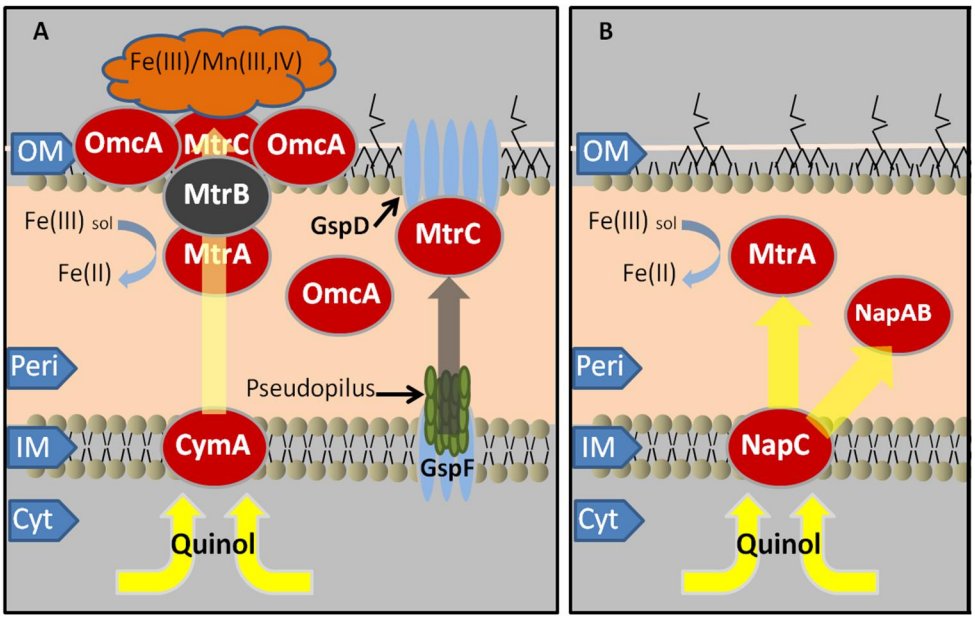

Figure 2.7 - Predicted method of extracellular electron transfer in S. oneidensis MR-1 (A) and E. coli heterologously expressing MtrA (B) - (Modified from Pitts et al (105)).OM – Outer membrane, Peri – Periplasm, IM – Inner membrane, Cyt - Cytoplasm

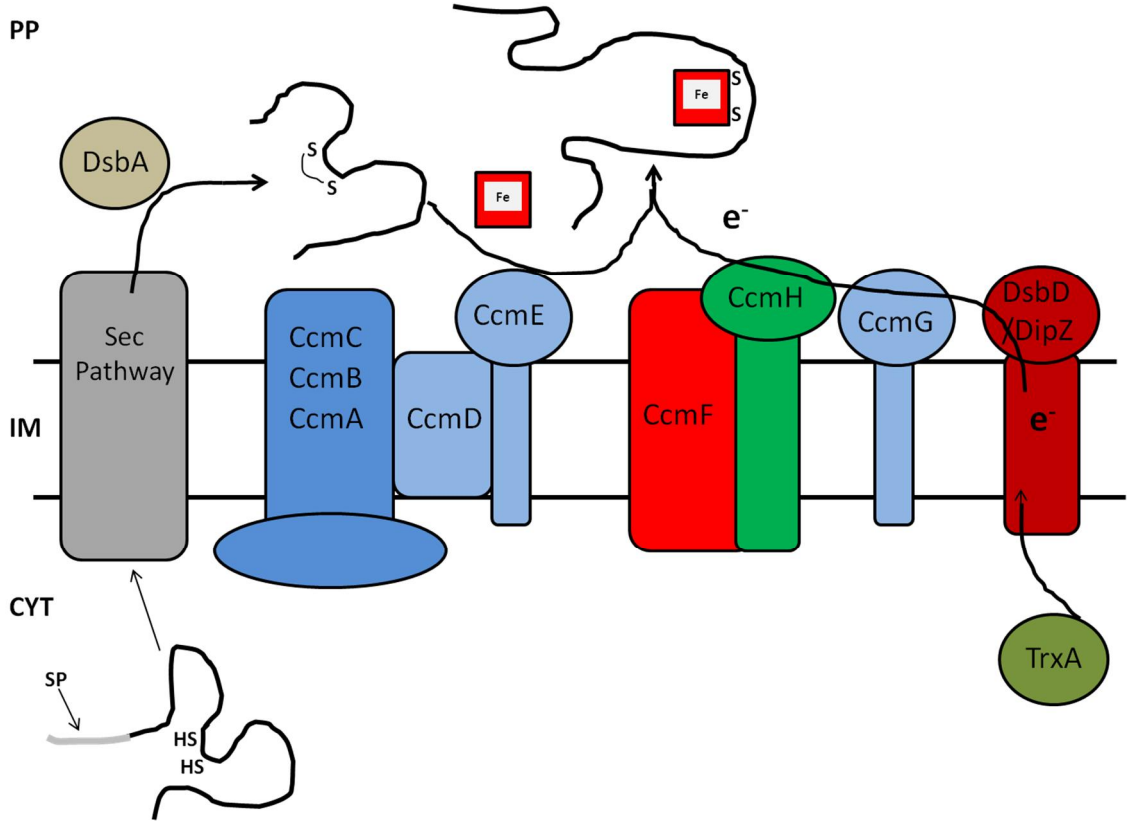

Figure 2.8 – The cytochrome maturation genes required for proper expression of c-type cytochromes. Holocytochromes are transferred from the cytoplasm to the periplasm where insertion of the haem group into the target cytochrome is carried out through the use of the cytochrome maturation genes ccmA-H and DsbD/DipZ. PP – Periplasm, IM – Inner membrane, Cyt – Cytoplasm.

There is, however, another way in which this could be explained. *E. coli* only has 7 naturally occurring *c*-type cytochromes, but *NapC* is one of these. It is a native tetrahaem cytochrome present in the inner periplasmic membrane, the same as *CymA* and has a very similar overall amino acid sequence (107). Both *CymA* and *NapC* are involved in electron transfer from menaquinol to *NapAB* – a periplasmic terminal reductase complex (119). It not only shares sequence homology with *CymA,* but it is also capable of reducing soluble Fe (III) on its own. Reduction occurs at a rate 2.6 fold lower than the strain containing *CymA* (107). The ability of this cytochrome to reduce

Fe (III) is not of real concern to this study but instead the rate in which it is capable of transferring its electrons to the next available cytochrome in the pathway (through the cell membrane).

Another attempt at transferring iron reducing capabilities into *E. coli* was also attempted by Donald et al. (120). This experiment was carried out using the outer membrane decahaem cytochrome *OmcA,* with the intention of being able to reduce insoluble Fe (III). This was again conducted with the simultaneous use of cytochrome maturation genes for the same reason as stated in the *MtrA* study. It was shown that *E. coli* K-12 was not capable of expressing this protein correctly due to the cryptic nature of the type-II secretion (in MC4100) pathway seen in this strain. The expression system is expressed in BL21 and this was then used to show that the recombinant strain was able to reduce insoluble Fe (III).

A more recent development along the same experimental path was the introduction of a "more complete" exoelectrogenic pathway through the introduction of 3 *c*-type cytochromes from *S. oneidensis* MR-1 into an *E. coli* strain. The chosen cytochromes were MtrA, B and C, as the proposed localisation of the proteins would permit a protein to interact with an inner membrane quinone reductase MtrA (to interact with NapC). The electrons would then be transferred to decahaem cytochrome, MtrC through the membrane spanning beta barrel protein MtrB, which acts as a sheath (121), covering transition space between MtrA and C. A diagrammatic representation of the proposed transfer is shown in Figure 2.9.

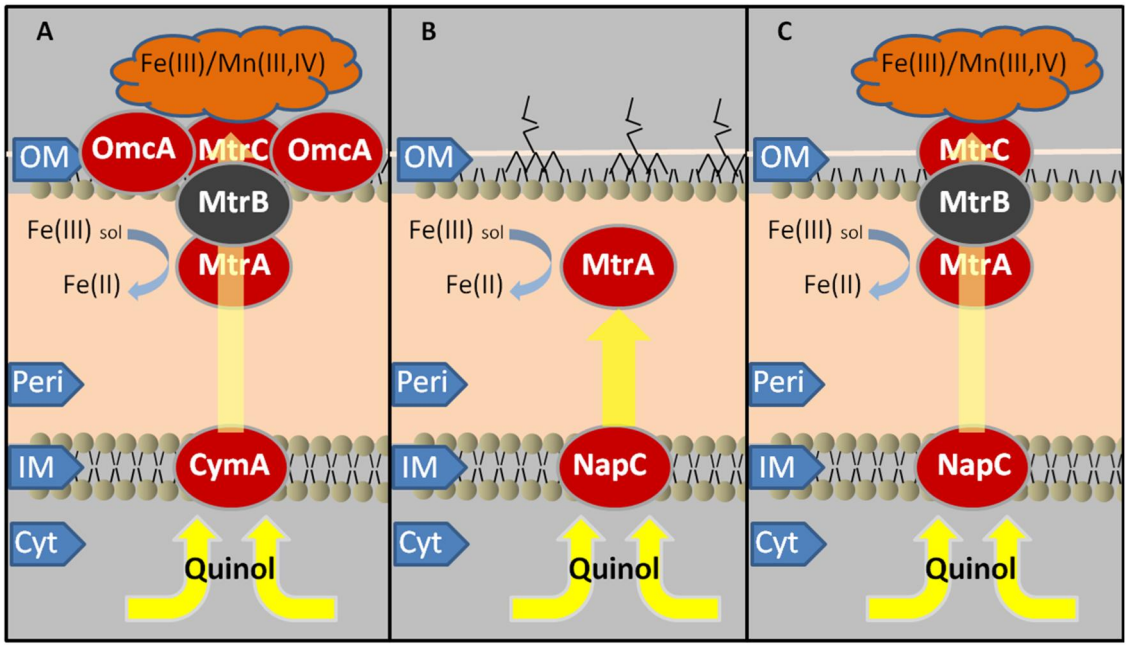

Figure 2.9 – The genes and proteins proposed to be involved in extracellular electron transfer to an insoluble metal. A) Proposed mechanism in Shewanella. B) MtrA expressed in E. coli to allow for reduction of soluble iron C) MtrCAB genes from Shewanella oneidensis MR-1 expressed within E. coli allow for extracellular reduction of iron. OM – Outer membrane, Peri – Periplasm, IM – Inner membrane, Cyt – Cytoplasm.

All of these experiments provide evidence for the ability to functionally express foreign *c*-type cytochromes in *E. coli* and suggest that extracellular electron transfer is possible in a non DMRB strain through the addition of a single outer membrane cytochrome. This experiment however does not demonstrate that the cells would be capable of producing current, as shown by the case of *Pelobacter carbinolicus,* which is able to reduce Fe (III) but is incapable of power output in an MFC (122).

A study carried out by White et al. (123) took a novel approach and introduced the same meta reduction pathway (MtrCAB) into a proteoliposome, effectively creating an artificial cell membrane. With the internal portion of the "cell" containing electron transporters, the artificial system with MtrA focussed internally and MtrC externally, with MtrB acting as a sheath between the two being tested for electron transfer. Not only was this shown to be possible, but electron transfer rates to oxide minerals such

as goethite were shown to be at levels similar to those seen by *Shewanella* cultures (123).

More evidence for transfer of exoelectrogenic activity into a non DMRB for current generation within a BES came from a paper by Goldbeck et al (124). This paper, from the same group that produced the metal reducing *E. coli* (125), presented the same exoelectrogenic transport chain but further engineered the plasmid setup to aid in current production. In order to do this, a degree of synthetic biology methodology was implemented through promoter tuning. The generated library was shown to have vastly different levels of MtrA and C between the different promoter sets. The cells producing the greatest level of MtrA and C were however not found to produce the greatest current output or be the "healthiest". An optimal expression level was reached, which provided the most morphologically typical *E. coli* but also the greatest current output. The exact mechanisms behind these observations have yet to be explained.

The purple cells shown in Figure 2.4 may make use of electrically conductive appendages known as nanowires. These appendages allow the bacteria to transport their electrons extracellularly without having to have direct contact with the anode. This morphological feature has been noted in both *Geobacter* and *Shewanella* where the expression of these pili is dependent on the absence of soluble electron acceptors (126). Once all soluble electron acceptors have been exhausted, the bacteria then synthesise pili and flagella to allow them to migrate towards Fe (III) oxides for electron transfer (126). This feature is however not unique to DMRB as it has also been observed in the oxygenic phototrophic cyanobacterium *Synechocystis* sp. PCC6803 and the thermophilic, fermentative bacterium *Pelotomaculum thermopropionicum* (127) and may therefore be a feature of a variety of species to allow for electron transfer. The appendages produced by these species only occur under certain nutrient limiting conditions which are different for each species but lower the metabolic load on the strain as needed. The appendages produced by these strains were highly electrically conductive and very similar in appearance and structure to those seen in MR-1 (127).

The production of electrically conductive nanowires is different to the production of standard pilus like appendages that generally do not permit electron transfer. It is believed that the production of these nanowires not only allows for the efficient transfer of electrons, but increases the surface area of the cells, providing them with a greater chance of binding to a TEA such as Fe (III) oxide or an anode (128). The deletion of the *S. oneidensis* MR-1 cytochromes MtrC and OmcA resulted in significantly impaired nanowires compared to the wild type, thereby highlighting the importance of these outer membrane proteins (127). As shown in Table 2.3, the deletion of *PilD*, *GspD* and *GspG* has a significant impact on the achievable power output in MR-1. These genes are responsible for type IV prepilin peptidase (PilD) and type II secretion pathway (GspD and GspG) (109). The type IV preplilin peptidase is a cytoplasmic membrane protein that cleaves signal sequences on the cytoplasmic side for transport towards the outer membrane (129). This is essential for the production of type IV pili within a number of species, including *E. coli,* although this appears to be within pathogenic strains (130,131). These type IV pili are not, however, expressed in *E. coli* under standard laboratory conditions. The type IV prepilin peptidase role makes them seem essential for the production of nanowires and may mean that expression of conductive pili within *E. coli* is possible. The type II secretion pathway is partially coded for by *GspD* and *GspG* and is one of 5 secretion pathways available to gram negative bacteria, but it appears to be essential for the proper expression of outer membrane cytochromes and nanowires (127,132). The type II secretion pathway appears to be cryptic within *E. coli* K-12, but is expressed under laboratory conditions in B type strains (120). The use of nanowires in MFCs has been shown to be very important, especially for DMRB strains such as *Geobacter,* which are incapable of producing endogenous mediators (44,133) and reported a 10-fold increase in power output when expressing nanowires. Lovley has postulated that if *Geobacter* were able to transfer electrons to the anode at the same rate as it is able to transport to its natural electron acceptor, ferric iron, it would be capable of producing a current four orders of magnitude higher than presently seen (62). The importance of pili and nanowires in *S. oneidensis* has in some cases been reported to be detrimental to the power output.

The construction of a mutant strain that was deficient in PilD was shown have very low power outputs due to the added effect that this has on the type II secretion system (109). A subsequent strain with the secretion system intact, but PilD deficient, produced greater power output than the wild type. This strain was capable of producing *c*-type cytochromes, but unable to produce pili or flagella (134).

The blue cells shown in Figure 2.4 illustrate the use of endogenous mediators that allow the cells to transfer their electrons to an intermediate molecule before being transported to the anode without having any contact with it. This has not been as thoroughly documented as the other methods of electron transfer, but several *Shewanella* species have been recognised as secreting electron shuttles in the form of flavin mononucleotide and riboflavin, which can then reduce Fe (III) (135–137).

Good mediators are capable of easily passing through the cell membrane and interacting with the electron transport chain of the cells and as well as other oxidising reducing agents such as NADH and reduced cytochromes(76). The reduced mediator is then able to move out of the cell, transfer its electrons to the anode and pass back through the cell membrane to harvest more (76). The mediators should also be stable within the anolyte, resist degradation and transfer the electrons to the anode at a high rate whilst also being non toxic to the cells.

The use of these mediators has allowed for much greater power outputs to occur in certain situations. Velasquez-Orta et al. (78) showed that the addition of mediators to an MFC inoculated with *Shewanella* cells allowed for a peak current four times higher than that noted when only *Shewanella*'s self produced mediators were present. The levels of mediators required for this increased current output were almost 10 times higher (4.5-5.5 µM) than those normally produced by *Shewanella* (0.2-0.6 µM) (78). The removal of these naturally occurring flavins from a developed anodic *Shewanella* culture has been shown to reduce the power output by more than 70% (136). This does however have a significantly detrimental effect on the coulombic efficiency that can be achieved, as CE values tend to range between 35 and 5% (138–140).

As this is highly concentration dependent, the analysis of the proteins involved could provide an opportunity for their upregulation to allow for greater production of these mediators to increase the power output.

There are other mediators that are naturally produced by a wide range of organisms and are found within wastewater. Some of these are humic acids, sulphate and thiosulphate, which are naturally occurring and have the ability to act as mediators (141) as shown in Figure 2.10. *Pseudomonas aeruginosa* can produce the secondary metabolite pyocyanin that can act both as an electron shuttle but also as an antibiotic that can kill off other microbes thereby helping to keep the culture pure (37).

Endogenous mediators are not as limited by the direct contact of the cell with the anode. The mediators are soluble and capable of diffusing through the culture and media allowing them to be reduced in the cell membrane and then travel to the anode where they are oxidised.

The use of the increased levels of flavins within the MFC anode provides the opportunity for much higher electron transfer rates compared to those seen in a biofilm. Velasquez-Orta et al. (78) claim to have rates 20 times higher than those seen in a MFC biofilm setup carried out by (136). This would of course be highly dependent on the experimental methodology used.

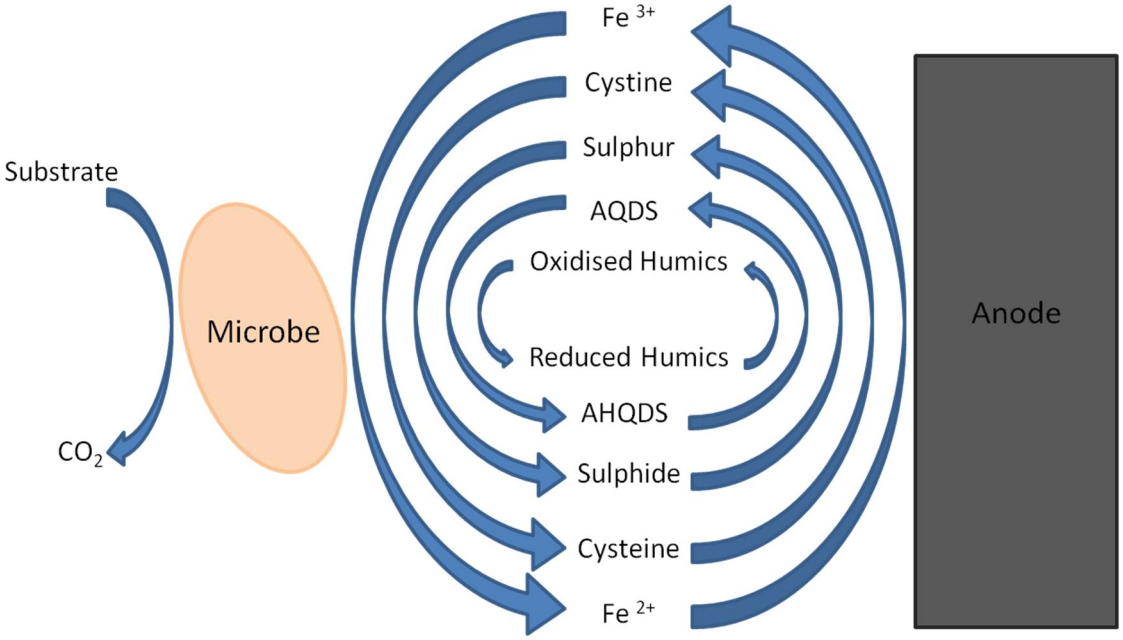

Figure 2.10 - Showing a variety of substances that can be used as endogenous mediators. AQDS – Anthraquinone-2,6-disulfonate, AHQDS - Anthrahydroquinone-2,6-disulfonate.

Naturally electrogenic bacteria have evolved to survive under conditions, where only insoluble electron acceptors are present and be able to reduce them. In order to achieve higher power densities from these bacteria, they will most likely require a mixture of synthetic biology and metabolic engineering. This will allow for the development of a strain or strains that have been engineered to remove undesired electron pools that prevent maximum electron transfer. The cells should also be able to express the most redox active proteins from a variety of organisms allowing for maximum transfer of electrons to the anode.

Although *Shewanella* may possess the three stated methods of electron transfer, the strain is not an ideal electrogenic bacterium, as it is not able to fully oxidise all organic compounds to carbon dioxide and then transfer the electrons to the anode (90). This can be seen with the example of lactate, which is incompletely oxidised to acetate by *Shewanella* but can be fully degraded by *Geobacter* and *Rhodoferax,* which are considered to be electricigens (90). This inability results in only a third of the electrons from lactate being harvested and transferred to the anode (90). This does however

present an opportunity to develop mixed communities “designed” for operation under specific circumstances.

There is no direct link between the ability of a bacterium to reduce Fe (III) and its ability to produce a current within an MFC. There are many examples where these abilities are seen together such as in *Shewanella* (96)*, Geobacter* (102)*, Desulfuromonas* (142) and *Pseudomonas* (143,144), but the exact link between these abilities has not been deciphered. It would seem reasonable to presume that the transfer of electrons to insoluble Fe (III) would also allow for the transfer of electrons to an insoluble electron acceptor in the form of an anode. This, however, has proven not to always be the case as shown with the example of *Pelobacter carbinolicus* (122). This is the first documented example of an organism that is capable of insoluble Fe (III) reduction yet unable to produce current within a MFC.

The use of only a single method of extracellular electron transfer will greatly limit both the achievable power density and also the coulombic efficiency. Direct contact methods tend to have high efficiency, but when used as the sole transfer method provide a limited power output (44). As the cells must make contact with the anode, or at least form a biofilm for this method, it is necessary to have an anodic electrode with a large surface area. The reverse tends to be true of endogenous mediators, as they are capable of producing high power outputs, but are done at a reduced efficiency due to the production of electrochemically inactive side products (44).

2.1.7 Biofilm development

Although not directly involved with electron transfer, the development of a healthy anodic biofilm has been shown to greatly increase the achievable power output (138,145,146). This may be the most important factor in the biological side of the MFC electron transfer. Hou et al. (145) demonstrated that the development of a mature biofilm allowed for over an order of magnitude difference in power output. A 30 day biofilm provided a power density of 594 mW/m^2 compared to 33.4 mW/m^2 seen in the MFC on day 5. In nature, the biofilm provides protection from the environment and allows for transfer of nutrients between cells. In MFCs the full colonisation of the

anode allows for maximum contact with the electrode, therefore increasing the amount of electrons that are transferred. As direct contact is a significant method of electron transfer (although not the main method of electron transfer in *Shewanella* - (104)) biofilm formation is an important factor to consider. This means that the choice of anodic electrode is important as it needs to have a large surface area and allow for proper adherence. A carbon brush anode, is one design that is well suited to this requirement (94). Figure 2.11 provides an example of the 3 main stages that occur in the life cycle of a biofilm although these can be further subdivided. The initial stage can be the deposition of a conditioning film on the surface to provide an opportunity for the cells to bind. The cells undergo reversible attachment to the surface and then through quorum sensing the cells are able to detect a change in environment (147). They alter their gene expression to suit their new environment and begin production of extracellular polymeric substance (EPS) (148). This allows them to bind more tightly to not only the anode surface but also to other cells. This is referred to as irreversible adherence. The biofilm then develops into a three dimensional structure of cells and EPS and once it reaches a certain size begins to disperse cells into the surrounding environment (149–151). A developed biofilm is able to transfer compounds between the cells contained within it and permits the transfer of electrons between cells to allow terminal transfer to the anode (152).

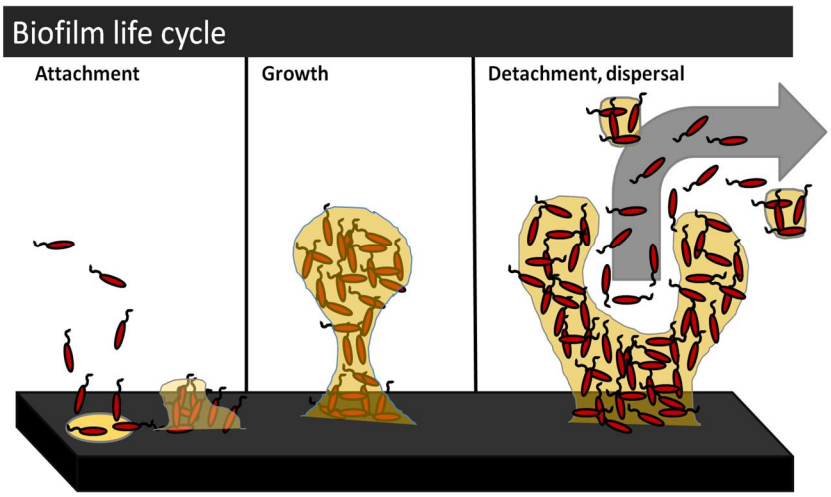

Figure 2.11 – Biofilm life cycle. Illustrates attachment, growth and dispersal/detachment stages of cycle.

The genetic factors involved in the development of biofilms are different for each species and this becomes more complex when a mixed microbial community is present. Biofilms use what is known as quorum sensing in order to be able to communicate with each other and also the secondary metabolite cyclic-di-GMP (153). Quorum sensing makes use of hormone like molecules known as auto-inducers (154) that allow the cells within the biofilm to regulate expression of proteins in order to suit their current environment.

The ease with which the bacteria are able to bind to the anode and form a biofilm depends on a variety of conditions. These range from the microstructure of the anode to the pH, temperature, hydrophobicity of the cell membrane and the substrates available to the bacteria (153,155). Gram negative bacteria such as *E. coli* have a lipopolysaccharide outer membrane, which imbues the cell with a negative charge. This allows the cells to more easily bind to positively charged structures. As the anode has a negative charge, this could make it harder for the cells to bind. The use of fimbraie and flagella increase the ability of the bacteria to adhere to a surface (156,157) and has even been reported to be essential for early attachment in *E. coli* along with the outer membrane protein Ag43 (158). The necessity of these appendages ties in with the results seen in Table 2.3, where the removal of *PilD* in MR-1 reduced the current production and greatly impacted upon biofilm production as seen in Figure 2.12. The deletion of a flagellar specific sigma factor (FliA) involved in the development of bacterial flagella has been shown to greatly decrease the ability of *E. coli* K-12 to form a biofilm (155). The same study however showed that the deletion of the master regulator in flagella biogenesis (FlhD/FlhC) resulted in a much smaller reduction in ability. The overexpression of this FlhD/FlhC complex, resulted in bacteria becoming overly motile and not settling to form a biofilm and therefore suggests that the overexpression of flagellar protein does not appear to be a suitable method for increasing biofilm formation. It may be possible that the over expression of nanowires within *E. coli* could allow for an increased biofilm forming capability although this is purely speculative. If this is not found to be sufficient, the addition of other factors that have been identified in biofilm development could be cloned into *E. coli*. It has

been reported that *E. coli* K-12 will not form a biofilm in minimal media unless supplied with amino acids (158) and that growth in media that contains substrates that are metabolised to acetyl phosphate and acetate, are highly supportive of biofilm formation (155). *Staphylococcus epidermidis* produces autolysin E in order to allow it to bind to bare surfaces (159). These factors could potentially be employed to increase the rate in which biofilm formation is initiated. The molecules responsible for quorum sensing have been identified in a number of species including *E. coli,* but the exact information that is sent by these molecules is yet to be determined (160). The concentration of the auto-inducer must reach a certain threshold before the cells alter their gene regulation (161), with the production of EPS being a direct result of the change in gene regulation following the detection of threshold levels of auto-inducers. The biofilm is believed to consist of 75-90% extracellular polymeric substances (EPS) and only 10-25% organisms although the specific makeup of this is dependent on environmental conditions (161). This demonstrates the importance of EPS in order to create a developed biofilm. There are a number of factors, which have been identified as important within biofilms formed by *E. coli* such as colonic acid and β-1,6-GlcNac polymer (162). The conductivity of the EPS is not very easily analysed, as there is a wide variety of compounds that are used to make it up and which can vary under different environmental conditions (163). The composition of EPS from a mixed bacterial culture studied within wastewater was shown to be mostly protein, then polysaccharide and finally DNA (163). However, when more complex organic substrates were contained within the wastewater, the protein levels decreased and DNA became the predominant factor in the EPS (163,164).

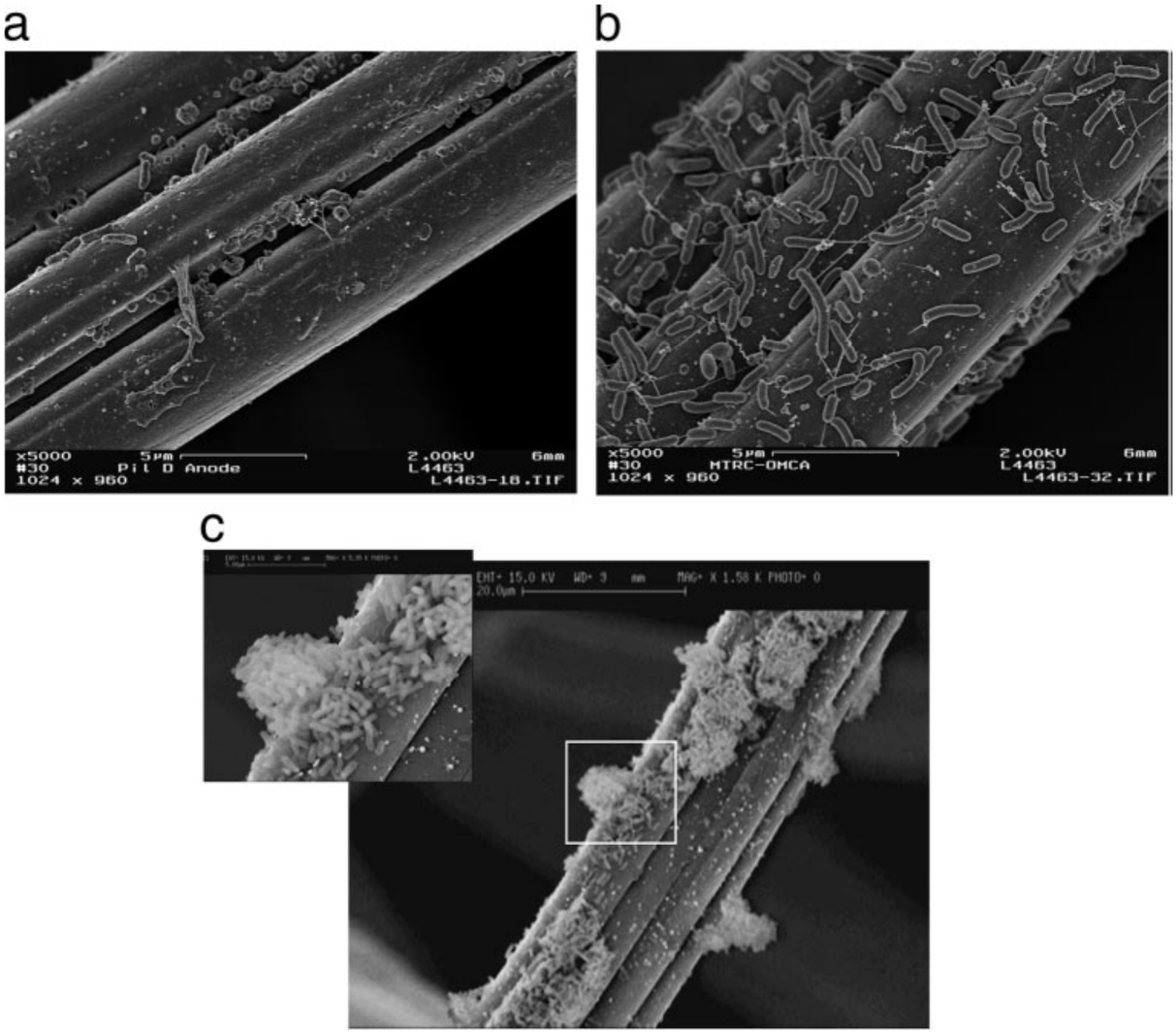

Figure 2.12 – SEM images of wild type S. oneidensis MR-1 and mutants. A) ΔpilD mutant B) ΔomcA/ΔmtrC mutant C) Wild type MR-1 (reproduced from Bretschger et al. (109))

Beloin & Ghigo (162) provide an analysis of regulatory genes within bacterial species looking for possible genetic factors that are activated under different environmental conditions in a biofilm. Table 2.6 presents a list of regulatory genes within biofilms and describes the role that each of them play in their host. There are a number of factors listed that are shown to repress the formation of a biofilm such as *crp, csrAB* and *hns*. These are unlikely to be the only genes involved in these actions, but the removal of them may increase biofilm formation. Production of the opposite effect, i.e. increasing the biofilm formation, could possibly be achieved through the overexpression of genes

such as *barA* and *uvrY*. The analysis of transcriptome studies of biofilm formation, has shown that a high number of stress related genes are expressed when biofilms are undergoing development (165–167).

Table 2.6 – Presents regulatory genes and their role in biofilm development (Modified from Beloin & Ghigo,* (162)*)

Regulatory gene (s)	**Bacterial species**	**Function in biofilm formation**
Gram-negative bacteria		
barA/uvrY	*E. coli*	Activates biofilm formation
cpxRA	*E. coli*	Senses surface perturbation and required for optimal cell-to-cell interactions
crp	*E. coli*	Represses biofilm formation (catabolite repression)
csrAB	*E. coli*	Represses biofilm formation and activates detachment
hns	*E. coli*	Reduces adhesion in anoxic conditions
ompR/envZ	*E. coli*	Increases attachment via curli and cellulose gene activation
rcsB-yojN=rscC	*E. coli*	Activates biofilm formation via remodelling of cell surface composition
rpoS	*E. coli*	Reduces or increases depth of the biofilm
	P. aeruginosa	Reduces depth of the biofilm
crc	*P. aeruginosa*	Required for normal biofilm development (activation of type IV motility)
gacAS	*P. aeruginosa*	Required for microcolonies formation
mvaT	*P. aeruginosa*	Reduces adhesion to abiotic surfaces via *cup* gene repression
rpoN	*P. aeruginosa*	Role in initial adhesion and biofilm architecture

	V. fisheri	Role in biofilm architecture
Gram-positive bacteria		
abrB	*B. subtilis*	Represses biofilm formation
ccpA	*B. subtilis*	Reduces depth of the biofilm (catabolite repression)
	S. mutans	Necessary for full biofilm maturation
spo0A	*B. subtilis*	Required for mature biofilm development (represses *abrB*)
spo0H	*B. subtilis*	Required for mature biofilm development
artRS	*S. aureus*	Reduces primary adherence to polystyrene
rbf	*S. aureus*	Required for mature biofilm formation of abiotic surfaces
SarA	*S. aureus*	Activates biofilm formation via PIA/PNAG activation
SigmaB	*S. epidermidis*	Activates biofilm formation
bfrAB	*S. gordonii*	Activates PVC and saliva-coated hydroxyapatite biofilm formation
hk11/rr11	*S. mutans*	Role in biofilm architecture
brpA	*S. mutans*	Required for mature biofilm formation on abiotic surfaces

All of these factors discussed are important in the development of a biofilm to allow for efficient electron transfer in a high power density MFC.

2.1.8 Constructing electrogenic activity in a non electrogenic strain

In order to create a fully electrogenic organism capable of completely oxidising a wide range of substrates to CO_2, efficiently transferring these to the anode, whilst still producing a high power output, will require the use of a wide variety of techniques. This includes the use of synthetic biology but will also necessitate the use of techniques such as metabolic engineering.

Alfonta (128) described the possible methods that could be applied in order to create an electrogenic organism, although some methods appear less feasible than others whilst also appearing to disregard other possibly simpler methods. The use of methods such as directed evolution of redox enzymes present within the non electrogenic strain such as *E. coli* seems like a potentially lengthy procedure due to the lack of redox proteins present within the periplasm and outer membrane. The only potential redox protein present within the inner membrane of *E. coli* is *NapC* which is capable of reducing soluble Fe (III) but at a third of the rate seen by its homologues *CymA* from *S. oneidensis* MR-1 (107). This idea of directed evolution on pathway components from an already electrogenic organism could allow it to be better suited to the new environment within a host organism such as *E. coli* and also provide better affinity for the anode. The use of random mutagenesis on outer membrane proteins and those associated with the pathway through the use of techniques such as error prone PCR and high throughput analysis, could allow for increased transfer rate through greater binding with the target TEA.

The use of gold coated bacteria to provide higher transfer efficiency stated in the discussed paper (128) is the same as coating the electrodes in platinum. These will both increase productivity but come at a significant cost, especially when considered for up scaling the systems. There are methods to allow the biosynthesis of gold nanoparticles that can coat the surface of the cells, but this appears an undesirable method due to the associated costs.

A further method for developing an increasingly electrogenic cell line has been proposed through the use of bacterial surface display of redox proteins. A promising method for doing this is through the attachment of a signal peptide recognised by the host cell to a heterologously expressed protein. An example is the AIDA-I based autodisplay system that allows more than 10^5 recombinant proteins to be transported to the outer membrane of the cell where they could allow electron transfer to an anode (168). This method is illustrated in Figure 2.13 and could possibly be used to export a redox protein to the membrane to oxidise substrates.

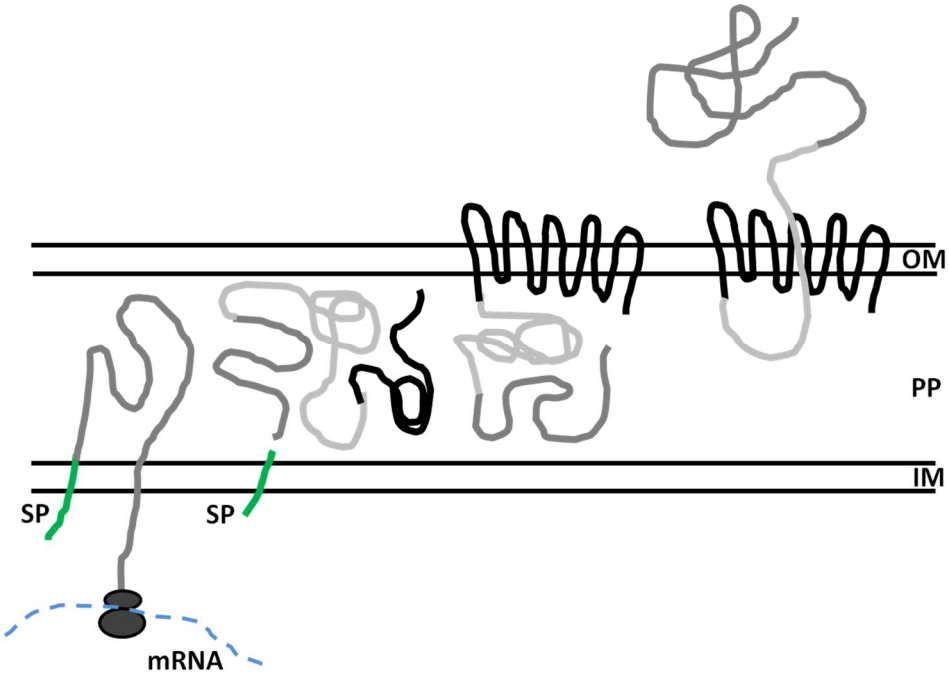

Figure 2.13 - AIDA-I based autodisplay system showing the transport of the heterologously expressed protein through the cell membrane. Dark Grey is recombinant protein, black is native membrane protein, light grey is peptide linker sequence. OM – Outer membrane. PP – Periplasm. IM – Inner membrane. SP – Signal peptide.

A similar system has already been applied for use within MFCs where a glucose oxidase enzyme was expressed on the outer membrane of *Saccharomyces cerevisiae* to increase the power output (169). The noted increase in this case was only from an open circuit value of 700 mV to 884 mV in the modified strain within a setup that also made heavy use of added mediators. This method also seems relatively unfeasible as the electrons released are not being directed towards the anode in anyway. A more practical method for increasing the power output could instead be to express a greater number of outer membrane cytochromes in a cell to allow it to transport its electrons directly to the anode. The overexpression of these outer membrane cytochromes has however been demonstrated to be a delicate balance between cellular fitness and the

correct expression and localisation of functional *c*-type cytochromes in order to obtain the greatest power output (124).

Developments in recent years have shown that the transfer of exoelectrogenic activity to an organism without this capability, can be achieved through the introduction of the functional Mtr pathway from *Shewanella oneidensis* MR-1 alongside upregulated native cytochrome maturation proteins (124,125). The first study to conclusively demonstrate the ability of *E. coli* to be able to produce exoelectrogenic activity was Jensen et al (125). The expression of MtrA, B and C, expressed functionally and correctly localised, allowed for the reduction of insoluble iron particles residing outside the cell.

The second, and perhaps more relevant study, was the demonstrated interaction of a genetically modified *E. coli* strain with an electrode within a MFC (124). This system again made use of the same section of the *Shewanella* Mtr pathway alongside overexpressed cytochrome maturation genes. In this case, however, the experimentalists strove to optimise the system through the use of a synthetic biology styled promoter screening system. The overexpression of the outer membrane Mtr cytochromes was demonstrated to be a delicate balance between cellular fitness and the correct expression and localisation of functional *c*-type cytochromes in order to obtain the greatest power output.

2.1.9 – Strain activation

There is a method for increasing the electrogenic activity of a microbial strain, without requiring any genetic or metabolic modifications. This technique makes use of the strict anaerobic environment seen within the anode chamber of an MFC. Due to the lack of TEA seen in the anode of an MFC, the bacteria must be able to make use of the carbon electrode as the TEA. As all organisms require a TEA of some sort, the bacteria that are best able to transfer their electrons to the anode will be most likely to survive there.

The first example of this can be seen in the development of an electrogenic *E. coli* strain through the use of this technique. The bacteria were grown in an operating MFC

under strict anaerobic conditions until the voltage had decreased to below 10% of that seen initially. A sample of these cells were then grown anaerobically in fresh media and then re-inserted into the MFC for further development (170). This provides the opportunity to develop an electrogenic organism that is capable of metabolising a wide range of compounds that many DMRB are unable to do. An example can be seen with the development of an electrogenic strain of the highly metabolically versatile purple photosynthetic *Rhodopseudomonas* species (171). This could well be an important part in the development of MFCs as the ability to degrade a wide array of compounds is one of the methods that allows for the higher power densities achieved by mixed cultures.

2.1.10 – Metabolic engineering

In order to be able to develop a cell strain capable of fully committing to the required need, the use of synthetic biology except in the case of simply building from scratch (100) is not sufficient (172). There must also be the use of metabolic engineering to allow for metabolic pathways to be upregulated, enhanced or even re-designed to provide the best opportunity for efficient electron transfer where it is required (172). In this case, this would be the transfer of electrons from the complete degradation of organic compounds in the cytoplasm, through the periplasm and exported through the outer membrane. As molecular and synthetic biology consider using the best individual components to make up an organism, metabolic engineering and systems biology consider the organism as a whole and how these components interact (172–174). This can then be used to determine how the energy can be channelled in the desired direction instead of it being used for the formation of undesired compounds. The first defined example of metabolic engineering can be seen with the use of glutamate dehydrogenase from *E. coli* to replace glutamate synthase in *Methylophilus methylotrophus* and allow for greater conversion efficiency of methanol into cellular carbon (175). The researchers identified the limiting junction (branching point or node) within the pathway and acknowledged that there was an alternative to this method which would allow for greater yields. In order to reduce the amount of time taken for

a suitable modification to be deciphered, the type of alteration required must be known (174).

Uses of metabolic engineering can be directly applied to microbial strains that are to be adapted for high efficiency within an MFC. This is expressed within MFC results as the coulombic efficiency of an organism, and refers to the energy percentage transferred to the anode from the oxidation of a certain organic compound. As pure, relatively simple substrates such as acetate and lactate require the use of commonly expressed enzymes for their oxidation, there is a higher coulombic efficiency achieved from these compared to using wastewater. This is due to the fact that wastewater contains a wide variety of organic compounds, which will be of a more complex nature than acetate and lactate and therefore require the production of a broad range of enzymes for their degradation. The expression of these enzymes comes at a price and means that a proportion of the electrons produced from the oxidation of substrates will be siphoned into this process. Cameron & Tong (176) discussed extending the range of substrates that an organism can metabolise whilst also elaborating on the modification of the cells catabolic activities to help degrade toxic compounds.

There are also inherent control mechanisms within biological systems that ensure growth within the cells is balanced. This prevents the transfer of all the energy through a certain pathway that could be detrimental to the organism and prevent the cells from developing in their natural environment. The resistance of these pathways against a change in the energy flux is described as its metabolic rigidity (174). Within an MFC, the cells are under artificial conditions that will be different to their natural environment. The cells will therefore not require some of the functions coded for in its genome that may only limit the rate in which the cells are able to release electrons for transfer. An example of reduced genome organisms that provide a more stable cell line can be seen in the strains produced by companies such as Scarab Genomics. Scarab Genomics have developed rationally designed *E. coli* genomes that take into account the genomic code for a variety of *E. coli* strains to determine the core genome common to all. The K-12 genome is 4.6 Mb (177) but the core genome of *E. coli*

continues to reduce as more genomes are sequenced (178). This has allowed Scarab genomics to remove over 15% of the *E. coli* genome, which includes non-essential genes, potential pathogenicity genes and many K-islands (179). Although 87.8% of the genome consists of protein coding genes and 11% regulatory functions, there are claims that this reduced genome provides substantial advantages over common *E. coli* strains (180). These include robust cell growth in minimal media, increased transformation efficiency and increased plasmid stability. Through continued development, they have managed to reduce the genome of the parental strain K-12 MG1655 genome of 4.7 Mb to 3.9 Mb in strain MDS42 and further down to 3.2 Mb in MDS73 (179).

It is vital within the metabolic engineering of organisms that all the branch points within a metabolic network are identified to determine where the energy flow may be directed and will therefore also provide an idea of how to redirect it. This allows the determination of the various desired pathways that may occur within a cell and also those that may produce undesired side products as shown in Figure 2.14. The degradation pathway for the oxidation of organic compounds can vary depending on the environmental conditions the cells are under and also the substrate conditions. As certain products will provide a better energy output and an less complex catabolic pathway using common enzyme mechanisms, there is a tendency for the cells to move towards this pathway (181). Under varying conditions, the cells may however choose to produce different compounds and secondary metabolites (182) that will decrease power output and as this may occur within an MFC, the removal of one of these enzymes may allow for complete oxidation of compounds and increase the energy yield. An example of metabolic engineering methods outperforming synthetic biology techniques, can be seen in the development of a lycopene producing *E. coli* (183,184). The use of synthetic biology techniques to introduce a wide variety of foreign genes into *E. coli* resulted in a maximum lycopene production of 9000 ppm. This was dwarfed by the 18000 ppm obtained through metabolic engineering by characterising the metabolic landscape and removing competing pathways (172). In the branch example shown in Figure 2.14 the inhibition of the undesired enzyme will allow for a greater

yield of the desired product as long as the enzyme is capable of dealing with the increased substrate yield. There may therefore be a need to increase the expression of the enzyme, seek out a similar enzyme from another organism with increased activity or perform random or directed mutagenesis on the gene, in order to try and increase its activity (172).

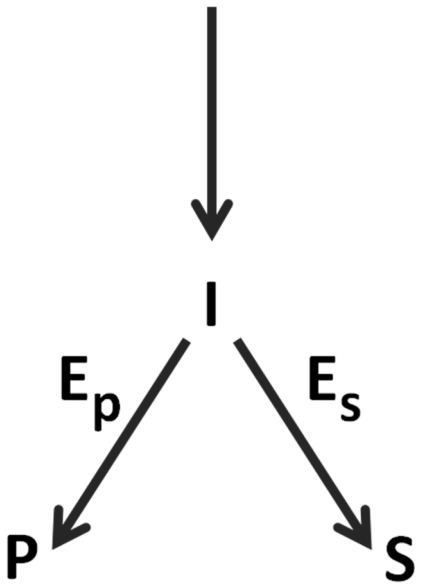

Figure 2.14 – Example of a branch point within a metabolic pathway. The substrate or intermediate (I) can either be converted to the desired product (P) or an undesired side product (S)

As discussed earlier, *Shewanella* species are unable to completely oxidise lactate to carbon dioxide and are instead only able to produce acetate from it (90). This means that in order to construct an electrogenic strain that is able to completely oxidise all the organic matter provided, and also produce a high rate of electron transfer, it will most likely require the acquisition of genes and pathways from a variety of organisms.

The use of synthetic biology makes this process much easier due to the ability to rapidly construct a wide variety of gene variants in different strains and then test the efficiency of each system using high throughput analysis (172). Although the

introduction of a heterologous pathway into the host organism may provide certain enzymes with increased specificity or activity, the pathway is unlikely to harmonise with the pathways already present within the organism. The best option may instead be to refine the current pathways within the host organism in order to streamline its operation and increase activity (172).The mapping of a cells metabolic landscape, which has been documented in several strains of *E. coli* as well as a number of *Shewanella, Geobacter* and *Rhodoferax* strains (185–187), is a vital starting point. This will then allow for the identification and sequential removal of competing enzymatic pathways (172). As analysed in the MR-1 mutants study conducted by Bretschger, et al. (109), the removal of some of the other terminal reductase genes within MR-1 increased its power output. This principle could, in theory also work effectively for *E. coli* as this has a number of terminal reductase genes. The ones that are involved in electron transfer under anaerobic conditions would be in direct competition with the *c*-type cytochromes transformed in from *S. oneidensis* MR-1. These enzymes can be seen in Table 2.7, where there are a number of nitrate reductases present. The removal of a number of these could allow for increased electron transfer to outer membrane MR-1 *c*-type cytochromes, although this may affect the delicate balance within the cell. The most obvious periplasmic nitrate reductases to remove would be the periplasmic reductases such as *NapC,* which would be in direct competition with the *CymA* inserted. This is due to the fact that *NapC* normally transfers electrons to a periplasmic nitrate reductase, in the presence of a *NapC-F* gene cluster in *E. coli.* Bretschger et al. (109) suggests that a deletion of *napB* in MR-1 leads to an increase in power output (188) making it a suitable candidate for removal as a competing pathway. Further studies looking into the proteins interacting with CymA and MtrA have shown transient protein interaction between most abundant periplasmic cytochromes STC, FccA and ScyA (189) to be highly important. These proteins may well have homologous partners in *E. coli* providing further targets for metabolic engineering.

Table 2.7 – Oxido – reductases of the respiratory chains of E. coli (Modified from Unden & Bongaerts* (190)*)

Enzyme	**Redox couple** **Pair** **E_m (V)**		**Genes**	**Map position (min)**	**Signal sequence subunit (AA residues)**
Primary dehydrogenases (DH):					
Formate DH_N	HCO_3/HCO_2	-0.43	*fdnGHI*	33.0	FdnG (1-33) (pot.)
Formate DH_O	HCO_3/HCO_2	-0.43	*fdoGHI*	88.03	FdoG (1-33) (pot.)
Formate hydrogen-lyase			*fdhF, hycA-H*	92.6; 61.35	n.s.
Hydrogenase 1	H^+/H_2	-0.42	*hyaABCDEF*	22.26	HyaA (1-45)
Hydrogenase 2	H^+/H_2	-0.42	*hybABCDEFG*	68.53	HybA (1-26/27)
NADH DH I	NAD^+/NADH	-0.32	*nuoA-N*	51.64	n.s.
NADH DH II	NAD^+/NADH	-0.32	*ndh*	25.17	n.s.
Glycerol-3-P DH_O	DHAP/Gly-3-P	-0.19	*glpD*	76.89	n.s.
Glycerol-3-P DH_N	DHAP/Gly-3-P	-0.19	*glpACB*	50.76	n.s.
Pyruvate oxidase	Acetate + CO_2/Pyruvate		*poxB*	19.42	n.s.
D-Lactate DH	Pyruvate/D-lactate	-0.19	*dld*	47.80	n.s.
L-Lactate DH	Pyruvate/L-lactate	-0.19	*lctD*	81.55	n.s.
D-amino acid DH	2-Oxoacid + NH_4/Amino acid		*dadA*	26.64	n.s.
Glucose dehydrogenase	Glucose/gluconate	-0.14	*gcd*	2.97	n.s.
Succinate DH	Fumarate/succinate	+0.03	*sdhCDAB*	16.37	n.s.
Terminal reductases:					

Quinol oxidase *bo*$_3$	O_2/H_2O	+0.82	*cyoABCDE*	9.78	CyoA (1-24) (pot.)
Quinol oxidase *bd*	O_2/H_2O	+0.82	*cydAB*	16.67	n.s.
Quinol oxidase III (Cyx)	O_2/H_2O	+0.82	*appBC (=cyxAB)*	22.42	n.s.
Nitrate reductase A	NO_3/NO_2	+0.42	*narGHJI*	27.53	n.s.
Nitrate reductase Z	NO_3/NO_2	+0.42	*narZYWV*	33.09	n.s.
Nitrate reductase, periplasmic	NO_3/NO_2	+0.42	*napFDAGHBC*	49.5	NapB (1-34)(pot.)
Nitrate reductase	NO_3/NH_4	+0.36	*nrfABCDEFG*	92.42	NrfA (1-26) NrfB (1-31) (pot.)
DMSO reductase	DMSO/DMS	+0.16	*dmsABC*	20.32	DmsA (1-16)
TMAO reductase	TMAO/TMA	+0.13	*torCAD*	21.61	TorA (1-39)
Fumarate reductase	Fumarate/succinate	+0.03	*frdABCD*	94.4	n.s.

If more reductase genes were to be removed, especially those expressing signal peptides that are therefore likely expressed in the membrane, the heterologously expressed proteins from MR-1 would need to be able to cope with the increased load of electrons. There may need to be modifications made in order to increase the transfer kinetics between these proteins and ensure efficient transfer to the anode.

In order for a host organism to be able to degrade a wider range of substrates to produce energy, it may only require the addition of a few enzymes from other organisms. These enzymes will then allow the previously indigestible compound to be converted to a product that is readily degraded by the host organism's inherent metabolic pathways (173).

The addition of individual foreign enzymes into a host organism is unlikely to provide the same activity as seen within the species of origin unless they are optimally expressed or structurally modified to allow them to adapt to the new environment (172). This infers that the development of metabolic engineering relies heavily upon systems biology for a whole cell understanding.

Systems biology is a combination of a wide variety of subject groups including biology, computer science and biophysics in order to determine interactions within a cell. This type of analysis views the cell from a holistic viewpoint instead of individual components. Knowing what each particular part is responsible for has largely been established but the interactions of these components within a system provides much more valuable information. Data collected detailing all the cellular transcripts (transcriptome), proteins (proteome) and also the cell metabolism (metabolome) under a given set of conditions are required for the most effective construction of these models (191). These data can then be used to construct computer models of cell types to help determine how cellular components will vary. These models can be applied for metabolic engineering to help predict how the modification of a particular protein or pathway will affect the overall balance within the cell.

2.1.11 Inverse metabolic engineering

This method was first termed by Bailey et al. (192) as ‘‘The elucidation of a metabolic engineering strategy by: first, identifying, constructing, or calculating a desired phenotype; second, determining the genetic or the particular environmental factors conferring that phenotype; and third, endowing that phenotype on another strain or organism by directed genetic or environmental manipulation.”. Inverse metabolic engineering (IME) was proposed by Bailey et al. (192), as a solution to the limited success by earlier metabolic engineering methods. In early IME methods, the identification of the genes responsible for the given phenotype firstly needs to be made through sequencing and 2D gel electrophoresis, but this was a lengthy procedure. The development of advanced sequencing technology that permits the elucidation of a genome sequence within a vastly reduced timeframe, use of DNA microarrays and expansion of –omics studies, has allowed for the rapid identification of cell components that are involved in desired phenotypes (193). Gill et al. (194) developed a method of deciphering the genetic components of the desired phenotype. This was done through digesting the genome into a variety of different sized fragments and inserting them into a plasmid thereby, creating a genomic library. Through the transformation of these plasmids into *E. coli* strains, they were able to identify the

ones expressing the desirable phenotype. Examination of the strains expressing the desired phenotype then allowed for further analysis of the genes required, and permitted opportunities for further genetic tuning for upregulation. This technique also has its downsides, one of them being that it can be hugely time consuming. The use of DNA microarray technology to analyse the difference in transcript levels of genes under varying conditions allows for the identification of the relevant genes, which can then be modified or transferred onto plasmids allowing increased expression rates (195). This methodology has been successfully used in other cases to increase the efficiency of the less well studied *Saccharomyces pastorianus* (196) and also to increase solvent tolerance (197). The use of IME has significant potential within MFC strain development, especially in order to be able to produce patentable opportunities following the isolation of electrogenically active strains following enhancement of sewage sludge using an MFC. The challenge of high throughput analysis of a large number of cell types could be accomplished through the use of one of the multiwell MFC devices that will be discussed following discussion of the issues surrounding codon optimisation.

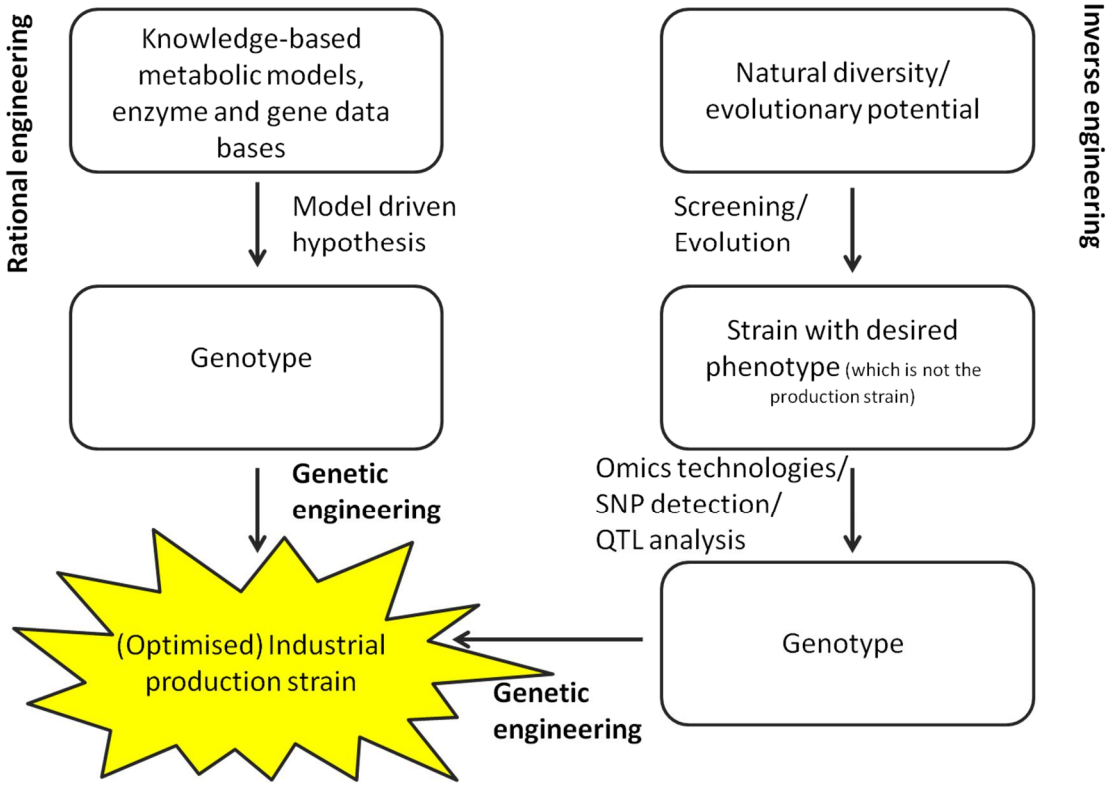

Figure 2.15 – Comparison between rational engineering and IME – (Modified from Saerens et al. (196))

Once the proteins responsible for the increase in activity have been identified through MS analysis they can then be codon optimised for the host organism to aid in the recombinant production of the desired proteins.

This literature review has illustrated that in order for the use of MFCs to be economically viable, replace the use of inefficient anaerobic digesters and create a water industry that can move closer to becoming self sufficient there is still a wide range of research required.

2.1.12 Codon optimisation

For the optimal expression of foreign proteins within *E. coli,* the protein will most likely need to have the codons altered to allow for proper interaction with the most common tRNA molecules present within the host. This can be done when planning the construction of a synthetic gene. This allows for the insertion and deletion of

restriction sites within the sequence to reduce the chance of digestion by the host cell and provides the researchers involved with greater cloning flexibility. The traditional method of codon optimising a sequence was to analyse the amino acid sequence of the protein and alter the codons in order to fit in with the most common codons seen within the host organism. Although this method of codon optimisation made sense, there was no experimental work conducted to support it. With an increase in the level of synthetic genes being produced, a study was conducted in order to test this in an attempt to further optimise heterologous protein production (198,199). It was noted from this study that expression of proteins within *E. coli*, was highly dependent on the codons used but not as classically predicted. Instead of using the most abundant codons seen in *E. coli* proteins, it was seen that the most favourable codons were those that were read by tRNAs that are highly charged (amino acetylated) during amino acid starvation (199). Through this information, the researchers were able to develop a model for the optimisation of the proteins and showed that differences in the codons used can result in up to a 40-fold difference in the amount of protein expressed (Welch et al. 2009).

2.1.13 Strain development

All of the above mentioned techniques require a high throughput analysis technique that is able to provide information about the developed strain and allow a rapid comparison between variants to determine those with the greatest current production potential. The use of colorimetric iron reduction assays is insufficient due to the inability to distinguish between the current production ability of a strain and merely its capability to transfer electrons to insoluble iron (122). A multiwell MFC as shown in Figures 2.16 and 2.17 would allow for the analysis of a large number of strains in a much quicker time than capable using a single twin chamber MFC setup**.** This is, however dependent on the analysis wanting to be undertaken, with it realistically being focussed on short term analysis.

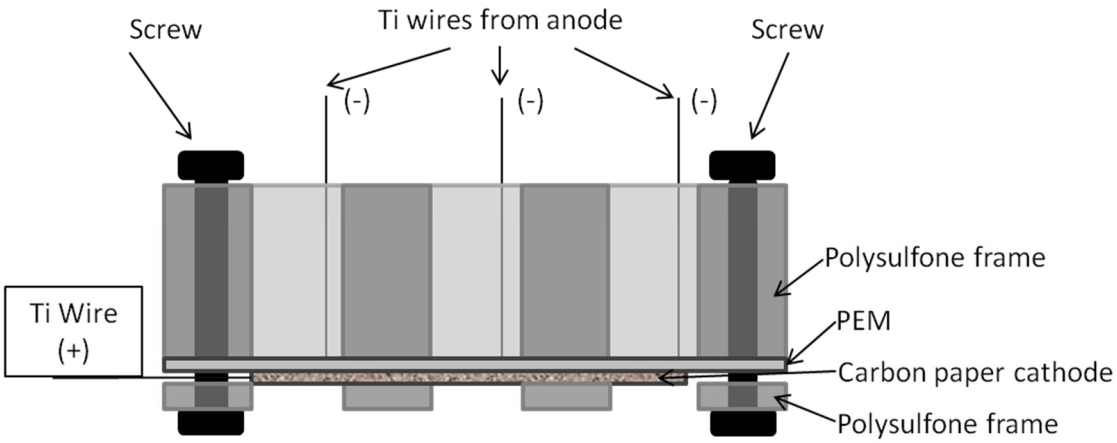

Figure 2.16– Provides an example of a simple mutliwell MFC – here shown with 9 separate compartments. This provides a graphical, cross sectional illustration of the multiwell MFC.

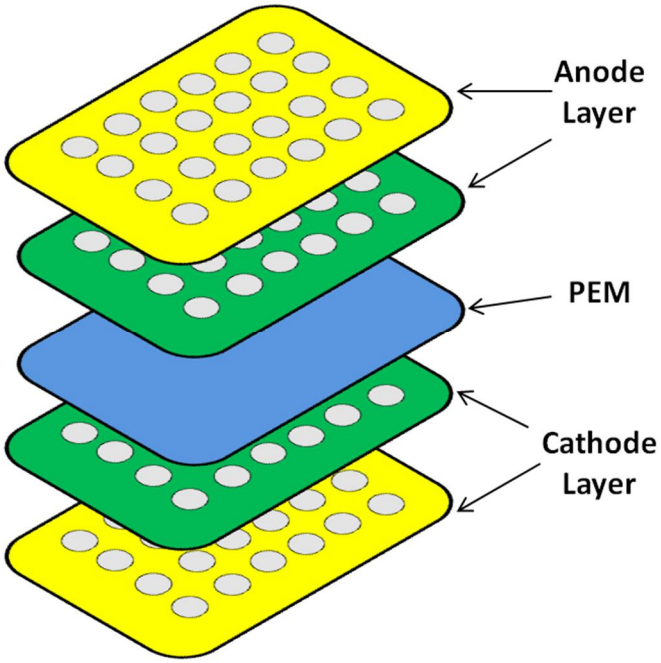

Figure 2.17 - A further example of multiwell chamber MFC that allows for the simultaneous analysis of 24 different strains.

The analysis of strains using such minute volumes of cells would require multiple replicates due to the chance of false results. As the strain being tested would need to be grown within a separate container beforehand, this allows for the development of

subpopulations within the culture (200). This refers to the fact that although the cells may all be genetically identical, there is often a wide degree of heterogeneity seen between the phenotypes in a culture (200). Using small volumes may result in the acquisition of one abnormal phenotype. The only real method of rectifying this is to ensure that the culture is fully mixed before use, to allow for homogeneity and also carry out multiple replicates.

2.1.14 Proteomic analysis

Following the introduction of foreign genes into a host organism, they and the proteins they express will need to be identified. This can be done in a number of ways such as sodium dodecyl sulphate polyacrylamide gel electrophoresis (SDS PAGE), which allows for the proteins to be identified according to their molecular weight (201). The use of gel based analysis for the identification of proteins has largely been superseded due to the developments in mass spectrometric analysis. This latter type of analysis is coupled with protein labelling techniques that allow for not only the identification but also accurate quantitation of the identified proteins (202,203). Examples of protein labelling techniques can be seen with stable isotope labelling by amino acids in cell culture (SILAC) (202), isotope-coded affinity tags (ICATs) and the more recently developed isobaric tag for relative and absolute quantitation (iTRAQ) (204).

The use of iTRAQ provides an advantage over other quantitative proteomic analysis methods such as ICAT, as it is possible to use either a 4- or 8-plex setup compared to ICAT's 2-plex (203). This allows the user to analyse a multitude of phenotypes simultaneously without having to do numerous 2-plex analysis, where the data could be compiled at a later date. The use of multiple 2-plex analysis can introduce variance into the results due to the differential treatment of the samples. Although all the samples used in iTRAQ are combined before analysis, the quantitation of individual peptides, and the relevant sample group they were derived from, can be identified due to the reporter ions released (205). The ability to quantify the regulation in protein levels is incredibly useful within biological studies, providing a powerful insight into the workings of the cells under different conditions (205).

2.1.15 Conclusions

The developments within the field over the course of this study are significant, with the major developments with the closest relevance to this study being surmised by a few choice papers:

The work carried out by the Caroline Ajo-Franklin's group within the University of California, Berkeley has produced two papers (124,125) that are in direct competition with the work that has been carried out during the course of this project.

The first of the papers published by this research group, in many respects built upon the work by Pitts et al (105) and Donald et al (120). The work carried out by Pitts et al was the first known use of heterologously expressed *c*-type cytochromes within *E. coli.* During this study, they demonstrated that it was possible for *E. coli* to reduce iron, even though in this case it was in its soluble form as Fe (III) citrate. Further studies have shown that the native *E. coli* protein, NapC, that was believed to supply MtrA, when expressed in *E. coli,* was also capable of reducing soluble Fe (III) in the absence of heterologous MtrA(107).

The work carried out by Donald et al (120) was a further addition to this thread of experiments whereby an outer membrane *c*-type cytochrome in the form of OmcA from *S. oneidensis* MR-1 was expressed in a B-type *E. coli* strain. This work showed that the protein was both functional and correctly localised, and capable of reducing insoluble Fe (III).

Work within this area was subsequently carried out by the Ajo-Franklin group in the form of the paper by Jensen et al (125). This paper built on the work done by Donald et al and Pitts et al, although Jensen et al used a larger, "more complete" extracellular electron transfer pathway comprising of MtrA, B and C. The experiments further confirmed the capability of utilising *E. coli* as a DMRB with the addition of minimal genetic modifications to allow it to reduce insoluble iron. The study also highlighted the fact (through knocking out native NapC) that there are multiple inner membrane proteins in *E. coli* that are able to interact with the quinone pool and donate electrons to the recombinant Mtr pathway.

The second paper in this thread (124) produced by the Ajo-Franklin group was a further extension of the work carried out in the last paper. Although there is no direct link between insoluble metal reduction (especially iron) and current generation within a BES, these two capabilities are still relatively suggestive that an organism that can do one, can do the other. In order for extracellular electron transfer to occur within *S. oneidensis* MR-1, it relies upon the transcript being copied from the genome, component parts of the Mtr pathway (namely MtrCAB being produced), proper expression of the cytochrome maturation gene system within the membrane, localisation of the haem groups within the *c*-type cytochromes and the correct folding, localisation and ratios of the Mtr proteins. This is a delicate balance between a large number of elements within the complexity of the whole cell, made even harder due to the fact that the vast majority of the work is done in the membrane. Trying to replicate this activity artificially through a recombinant DNA expression system has numerous potential complications due to the high level of complexity in the system.

The recombinant extracellular electron transport system is coded with the *sec* signal peptide attached to ensure localisation towards the membrane along with the essential CXXCH sequence (206) to allow for the apocytochromes to interact with the cytochrome maturation protein machinery (124). There is a limit to the amount of protein that the sec secretion pathway is able to deal with before being overloaded, resulting in a proportion of the proteins remaining without haem groups. Relying upon high level expression systems such as T7, where huge transcript levels are being produced and protein translated, resulted in the cell being unable to cope. This appeared to show a massive metabolic burden upon the cell, potentially with the sec system unable to cope with the huge amount of protein trying to be transferred through it and the Ccm proteins being overloaded. Through the creation of a promoter library, the group was able to test a large number of tuning permutations to help determine the one that would yield the highest number of functional *c*-type cytochromes, but also the greatest current density.

Previous work carried out has demonstrated that the overexpression of membrane proteins within *E. coli* leads to the formation of aggregates within the cytoplasm alongside the required chaperones and precursors (207). All of this resulted in low level accumulation of the proteins within the membrane compared to overexpressed soluble proteins. This is possibly expectedly due to the saturation of the translocation machinery (207).

During this thesis, there was however no attempt at potentially alleviating this issue of overexpressed membrane proteins through the upregulation of the translocation machinery. This would indeed have added another level of complexity and depending on the design of experiments, may have resulted in a far greater number of genetic permutations from promoter set tuning, but may have yielded some interesting results with greater current densities. This assumes that the translocation machinery is the limiting factor and there may well be other, quicker and better ways of increasing yields.

With all this being said, this literature review has identified significant areas of potential development for the construction of a fully electrogenic *E. coli*. The areas that would need to be addressed primarily would be the transfer of *c*-type cytochromes such as *CymA* (knockout *NapC), MtrA, MtrB, MtrC* and *OmcA* in an attempt to create a functional high level transfer of electrons to the anode. Increasing the biofilm forming capacity of *E. coli*, to allow for greater colonisation of the anode should then hopefully increase this capacity further. The next steps would require a more thorough metabolic engineering strategy and analysis of activity changes, following the rational modification or removal of cell proteins and pathways. The removal of genes encoding proteins responsible for the reduction of other terminal electron acceptors such as nitrate and sulphur, could allow for greater electron transfer to the anode reducing pathway as seen in *S. oneidensis* MR-1.

Chapter 3: Materials and Methods

3.1 Bioinformatic analysis

As detailed in chapter 2, analysis of the literature revealed that the genes encoding *c*-type cytochromes believed to be responsible for electrogenic activity in *S. oneidensis* MR-1 were shown to be located on a single gene cluster (108).

In order to be able to clone the electrogenic gene cluster, a bioinformatic analysis of the genes had to be carried out. This was done in order to determine the feasibility of amplifying the fragment from the *Shewanella* genome, ligating into a suitable plasmid and then expressing the proteins within a compatible *E. coli* strain.

The first step for this was to determine the sequence of the gene cluster including all spacer regions which was collected from NCBI (http://www.ncbi.nlm.nih.gov/). As the entire gene cluster amounted to over 13 kb and there may well be redundancy within the genome, it was decided that it would be advantageous to try the simultaneous production of several plasmids using different fragments of the cluster. Following consideration of the literature it was decided that the minimum gene cluster (Fragment 1) should consist of the genes from *OmcA* to *MtrB* since this would contain the outer membrane cytochrome *OmcA* and the periplasmic cytochrome *MtrA* that had already demonstrated functional heterologous expression in *E. coli* strains (105,120) (Figure 3.1). This also provided the cytochrome *MtrB* that has been stated to be required for proper incorporation of *OmcA* and *MtrC* into the outer membrane of *Shewanella putrefaciens* (112). This fragment was designed in consideration of the fact that the full gene cluster may well be very difficult to amplify in a single PCR reaction. As this was roughly half of the gene cluster, it provided the option to potentially try and join this and a fragment containing MtrDEF together to make the full gene cluster following their individual amplification.

***Figure 3.1 – S. oneidensis MR-1 electrogenic gene cluster (modified from Fredrickson et al* (108))**

The overall fragment sizes were as follows:

OmcA, *MtrC, MtrA and MtrB* – 7,728 bp

MtrC, MtrA and MtrB – 5,192 bp

OmcA, MtrA and MtrB – 5,713 bp

MtrD, E, F, OmcA, MtrC, A, B – 13,003 bp

Several bioinformatic tools were used to try and determine more about the proteins that were to be expressed:

3.1.1 Signal P

This program (http://www.cbs.dtu.dk/services/SignalP/) allowed for the identification of predicted signal peptides within the proteins that would show whether they would be transported to the outer membrane. Inserting the amino acid sequence of the protein in FASTA format into the program provided details of the location and length of the signal protein. As all of the proteins being considered were thought to reside in the membrane of *S. oneidensis* MR-1, they were all expected to contain signal peptides.

3.1.2 TMHMM

This tool (http://www.cbs.dtu.dk/services/TMHMM/) provided an opportunity to determine the location of predicted transmembrane regions within the protein. This would show whether the protein was thought to reside in the membrane of the cell.

3.1.3 Webcutter

Inserting the nucleotide sequence of the gene into webcutter 2.0 (http://rna.lundberg.gu.se/cutter2/) and NEBcutter 2.0 (http://tools.neb.com/NEBcutter2/) allowed for the identification of all the restriction sites that cut the sequence and provided the details of where these sites were. This allowed restriction sites that were present within the MCS of the pACYCDuet-1 vector to be chosen that did not cut the sequence of the desired fragment. This allowed for insertion of the fragment into the vector.

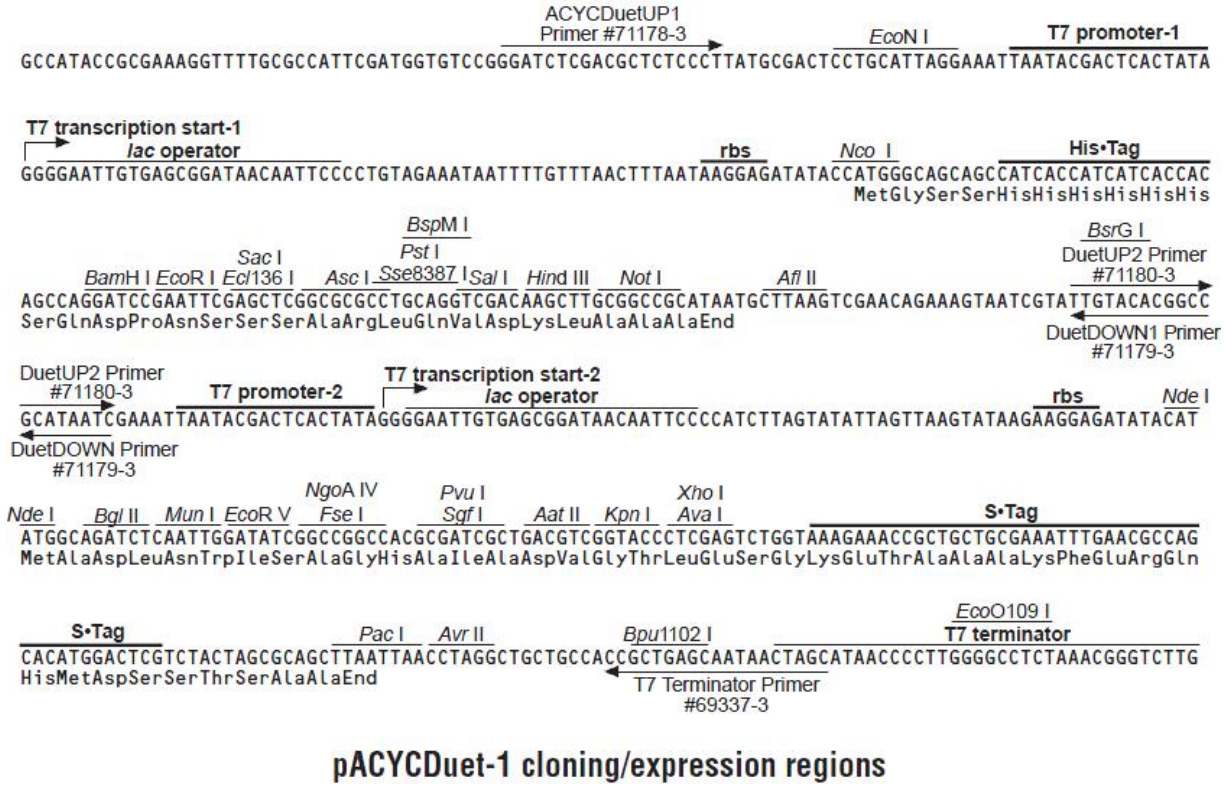

pACYCDuet-1 cloning/expression regions

Figure 3.2 – Multiple cloning sites within pACYCDuet-1

3.1.4 Molecular weight/pI

The molecular weight and pI of the proteins were predicted by inserting the amino acid of the protein into the ExPASY compute mW/pI tool (http://expasy.org/tools/pi_tool.html).

3.1.5 Primer design

Primer design was carried out using the program SnapGene (GSL biotech LLC, IL,USA). Inserting the nucleotide sequence of the gene into the program allowed for the design of primers for PCR that would allow the desired fragment to be amplified. After the primers had been designed, they then had the additional restriction sites added to the 3' end, to allow for insertion of the fragments into the plasmid. Primers were synthesised by Invitrogen (Paisley, UK).

3.1.6 – Theoretical plasmid construction

Theoretical construction of plasmids for identification of restriction sites, details of origins of replication, resistance cassettes and selected ORFs were carried out using SnapGene (Biotech LLC – Chicago, IL, USA).

3.2 Molecular biology

3.2.1 Sterilisation and aseptic technique

Unless stated otherwise, all solutions and apparatus were sterilised by autoclaving at 121 °C, with a pressure of 1.05 bar for 20 min. The benches were regularly washed down with 1% Virkon, followed by 70% ethanol. A blue flame Bunsen was kept on throughout experiments where contamination was an issue. Lab coat, goggles and gloves were worn in the lab at all times to ensure that health and safety rules were adhered to, and therefore reduced the risk of injury from chemicals.

3.2.2 Preparation of genomic DNA

For amplification of Mtr genes to occur the genomic DNA firstly needed to be extracted. This came from the DMRB organism *S. oneidensis* MR-1. Before this amplification could occur the genomic DNA needed to be prepared to allow for Polymerase Chain Reactions (PCR). Frozen aliquots of spun down cell cultures that had the supernatant removed were used to extract the genomic DNA from. The protocol for this was followed exactly as stated in the Qiagen DNeasy® Blood and tissue Handbook (July 2006 edition). The only step that was modified slightly was after the

addition of the proteinase K, as the protocol only states to leave the sample at 56°C for 30 min to allow the cells to lyse. The samples were instead left for roughly 6 h.

3.2.3 Agarose gel (1%w/v)

Agarose gels were made by using either 0.3g of agarose and 30 mL of 1 x TAE (recipe in appendix) (for small gels) or 1.2 g of agarose and 120 mL of 1 x TAE (for large gels) mixed together in a conical flask. The solution was heated up using a microwave making sure that it was removed as soon as the solution began to bubble. This was done until all the agarose had dissolved.

Once the solution had cooled down to around 60°C, 10 µL of ethidium bromide was added, mixed, then poured into the gel casting tray of the desired size with the corresponding comb in place. The gel was given around 20 min to allow it to set and could be seen to become slightly opaque on setting. The gel was then placed into the running position and was covered with 1 x TAE buffer. The comb was removed carefully and 5 µL of Hyperladder I DNA size standard (Bioline, London, UK) (10.0, 8.0, 6.0, 5.0, 4.0, 3.0, 2.5, 2.0, 1.5, 1.0, 0.8, 0.6, 0.4, 0.2 kb) was added to the first well of the gel and then the remaining samples were added. All gels were run at a constant current of 120 mA, with the small gels being run for 35 min and large gels being run for 60 min for PCR samples and 4 h when gel purification of a vector was being done.

After the gels had run sufficiently they were removed from their tanks and then viewed using a UVP GelDoc-It TS. The images of the gels were saved onto a memory stick, transferred to a computer and printed off.

3.2.4 Plasmid preparation of pACYC-Duet-1

Glycerol stocks of *E. coli* TOP10 carrying intact plasmids were frozen at -80°C. In order to make up a new batch of the plasmid vector a 2 µL aliquot of the glycerol stock was taken and put into 100 mL of Luria-Bertani (LB) media (appendix) in a 250 mL conical flask and then put into an incubator at 200 rpm at 37°C for 16 hrs. The solution was split into 2 separate 50 mL falcon tubes and the pellet was then used in a maxiprep (as described in section 3.2.18).

3.2.5 PCR

Polymerase chain reaction was used to amplify the DNA of the desired gene. This was done using Phusion Hot Start II High-Fidelity DNA Polymerase kit (provided by New England Biolabs, Hitchin, UK). The advantages of using this polymerase is that it is highly specific and also contains an Affibody ® molecule supposedly allowing for removal of any annealing temperature limitations.

An example PCR reaction set up is shown in Table 3.1:

Table 3.1 - PCR reagents

Reactant	Volume/µL	Final Concentration
5X HF Buffer for Phusion DNA polymerase*	10	1X
dNTPs (2mM each)	1	0.2mM (each)
PCR Grade Water	35	-
Sense (5') Primer /10µM	1	0.3µM
Anti-Sense (3') Primer/10µM	1	0.3µM
Template DNA	1 (1 in 10 dilution)	-
Phusion Hot Start II DNA Polymerase (2U/µL)	1	0.04U/µL
Total reaction volume	**50 µL**	**-**

* 1X Buffer provides 1.5 mM $MgCl_2$

This set up is designed to produce the best result from the enzyme. The buffer is used to maintain the optimum conditions for the enzymes throughout the procedure. The order in which the components were added was done to prevent any reactions occurring before all the components were present within the PCR grade 0.2 mL microcentrifuge tubes. The Phusion Hot Start enzyme was the last component added, as this ensured that the reaction did not begin prematurely. The 200 µL microcentrifuge tubes that the samples were loaded in were spun down quickly before being put into the PCR thermocycler so that the components were properly mixed.

The annealing temperatures that had been determined were used to set up the PCR program used for the amplification procedure. As there are 2 primers used in each

reaction and each one has a separate defined annealing temperature the higher of the 2 annealing temperatures was used in each case.

The PCR procedure was set up as shown in Table 3.2:

Table 3.2 – PCR set up

1. T = 98°C	2 min
2. T = 98°C	15 s
3. T = Calculated 1° Annealing Temperature	30 s
Ramping speed = 3.0	
Gradient across heating block = 10.0°C	
4. T = 72°C (1kb/30s)	
5. GO TO 2 – REPEAT 4	
6. T = 98°C	15 s
7. T = calculated 2° Annealing Temperature	30 s
8. T = 72°C (1kb/30s)	
9. GO TO 6 – REPEAT 29 TIMES	
10. T = 72°C	10 min
11. Hold 4°C	

3.2.6 PCR overlap

As the project developed, more advanced polymerase techniques were employed. One of these was the use of PCR overlap. This technique allows for the addition or removal of genetic sequences using PCR, followed by the removal of the initial template plasmid, yielding purely recombinant vector. This technique was employed for the construction of the SPA-tagged (208) Mtr vectors in chapter 6.

An example methodology, with the addition of a SPA-tag to pACYCOmcA is as follows, with full detailed description found in (209):

1. SPA-tag nucleotide sequence was identified within pJL148
2. Primers designed to amplify sequence using 30 bp on FP and RP.
3. Addition of nucleotides to the 5’ region of the FP to allow for 3’ reading into OmcA. This was designed to remove the stop codon of OmcA and allow for the 3’ attachment of the SPA-tag to OmcA.

4. Addition of nucleotides to the 5’ region of the RP to allow for reading into region downstream of the GOI. The gap between the FP and RP binding regions wants to ideally be roughly 50 bp.
5. Amplify the SPA-tag from pJL148 using a standard PCR protocol, taking into consideration primer annealing temperatures and allowing for sufficient extension time depending on polymerase used.
6. Purify the correct band (roughly 200bp) using gel purification.
7. Use the purified PCR product alongside desired template for modification (In this case pACYCOmcA) in a PCR reaction. The purified PCR product from step 6 acts as FP and RP to the desired template allowing for simultaneous introduction of additional genetic material (SPA-tag) and then amplification of the remaining plasmid. Use standard PCR procedure as described in section 3.2.5.
8. Add DpnI to the mixture following PCR amplification to selectively digest *dam* methylated template DNA. Leave at 37 °C for 2 hrs. This leaves only recombinant, modified plasmid in a nicked form.
9. Transform mixture into competent cloning strain such as DH5alpha and select based on original resistance of plasmid (Cm).
10. Purify plasmid from culture, PCR amplify for detection of correct insertion and sequence for full verification.
11. Plasmid is now ready for use and expression in desired strain.

3.2.7 PCR for recombination

An additional method of modifying either plasmid of chromosomal genetic sequences is through the use of recombination. In the method, a lambda red recombination method, widely popularised by Datsenko and Wanner (210) is described. The technique was originally specified as a deletion tool using a single PCR reaction but can be modified to allow for more complicated insertion events or with careful design, even simultaneous deletion and insertion.

An example of recombination used within this thesis was for the modification of pUC19 to replace the Ampicillin resistance cassette with that of the Chloramphenicol resistance cassette from pACYCDuet-1. This was done to help provide a 2 plasmid system of chromosomal insertion as described in chapter 6.

In order to be able to do this, PCR primers were designed to amplify the Chloramphenicol cassette from pACYCDuet-1 that would also be homologous to the region immediately upstream and downstream of the Ampicillin resistance cassette in pUC19. This would involve an initial amplification of the Chloramphenicol resistance cassette from pACYCDuet-1 and electroporation into a strain harbouring pUC19 and an induced pKD46 Kan.

An example is shown below:

1. Primers were designed to the Chloramphenicol cassette:

2 Primers

Primer	Length	Binding Sites		Tm
Duet Cm PCR FP	16-mer	729 .. 744	→	61°C
/sequence = ttacgccccgccctgc 75% GC				
Duet Cm PCR RP	31-mer	1358 .. 1388	←	60°C
/sequence = atggagaaaaaaatcactggatataccaccg 39% GC				

2. The region immediately upstream and downstream of the Ampicillin cassette was identified:

Upstream of Amp – aaaaggaagagt

Downstream of Amp – aagtatatatgagtaaacttggtctgacag

3. The sequences were combined to allow for the initial amplification of Cm from pACYCDuet-1 with extensions for insertion into pUC19:

Duet Cm lambda Amp FP – **aaaaggaagagt**ttacgccccgccctgc

Duet Cm lambda Amp both RP -

aagtatatatgagtaaacttggtctgacagatggagaaaaaaatcactggatataccaccg

Bold section is from Amp, as shown above. Underlined sequence is from Cm cassette.

4. PCR is setup as described in section 3.2.5
5. Recombination event is described in section 3.2.27

3.2.8 Restriction enzyme digest of vector and PCR products

The digestion of the vector depended upon which type of restriction endonuclease was being used to digest it. All restriction enzymes and buffers were purchased from New England Biolabs (Hitchin, UK) apart from multicore buffer, which was purchased from Promega (Southampton, UK).

The reaction was setup with the least reactive solutions first (i.e. 18.2 MΩ water), gradually building up to the most reactive (restriction enzymes). The solution was pulse spun in a micro centrifuge and then stored in a water bath at 37°C for at least 2 hrs. In order to prevent re-ligation of the cleaved vector fragment, 2µL of alkaline phosphatase was added to the solution to remove the terminal phosphate groups from the DNA strands. To inactivate the restriction enzymes and alkaline phosphatase, the temperature of the water bath was increased to 42°C for 10 mins and then stored in the freezer for later use.

Table 3.3 - Example AscI and NotI digest of pACYCDuet-1

Reactant	**Volume used**
18.2 MΩ/cm water	6 µL
10 x Buffer 4	17 µL
BSA (10mg/mL)	17 µL
Uncut pACYCDuet-1 (10 µg)	120 µL
*Asc*I enzyme (20U/µL)	5 µL
NotI enzyme (20U/µL)	5 µL
Total volume	**160 µL**

Restriction enzyme digest also needed to be carried out on PCR products but this was normally done following gel purification (as detailed in section 3.2.7) to remove any other DNA fragments that had been unintentionally amplified during PCR. Following gel purification the PCR products could then be digested as shown in Table 3.4.

Table 3.4 - Example PCR digest

Reactant	Volume used
18.2 MΩ/cm water	8 µL
10 x Multicore buffer	5 µL
BSA (10mg/mL)	5 µL
Purified PCR product	30 µL
AscI enzyme (20U/mL)	1 µL
NotI enzyme (20U/mL)	1 µL
Total volume	**50 µL**

3.2.9 Gel purification

Qiagen gel purification kits were used for all DNA purification following transfer through an agarose gel. The procedure used for this technique was as detailed in the manufacturer's instructions.

3.2.10 PCR cleanup – SURECLEAN

As gel purification often results in a large loss of DNA, this step is considered unnecessary for PCR products following enzymatic digestion and instead have the enzymes and unwanted DNA removed using a PCR cleanup procedure. The version was used in this thesis was Sureclean from Bioline (London, UK). The procedure use was as detailed in the manufacturers protocol

3.2.11 Ligation

Ligation reactions were set up in 3 different ways where the ratio of ligation to vector was altered. All the reactions contained 1 µL of T4 DNA ligase (purchased from Promega, Madison, WI, USA) and were made up to a total volume of 10 µL. The 3 different ratios used were:

1:3, 1:1 and a 3:1 ratio of vector to insert

The different amounts of vectors were calculated using the following calculation:

Length of insert (in kb) x ng of vector = ng of insert needed for a 1:1 ratio

Length of vector (in kb)

This was done using the ligation calculation tool on: http://www.insilico.uni-duesseldorf.de/Lig_Input.html

Table 3.5 - Example ligation

Reactant	Volume used
10 x Ligation Buffer	1 µL
Ligase enzyme (1U/mL)	1 µL
Purified PCR product	6 µL
Digested pACYC vector	1 µL
18.2 MΩ H_2O	1 µL
Total volume	**10 µL**

An example of the different ratio ligations is shown below with a 9895 bp insert and 4000 bp vector:

1:3 = 20 ng (1 µL) vector to 150 ng (6 µL) insert

1:1 = 20 ng (1 µL) vector to 50 ng (2 µL) insert

3:1 = 20 ng (1 µL) vector to 17 ng (1 µL) insert

The components were added in an order that ensured that the ligase enzyme was the last to enter the microcentrifuge tube. The tube was pulse spun down in a centrifuge to collect all the reactants in the bottom and then put into a PCR machine at 16°C for 16 h. After samples were removed from the PCR machine they could then be stored in the -20°C freezer ready for use in transformations into an *E. coli* cloning strain such as TOP10.

3.2.12 Preparation of chemically competent cells

The day before the competent cells were made, 100mM $CaCl_2.2H_20$ (147.02) (1.47g in 100 mL), 100mM $MgCl_2.6H_2O$ (201.31) (2.01g in 100 mL), 10 mL of sterilised 50%

glycerol, 80 x 1.5 mL sterilised microcentrifuge tubes were all sterilised. A 10 mL culture of the chosen *E. coli* strain/ LB /antibiotic was also setup overnight.

The next day, 1 mL LB was put aside for OD600 (zero) blank. 2 mL of the overnight culture was added to 200 mL LB/antibiotic in 500 mL flask and incubated for 1.5 hrs with OD_{600} readings being taken (every 15 mins) in a spectrophotometer. When the cells were at an OD_{600} of roughly 0.5 (not more than 1.0) the culture was put on ice for at least 10 mins with occasionally swirling. The 200 mL of cells were spun down in 4 red topped 50 mL falcon tubes at 4500rpm for 10 mins at 4°C. The supernatants were discarded and the pellets were very gently resuspend in 20 mL 100mM $MgCl_2$ each by swirling and then spun down again at 4500rpm for 10 mins at 4°C. The supernatant was again discarded and the first pellet (of 4) was very gently resuspend in 6 mL 100mM $CaCl_2$, by swirling and poured into the tube containing the second pellet (sterile conditions are essential). All pellets were resuspended in this manner until all 4 pellets were resuspended in 6 mL and the combined pellet was then put on ice for 1.5 hrs to become competent. 1.8 mL of sterile 50% glycerol was added to 6 mL cell "solution" and swirled very gently until the glycerol was mixed to homogeneity and cells were resuspended. 150 µL aliquots of the cells were taken and transferred into sterile, cooled (-20°C) 1.5 mL microcentrifuge tubes. The cells were then flash frozen or left in the -80°C to freeze. They were then stored at -80°C until needed.

3.2.13 Transformation into chemically competent *E. coli* TOP10, DH5α and BL21 (DE3)

The following protocol was used to transform ligated plasmids or control plasmid into competent *E. coli* cells. A 150 µL aliquot of competent cells was taken out of the -80°C freezer and stored on ice. A thawed ligation product or plasmid was then removed from the microcentrifuge tube and an aliquot was inserted into the correctly labelled tube containing the competent cells. The sample was left on ice for 30 min before being heat shocked at 42°C in a water bath for 90 s to allow the ligated vector or plasmid to be transformed into the cells through the disruption of the cell membrane. The cells were then put back onto ice for a few min before having 200 µL of LB added

to them and then stored at 37°C, 180 rpm for at least an hour to allow the cells to repair. Following the cells storage at 37°C, 180 rpm they were then plated out on LB agar plates containing the desired antibiotic (section 3.2.16) ensuring that strict aseptic technique was adhered to.

Table 3.6 - Transformation into TOP10

Reactant	Volume used
E. coli TOP10	150 µL
Ligation product	10 µL
LB	200 µL
Total volume	**360 µL**

3.2.14 - Preparation of electrocompetent cells

Electrocompetent cells provide another method of transferring DNA into bacteria. The day before making electrocompetent cells, 100 mL of MQ water, 50 mL of 10% glycerol, 100 mL of LB and ~100 1.5 mL microcentrifuge tubes were sterilised. Water and 10% glycerol was stored at 4°C. An overnight culture of the desired *E. coli*/LB/antibiotics was put up.

The next day, 1 mL of LB was put aside for an OD_{600} (zero) blank. 1 mL of the overnight culture was added to 100 mL of LB in a 250 mL flask and incubated at 37°C, 200 rpm (unless temperature sensitive plasmids were involved) for 1.5 hrs with OD_{600} readings then being taken every 15 mins in a spectrophotometer. When the OD_{600} reached roughly 0.5 (not more than 1.0) the culture was put on ice for at least 10 mins, with occasionally swirling. The 100 mL of cells were spun down cells in 2 red topped 50 mL falcon tubes at 4500rpm for 10 mins at 4^{o}C. The supernatants were discarded and the pellets resuspended and combined in 25 mL of ice cold MQ. The centrifugation, discarding of supernatant and resuspension in 25 mL of ice cold MQ was repeated twice more. The cells were spun down at 4500rpm for 10 mins at 4^{o}C and resuspend in 2 mL of ice cold 10 % glycerol. The cells were the split into 150 µL aliquots in each sterile microcentrifuge tube. The cells were then ready for electroporation or storage at -80°C for later use.

3.2.15 - Electroporation into electrocompetent cells

Electrocompetent cells were used throughout this thesis for recombination events as described in section 3.2.27. The following protocol details how this was done.

150 µL aliquot of electrocompetent cells was taken and no more than 10% DNA was added to it, followed by mixing and incubation on ice for 30 mins. Cells were added to 0.1 cm electroporation cuvettes and tapped to ensure removal of any bubbles. The cuvette containing the sample was then inserted into the electroporation holder attached to the Biorad gene pulser Xcell (Hercules, CA, USA). The pre-set *E. coli* protocol listed under bacteria was used with the following parameters; Exponential decay pulse type, pulse length – 25 ms, capacitance, 200 pF, for a 0.1 cm cuvette. Recommended sample volume is 20 µL but 150 µL was successfully used on numerous occasions. A time constant between 4.8 and 5.1 was preferable for successful transformations but this cannot be controlled.

Following electroporation, 1 mL of LB media was immediately added to the electroporation cuvette. The cells were gently mixed in the LB solution then transferred to a sterile 1.5 mL microcentrifuge tube. Unless temperature sensitive, the cells were transferred to a 37 °C incubator, 200 rpm for 1.5 hrs and then plated onto selective antibiotic agar plates.

3.2.16 Plating bacteria

Prior to plating, LB agar plates were surface dried by placing open face down at 65 °C for 10 min. A glass spreader was sterilised by immersion in 70 % (v/v) ethanol and the excess ethanol was removed by passing the spreader through a blue Bunsen flame. Once the spreader had cooled it could then be used to spread 50-200 mL of bacterial suspension evenly over the surface of the agar until the solution had adsorbed sufficiently into the agar.

The plates were then stored at 37°C for 16 h to allow the cells to grow.

The cultures that were present on the plates after they had been left in the incubator were regarded as containing the recombinant gene and were then grown in liquid

culture containing the desired antibiotic. If this was successful then the cells were ready to have minispin DNA extracted from them.

3.2.17 Minispin plasmid DNA purification protocol

The minispin DNA preparation technique provides a method for obtaining a very high purity plasmid DNA product. The procedure used for this was followed as detailed in the manufacturer's manual.

3.2.18 Maxiprep plasmid DNA purification protocol

The Qiagen Maxiprep kit provides a method to harvest a much greater yield of high quality plasmid than a minispin column. This procedure requires a much larger volume of culture to harvest the plasmid. The copy number of the plasmid determines the volume of the main prep culture. A low copy number plasmid will require between 200 and 500 mL of culture (ensure that media makes up a max of 2/5 of the available volume in flask) whereas a high copy number plasmid will require between 100 and 200 mL of culture. The protocol is as detailed.

10 mL overnight starter culture was grown up from a plate containing the desired plasmid. This was (unless temperature sensitive) kept at 37°C, 200 rpm for 16 hrs. A 1 in 100 dilution of overnight culture into LB media was done. The volume used depended on the plasmid to be harvested. The culture was kept at 37°C (unless temperature sensitive), 200 rpm for 16 hrs. The culture was spun down at 6000 rpm, 15 mins with the supernatant being discarded. The pellet was resuspended in 10 mL of buffer P1, containing lyseblue and RNase A. 10 mL of buffer P2 was then added and the sample was mixed by inverting 4-6 times. The sample was then left a room temperature for no longer than 5 mins. Due to the prior addition of lyseblue, the solution all turned blue. 10 mL of pre-chilled buffer P3 was then added and the solution was mixed by inversion again. The sample changed from blue to yellow (cell lysates) with white particulate matter (cellular debris, including cell membrane and proteins). Sample was then kept on ice for 20 mins. Sample was centrifuged at ≥20,000 x g for 30 mins at 4°C. Supernatant was immediately transferred to a fresh container. Cell debris, pelleted at the bottom of old container was discarded. Centrifugation was

carried out on the sample again. ≥20,000 x g for 15 mins at 4°C. Supernatant was immediately removed and kept, with any remaining pellet discarded. A Qiagen-tip 500 was equilibrated by applying 10 mL of buffer QBT to the top and the solution allowed to flow through by gravity. The retained supernatant was then added to the equilibrated column. Following binding of sample to the column, the flow through was discarded and the column was washed with 2 x 30 mL of buffer QC. The column was moved to a fresh container and the DNA was then eluted with 15 mL of buffer QF. DNA was precipitated by adding 10.5 mL of room temperature isopropanol to the eluted DNA. This was then mixed and centrifuged immediately at ≥15,000 x g for 30 mins at 4°C. The solution was then carefully decanted, ensuring the pellet was not disturbed. 5 mL of room temperature 70% ethanol was then added and the sample was centrifuged at ≥15,000 x g for 10 mins at 4°C. The solution was then decanted, ensuring the pellet was left undisturbed, any remaining supernatant was the aspirated and the sample was left to air dry for 10-15 mins. The DNA pellet was then resuspended in between 250 and 400 µL of 1 x TAE and the sample was stored at -20°C for later use.

3.2.19 DNA sequencing

All sequence verification was carried out at the University of Sheffield Medical School core genomic facilities. Data files were sent back as SEQ (notepad readable) and ABI format chromatogram file (FinchTV compatible), providing the option to look through a FASTA type format of the data or view the chromatogram for manual identification.

3.2.20 Protein extraction protocol

Based on T7 extraction protocol (TB125 T7 Tag Affinity Purification Kit) using Wash Buffer 10x (1.5 M NaCl and 1 M Tris-HCl pH 8.0) – i.e. no EDTA for Metalloproteins; 1.5 M NaCl, 1 M Tris-HCl, 10 mM EDTA, pH 8.0 for other proteins.

Protein extraction solutions

120 mL	1X Wash Buffer (150 mM NaCl, 100 mM Tris-HCl, 1 mM EDTA, pH 8.0) used for non-metalloproteins
25 mL	1X Elution Buffer with biotin (150 mM NaCl, 100mM Tris-HCl, 1 mM EDTA, 2 mM D-biotin, pH 8.0)

Additional components required:

- Ice
- 0.45 micron membrane syringe-end filters
- Glass beads, acid washed, 425-600 µm (G8772 Sigma Aldrich)

Prepare reagents:

10x Wash Buffer for metalloproteins - 1.5 M NaCl and 1 M Tris-HCl pH 8.0 (100 mL)

Take 60 mL of ddH_2O

Add 8.766 g of Sodium Chloride (NaCl MW 58.44)

Add 12.114 g Trizma (Tris(hydroxymethyl)aminomethane - $C_4H_{11}NO_3$ MW 121.14)

Adjust pH to 8.0 with HCl

Take up to 100 mL with ddH_2O

1x Wash Buffer for extracting insoluble proteins – 6 M Urea, 150 mM NaCl , 100 mM Tris-HCl, 1 mM EDTA, pH 8.0 (100 mL)

Take 30 mL of ddH_2O

Add 36.036 g of Urea (mW 60.60)

Add 0.8766 g of Sodium Chloride (NaCl mW 58.44)

Add 1.2114 g Trizma (Tris(hydroxymethyl)aminomethane - $C_4H_{11}NO_3$ mW 121.14)

Add 0.0292 g EDTA (mW 292.24)

Adjust pH to 8.0 with HCl

Take up to 100 mL with ddH_2O

1x Wash Buffer for Bind/Wash insoluble proteins – 2 M Urea, 150 mM NaCl , 100 mM Tris-HCl, 1 mM EDTA, pH 8.0 (100 mL)

Take 30 mL of ddH_2O

Add 12.012 g of Urea (mW 60.60)

Add 0.8766 g of Sodium Chloride (NaCl mW 58.44)

Add 1.2114 g Trizma (Tris(hydroxymethyl)aminomethane - $C_4H_{11}NO_3$ - mW 121.14)

Add 0.0292 g EDTA (mW 292.24)

Adjust pH to 8.0 with HCl

Take up to 100 mL with ddH_2O

1x Elution Buffer for with biotin for insoluble proteins – 2 M Urea, 150 mM NaCl, 100mM Tris-HCl, 1 mM EDTA, 2 mM D-biotin, pH 8.0 (100 mL)

Take 30 mL of ddH_2O

Add 12.012 g of Urea (mW 60.60)

Add 0.8766 g of Sodium Chloride (NaCl mW 58.44)

Add 1.2114 g Trizma [Tris(hydroxymethyl)aminomethane - $C_4H_{11}NO_3$ mW 121.14]

Add 0.0292 g EDTA (mW 292.24)

Add 0.0490 g D-biotin (mW 244.3)

Adjust pH to 8.0 with HCl

Take up to 100 mL with ddH_2O

3.2.20.1 Cell Extract Preparation – Soluble Proteins:

1. The extraction of metalloproteins was done (as must be) with 1 x wash buffer without EDTA with all other proteins suitable to be extracted with EDTA in 1 x wash buffer. Buffers were kept ice cold for cell resuspension.
2. Cells were harvested by centrifugation at 2800 RPM for 10 mins. The supernatant was decanted and the cell pellet allowed to drain as completely as possible. Cells were resuspended in 1-15 mL of ice-cold wash buffer (volume as required), depending if metalloprotein or not (check step 1).
3. Using 425-600 µM glass beads, the following steps were applied:
    a. The same weight of glass beads as to the volume of the cell pellet was added, i.e. 0.2 g for 0.2 mL.
    b. Sample was placed on a bead beater for 3x1 min, allowing for 5-10 sec rest between each 1 min to prevent overheating.
    c. Tubes were placed on ice for 5 mins to prevent overheating and step b was repeated again.

Tip: Check carefully for beads between the lid and the tube as this can cause leaks and result in sample loss.

4. Lysate was centrifuged at 21,000 x *g* for 30 min at 4°C to remove debris. Lysate was then stored at -20°C.
5. If stored, lysate was centrifuged at 13,000 RPM for 5 min at 4°C, to remove aggregates that may have formed during storage.

3.2.20.2 Cell Extract Preparation – Insoluble Proteins:

This procedure was used for the extraction of insoluble proteins. This was done on cell samples following the extraction of soluble proteins. The addition of 6M urea to the bind/wash buffer aided in the solubilisation of proteins. This following protocol details extraction of proteins starting from cell harvesting:

1. Cells were harvested by centrifugation at 2800 RPM for 10 mins. Supernatant was decanted and excess liquid removed by aspiration. Cell pellets were resuspended in 1-15 mL 1X Bind/Wash buffer that does not contain urea (volume as required).
2. Samples were vortexed to resuspend the pellet followed by the use of glass beads to shear DNA:
3. 425-600 µM glass beads were used with application of the following steps:
    a. The same weight of glass beads was added equal to the volume of the cell pellet, i.e. 0.2 g for 0.2 mL.
    b. Pellet was placed on a bead beater for 3x1 min, allowing for 5-10 sec rest between each 1 min to prevent overheating.
    c. Tubes were placed on ice for 5 mins to prevent overheating with step b being repeated again.
4. Samples were centrifuged at 20,000×*g* for 15 mins to collect the inclusion bodies and cellular debris while leaving other proteins in solution.
5. Supernatant was removed and the pellet was resuspended in same volume of 1X Bind/Wash buffer (without urea) used in step 1. Vortex was sometimes necessary to resuspend the pellet. Steps 3-5 were repeated.

6. Supernatant was removed from the final centrifugation and the pellet was resuspended in 1 mL of 1X Wash Buffer containing 6M urea. Sample was incubated on ice for 1 hour to completely dissolve the protein. Insoluble material was removed by centrifugation at 21,000 x *g* for 30 min at 4°C and the supernatant harvested as the insoluble fraction.

3.2.20.3 Protein extraction in specific relation to MFC iTRAQ

The following describes the method used for the collection of cells and protein extraction used within the iTRAQ detailed in chapter 5.

The electroactive biofilms in the MFCs were extracted into 40 mL phosphate buffered saline (PBS) and, taking into account the production of cells in the MFC effluent, their specific growth rate was calculated with methods as described in (211,212). The specific formula used was:

μ (h^{-1}) = production rate of cells in culture (cells h^{-1})/ biofilm population (total number of cells)

The M1 supply-rate to planktonic continuous-culture in the chemostat was subsequently adjusted so that the growth rate of these cultures would match the calculated MFC biofilm growth rates, following which samples from the chemostat were also acquired (2x20 mL).

From each phenotype, insoluble and soluble proteins were extracted from 2 biological replicates each before an iTRAQ-based quantitative proteomic analysis was carried out. The extraction of insoluble and soluble proteins followed two protocols (213,214), with some modifications as detailed elsewhere (215). Cells were resuspended with 43 mM NaCl, 81 mM MgSO4, 27 mM KCl buffer or 1 M TEAB (triethyloammoniumbicarbonate; pH 8.5), 0.12% SDS buffer for the insoluble and soluble protein extraction, respectively. The former buffer used was devoid of detergents to achieve the isolation of the insoluble fraction (i.e. fraction not dissolved in high salt contents buffers used for extractions), whilst the latter buffer used both TEAB and SDS to achieve more denaturation of proteins as well as solubilisation of

membrane proteins. Protein extraction of both fractions was carried out using an ultra sonicator (Sonifier 450, Branson) 10 times (alternatively 30 s of sonication and 1 min on ice) at 80% duty cycle, followed by liquid nitrogen cracking and water bath sonication with ice for 15 min. Samples were then centrifuged at 2,000 x *g* for 5 min at 4 °C to discard unbroken cells and debris, the supernatant collected was then centrifuged at 100,000 x g for 2 hrs or 21,000 x g for 30 min for insoluble and soluble fractions, respectively. Before the total protein concentration was determined from both fractions using the RC-DC Protein Quantification Assay (Bio-Rad, UK), soluble and peripheral membrane proteins were removed from the insoluble fraction by washing the pellet with ammonium carbonate (pH 11)(216) and the pellet resuspended in 1 M TEAB, 0.12% SDS buffer.

3.2.21 Protein quantification assay – Bradford ultra

For quantification of proteins a Bradford ultra (Expedeon, Harston, UK) assay was carried out. Bradford ultra provides an advantage over standard Bradford due to its tolerance of detergents (up to 1%).

In order to be able to determine the concentration of a protein a standard curve must be made using a suitable protein standard, such as bovine serum albumin (BSA). The range of the standard curve will depend on the approximate concentration range the target protein lies.

For high protein range, a dilution series between 0.1 mg/mL and 1.5 mg/mL was required. For a low protein range this may lie between 1 µg/mL and 25 µg/mL. The following methodology considers a high protein range.

1. The test samples, standards (for the defined protein range) and blank (same buffer as protein samples are stored in but with no protein) were mixed with Bradford ultra reagent in a 1:15 ratio of sample to reagent. The cuvette based method made use of 100 µL of sample and 1.5 mL of reagent. All samples, standards and blanks were done in triplicate.
2. Absorbance was read at 595 nm.

3. Sample readings were corrected against the blank, the standard curve plotted and the protein concentration read off protein samples against this.

3.2.22 Sodium dodecyl sulphate polyacrylamide gel electrophoresis (SDS PAGE)

SDS-polyacrylamide gels were cast between two glass plates that had been cleaned using 50% (v/v) ethanol. The dimensions of these plates were (10.1 x 7.2 and 10.1 x 8.2 cm) with the larger plate having 0.75 mm spacer ridges attached to it. The two plates were clamped together, making sure that they were correctly positioned with both their bottoms flush. The components for the 12% (w/v) resolving gel were mixed together in a plastic universal and then pipetted between the two plates until the solution was approximately 2cm from the top of the smallest plate. To ensure that the resolving gel had a straight top edge, water was pipetted over the top of the gel until it began to overflow from the top. The gel was left like this for around 20 min to allow it to polymerise. After this period, the water was poured off, leaving a solid, straight topped resolving gel. To ensure that no water was left sitting on top of the gel, thin strips of blotting paper were dabbed lightly just above the top of the gel. The components of the stacking gel were mixed together in a small conical flask and then pipetted into on top of the resolving gel until the top of the small plate. A 10 – toothed comb was then immediately inserted into the gap between the plates and the gel was allowed to set for 20 min before the comb was removed. The wells of the gel were rinsed with distilled water to remove any gel debris. The gels were then removed from the clamps that were used to set the gels and moved into the electrophoresis module ensuring that the smaller plates were facing inwards to create a central reservoir.

Table 3.7 - Resolving gels

Reactant	Volume used
40% (w/v) solution 37.5:1 acrylamide: bisacrylamide	3.0 mL
Solution B (appendix section 7.2)	2.5 mL
18.2 MW/cm H_2O	4.5 mL
10 % (w/v) ammonium persulphate	20 µL
Tetramethylethylenediamine (TEMED)	10 µL
Total volume	**10.03 mL**

Running buffer (1x) (Appendix) was poured into the tank up to the desired level, making sure that no bubbles were produced that could affect the running of the gel.

The gels had 5 µL of broad range molecular weight marker (191, 97, 64, 51, 39, 28, 19 and 14 kDa) added to one of the wells. The CFE samples that were frozen away were boiled again and the 25 µL sample was loaded onto the gel along with 25 µL of the solubilisation buffer samples. The gels were then run at a constant 200V for 40 min.

3.2.23 Staining and transfer of SDS-PAGE

Depending on the type of work being carried out, different stains were employed on SDS-PAGE gels:

3.2.23.1 Instant Blue

Table 3.8 - Stacking gels

Reactant	Volume used
40% (w/v) solution 37.5:1 acrylamide: bisacrylamide	0.5 mL
Solution C (appendix section 7.2)	1.0 mL
18.2 MW/cm H_2O	2.5 mL
10 % (w/v) ammonium persulphate	30 µL
Tetramethylethylenediamine (TEMED)	10 µL
Total volume	**4.04 mL**

Once the gels had run for a sufficient amount of time, they were then carefully removed from the electrophoresis module and taken out from between the plates. The gels were

placed into plastic containers and had Instantblue (Expedeon, Harston, UK) stain poured over them until covered and then were left for 10 min. The stain was then poured off and the gels were washed in distilled water to remove any residual stain. Gels were then suitable for visualisation and further analysis if required.

3.2.23.2 Silver stain

Silver stain provides a more sensitive method of visualising proteins from SDS-PAGE gels. The added flexibility of choosing the period to halt the staining and the compatibility with mass spectrometry downstream makes the Pierce (Rockford, IL, USA) "sliver stain for mass spectrometry - 24600" a very appealing option. It is important that no metal utensils are used during this procedure.

The following solutions were required and must be made up for this procedure. Any other solutions mentioned with the recipe not stated are supplied in the kit:

Fixing solution

60% distilled water, 30% ethanol, 10% acetic acid

Stop solution

95% distilled water, 5% acetic acid

Ethanol wash

90% distilled water, 10% ethanol

The procedure for this stain was followed as detailed:

1. The gel was washed in ultrapure water for 5 mins. The water was replaced and the gel was washed for another 5 mins.
2. Water was poured off and 20 mL of fixing solution was added to the gel. Gel was incubated at room temperature for 15 mins. The solution was replaced and left for another 15 mins.
3. The gel was washed with ethanol wash for 5 mins. The solution was replaced and the gel was washed for a further 5 mins.

4. The gel was washed in HPLC grade water for 5 mins. The solution was replaced and the gel was washed for a further 5 mins.
5. Immediately prior to use, sensitiser working solution was prepared by mixing 1 part silver stain sensitiser with 500 parts ultrapure water (50 µL sensitiser with 25 mL distilled water).
6. The gel was incubated in sensitiser working solution for exactly 1 min then wash with 2 changes of HPLC grade water for 1 min each.
7. 1 part silver strain enhancer was mixed with 100 parts silver stain (250 µL enhancer with 25 mL stain) and immediately added to the gel following removal of HPLC water and incubated for 5 mins.
8. Developer working solution was prepared by mixing 1 part silver stain enhancer with 100 parts silver stain developer (250 µL enhancer with 25 mL developer). Making sure not add to the gel at this point.
9. The gel was quickly washed with two changes of HPLC grade water for 20 secs each.
10. Developer working solution was immediately added and incubated until protein bands appear (2-3 mins). This was the optimal recommended time and background was noted to increase past this point although at times development has been extended up to 5 mins. Must be watched at all times.
11. At the point where desired band intensity was reached, developer working solution was replaced with stop solution. Gel was washed briefly then replace with fresh stop solution and incubate for 10 mins.
12. The gel was then ready for image analysis or further downstream processing.

3.2.23.3 Western blot

Western blots provide a very simple method for specifically detecting proteins within a sample. This antibody based method can target a defined region and help provide verification or absence of the protein of interest. Developments in the use of western blotting have allowed for increased simplicity in the technique, the Invitrogen iBlot system is an example of this. The following protocol was used for transferring the

protein from an SDS-PAGE gel to nitrocellulose paper and then performing a western blot following using this setup:

Protein transfer to nitrocellulose paper

1. The iBlot device was opened, the anode stack unsealed, making sure to keep it in its plastic tray. The anode stack was inserted, with the plastic tray touching the bottom, securely onto the iBlot device.
2. Following the running of an SDS-PAGE gel, the plates were carefully "cracked" open and the gel placed on top of the anode stack making sure not to leave any bubbles. Any bubbles were removed using a plastic roller.
3. Place pre-soaked filter paper over the top of the gel and use plastic roller to remove any bubbles.
4. The cathode stack was unsealed, the plastic tray discarded and the gel coated side placed down on top of the filter paper. The roller was to ensure good contact.
5. The disposable sponge was placed on top of the cathode stack with the metal contact facing upwards.
6. The iBlot device was switched on.
7. The lid of the iBlot was sealed, ensuring that the red light was shown. This denoted proper contact throughout the setup.
8. The desired program was chosen (default of P3: 20V, 7 mins) and the red button pressed to start the transfer of the proteins to the nitrocellulose paper.
9. Following the 7 min transfer time, the lid was opened, the sponge, cathode stack, filter paper and gel removed and discarded.
10. The nitrocellulose paper was removed and transferred to a suitable container for blocking.
11. The remaining anode stack was removed and the iBlot machine switched off if no longer needed.

Blocking and detection of antibodies

Materials required:

1 x Tris buffered saline with 0.1% Tween 20 (TBS/T)

Blocking buffer – TBS/T with 5% skimmed milk powder

1. The nitrocellulose paper obtained from the iBlot transfer was left in 20 mL blocking buffer for an hour at 4°C.
2. Blocking buffer was poured away and replaced with fresh blocking buffer plus an appropriate dilution of a primary antibody (1:10,000 of blocking buffer to antibody is relatively standard). The sample was left overnight at 4°C.
3. Blocking buffer was poured away and the sample was washed three times with TBS/T for 5 mins each. To ensure a clean sample the container was washed multiple times with TBS/T to help remove any remaining blocking buffer.
4. The membrane was blocked in blocking buffer with the recommended dilution of the secondary antibody for 1 hour at room temperature.
5. Blocking buffer was poured away and the sample was washed three times with TBS/T for 5 mins each. To ensure a clean sample the container was washed with TBS/T to help remove any remaining blocking buffer.
6. Abcam chemiluminescent reagent kit (ab79907 - Abcam, Cambridge, UK) was used to detect samples. 1 drop of oxidant reagent B was added to 1 mL of substrate reagent A and poured over the membrane immediately.
7. The membrane was then be visualised on a gel doc using the chemiluminescent feature.

3.2.24 Culture media

The culturing of bacteria, unless otherwise stated was carried out using Lysogeny broth at 37 °C, 200 rpm.

3.2.25 Cell growth

As some of the cells that were to be tested in the MFC contained multiple plasmids and therefore required the use of different antibiotics simultaneously, a single culture was taken from a plate and inoculated into 100 mL of LB in a 250 mL conical flask 2 days before it was required for testing. The culture was then incubated at 37°C and 200 rpm for 16 hrs. 1 mL of this culture was then transferred to another 100 mL conical

flask of LB at 2 pm the day before it was required for testing and stored at 37°C and 200 rpm until 10 am the next day.

3.2.26 Induction

Unless otherwise stated, inductions were carried out as follows:

1. Single colony picked from plate and transferred into LB with appropriate antibiotics. Grown at 37°C and 200 rpm overnight.
2. 1 mL of the culture was taken and transferred to 100 mL conical flask on LB along with the appropriate antibiotics. This was transferred to a shaking incubator at 37°C and 200 rpm for 1.5 hrs.
3. OD 600 checked every 20 mins until an OD of 0.5 was reached.
4. Protein expression was induced with 1 mM IPTG and cells were returned to 37°C and 200 rpm overnight.

3.2.27 Recombination

Lambda red recombination was employed during this project for the modification of plasmids. The protocol used for this was adapted from Datsenko and Wanner (210). The use of the pKD based lambda red recombination system required growth at 30°C with induction of the recombination machinery through the use of arabinose. During this thesis, it was noted that the cells grew too slowly at 30°C to be able to effectively work with them on the same day as starting the culture. A culture was instead setup the night before needed for use and the cells induced with arabinose at that point:

1. A single colony containing the recombination plasmid pKD46 was picked from a plate and transferred to 10 mL LB with 10 µg/mL ampicillin.
2. This was grown at 30°C and 200 rpm overnight.
3. 18 hrs before cells were needed, 10 µL of culture was taken and transferred to a fresh 10 mL LB culture with 10 µg/mL ampicillin and 5 mM arabinose. This was grown at 30°C and 200 rpm for 18 hrs.
4. Cells were spun down at 4000 rpm for 10 mins at 4°C.
5. The supernatant was discarded and the cell pellet gently resuspend in 1 mL of ice cold sterile distilled water.

6. Solution was spun down at 4000 rpm for 2 mins at 4°C. The water was then removed.
7. Steps 5 and 6 were repeated twice more.
8. The cell pellet was resuspended in 100 µL of sterile distilled water.
9. 30 µL was removed and set aside as a control.
10. 100 ng of purified PCR DNA was added to the remaining cells.
11. Protocol detailed in 2.2.14 was followed for electroporation procedure.
12. Outgrowth was done at 37°C as temperature sensitive pKD46 was no longer required.
13. To increase efficiency, plating out was done on lower concentration resistance plates (typically 40% of normal concentration) as this boosted the number of colonies.
14. Screen was carried out as required with PCR and sequencing verification.

3.2.28 Transposon based insertion

A method of chromosomal insertion fixed to a defined position in the chromosome compared to the much more versatile recombination method. This was adapted from McKenzie and Craig (217). This paper details the potential for this system to be able to insert sequences up to 14 kb in size and has function in multiple organisms. Other notable references - (218)(219). The methodology for chromosomal insertion using attenuation is detailed below:

Note – pGRG36 is temperature sensitive and must be grown at 30°C to allow for plasmid replication

1. The GOI was cloned into the MCS of pGRG36 making sure that the Tn7 flanking arms are left intact.
2. The recombinant plasmid was transformed into the desired host strain for chromosomal insertion and colonies selected for on Ampicillin LB plates overnight at 30°C.
3. Colonies were then grown in 10 mL of antibiotic free LB media at 200 rpm, 30°C for 18 hrs.

Note – the original paper (217) **reports that no induction was required for the chromosomal insertion of the GOI due to leaky expression. pGRG36 is arabinose inducible to allow for increased expression if required. Repression of the transposase system can also be done using 0.1% glucose.**

4. Cells were plated out on antibiotic free LB agar plates and stored overnight at 42°C for removal of the plasmid.
5. Colonies were selected for detection of insertion using PCR with the following primers that flank the *attTn7* site:
   FP: 5'GATGCTGGTGGCGAAGCTGT
   RP: 5'GATGACGGTTTGTCACATGGA
6. Determination of the removal of the plasmid was then determined by Ampicillin sensitivity.

3.2.29 Tandem affinity purification

Tandem affinity purification provided a method of doubly purifying the desired target protein. This was done through the use of two affinity tags, in this case a SPA tag was used (3 x FLAG tag and a calmodulin binding peptide with a TEV protease site between the two tags). This technique allows for either very high purification of a target protein or can be adapted for use in protein interaction work. The original paper detailing this is by Zeghouf et al (220) and further application in *E. coli* (208). The SPA-tag was attached to the C-terminus of target proteins in this study with overlap PCR being used to achieve this (details of overlap PCR in section 3.2.6). The following describes the process of tandem affinity purification of a SPA-tagged protein for interaction work with for the expression of a SPA tagged OmcA protein in pACYCOmcA:

The following reagents and solutions were required:

Wash buffer

Tris-buffered saline (TBS, Product No. 28360) containing 0.05% Tween-20 Detergent and 0.5M NaCl

AFC buffer

30 mM Tris-HCl, 150 mM NaCl, 0.1% detergent, and 0.1-0.5 mM TCEP [tris (2-carboxyethyl) phosphine-hydrochloric acid]

TEV protease buffer

~5 to 10µl (50 units) of TEV protease and 400 µL of 1X AFC buffer

Calmodulin elution 1X stock buffer:

10 mL of 1X calmodulin elution stock buffer containing 50 µL of 2 M Tris-HCl (pH 7.9), 1 mL of 1 M ammonium hydrogen carbonate (NH 4 HCO 3), 150 µL of 0.2 M EGTA, 7 µL of 14 M β-mercaptoethanol, and 8.8 mL of sterile distilled water.

1. Primers were designed for insertion of the SPA-tag by amplifying the desired region from pJL148 and attachment of the genetic sequence to the target protein sequence (OmcA).
2. Sequence verified tagged plasmid was transformed into the desired expression strain (BL21 DE3) and plated onto selective antibiotic plate (Cm).
3. A single colony was picked and grown in 10 mL LB media at the required temperature (37°C), with antibiotics (20 µg/mL Cm) and rotation (200 rpm) and grown overnight.
4. 1 mL of overnight culture was taken and transferred to 100 mL of LB in a 250 mL flask with fresh antibiotics. Grow at 200 rpm, 37°C for 18 hrs.
5. Cell pellets were harvested by spinning down the culture at 4000 x g for 15 mins at 4°C.
6. The desired cell extract as produced as described in section 3.2.20.
7. A 50 µL sample was taken and combined with 10 µg of antibody. The sample volume was adjusted to 500 µL with cell lysis buffer. This was rocked at room temp for 1-2 hrs.
8. 25µL (0.25mg) of Pierce Protein A/G Magnetic Beads were placed into a 1.5mL micro centrifuge tube.
9. 175µL of Wash Buffer was added to the beads and gently vortexed to mix.

10. The tube was placed into a magnetic stand to collect the beads against the side of the tube. The supernatant was removed and discarded.
11. 1mL of Wash Buffer was added to the tube, inverted several times or gently vortexed to mix for 1 minute. The beads were collected with a magnetic stand. The supernatant was removed and discarded.
12. The antigen sample/antibody mixture was added to a 1.5mL micro centrifuge tube containing pre-washed magnetic beads and incubated at room temperature for 1 hour with mixing.
13. The beads were collected with a magnetic stand and the flow-through removed and saved for analysis.
14. 500µL of Wash Buffer was added to the tube and gently mixed. The beads were collected and the supernatant discarded. Wash step was repeated twice.
15. 500µL of purified water was added to the tube and gently mixed. The beads were collected on a magnetic stand and the supernatant discarded.
16. Cleavage of the TEV protease site was then performed by adding ~5 to 10µl (50 units) of TEV protease and 400 µL of 1X AFC buffer onto the column. The top of the column was closed with a cap. The column containing the beads were rotated gently overnight at 4 °C using a LabQuake shaker.
17. Eluate was collected and transferred into a tube with 10 µg of Anti-CBP.
18. Steps 2 to 9 were continued as before and the proteins eluted with 1 x calmodulin elution buffer.

3.2.30 Immunoprecipitation

The following protocol was provided for manual immunoprecipitation using Pierce A/G magnetic beads (88802 – Pierce, Rockford, IL, USA):

Materials and solutions required:

• 1.5mL micro centrifuge tubes

• ***Wash Buffer:*** Tris-buffered saline (TBS, Product No. 28360) containing 0.05% Tween-20 Detergent and 0.5M NaCl

• ***Low pH Elution Buffer***: IgG Elution Buffer, pH 2.0 (Product No. 21028) or 0.1M glycine, pH 2.0

• ***Alternative Elution Buffer***: SDS-PAGE reducing sample buffer

• Antibody for immunoprecipitation

• Antigen Sample

• Cell Lysis Buffer (used to adjust IP reaction volume)

• ***Neutralisation Buffer***: High-ionic strength alkaline buffer such as a 1M phosphate or 1M Tris; pH 7.5-9

•Magnetic stand (e.g., MagnaBind Magnet for 6 ×1.5mL Micro centrifuge Tubes, Product No. 21359)

Note: This protocol provides a general guideline for immunoprecipitation but required optimisation for each application.

1. The antigen sample was combined with 10µg of antibody. The reaction volume was adjusted to 500µL with the Cell Lysis Buffer. The reaction was incubated for 1-2 hrs at room temperature or overnight at 4°C with mixing.
2. 25µL (0.25mg) of Pierce Protein A/G Magnetic Beads were placed into a 1.5mL micro centrifuge tube.
3. 175µL of Wash Buffer was added to the beads and gently vortexed to mix.
4. The tube was placed into a magnetic stand to collect the beads against the side of the tube. The supernatant was removed and discarded.
5. 1mL of Wash Buffer was added to the tube. The tube was inverted several times or gently vortexed to mix for 1 minute. The beads were collected with a magnetic stand. The supernatant was removed and discarded.
6. The antigen sample/antibody mixture was added to a 1.5mL micro centrifuge tube containing prewashed magnetic beads and incubated at room temperature for 1 hour with mixing.

7. The beads were collected with a magnetic stand and the flow-through removed and saved for analysis.
8. 500µL of Wash Buffer was added to the tube and gently mixed. The beads were collected and the supernatant discarded. The wash step was repeated twice.
9. 500µL of purified water was added to the tube and gently mixed. The beads were collected on a magnetic stand and the supernatant discarded.
10. Low-pH Elution: 100µL of Low-pH Elution Buffer was added to the tube. The tube was incubated at room temperature with mixing for 10 mins. The beads were magnetically separated and the supernatant containing target antigen saved.

To neutralise the low pH, 15µL of Neutralisation Buffer was added for each 100µL of eluate.

Alternative Elution: 100µL of SDS-PAGE reducing sample buffer was added to the tube and the samples heated to 96-100ºC in a heating block for 10 mins. The beads and were magnetically separated and the supernatant containing target antigen was saved.

3.3 Proteomics techniques and mass spectrometric analysis

3.3.1 In gel digest

Following gel staining, further analysis of particular protein bands was at times carried out using mass spectrometry. The method used following coomassie or instant blue staining is detailed here:

When using 1-D gels, reduce the size of gel pieces to 1-2 mm in each dimension with a clean scalpel. Pieces that are too large will resulted in reduced peptide recovery. Pieces that are too small can be lost during pipetting steps.

1) Stock Solution Preparation

Reduction buffer

10mM Dithiothreitol (DTT) solution

- 2.3145 mg DTT = 0.0023 g

- 1500 µl 50 mM NH_4HCO_3

Alkylation buffer:

- 55mM Iodoacetamide in 50mM NH_4HCO_3
- 15.26mg Iodoacetamide = 0.0153 g
- 1500µl 50 mM NH_4HCO_3

Trypsin solution (The final concentration of the trypsin solution is 20µg/ml.) (4°C?)

- 100µl 1mM HCl
- 1 vial of trypsin

Use necessary amount of trypsin reconstituted in HCl, as hereby indicated:

Prepare 100 µL of trypsin solution (5 digestions using 20 µL of solution) by mixing:

- 10 µL reconstituted trypsin in HCl

- 90 µL 40mM ammonium bicarbonate in 9% acetonitrile solution

Wash and De-stain Gel Pieces

1. The gel was washed in 20 mL of water for 5 mins.
2. The band of interest was carefully cut from SDS-PAGE gel using a scalpel or razor blade, taking care to include only the desired region. The gel piece was lifted out using clean flat nosed tweezers.
3. The gel piece was placed in a siliconised Eppendorf tube or equivalent. A siliconised tube reduces binding of the peptides to the tube surface.
4. The gel piece was covered with 200 µL of 200 mM ammonium bicarbonate with 40% acetonitrile and incubated at 37^{o}C for 30 mins. The solution was removed and discarded from the tube.
5. Step 4 was repeated one more time.
6. 100 µL of acetonitrile was added and incubated for 5 min until the gel pieces appeared shrunken and opaque. The gel particles were spun down the liquid was discarded.

7. The gel pieces were dried in a Speed Vac for approximately 15 to 30 mins.

Reduction and alkylation.

1. *The gel pieces were swollen in 100 µL of reduction buffer and incubated for 30 min at 56°C to reduce the proteins.*
2. The gel particles were spun down and the liquid discarded. The gel pieces were shrunk with 50 µL of acetonitrile.
3. Acetonitrile was replaced with 100 µL of Alkylation buffer to block reactive cysteines. The sample was incubated for 20 min at room temperature in the dark. Iodoacetamide solution was then discarded.
4. The gel particles were washed with 100 µL of 50mM NH_4HCO_3 for 10 min.
5. 100 µL of acetonitrile was added and incubated for 5 min until the gel pieces shrank. The gel particles were spun down and the all the liquid discarded.
6. Step 12 was repeated one more time.

Enzymatic digestion

1. The gel pieces were dried in a Speed Vac for approximately 15 to 30 mins.
2. 20 µL (0.4 ug of trypsin – as an example) of the trypsin solution prepared for in-gel digests was added to the gel sample.
3. 50 µL of 40 mM ammonium bicarbonate in 9% acetonitrile solution was added to the gel sample.
4. Made sure that the gel piece is at the bottom of the tube and covered with liquid.
5. The gel piece was incubated overnight at 37^{o}C.

Peptide extraction

1. After overnight incubation, the samples were spun down to collect all the water droplets condensed inside the lid of the microcentrifuge tube.
2. All the liquid from the gel piece was removed, transferred and saved in a new, labelled tube.
3. Peptides were extracted from the gel matrix by adding 10 to 15 µL of 25 mM NH_4HCO_3 (ammonium bicarbonate). Samples were vortexed briefly, incubated

at room temperature for 10 min, and the supernatant recovered after a brief spin.

4. 1 to 2 times the volume of the gel particles worth of acetonitrile was added and left to incubate at 37°C for 15 min with agitation. The gel particles were spun down and the supernatant collected.
5. 40 to 50 µL of 5% formic acid was added and then left for 15 min at 37°C with agitation. The gel particles were spun down and the supernatant collected.
6. 1 to 2 times the volume of the gel particles worth of acetonitrile was added and the samples incubated at 37°C for 15 min with agitation. The gel particles were spun down and the supernatant recovered.
7. All extracts were pooled and dried down in a vacuum centrifuge. Dry digests were stored in a freezer at –20°C until needed.
8. Resuspension of the samples was carried out in 0.1% trifluoroacetic acid, 3% acetonitrile with the rest of the volume being HPLC grade water.

3.3.2 Silver destain and in gel digest

Silver stain in gel digest was carried out exactly the same except that a further initial destain protocol was required. This procedure was initially followed and then the protocol in 3.3.1 was continued in order to finish:

1. The gel was washed in HPLC grade water for 10 mins. The water was replaced and the gel was washed for another 10 mins.
2. The desired protein bands were excised and transferred to siliconised Eppendorf tubes.
3. Destain solution was prepared by combining 74 µL of silver destain reagent A with 245 µL of silver destain reagent B and 4 mL of HPLC grade water. This is sufficient to treat 10 gel pieces and was must be used within the same day as being made up.
4. 0.2 mL of the destain solution was added to the gel pieces, mixed gently and incubated at room temp for 15 mins.
5. The destain solution was removed and replaced with fresh solution followed by incubation for a further 15 mins.

6. The destain solution was removed and gel pieces were washed three times with 0.2 mL of wash solution for 10 mins each time.
7. The gel bands were then ready to follow the in gel digest protocol listed in 3.3.1.

3.3.3 In solution digestion

Prior to labelling protein samples with iTRAQ for quantitative proteomics, it was necessary to determine the concentration of the protein within the sample. This was done using a Bradford Ultra assay as described in section 3.2.21. Running samples on an SDS-PAGE gel will also show if the samples have roughly the same amount of protein. It is highly advised to run an SDS-PAGE gel following digestion as this will give a good indication to if the proteins have been fully digested. The following protocol describes the digestion of 100 µg of protein sample from each phenotype. The protocol and required reagents are hereby listed:

Required reagents:

- Dithiothreitol (DTT – Sigma Aldrich, Dorset, UK)
- Tris-(2-carboxymethyl phosphine) (TCEP – Sigma Aldrich, Dorset, UK) OR Iodoacetamide (IAA – Sigma Aldrich, Dorset, UK)
- Sequencing grade modified Trypsin (Promega, Southampton, UK)
- Sodium dodecyl sulphate (SDS – Sigma Aldrich, Dorset, UK)
- Sodium deoxycholate (Sigma Aldrich, Dorset, UK)

1. 20 µL of 0.5 M triethyloammoniumbicarbonate (TEAB) at pH 8.5 was added to 100 µg of almost completely dry sample to give a protein concentration of ~ 5 mg/ mL.
2. 1 µL of 2% SDS was added and vortexed.
3. 1 µL of 110 mM of TCEP was added to each sample and vortexed.
4. Samples were incubated at 60°C for 1 hour.
5. Samples were centrifuged to collect all solution.

6. 1 µL of freshly prepared 84 mM IAA was added followed by vortexing of the sample and centrifugation to collect the solution.
7. Samples were incubated in a dark cupboard for 30 mins at room temperature. Wrapping tubes in foil is preferential to prevent exposure to light.
8. Samples were vortexed and centrifuged.
9. 1 mg/mL solution of trypsin using 1 mM HCL and 40 mM ammonium bicarbonate with 9% acetonitrile was prepared and 10 µL was added to each sample followed by vortexing and a spin down to collect sample.
   Note – For insoluble fractions, sodium deoxycholate (SDC) was added to a final concentration of 0.007% before tryptic digestion (1:10 w/w ratio) overnight. A combination of trypsin and chymotrypsin was then used at a 1:10 (w/w) ratio of enzyme/protein for the second day.
10. Samples were incubated at 48°C overnight (221).
11. Samples were centrifuged to collect all sample.

3.3.4 iTRAQ labelling

The following is a description of iTRAQ labelling used following the in solution digest that was carried out as described in section 3.3.3.

1. iTRAQ reagents were allowed to reach room temperature and 70 µL of ethanol was added to each tube, with the samples then vortexed and centrifuged.
2. The contents of one of the iTRAQ reagent vials was transferred to one sample tube and vortexed to mix.
3. The samples were then incubated at room temperature for 1 hour
4. Before combining samples, a small aliquot of each sample was taken, the organic solvent removed and cleaned using a C18 Zip tip as described in section 3.3.6 and analysed through LC-MS/MS to check for identification of correct m/z charge for each iTRAQ label
5. The samples of each iTRAQ reagent labelled tube sample were combined in a fresh tube.
6. Samples were be desalted (as necessary) before transfer to LC-MS/MS. Due to the complex nature of the sample (global proteomic analysis) then

fractionation of samples through strong cation exchange (SCX) or hydrophilic interaction chromatography (HILIC) was needed as described in section 3.3.5.

3.3.5 Strong Cation Exchange (SCX)

After incubation at room temperature, labelled samples were combined before being dried in a vacuum concentrator. Off-line (to the LC-MS/MS) first dimensional fractionation of samples using SCX was performed on a BioLC HPLC system (Dionex, UK) prior to online second dimension RP (reverse phase) - LC MS/MS analysis. The SCX fractionation was carried out using a PolySULFOETHYL-A Column (PolyLC, USA) with a 5 μm particle size, 10 cm length x 4.6 mm diameter and 200 Å pore size. The system was operated at flow rate of 0.4 mL/min with an injection volume of 70 μL. Transfer and elution of peptides was achieved using binary mobile phase buffers A and B (buffer A: 10 mM KH_2PO_4 and 25% ACN at pH 3; buffer B: 10 mM KH_2PO_4, 25% ACN and 500 mM KCl, at pH 3). Separation was performed using a 60 min gradient, starting with 5 min at 100% buffer A, followed by a linear ramp to 30% buffer B over 40 min, then 30% to 100% B over 5 min, and finally holding at 100% A for 5 min. A UV detector UVD170U calibrated at 214 nm and Chromeleon Software (Dionex, Netherlands) were used to record the SCX chromatography. Labelled peptide fractions were collected every minute, and later dried in a vacuum concentrator.

3.3.6 C18 cleanup columns

In order to clean up peptide samples following digestion non complex samples were cleaned up using C18 zip tip columns. The protocol for this is hereby detailed:

Samples are noted to have been dried using a vacuum concentrator

Required solutions:

Hydration solution:

50:50, ACN: HPLC purity water, 0.1% TFA

Wash solution:

0.1% TFA in HPLC purity water

Peptide elution solution:

60:40 ACN: HPLC purity water, 0.1% TFA

Reconstitution buffer:

5:95 of ACN to HPLC purity water plus 0.1% TFA

1. Dried samples were resuspended in 13 µL of reconstitution buffer, vortexed and centrifuged.
2. Sample pH was checked and adjusted to pH ≤ 3 with 10 % TFA.
3. P10 pippetor was to 10 µL and a ZipTip was placed on the pipette.
4. The tip was hydrated by aspirating 10 µL of hydration solution and discarding it.
5. Step 4 was repeated.
6. The tip was then washed by aspirating 10 µL of wash solution and discarding it.
7. Step 6 was repeated.
8. The peptide sample was then loaded onto the tip by repeated aspiration and expulsion back into the sample holding tube. This was done 5-6 times
9. The sample was then washed by aspirating 10 µL of wash solution into the tip and then expelling to waste.
10. Step 9 was repeated 5 times.
11. Sample was eluted from the tip using 5 µL of peptide elution solution.

3.3.7 Liquid Chromatography-Tandem Mass Spectrometry (LC-MS/MS)

3.3.7.1 – Standard identification of proteins

Detection of proteins within a sample has been a desired technique within life sciences for a substantial period of time. Western blots provide a very simple solution to this issue although there is a limited amount of information generated from them. The development of mass spectrometry allows for analysis of the polypeptide chain to further confirm the identification of proteins instead of relying on a visual result.

For the general detection of samples, LC-MS/MS analysis was typically carried out on either an HCT ultra PTM discovery electrospray ionisation (ESI)-Ion Trap MS/MS

(Bruker Daltonics, Coventry, UK) or a Bruker amaZon Ion-Trap MS/MS (Bruker) coupled with an Agilent Ultimate 3000 nano-flow HPLC (Dionex). Samples for these experiments were typically prepared as described in section 3.3.1.

3.3.7.2 – Quantitative analysis of proteins

For the quantitative analysis of proteins using iTRAQ, fractionation was carried out as described in section 3.2.5. Prior to tandem MS analysis, each fraction was first desalted using UltraMicroSpin Column (The Nest Group, Southborough, MA, USA) following the manufacturer's protocol, detailed in section 3.2.6. 2D Liquid chromatography tandem mass spectrometry (LC MS/MS) of iTRAQ labelled samples was carried out on a QStarXL hybrid QToF system (AB-SCIEX, Foster City, USA) and a maXis hybrid UHR-QToF system (Bruker Daltonics, Coventry, UK), both coupled to an Ultimate 3000 nano-flow HPLC (Dionex). All iTRAQ-labelled samples were further desalted online using a 5 mm x 300 μm ID LC-Packings C18 PepMap trap cartridge under 0.1% TFA and 3% ACN for 15 min, and eluted to a 15 cm, 75 μm ID LC-Packings C18 PepMap analytical column in 0.1% formic acid with an ACN gradient performed over a 90 min gradient (3-35% ACN).

3.3.8 Multiple reaction monitoring (MRM)

In order to be able to focus in on a specific protein or peptide within a sample a method called multiple or selective reaction monitoring is used. This is based upon a protocol described in Anderson and Hunter (222). To determine the peptides to search for they can either have been previously identified through the use of AutoMS or a theoretical digest can be done on the polypeptide chain of the protein to determine the resulting peptides. From this the mass over charge (m/z) of the peptide will be known providing the information required. In order to target a specific peptide from within a protein it must meet the following criteria:

- Must be doubly or triply charged
- Ideally not containing Methionine as this can be variably oxidised leading to fluctuations in the m/z of the peptide

- If containing Cysteine then this carboxymethylation must be considered following alkylation

The MRM procedure was carried out on either an HCT ultra PTM discovery electrospray ionisation (ESI)-Ion Trap MS/MS (Bruker Daltonics, Coventry, UK) or a Bruker amaZon Ion-Trap MS/MS (Bruker) coupled with an Agilent Ultimate 3000 nano-flow HPLC (Dionex). The HPLC aspect of the setup was carried out as specified in 3.3.7.

In order to program the setup of the Bruker trapControl software had the mode changed to MRM The precursor m/z of the desired peptides was input into the precursor column. Isolation was selected with a width window of 2 m/z to ensure the desired ion was captured whilst providing room for low levels of instrument error. Essentially, the reaction selection was chosen to ensure that any ion isolated within the desired m/z window were then fragmented to determine their component ions. The MS was run in positive mode along with a target window of 200000 and an accusition time of 0.30 ms.

3.3.9 Mass spectrometry analysis and data searching

The protein identification and quantification processes were mainly carried out as described by Ow et al (223). Tandem MS data generated from QStarXL instrument were used to find peaks and converted to MGF format using the mascot.dll embedded script (V1.6) coupled with Analyst QS 1.1.1 (Applied Biosystems / AB-SCIEX). MGF data were interrogated (for identifications only) using an in-house cluster running the Phenyx algorithm (224) (binary version 2.6; Genebio, Geneva). Protein sequences for interrogation were obtained from the ftp site (ftp://ftp.ncbi.nih.gov/) of NCBI databases. Details on the identification parameters and target-decoy database strategies for the identification are based on search criteria established elsewhere (225). Only proteins satisfying a 1% global peptide false positive identifications or False Discovery Rate (FDR) (226) and observed with ≥ 2 peptides were considered for further quantitative analysis. The intensities of the iTRAQ reporters were automatically exported from all qualified (as above) spectra and were processed as described by Pham et al (213).

3.3.10 Analysis of iTRAQ quantification and statistical validation

The analysis of iTRAQ ratio, statistical tests, and their distributive estimations were all performed as described by Pham et al (224). Briefly, protein quantifications were obtained by computing the geometric means of the reporters' intensities. A global median correction and isotopic impurity correction was subsequently applied to every reporter in order to compensate for experimental and systematic errors. A *t*-test comparison between the reporter ions' intensities was carried out employing these corrected intensities. The distribution of the values was tested to see if it had a mean different from zero, and reported the *p*-values associated with the said distribution, based on a threshold ($\propto$ = 5%) for significance. Since two replicates are available for each condition, a change is reported only if it is significant regardless of which replicate is chosen to perform the comparison. This was carried out for every protein. In the remainder of the thesis, proteomic probability scores are defined as -log10 (p) to measure significance, and only report quantitative results that are statistically significant, thus requiring a score > 1.3 [i.e. -log10 ($\propto$)].

3.4 MFC and Half Cell techniques

3.4.1 MFC Setup

3.4.1.1 UWE MFC setup

The electrode material used within the MFC chambers was pure carbon fibre veil (PRF Composite Materials, Poole, U.K.) cut into 6 x 20 cm oblongs and folded in the middle 3 times until they measured (H x W x D) 5 cm x 3.5 cm x 0.5 cm. The surface area was calculated as 120 cm^2 and the electrodes were then attached to Ni/Ti wire. The MFCs used are a two chamber set up as shown in Figure 1.2 that have a void volume of 15 mL. The two chambers are separated by a proton exchange membrane (PEM) (VWR, Leicestershire, U.K.) that had been stored in 1% NaCl solution for at least 24 hrs before use in the fuel cell.

The MFC had heated (25°C) and aerated tap water flowing through the cathode chamber overnight at a flow rate of 10 mL/min, before any culture was loaded into the

anode chamber. This flow rate was chosen as the highest rate that could be flowed through the cathode without any effect on the PEM and interference with the anode. The anode chamber had distilled water passing through overnight at the same flow rate. This was done to ensure that the fuel cell voltages were low and stable before the test began as to minimise errors.

The anode chamber was completely emptied before the culture was loaded into the chamber and the anode run in batch mode. A sample of 15 mL of culture was measured out aseptically and then loaded into the chamber using a peristaltic pump set at a flow rate of 10 mL/min. After the cells were loaded, the MFC was connected to the computer through the use of an interface box, ADC-24 A-D converter computer interface (Pico Technology Ltd., Cambridgeshire, U.K.) left at open circuit (No load set on the device) for 4 hrs to allow the cells to stabilise. A polarisation curve was carried out to determine the maximum power density of the engineered strains by applying an external resistance which was decreased every 500 s. The initial starting resistance was 111 kΩ, gradually decreasing to 1.11 kΩ over 16 steps. Data obtained was then analyzed using Microsoft Excel.

3.4.1.2 Cambridge MFC setup

A sample of 10 mL of dense cell cultures were diluted to a final OD_{600} of 1.0 with fresh LB, along with replenishing required antibiotics (20 µg mL^{-1} Cm, 100 µg mL^{-1} Amp) and 0.5 mM IPTG. 200 µl of sample was injected into the anodic chamber of a microfludic-scale microbial fuel cell with the cathode chamber facing upwards to allow full exposure to the air. The device was then connected to the computer through the use of an interface box, ADC-24 A-D converter computer interface (Pico Technology Ltd., Cambridgeshire, U.K.) and allowed to settle for 30 mins with no external resistance applied. A polarisation curve was carried out to determine the maximum power density of the engineered strains by applying an external resistance which was decreased every 500 s. The initial starting resistance was 111 kΩ, gradually decreasing to 1.11 kΩ over 16 steps. Data obtained was then analyzed using Microsoft Excel.

3.4.1.3 Bacterial culture and nutrient supply

The following describes the procedure used for culturing bacteria for use within the iTRAQ study detailed in this study:

Bacterial cell cultures were grown as described in previous work (212) and, as before, a high cell density of *Shewanella oneidensis* MR-1 was obtained with supplemented M1 medium containing among other things the electron donor sodium lactate (Recipe detailed in appendix). Cultures of *S. oneidensis* were taken from a glycerol stock and sub-cultured onto an LB agar plate, overnight at 28°C. A single resulting colony was then transferred to 100 mL of M1 medium (227) containing 0.4% (w/v) sodium lactate as a single carbon source and allowed to grow for 16 h at 28°C, 180 rpm. A volume of 1 mL from this dense culture (OD_{540nm} = 0.250) was then used to inoculate 4 x 25 mL flasks of M1 for each of the different setups (2 for MFC inoculation and 2 for continuous culture in a chemostat). The cells were then transferred to their relevant containers, generating two different phenotypes: (i) electroactive anodic anaerobic biofilms inside the MFC; and (ii) chemostat planktonic microaerobic cells. A peristaltic pump was used to continuously supply anolyte (M1 medium) and catholyte (tap water) to the MFC chambers with the flow rate set to 62.5 $ml.h^{-1}$ for each UWE fuel cell used. All MFC experiments were conducted at room temperature (23 ± 2 ºC).

3.4.1.4 MFC design and operation for iTRAQ experiment

The following MFC method was adapted from those used in Ieropoulos et al. (76) as this experiment was done in collaboration with this group.

The MFCs utilised for this experiment were a standard two-chamber type, separated by a 12 cm^2 cation-exchange membrane (VWR, UK) and with 20 mL reactor volume per chamber (anode/cathode). These fuel cells were fabricated by 3D-printing in biocompatible polycarbonate (212). Each chamber contained a folded sheet of carbon fibre veil with a total surface of 270 cm^2 each (212) (20m^2 g^{-1}; PRF Composite Materials, Dorset, UK) as the electrode and a resistance of 5 Ω m in the machine direction and 9 Ω m in the cross direction. The folded electrodes were pierced with a 5cm long nickel–chrome wire coming out of one of the two top holes to provide the

connection points for the external circuit. The electrode conformation was such that 270 cm^2 surface area of carbon veil was 'folded down' to 5 cm^2, in order to reduce the resistance of the material, and hence reduce the internal resistance of the fuel cell.

3.4.2 Polarisation curves

Polarisation curves were generated by connecting the MFC up to a decade resistance box (Farnell, U.K.) set at a starting resistance of 100 kΩ and decreasing in steps of 10 kΩ down to 10 kΩ. The resistance was then decreased by 2 kΩ down to 2 kΩ and moved a single kΩ down to 1 kΩ. The final set of resistance changes were from 1 kΩ to 200 Ω in 200 Ω decrements. The MFCs were left for at least 500 secs between each resistance change to allow to cell voltage to level out. The data was acquired in millivolts (mV) using an ADC-16 A-D converter computer interface (Pico technology Ltd., Cambridgeshire, U.K.). Recorded data was then analysed using Microsoft Excel.

In order to be able to directly compare one strain to another, the maximum power density was calculated. This provided more information than the voltage output as it allows the resistance at which the greatest power is output is achieved to be determined. The point of external resistance at which this occurs is equal to the internal resistance of the MFC (Ieropoulos et al., 2008). In order calculate the power density achieved in the MFC, the current (I) firstly needed to be calculated using Ohm's law, I=V/R, where V is the measured voltage and R is the known external resistance. Power was then calculated (W) by multiplying current by voltage, P=IxV. This then allowed the power density to be determined by dividing the power by the surface area of the electrode PDensity = P/SA. The power density is presented as mW/m2. However, it should be noted that although power density can be used to compare between MFC models, it is highly dependent on what the authors chose to consider as their "projected surface". Different interpretations of electrode surface area lead to orders-of-magnitude-differences in current density estimation (76,228) so the use of this parameter is not helpful to estimate if the bacterial cultures are limited in nutrients.

3.4.3 Half cell setup

The use of a half cell provided an opportunity to test strains over a longer period of time that was not possible with the microfluidic Cambridge MFCs. The design and setup for these was adapted from Carmona-Martinez et al (229) and Pereira-Medrano et al (230).

3.4.3.1 Strain testing in a sedimentary half cell using LB

A 10 mL sample of a dense, uninduced culture of engineered *E. coli* cells was condensed down to an OD_{600} of 5. Within a flow hood, 1 mL of this sample was loaded into a sterile 250 mL Duran bottle of LB alongside the relevant antibiotics (20 µg mL^{-1} Cm, 100 µg mL^{-1} Amp) and 0.5 mM IPTG. The final initial OD of the culture was therefore diluted to 0.2. A sterile carbon paper electrode (PRF Composite Materials, Poole, U.K.), woven with Ni/Ti wire, and a Ag/AgCl red rod reference electrode (Hach Lange, Salford, UK) were inserted into the 250 mL Duran bottle, ensuring the carbon electrode was flat against the bottom. The Ni/Ti wire was fed through a small hole of the lid and the end of the reference electrode came through a similar hole. Aquarium Silicone Sealant was used to seal any gaps left in the lid (Aquatics Online Ltd, Bridgend, UK) after it was tightly screwed. The completed half cell was then transferred to a 37°C water bath and connected up to the computer via an ADC-24 A-D converter computer interface (Pico technology Ltd., Cambridgeshire, U.K.). Readings were taken every min for 15 hours, with data being analyzed in Microsoft Excel.

3.4.3.2 Strain testing in a sedimentary half cell using a minimal media

The engineered strains were also tested over an 8 day period in order to determine the negative potential within a sparged minimal media with a defined carbon source. M9 minimal media) was chosen with 0.4% sodium lactate as the sole carbon source (231). The media was filter sterilized using the Stericup system (Millipore, Watford, UK). Media was then sparged with Nitrogen gas for 15 mins within a flow hood, with a filter placed between the nitrogen source and the media. Following this, antibiotics (20 µg mL^{-1} Cm, 100 µg mL^{-1} Amp) were added alongside 0.5 mM IPTG. The cells were prepared as stated in section 3.4.3.1 and 1 mL of OD 5.0 culture was added to the media. The half cells were then sealed and placed in a water bath at 37°C and

connected to a picologger device (as in section 3.4.3.1) with readings being taken every minute for 8 days.

3.4.4 Chronoamperometry

A secondary testing method for the analysis of exoelectrogenic activity of the engineered and wild type strains was the use of a half cell with a poised potential of +0.2 V. The half cell was setup as follows:

1. 100 mL of a dense, uninduced culture of engineered cells was condensed down to an OD_{600} of 5.
2. Within a flow hood, 1 mL of this sample was loaded into a sterile 250 mL Duran bottle of LB alongside the relevant antibiotics (20 µg mL^{-1} Cm, 100 µg mL^{-1} Amp).
3. A sterile carbon paper electrode (PRF Composite Materials, Poole, U.K.), woven with Ni/Ti wire, platinum coated counter electrode poised at +0.2 V and a Ag/AgCl red rod reference electrode (Hach Lange, Salford, UK) were inserted, ensuring the carbon electrode was flat against the bottom. The Ni/Ti wire was fed through a small hole in the lid, the counter came through one of equal size and the end of the reference electrode came through a similar hole.
4. The completed half cell was then transferred to a 37°C water bath and the potential was poised at +0.2 V using a Uniscan PG-581 portable potentiostat connected up to the computer. Readings were taken every min for 900 mins, with data being analysed in Microsoft Excel.

3.5 Plasmid and strain development

Table 3.9 - Obtained vectors

Plasmid	Origin of Replication	Promoter	Antibiotic	Coding	Received from
pKP1	pBR322/ColE1	T7	AmpR	*MtrA*	Prof. Richardson
pEC86	p15A	pTrc/pTetA	CmR	ccmABCDEFGH	Prof Richardson
pRGK333	pBR322/ColE1	bla	AmpR	ccmABCDEFGH IPTG inducible	Prof. Kranz
p*OmcA*	p6K gamma	tat	AmpR	*OmcA*	Prof. Richardson
pKD46	OriR101	Ara	AmpR	*Bet, Gam, Exo*	Yale culture collection
pKD13	R6K gamma	n/a	KanR	*FRT flanked Kan cassette*	Yale culture collection
pKD32	R6K gamma	n/a	CmR	*FRT flanked Cm cassette*	Yale culture collection
pCP20	repA101ts temperature sensitive	bla	AmpR/CmR	*Flippase*	Yale culture collection
pGRG36	pSC101 temperature sensitive	Ara	AmpR	*TnsA-D*	Zdeno Levarski (Addgene)
pJL148	pBR322/ColE1	n/a	AmpR	*SPA-Tag*	Prof. Jeff Greenblatt
pACYCDuet-1	p15A	Lac T7	CmR	*Dual MCS*	Novagen
pRSFDuet-1	pRSF	Lac T7	KanR	*Dual MCS*	Novagen
pUC19	pBR322/ColE1	n/a	AmpR	*MCS*	NEB

Table 3.10 – Constructed vectors

Plasmid	Origin of Replication	Promoter	Antibiotic	Coding
pACYCOmcA	p15A	Lac T7	CmR	*OmcA*
pACYCMtrABO	p15A	Lac T7	CmR	*MtrA, B and OmcA*
pACYCMtrCAB	p15A	Lac T7	CmR	*MtrC, A and B*
pACYCMtrCABO	p15A	Lac T7	CmR	*MtrC, A, B and OmcA*
pACYCMR-1	p15A	Lac T7	CmR	*MtrD, E, F, OmcA, MtrC, A and B*
pKD46Kan	OriR101	Ara	KanR	*Bet, Gam, Exo*
pUC19 Cm	pBR322/ColE1	n/a	CmR	*MCS*
pUC19Cm-Tn7	pBR322/ColE1	n/a	CmR	*AttTn7 flanked MCS*
pACYCMtrOmcA-SPA-tag	p15A	Lac T7	CmR	*SPA tagged OmcA*
pACYCMtrABO-SPA-tag	p15A	Lac T7	CmR	*SPA tagged OmcA + MtrA, B*
pACYCMtrCAB-SPA-tag	p15A	Lac T7	CmR	*SPA tagged MtrB + MtrC and A*
pACYCMtrCABO-SPA-tag	p15A	Lac T7	CmR	*SPA tagged OmcA + MtrC, A and B*

Table 3.11 – Tested strains

Strain	Genotype	Plasmids	Resistance	Source
E. coli MG1655	F^- λ^- ilvG- rfb-50 rph-1	None	None	Novagen
E. coli BL21	*E. coli* B F- *dcm ompT hsdS*(r_B-m_B-) gal [$malB^+$]$_{K\text{-}12}$(λ^S)	None	None	Novagen
E. coli BL21 DE3	*fhuA2 [lon] ompT gal (λ DE3) [dcm] ΔhsdS λ DE3 = λ sBamHIo ΔEcoRI-B int::(lacI::PlacUV5::T7 gene1) i21 Δnin5*	None	None	Novagen
E. coli RGK103 (Delta ccm)	F^- λ^- ilvG- rfb-50 rph-1 *ΔccmABCDEFGH*	Δ(ccmA-H)	KanR	Prof. Kranz
E. coli MG1655 pEC86	F^- λ^- ilvG- rfb-50 rph-1/*ccmABCDEFGH*	pEC86	CmR	Made in this project
E. coli MG1655 *MtrA*	F^- λ^- ilvG- rfb-50 rph-1/*mtrA*	pKP1	AmpR	Made in this project
E. coli MG1655 pRGK333	F^- λ^- ilvG- rfb-50 rph-1/*ccmABCDEFGH*	pRGK333	AmpR	Made in this project
E. coli MG1655 p*OmcA*	F^- λ^- ilvG- rfb-50 rph-1/*omcA*	p*OmcA*	AmpR	Made in this project
E. coli JM109 pEC86 *MtrA*	endA1 glnV44 thi-1 relA1 gyrA96 recA1 $mcrB^+$ Δ(lac-proAB) e14- [F' traD36 $proAB^+$ $lacI^q$ lacZΔM15] hsdR17($r_K^-m_K^+$) /*ccmABCDEFGH mtrA*	pEC86, pKP1	CmR, AmpR	Prof. Richardson
E. coli K-12 pEC86 p*OmcA*	F^- λ^- ilvG- rfb-50 rph-1/*ccmABCDEFGH omcA*	pEC86, p*OmcA*	CmR, AmpR	Made in this project
E. coli BL21 pEC86 p*OmcA*	*E. coli* B F- *dcm ompT hsdS*(r_B-m_B-) gal [$malB^+$]$_{K\text{-}12}$(λ^S)/ *ccmABCDEFGH omcA*	pEC86, p*OmcA*	CmR, AmpR	Prof. Richardson
E. coli BL21 DE3 pEC86 p*OmcA*	*fhuA2 [lon] ompT gal (λ DE3) [dcm] ΔhsdS λ DE3 = λ sBamHIo ΔEcoRI-B int::(lacI::PlacUV5::T7 gene1) i21 Δnin5/ ccmABCDEFGH omcA*	pEC86, p*OmcA*	CmR, AmpR	Made in this project

E. coli BL21 DE3 pRGK333 pACYCOmcA	*fhuA2 [lon] ompT gal (λ DE3) [dcm] ΔhsdS λ DE3 = λ sBamHIo ΔEcoRI-B int::(lacI::PlacUV5::T7 gene1) i21 Δnin5/ ccmABCDEFGH omcA*	pRGK33, pACYCOmcA	AmpR, CmR	Made in this project
E. coli BL21 DE3 pRGK333 pACYCMtrABO	*fhuA2 [lon] ompT gal (λ DE3) [dcm] ΔhsdS λ DE3 = λ sBamHIo ΔEcoRI-B int::(lacI::PlacUV5::T7 gene1) i21 Δnin5/ ccmABCDEFGH mtrAB omcA*	pRGK33, pACYCMtrABO	AmpR, CmR	Made in this project
E. coli BL21 DE3 pRGK333 pACYCMtrCAB	*fhuA2 [lon] ompT gal (λ DE3) [dcm] ΔhsdS λ DE3 = λ sBamHIo ΔEcoRI-B int::(lacI::PlacUV5::T7 gene1) i21 Δnin5/ ccmABCDEFGH mtrCAB*	pRGK33, pACYCMtrCAB	AmpR, CmR	Made in this project
E. coli BL21 DE3 pRGK333 pACYCMtrCABO	*fhuA2 [lon] ompT gal (λ DE3) [dcm] ΔhsdS λ DE3 = λ sBamHIo ΔEcoRI-B int::(lacI::PlacUV5::T7 gene1) i21 Δnin5/ ccmABCDEFGH MtrCAB omcA*	pRGK33, pACYCMtrCABO	AmpR, CmR	Made in this project
E. coli BL21 DE3 pRGK333 pACYCMR-1	*fhuA2 [lon] ompT gal (λ DE3) [dcm] ΔhsdS λ DE3 = λ sBamHIo ΔEcoRI-B int::(lacI::PlacUV5::T7 gene1) i21 Δnin5/ ccmABCDEFGH mtrCABDEF omcA*	pRGK33, pACYCMR-1	AmpR, CmR	Made in this project
Shewanella oneidensis MR-1	*ATCC - MR-1 [CIP 106686]*	None	AmpR	Prof. Gralnik

3.6 SEM preparation and analysis

Before samples could be analysed using SEM they firstly had to be prepared. For the analysis of anodic biofilms the following protocol was adhered to:

The MFCs were disassembled and the carbon paper anode was removed and cut into 1.25 by 2.5 cm pieces. The samples were completely covered in 3% glutaraldehyde and then stored in flat bottom containers in the fridge (4°C) overnight. The following day the solution was carefully discarded and the samples were submerged in cold 0.1 M PBS for 30 mins. This solution was discarded and the sample was again covered in 0.1 M PBS and then left in the fridge until needed.

A secondary fixation of the samples was then required, where they were covered in 2% Osmium tetroxide for 2 hrs at room temperature and then washed in 0.1 PBS as above. The samples were then dehydrated by using a graded series of ethanol:

- 75% ethanol for 15 mins
- 95% ethanol for 15 mins
- X 2 100% ethanol for 15 mins
- X 2 100% ethanol dried over anhydrous Copper sulphate for 15 mins

All of these steps were carried out at room temperature.

The samples were then stored in a 50/50 solution of HDMS and ethanol for 30 mins and were then moved to 100% HDMS. The samples were then dried in the fume hood.

Infiltration of the sample was accomplished by placing the specimens in a 50/50mixture of propylene oxide/araldite resin and left overnight at room temperature.

The specimens were left in full strength araldite resin for 6-8 hrs at room temperature after which they were embedded in fresh araldite for 48-72 hrs at 60°C.

Araldite resin

CY212 resin	10 mL
DDSA hardener	10 mL
BDMA accelerator	1 drop per 1mL of resin mixture

The samples were thinly sliced thereby making them suitable for analysis using the SEM

Chapter 4 - Introduction of an electrogenic pathway into a foreign organism

This chapter was done in collaboration with Dr. Greg. J. S. Fowler, Dr. Ana. G. Pereira-Medrano and was supervised by Prof. Phillip C. Wright

4.1 - Introduction

Interaction between living systems and man-made technologies provides the means to bridge the gap between the analogue and the digital world, presenting massive potential for biosensing, biocomputation and bioenergy. Energy within US wastewater is estimated to contain 9.3-fold that required to power its treatment (37). The potential for simultaneous degradation of organic compounds and energy generation employing diverse bacterial metabolism within an MFC is an attractive prospect. Transfer of electrons between most natural and artificial systems is only possible in the presence of lipid-soluble mediators that can permeate the insulating cell membrane. These mediators diffuse into the membrane and strip electrons from intracellular redox enzymes (232,233) in order to reduce an acceptor. They are, however, in general only artificial additions (with the exception of natural couplers such as nitrate/nitrite and sulphate/sulphide – which aren't present in pure culture studies where minimal media is used), often introducing more problems than they solve, especially in wastewater treatment, due to high costs (233), need for replenishment (76) and cellular toxicity (45). These problems all require solutions.

A limited number of organisms are capable of transferring electrons to inorganic compounds. Most, notably DMRB, such as *Shewanella* species, are able to secrete such mediators (136), and although they are *Shewanella's* main method of extracellular electron transfer (104), they are not essential for activity (136). The activity of natural DMRB (e.g. *Shewanella* and *Geobacter*) capable of reducing insoluble electron acceptors without the use of artificial mediators under anaerobic conditions is well-

documented (69,234–236). The wide range of *Shewanella* studies carried out show a predicted model for electron transport from the cytoplasm to the outer membrane (OM) focusing on a highly conserved cluster of *c*-type cytochromes (85,108,237). These comprise CymA, a tetrahaem cytochrome that functions as a major hydroquinone dehydrogenase (238), accepting electrons from the intracellular menaquinone pool and transferring them through the inner membrane to the periplasmic decahaem MtrA (239). The electrons are then transported through to an OM complex of decahaem proteins formed by OmcA and MtrC, localised by the presence of the non-haem β-barrel protein MtrB (112). *Shewanella* and *Geobacter* species can also utilise electrically conductive appendages in the form of nanowires for the reduction of insoluble terminal electron acceptors (127,240,241). For *Geobacter*, there is a well documented alignment of *c*-type cytochromes along these nanowires that allows for direct transfer to insoluble TEA (114,241). In *Shewanella* species, OmcA has been implicated in metal oxide reduction (103), even though, in other works, OmcA appears to be incapable of facilitating metal oxide reduction (242). The removal of either of the decahaem cytochromes OmcA and MtrC results in a vastly diminished electron transfer ability (103,109). It has been suggested that OmcA, for example, localises to the outer membrane when heterologously expressed in *E. coli*, but only in the presence of a type II secretion system (120). The requirement for the type II secretion system for the correct localisation of OmcA and MtrC is also seen in wild-type *S. oneidensis* with further observations also identifying these two proteins being present in the external medium (243).

This chapter shows the development of a portable electron transporter harnessed from *S. oneidensis* MR-1 which allows for the introduction of an extracellular electron transfer ability into a non electrogenic strain. This synthetic electron transporter provides the genetic coding for a defined protein chain, allowing novel interaction between a strain incapable of extracellular electron transfer and a carbon electrode. To achieve this, different protein sets from the Mtr operon of *S. oneidensis* MR-1 were expressed in combination with overexpressed cytochrome maturation genes in *E. coli*. *Escherichia coli* was chosen for this project as it is the model prokaryotic organism for

synthetic biology techniques, with a vast number of studies documenting both heterologous expression of functional proteins and the introduction of foreign pathways (172,244–247). This versatile organism was chosen not only for these reasons, but also because functional expression of *S. oneidensis* MR-1 *c-type* cytochromes in *E. coli* has been shown to be possible for reduction of Fe (III) (105,107,120,125), but this does not confer the ability to produce current as demonstrated by the DMRB *Pelobacter carbinolicus* (122).

The highly conserved metal reduction genes within a large proportion of *Shewanella* species are MtrCAB and OmcA (108). These four proteins provide an electron transport pathway between the periplasm and insoluble extracellular terminal electron acceptors, all coded by genes located within a single operon on the genome. In order to channel electrons from the intracellular quinone pool to the periplasm, we relied on the *E. coli* host inner membrane electron donors as previously seen (105,107,125). The main hub of this activity was presumed to have originated from the *E. coli* orthologue of the *S. oneidensis* inner membrane tetrahaem cytochrome CymA, namely NapC (107). Some level of plasticity has been demonstrated within this network with residual iron reduction ability of MtrA in a *ΔnapC* mutant (125). The new construct relies on over-expression of cytochrome maturation genes and the type II secretion pathway found in B- type strains, both of which have been shown to be vital in previous experiments in which *S. oneidensis* outer membrane cytochromes were expressed (120,243).

This chapter demonstrates the importance of a complete electron transport chain from periplasmic tetrahaem cytochrome to outer membrane and extracellular decahaem cytochrome, acting as a terminal reductase within an engineered *E. coli*, permitting interaction with a carbon anode. At the time of experimentation this was the first documented example, to my knowledge, of a redundant strain, devoid of artificial mediators, being engineered through the introduction of a synthetic electron transport conduit to generate current within a bioelectrochemical system (BES). The subsequent publication of the paper by Goldbeck et al (124) employed a genetically

identical system to the one shown here with an added synthetic biology aspect that is discussed towards the end of this chapter.

In order to be able to determine the exoelectrogenic activity of strains, a BES was required. This chapter provides an insight into the many challenges of accurate, reproducible, high throughput testing of samples. A breakdown of the key points of each of the different BES tested is shown in Table 4.1.

Table 4.1 - Key points describing each of the different BES setups

MFC type (chapter section)	Anode/Cathode volume	Other notable mentions
UWE two chamber MFC (Chapter 4.2)	60 mL/60 mL	• Oxygenated cathode H_2O • Temperature kept at 25°C • Cathode water pumped through at 10 ml/min
Cambridge MFC (Chapter 4.4)	200 µL/200µL	• Multiple channel • Small volume • Quicker setup
Half cells (Chapter 4.6)	250 mL	• Single cell • Poised anode potential (Chronoamperometry)

4.2 University of West England (UWE) MFC

4.2.1 – MFC testing and strain analysis

The initial method of screening was through the use of a relatively large volume two chamber MFC with a 60 mL anode chamber volume and equal cathode chamber volume. This setup comprised a folded carbon veil anode and cathode (each with an area of 120 cm^2) with a Ni-chrome wire woven through and a VWR proton exchange membrane (PEM) separating the two compartments. Further descriptions of this can

be found in methods section (3.4.1.1). A diagrammatic representation of this MFC can be seen in Figure 4.1.

The main defining elements of this setup were the fact that the cathode solution was constantly replenished with fresh oxygenated distilled water in an attempt to increase the available oxygen and therefore capability for reduction to occur. The setup also had a relatively large volume with 60 mL of culture volume loaded into the anode chamber. This setup was left at open circuit potential for 1 hour to allow the large culture volume to settle and adapt to the environment. Once this was done, a polarisation curve was carried out as described in section 3.4.2.

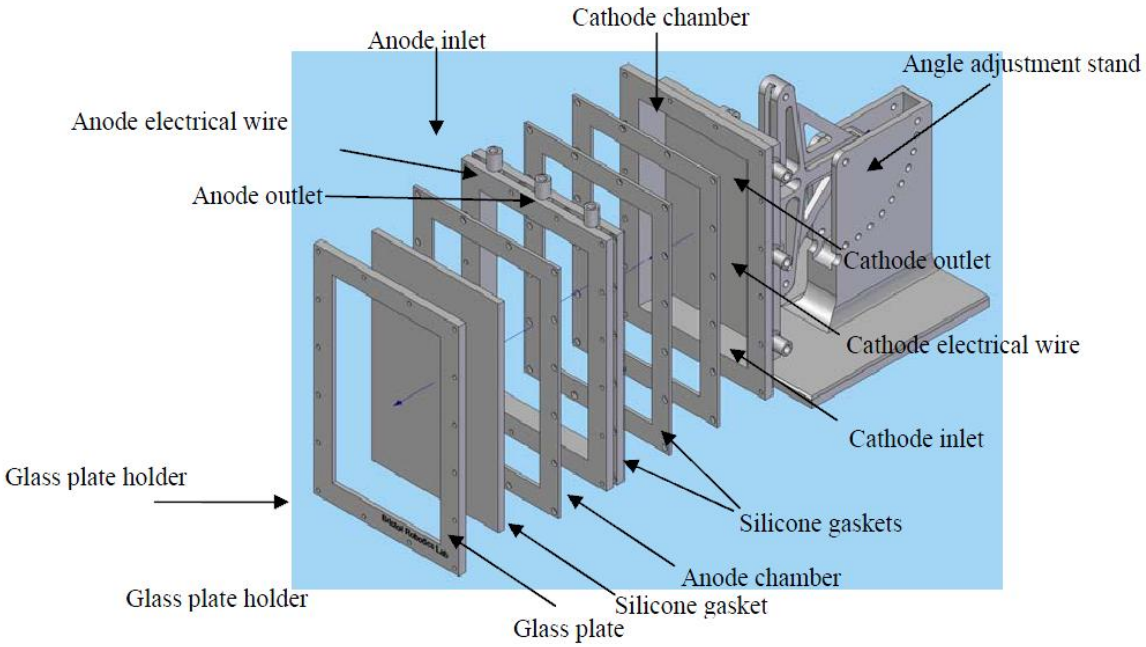

Figure 4.1 – Expanded view of the UWE MK1 MFC device

The results that were obtained required a number of calculations before more useful information could be acquired. The results that were collected during a polarisation curve were the change in voltage as the external resistance was reduced. An example of this can be seen in the Figure 4.2.

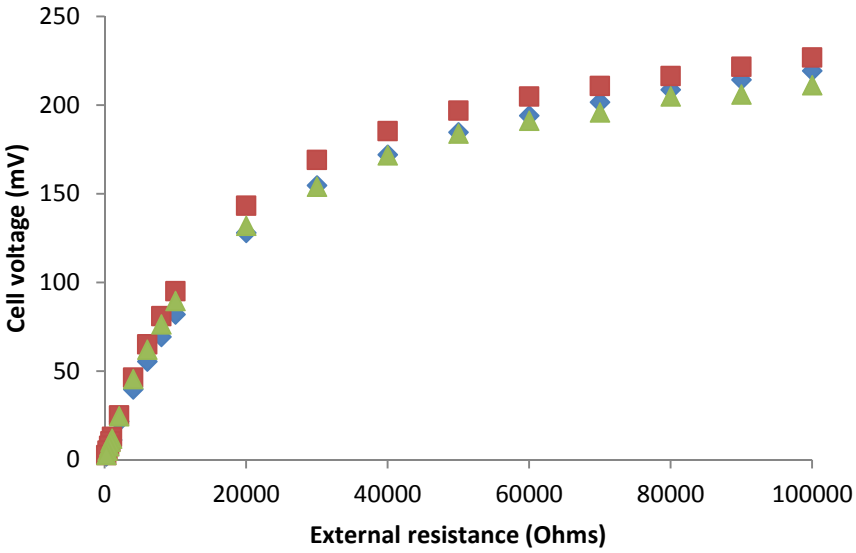

Figure 4.2 – Example of the results obtained from a polarisation curve of S. oneidensis MR-1. Results shown are for 3 biological replicates within a single UWE MFC showing the ability of the apparatus to reproduce results.

The example shown in Figure 4.2 is of the voltage values obtained from a triplicate analysis in a MFC of *S. oneidensis* MR-1 after applying a range of external loads (100kΩ-200Ω). The power density is then calculated from these results as detailed in section 3.4.2. Using the average of the results from the calculations the data was then plotted as a power density and cell voltage curves as shown in Figure 4.3. Figure 4.3 then allowed for the measurement of the resistance, in which the maximum power density was achieved. The point at which the greatest power density was achieved is equal to the internal resistance of the MFC. This is not just to do with the structural components of the cell, but also relates to the bacteria and their transfer mechanisms. The maximum power density achieved is a standard measure that is used to compare the power output achieved between different MFCs and strains. The analysis of the maximum power density achieved by two other strains (BL21 DE3 and BL21 DE3 pOmcA) is shown in Figures 4.4 and 4.5.

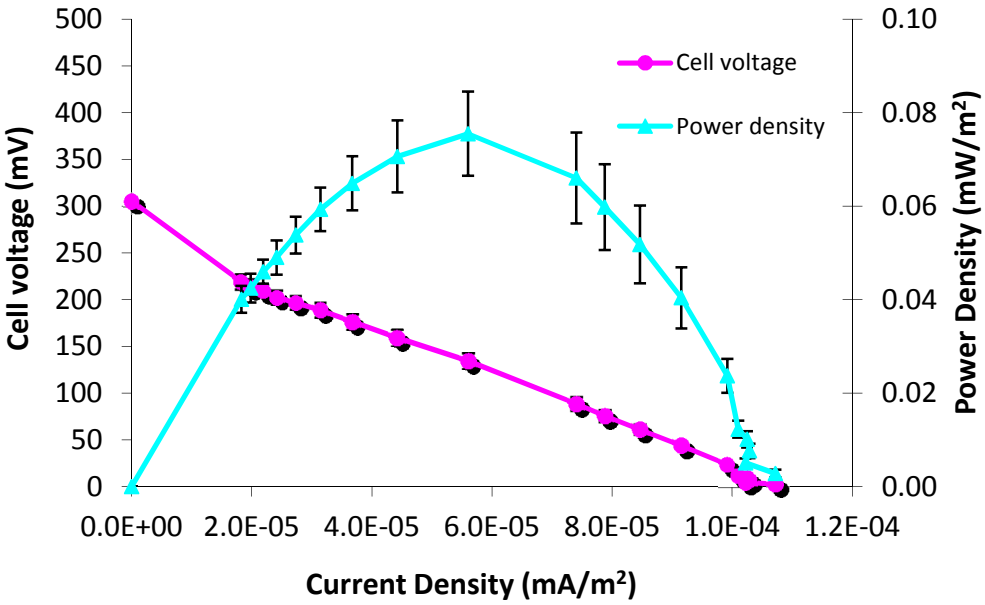

Figure 4.3 – Power density and cell voltage curves plotted using the average of the results from three biological replicate of S. oneidensis MR-1 following polarisation curves within 3 UWE MFCs. Results present show standard deviation from the median of the combined replicates.

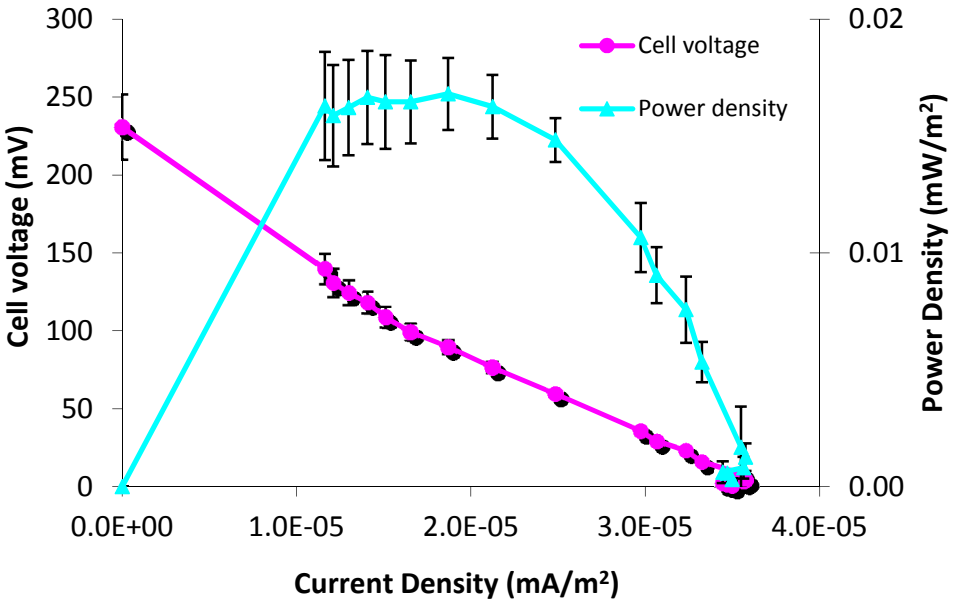

Figure 4.4 - Power density and cell voltage curves plotted using the average of the results from three biological replicates of BL21 DE3 following polarisation curves within 3 UWE MFCs. Results present show standard deviation from the median of the combined replicates.

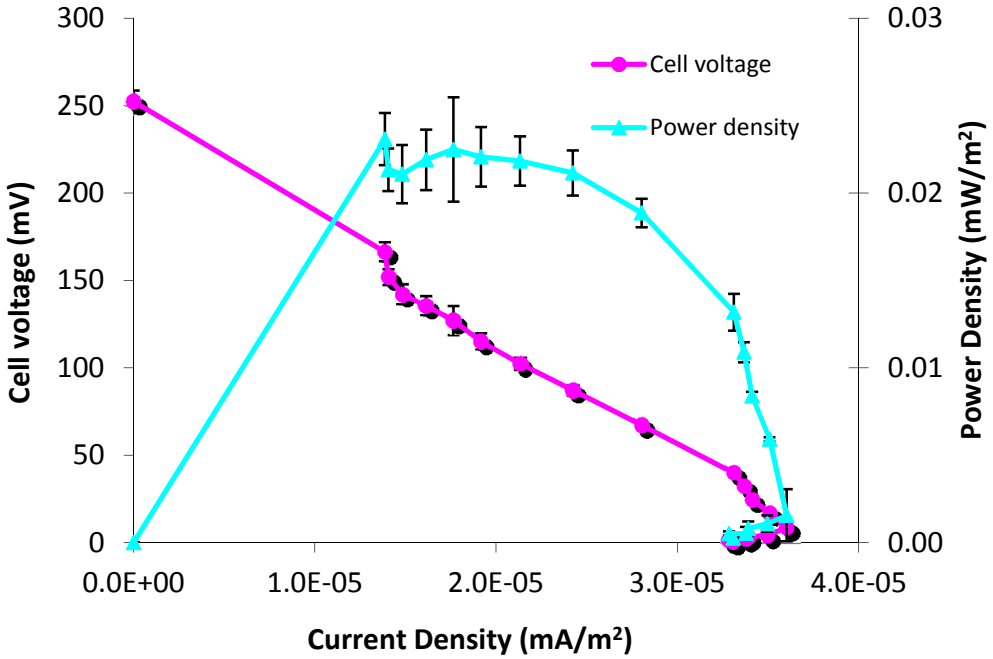

Figure 4.5 - Power density and cell voltage curves plotted using the average of the results from three biological replicates of BL21 DE3 pEC86 pOmcA following polarisation curves within 3 UWE MFCs. Results present show standard deviation from the median of the combined replicates.

The comparison of the maximum power density values from a variety of different strains (detailed in Table 3.11) allowed for the production of a bar chart of the results obtained in the initial MFC setup. The results were however, variable, as shown in Figure 4.6.

Figure 4.6 clearly shows a range of power outputs for the different strains that were tested in the MFC, with the highest power output being achieved by the naturally electrogenic DMRB *S. oneidensis* MR-1. All experiments were carried out in at least triplicate, often with many more. The median max power density from these runs is shown in Figure 4.6 with the standard deviation represented. In terms of the *E. coli* strains the lowest power output can be seen with the cytochrome maturation deficient strain Δ*ccm* (detailed in Table 3.11). There was a nearly 30% power increase with the use of the wild type *E. coli* strain *MG1655*, which may be due to the native

cytochrome maturation genes allowing expression of the endogenous *c*-type cytochromes present, which in turn may have allowed for electron transport to the anode. The results for strain JM109 pEC86 *MtrA* showed a return to the minimal power output observed for the control strain *delta ccm* even though cytochrome maturation genes and a periplasmic *c*-type cytochrome from *S. oneidensis* MR-1 are over-expressed in this strain. This could be explained by the observation that *MtrA* was thought to be a periplasmic protein in *S. oneidensis* and therefore *MtrA* may also be located solely in the periplasm even when over-expressed in *E. coli*; as a result it may not capable of transporting electrons outside of the cell. This correlates with the observation that heterologously expressed *MtrA* was unable to reduce insoluble Fe (III) as shown by Pitts et al (248), although it should be noted that the literature does not necessarily offer a direct correlation between electrogenesis and the ability to reduce Fe (III) (122). The expression of these additional proteins in this case may have caused an increased metabolic burden upon the cell and a further point of electron loss at *MtrA* as the electrons were not used for current production. The lack of power increase seen with K-12 pEC86 p*OmcA* could be explained by the cryptic nature of the type II secretion pathway in K-12, which prevents the expression of OmcA (249). The overexpression of cytochrome maturation genes and *OmcA* in BL21 DE3 produced an increased power output compared to wild type K-12. This appeared to show that the extracellular electron transfer ability demonstrated by Donald et al (249) where insoluble Fe (III) was reduced to Fe (II), did in fact also allow the engineered strain to transfer electrons to an anode.

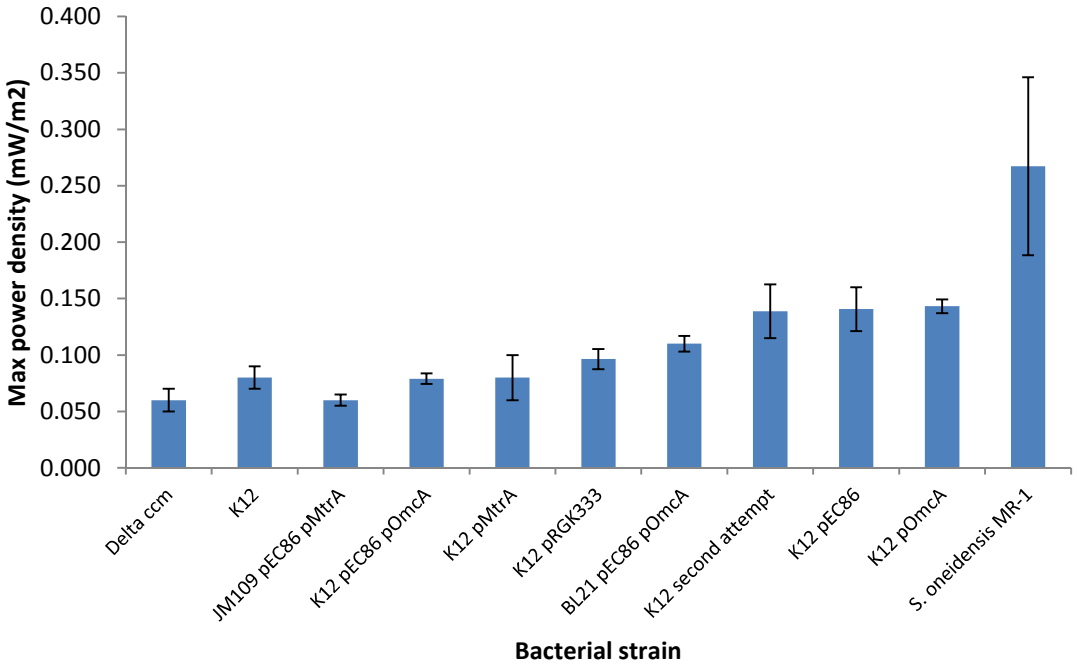

Figure 4.6 – Comparison of the power outputs achieved by a variety of bacterial strains within the first MFC setup. Results shown are the averages with standard deviation, from at least three biological replicates carried out within UWE MFCs. High level of variance can be seen between an initial batch of experiments compared to a later set.

4.2.2 Issues with UWE MFC

Although all of the strain tests were carried out in triplicate it was decided that K-12 should be retested. The variation in the obtained results being put into doubt as the power output produced this time was the highest yet achieved. This demonstrated a lack of reproducibility within the MFC setup being used.

This was not the only problem that was seen in this setup, as the MFC was made out of very pliable yet brittle plastic. The constant de- and reconstruction of them caused large cracks to occur at a certain point around the cell. Attempts were made to seal the MFC with silicon sealant, as shown in Figure 4.7**.** This was however only a very short term solution as the MFC would leak the next time it was assembled and would

in some cases not last the whole length of an experiment before beginning to leak, which could have affected the results.

Figure 4.7 – UWE MFC setup showing signs of wear and tear. Arrows indicate the points of the MFC that were breaking and required patching up with silicon sealant shown.

4.2.3 Alternative MFC options – Reading MFC

Following all of these issues, it was decided that an alternative setup should be used, one that would not be as awkward to assemble and that would be more resistant to wear and tear. This new fuel cell (schematic shown in Figure 4.8) consisted of a 2 chamber setup with internal volumes of 5 mL in the anode and cathode compartments. The device was much easier to assemble (7 layers but only 4 screws), primarily composed of Perspex (which provided greater durability) and with a total device size of approximately 55mm x 55mm it had a smaller demand on space. The cathode chamber still relied on the reduction of oxygen within distilled water, which was pumped into the cathode chamber at a rate of 1 mL/min. Cultures to be tested

were loaded into the anode chamber using a syringe and due to the smaller volume, in comparison to the UWE MFC, were allowed to settle for 30 mins in an open circuit configuration.

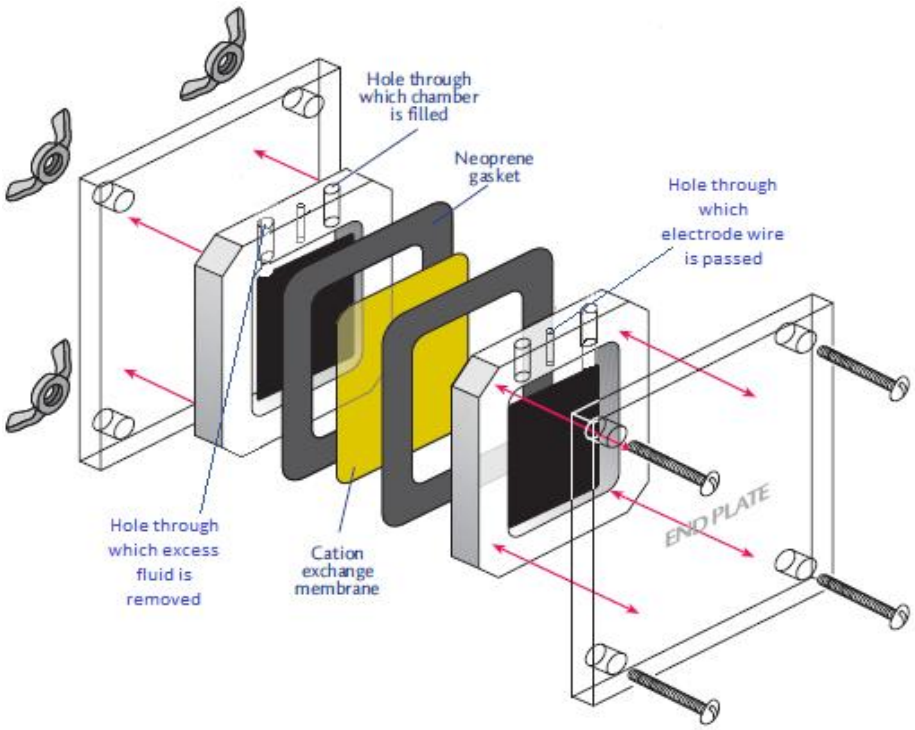

Figure 4.8 – A schematic for a smaller volume two chamber MFC – (Modified from Madden* (250)*)

The use of this MFC setup provided more reproducible results and allowed for the re-testing of the most promising initial engineered strain, BL21 DE3 pEC86 p*OmcA*. The testing and comparison of this strain against standard BL21 DE3 and *S. oneidensis* MR-1 produced the results seen in Figure 4.9.

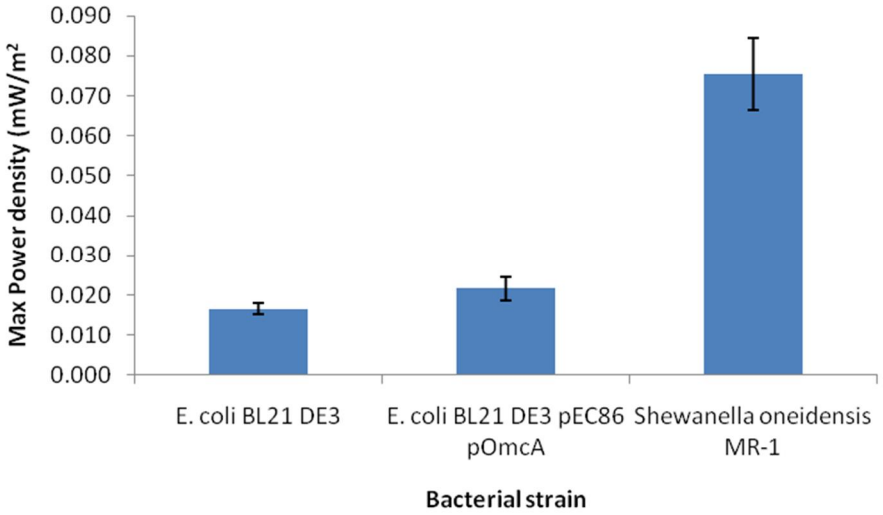

Figure 4.9 – Comparison of the maximum power density of E. coli strains to S. oneidensis MR-1. Results shown are the average and standard deviation of at least three biological replicates carried out within the Reading MFC. The difference observed between BL21 DE3 and BL21 DE3 pEC86 pOmcA was significant (p-value = 0.05)

Tests for the *E. coli* strains were carried out 5 times to ensure that the results obtained were reproducible. Figure 4.9 shows a statistically significant increase in activity in BL21 DE3 following the addition of pEC86 and p*OmcA* as determined by an unpaired *t*-test, *p*-value = 0.05. This was determined to be an increase of 29% from 0.017 mW/m^2 to 0.022 mW/m^2. This is obviously still significantly lower than that demonstrated by the naturally electrogenic *S. oneidensis* MR-1. This organism does however have a fully developed method for extracellular electron transport whereas this *E. coli* strain only has the addition of a single *c*-type cytochrome from this pathway. The theory postulated at this point in the project was that the addition of further cytochromes may well aid in increasing the achievable power output. As there are at least 4 *c-type* cytochromes that have been shown to be important in the production of power in *S. oneidensis* MR-1, it seemed reasonable to assume that the further addition of these may increase the ability of *E. coli* to transport electrons to an anode.

4.2.4 Post UWE MFC experiments

4.2.4.1 – Visual analysis of biofilm by SEM

At this point in the project it was decided that the analysis of biofilm formation within the MFC setup being used should be attempted. An *S. oneidensis* MR-1 culture was allowed to develop within an MFC for 30 days at a fixed resistance of 20 kΩ (resistance at which max PD previously noted in device – Figure 4.3) within the UWE MFC setup. Although issues were noted with this setup, it provided a much larger overall anode area for colonisation by *S. oneidensis* MR-1 and was much better suited to long term analysis instead of high throughput testing. The anode was then analysed using SEM as described in Section 3.6

Figure 4.10 clearly shows intimate contact of the cells with the carbon anode and appears to show the early stages of biofilm development as seen by the somewhat fluffy appearance to the cells in Figure 4.10 A. This could be caused by the production of EPS to allow the biofilm to grow. The cells appear to be the correct length of approx 2 µm which is easier to determine in Figure 4.10 B.

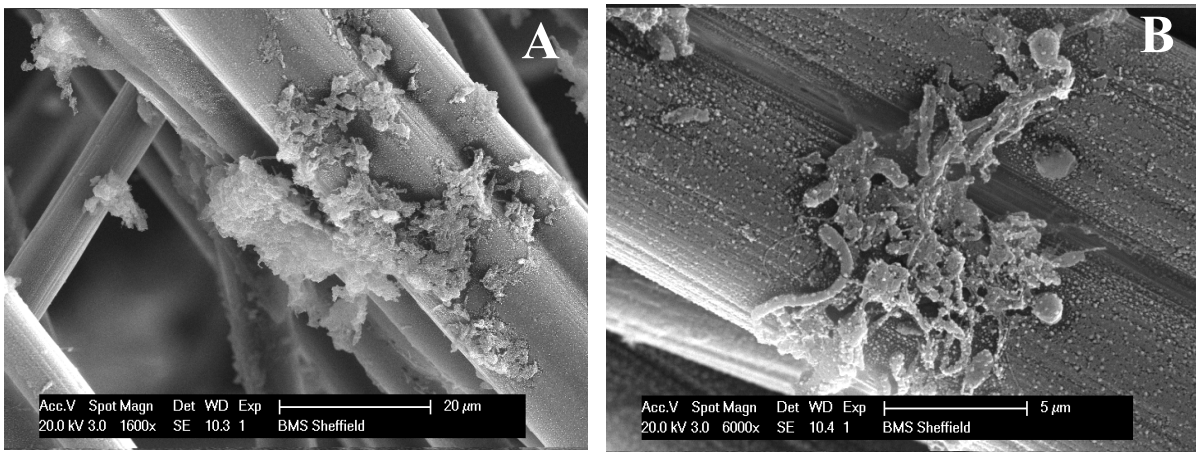

Figure 4.10 – SEM image of S. oneidensis MR-1 anodic biofilm A) 1600 x magnification B) 6000 x magnification

4.2.4.2 Construction of MR-1 electrogenic gene cluster plasmid

Following on from the initial experiments, it was decided that in order to try and increase the power density achieved in the MFC using an engineered *E. coli* strain, a more complete exoelectrogenic pathway was required. Instead of relying on the overexpression of the single *c*-type cytochrome OmcA alongside overexpressed cytochrome maturation genes, a variety of options with regard to the "completeness" of the Mtr pathway were proposed. These consisted of individual plasmids containing the following options:

- OmcA
- MtrCAB
- MtrCAB and OmcA
- MtrDEF, OmcA and MtrCAB

The following section gives a brief description into the considerations taken

4.2.4.3 Bioinformatic analysis

In order to determine if the construction of a plasmid containing the electrogenic gene cluster from *S. oneidensis* MR-1 was possible, a preliminary bioinformatic analysis of the genes and encoded proteins was carried out. Although only the restriction site analysis was required for the construction of the plasmid, the other tools provided valuable information about the expression and predicted localisation of the proteins.

4.2.4.3.1 Signal peptides

The results of the analysis of the amino acid sequence resulted in a signal peptide being predicted for every protein encoded within the gene cluster. An example of the results obtained from this analysis can be seen with the example of *OmcA* in Figure 4.11 (Details obtained from analysis of all other proteins can be found in the appendix).

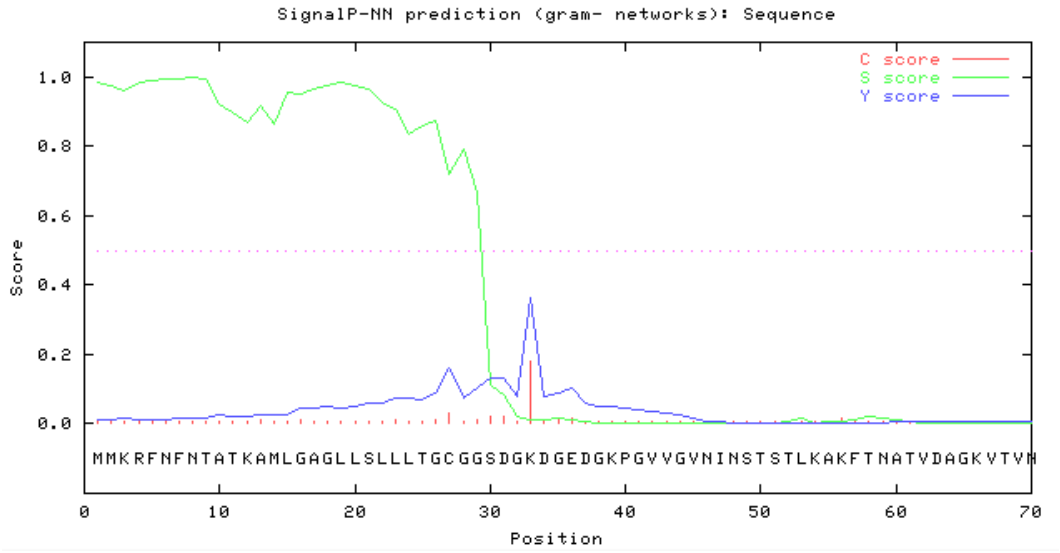

Figure 4.11 – Graphical output for the signal peptide prediction along the entire protein for OmcA from S. oneidensis MR-1. Analysis performed on SignalP 3.0 (251)

The S score is predicted for every amino acid within the protein with a high score being indicative of its role within a signal peptide, whilst low scores suggest a lack of involvement. The C score is the position of the predicted cleavage site; this point is considered the end of the signal peptide. All subsequent amino acids are considered part of the mature protein. This prediction can sometimes be seen numerous times within a sequence as shown at residue 27 in Figure 4.11 along with the other predicted site at residue 32. There is however only one true cleavage site, which is determined through the use of the Y-score. This is a combination of the S and C scores that provides a better prediction. This is done by combining the position of a significant C-score with a position where the slope of the S-score is steep. A prediction is also presented at the end of the results that indicates the probability of a signal peptide and also the position of the cleavage site. The higher the probability, the greater the chance of a signal peptide being present:

Prediction: Signal peptide

Signal peptide probability: 1.000

Max cleavage site probability: 0.908 between pos. 32 and 33

As all the proteins that were encoded within the cluster were predicted to be expressed in the periplasm or outer membrane in *S. oneidensis* MR-1 it is not unexpected that the proteins all have predicted signal peptides.

4.2.4.3.2 Transmembrane helices

The proteins were also analysed for the presence of transmembrane spanning regions. The results from this analysis predicted that only one of the proteins was believed to have a transmembrane spanning region. This protein was *MtrA*, which has been identified as a periplasmic protein within *S. oneidensis* MR-1, but also appears to cross between the membrane. Figure 4.12 presents the predicted transmembrane helices within *MtrA* (Details obtained from analysis of all other proteins can be found in the appendix). In this case there is a predicted membrane spanning region.

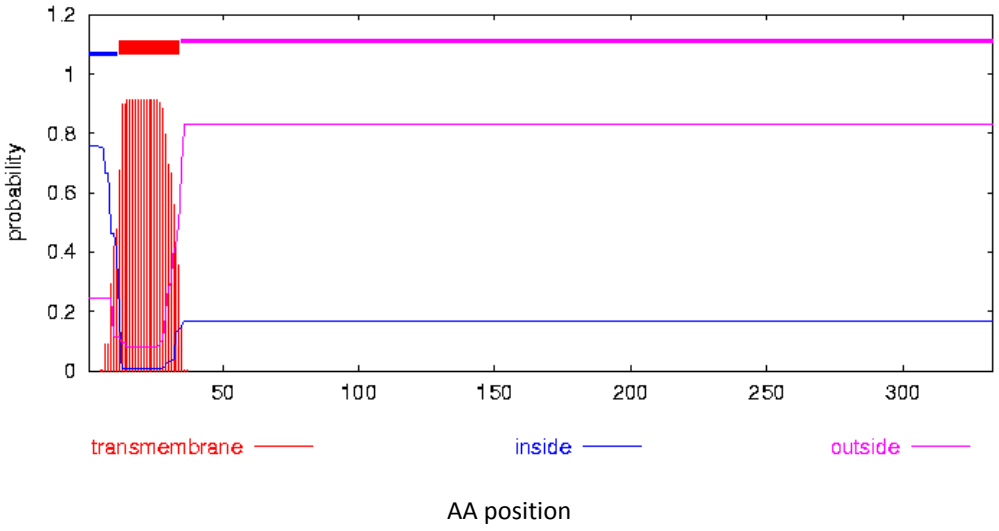

Figure 4.12 – Predicted transmembrane helices within MtrA

Sequence Length:	333
Sequence Number of predicted TMHs:	1
Sequence Exp number of AAs in TMHs:	20.26577
Sequence Exp number, first 60 AAs:	20.26558

Sequence Total prob of N-in: 0.75587

Sequence POSSIBLE N-term signal sequence

Sequence	***TMHMM2.0***	***inside***	1	11
Sequence	***TMHMM2.0***	***TMhelix***	12	34
Sequence	***TMHMM2.0***	***outside***	35	333

The position of this region is predicted as being between amino acid residue 12 and 34, with the N-terminal of the protein residing in the cytoplasm and the remainder of the protein predicted to be outside the cytoplasm.

4.2.4.3.3 Identification of restriction sites

In order to be able to clone the desired gene cluster into a plasmid of choice the available restriction sites must be identified to show which restriction enzymes digest the sequence. This then allows for the choice of restriction sites to attach to the end of the sequence through the use of primers that will allow for it to be inserted into a plasmid.

All of the gene clusters were searched through Webcutter 2.0 and NEBcutter 2.0. An example of the results obtained from this can be seen from the analysis of the entire gene cluster (*MtrD, E, F, OmcA, MtrC, A and B*) shown in Figure 4.13.

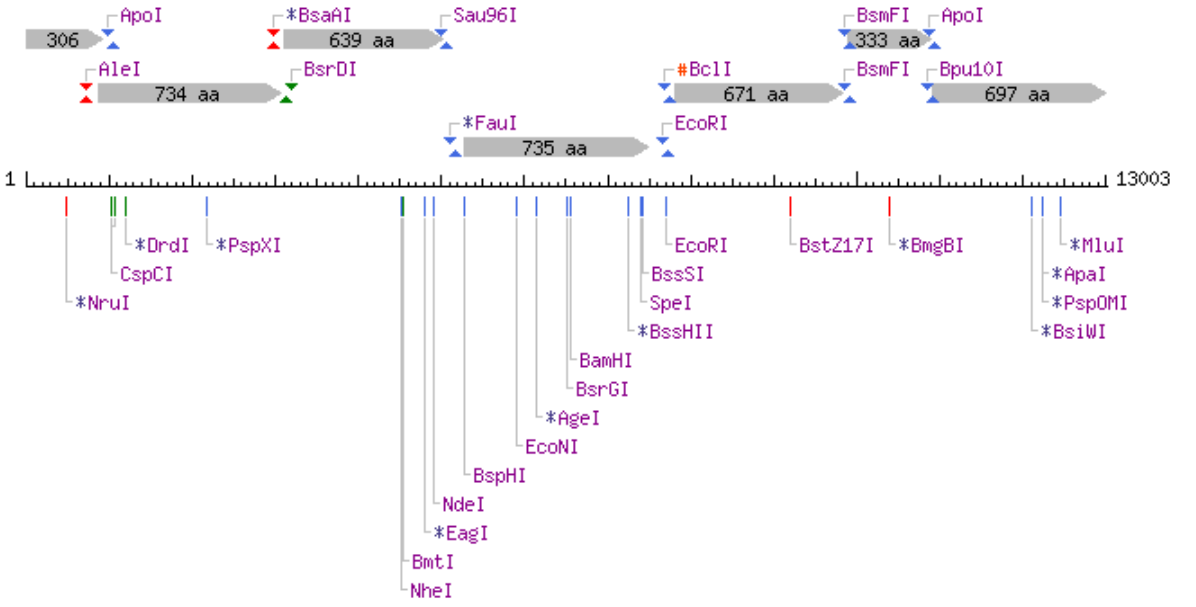

Figure 4.13 – Overview of some of the restriction sites seen within the MR-1 electrogenic gene cluster

As the programs allow for a comprehensive search for restriction sites using all NEB restriction enzymes, the list of the sites acquired is vast. A more useful piece of information in this case was the identification of enzymes that do not cut the sequence and are also present within the multiple cloning sites (MCS) of pACYCDuet-1.

The following endonucleases were selected but do not cut this sequence:

AatII, AccBSI, AscI, AspI, AtsI, BsrBI, BstD102I, CciNI, Cfr9I, CpoI, CspI, DraII, EcoO109I, FseI, NotI, PacI, PmeI, PpuMI, PshAI, Psp5II, PspAI, PspALI, RsrII, SapI, SbfI, SexAI, SgfI, SgrAI, SmaI, SmiI, SrfI, Sse8387I, SwaI, Tth111I, XbaI, XmaI.

From these results and the comparison to the MCS shown in Figure 4.14, the most suitable restriction sites to use were determined to be *AscI* and *NotI*.

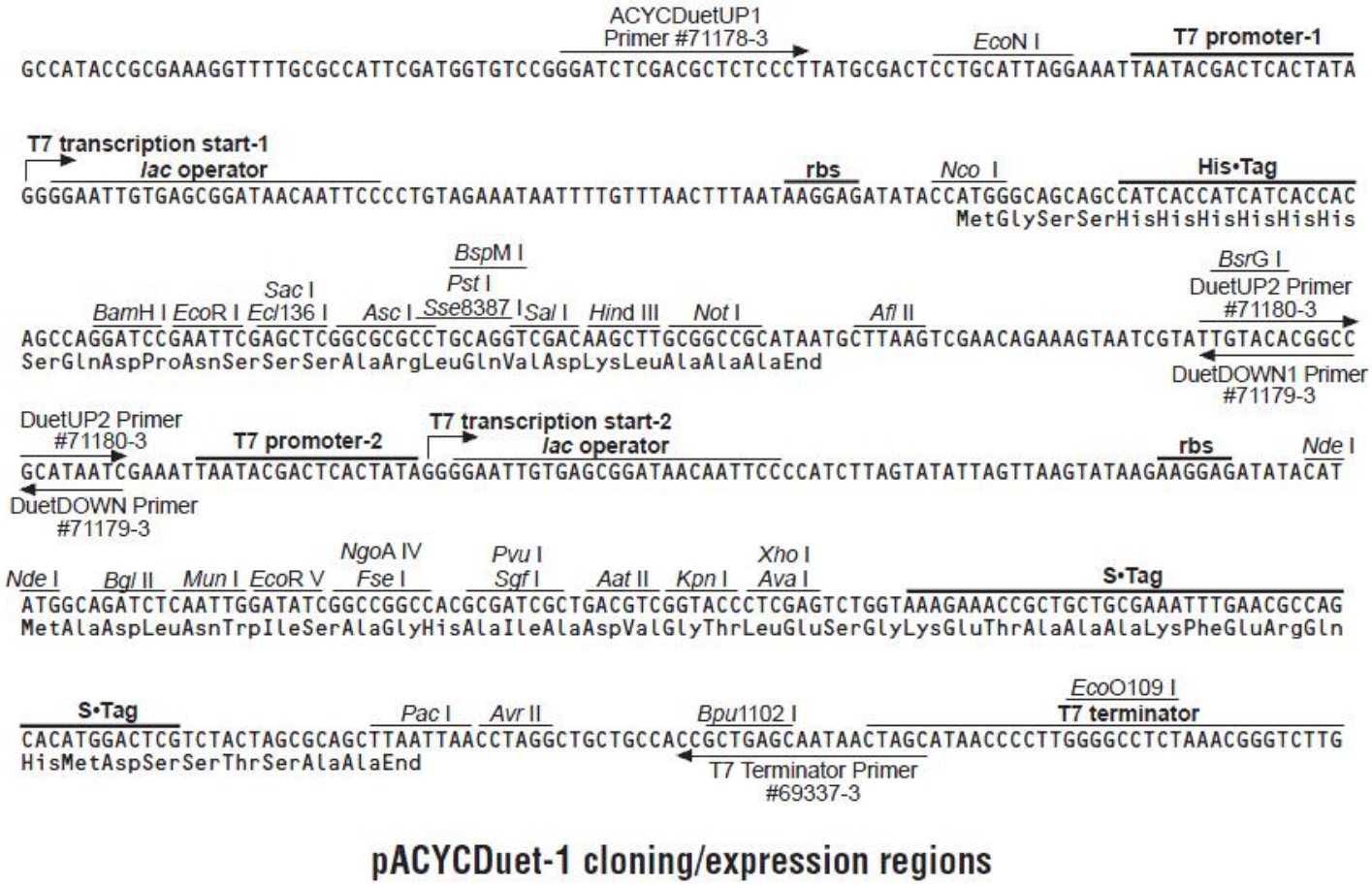

pACYCDuet-1 cloning/expression regions

Figure 4.14 – Multiple cloning sites of pACYCDuet-1

4.2.4.3.4 Predicted protein molecular weight

The predicted molecular weight and isoelectric point of each of the individual proteins within the gene cluster was calculated. The results can be seen in Table 4.2

Table 4.2 – Predicted molecular weight and isoelectric point of MR-1 proteins

Protein	Molecular weight (kDa)	Signal peptide (AA c.pos)
OmcA	79	Yes (32,33)
MtrA	36	Yes (33,34)
MtrF	67	Yes (23,24)
MtrD	33	Yes (15,16)
MtrE	79	Yes (31,32)
MtrC	71	Yes (21,22)
MtrB	78	Yes (21,22)

4.2.4.4 Agarose gel analysis of DNA fragments

In order to be able to construct an efficient current producing organism using proteins from highly electrogenic strains, the interaction of the proteins with the *E.* coli native metabolic pathways needed to be established. As discussed in the literature review in chapter 1, the work conducted by Pitts et al (248) and Donald et al (249) showed that it was possible for this to occur through the use of *OmcA* and *MtrA.* These examples however only allowed for the reduction of Fe (III) and this does not directly confirm or prove the ability to produce current. Our results show that the introduction of *OmcA* from *S. oneidensis* MR-1 only produces a 29% increase in power output. The addition of further cytochromes may then allow for further increase in power output as the extracellular electron transport pathway becomes more developed.

The genomic DNA (gDNA) from *S. oneidensis* MR-1 was successfully prepared as shown in Figure 4.15.

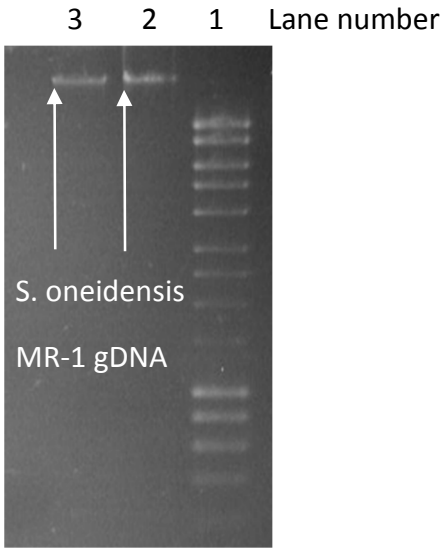

Figure 4.15 – S. oneidensis MR-1 genomic DNA – Lane 1 – Hyperladder I. Lane 2 and 3 – S. oneidensis MR-1 gDNA.

As the gDNA was now assumed to have been obtained, several PCR reactions were setup in an attempt to amplify the desired gene fragments. All of the fragments were believed to have been successfully amplified on the first attempt as shown in Figure 4.16. This can be seen in the production of clear bands of the correct size following the PCR reaction. These bands were all very bright and distinct from others present and therefore considered to have a high enough DNA concentration to be able to continue working with.

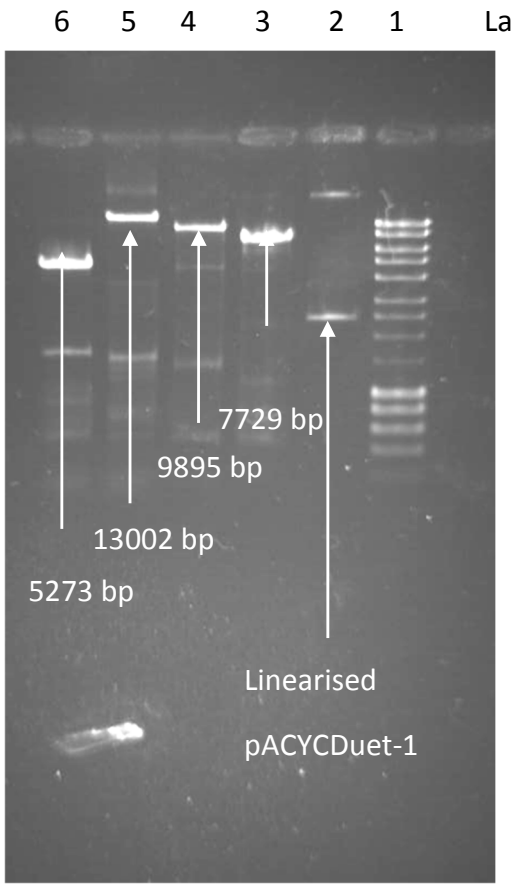

Figure 4.16 – S. oneidensis MR-1 PCR products – Lane 1 – Hyperladder I. Lane 2 – Undigested pACYCDuet-1. Lane 3 – MR-1 gene fragment 1 (OmcA – MtrB – 7729 bp). Lane 4 – MR-1 gene fragment 2 (MtrF – MtrB – 9895 bp). Lane 5 – MR-1 gene fragment 3 (MtrD – MtrB - 13002 bp).

The digested plasmid of pACYCDuet-1 shown in Figure 4.17 produced 2 bands showing that the plasmid had not been fully digested. The enzymes used are not compatible under the use of any of the supplied New England Biolabs buffer but the digest was done using a multicore buffer, which should have allowed for the reaction to occur unaffected.

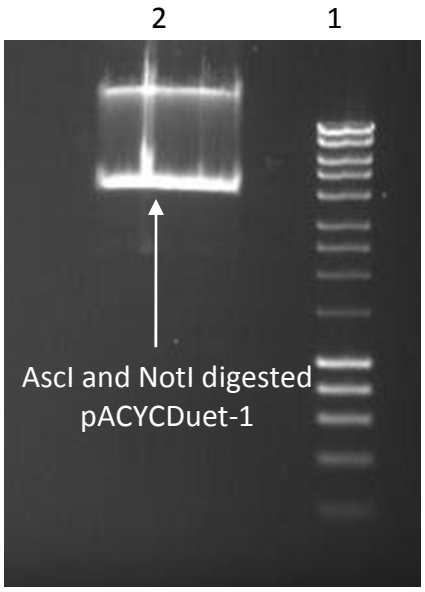

Figure 4.17- AscI and NotI digested pACYCDuet-1 – Lane 1 – Hyperladder I. Lane 2 – AscI and NotI digested pACYCDuet-1.

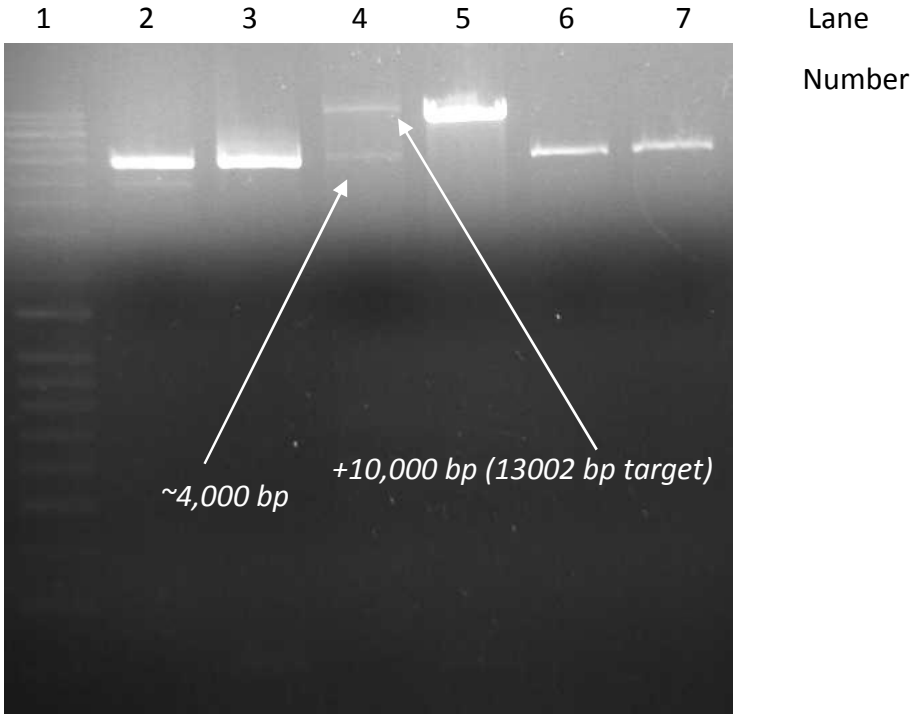

Figure 4.18 – Clone screening for pACYCMR-1 (MtrDEF,OmcA,MtrCAB) AscI and NotI digested. Lane 1 – Hyperladder, Lane 2 – Empty plasmid, Lane 3 – Empty plasmid, Lane 4 – Successful clone, Lane 5 – Unknown, Lane 6 – Empty plasmid, Lane 7 – Empty plasmid

4.2.5 Concluding remarks

The results obtained from the initial MFC setup demonstrated for the first time the ability to introduce electrogenic activity into a foreign organism although not to a particularly substantial level. The first published demonstration of this activity was by Goldbeck et al (124). There were differences between the two approaches as Goldbeck et al chose to focus on a single Mtr system with MtrCAB and instead tune the expression of it through promoter modifications to alter transcript levels. The thoughts considered at the time of discovery was that activity may be able to be further developed through the use of additional cytochromes, synthetic biology techniques and metabolic engineering. The development of the plasmids using various gene fragments of the MR-1 electrogenic cluster was done to help determine the genes essential to power production and which ones present a metabolic burden.

The limitations of the initial MFC were considered too great to carry on working with this type of device and so a new device was sought to combat the following limitations:

- This MFC had a large anode area but only a very small area of it was actually in contact with the cells. The large culture volume and sedimentation of the cells meant that this was only at the bottom of the anode. The MFC was tilted to try and alleviate this issue but the fact that the anode was run in batch mode didn't aid in the movement of bacteria within the chamber.
- The device was a pretty large size and when testing was being attempted in triplicate on a daily basis this meant:
    - Setting up three large MFCs
    - Loading the cells
    - Settling for an hour
    - Doing a polarisation curve
    - Processing the data
    - Cracking open the MFCs
    - Cleaning the MFCs and having them ready for the next day

The relatively complex nature of the setup meant that this was not really feasible, especially if trying to attempt any other work simultaneously.

- Managing to setup three MFCs was hugely time consuming and size of the equipment setup for this (including water tank, heater, oxygenator and MFCs) was very large, meaning that it would have been impossible for a single person to do any more replicates in one go.
- On top of this, the setup was fairly delicate making it unsuited to continual assembly and disassembly. Doing this resulted in high levels of wear and tear, including ripping of PEM leading to leaking from the cathode to anode. This then had the knock on effect of altering the available volume to load into anode.

Knowing all the limitations of the current device, the desired characteristics were also known. These were as follows:

- A more durable setup, capable of withstanding repeated assembly and disassembly
- A smaller scale system to allow for quicker setup, cleaning, less parts susceptible to damage
- Multiplexing capabilities to allow for more rapid testing of strains
- A high level of reproducibility

The advantages of the smaller setup provided by the Reading MFC due to the smaller testing setup, reduced setup time and more durable material made it a much better testing setup than the first MFC. This was however, still not considered to meet the testing criteria (especially with regards to the high throughput aspect) for the project and so other options were sought.

4.3 University of Cambridge MFC

4.3.1 MFC testing and strain analysis

With the information in hand about the desired MFC, a search of other groups with suitable devices was carried out.

The strains that were tested in chapter 4.2 were sent to a lab in the University of Cambridge for testing in a small volume, dual chamber, multiple channel MFC.

Results are presented in Figure 4.19:

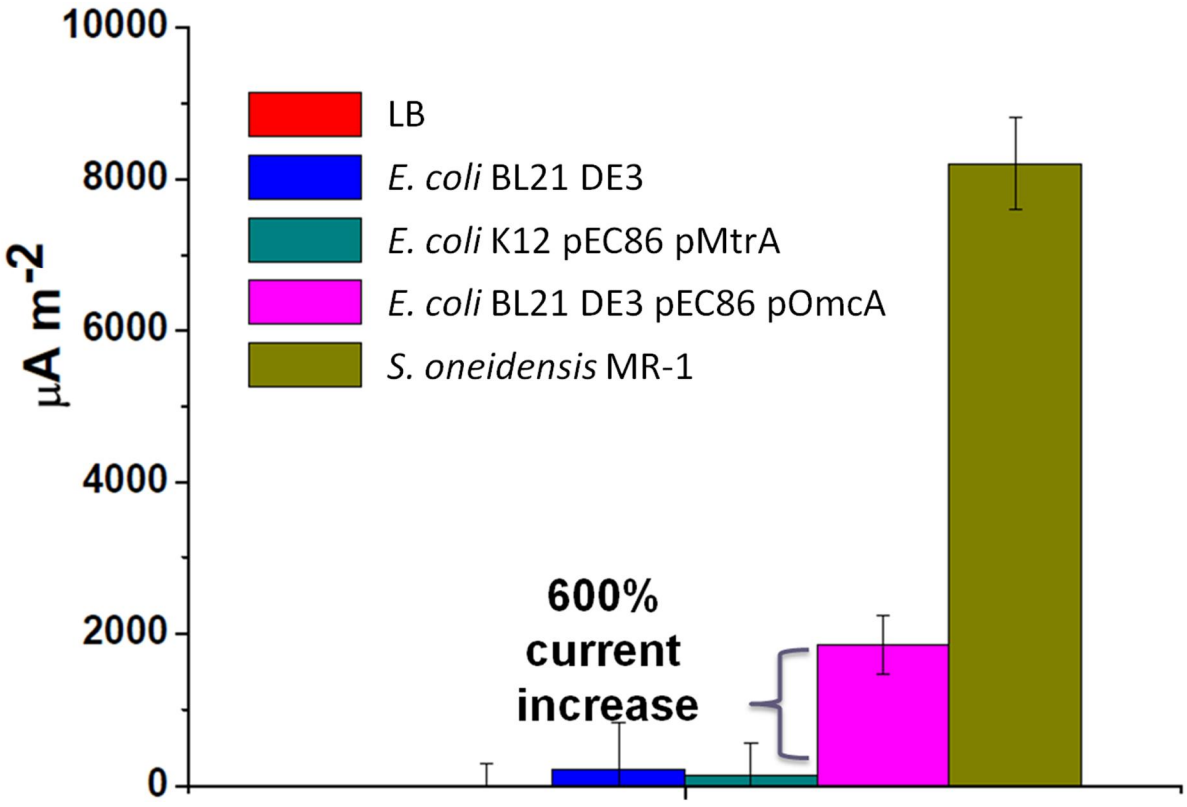

Figure 4.19 – Current generation in a Cambridge, low volume, multiple- independent channel MFC. Results shown are averages with standard deviation from at least three biological replicates carried out within the University of Cambridge MFC. Differences between BL21 DE3 and BL21 DE3 pEC86 pOmcA were statistically significant (p-value=0.0001)

The Cambridge MFC was built and transferred to Sheffield. This MFC setup utilised a much lower volume than the UWE MFC, permitted much quicker assembly and had multiple channels. All of these advantages made this a much simpler device to work with although the low chamber volumes (200 µL) brought challenges with it as well. The device was very delicate and needed to be handled very carefully, ensuring proper alignment of all components. The chamber volume was so low that the chamber vessels had to be loaded with a syringe, this is itself is not an issue but it meant that air pockets could form in the chamber that could not be removed easily and sometimes required the device to be opened and cleaned out to ensure no gaps.

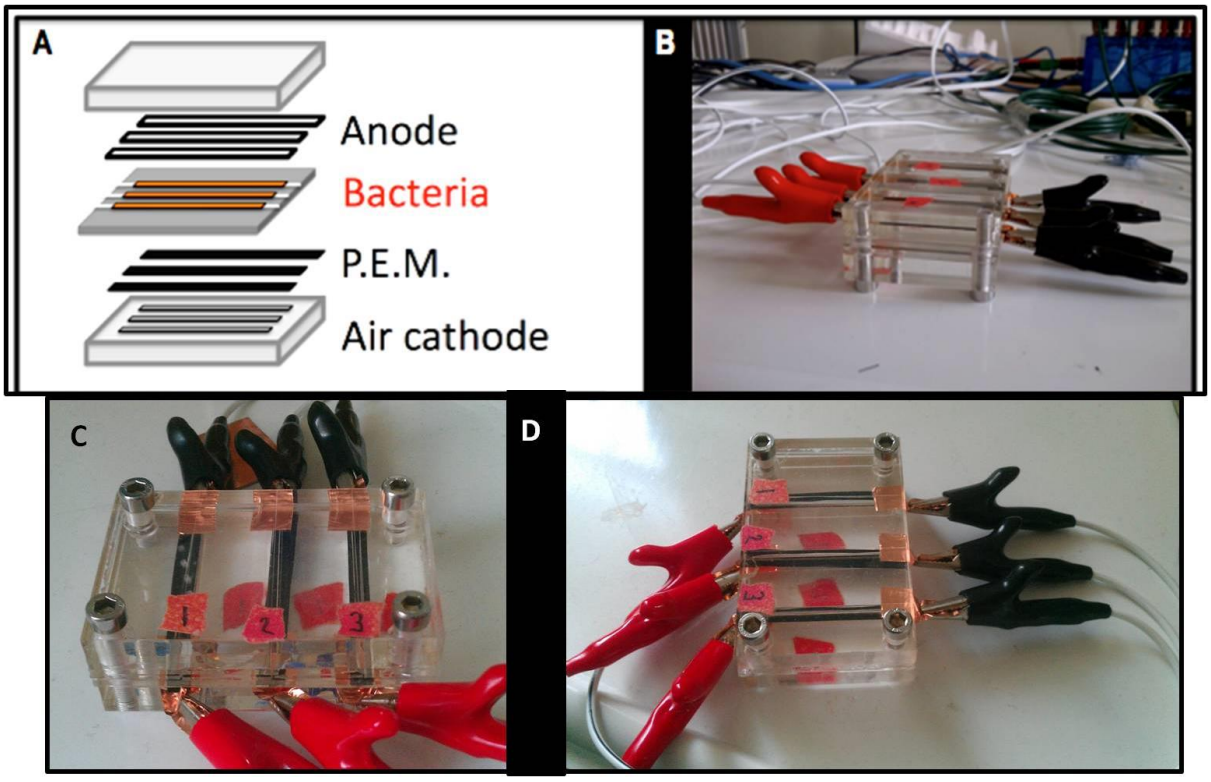

Figure 4.20 – Schematic diagrams and photographs of the Cambridge microfluidic microbial fuel cell (µMFC). (A) Schematic representation of the microfluidic microbial fuel cell (µMFC). (B-D) Photographs of the µMFC.

The initial assessment that had to be carried out once the MFC was delivered and built was to replicate the results obtained in Cambridge apart from K12 pEC86 pMtrA. This

was due to the fact that this single *c*-type cytochrome was shown not to be capable of insoluble metal reduction or generating current in previous experiments. The results from the in house test are shown in Figure 4.21.

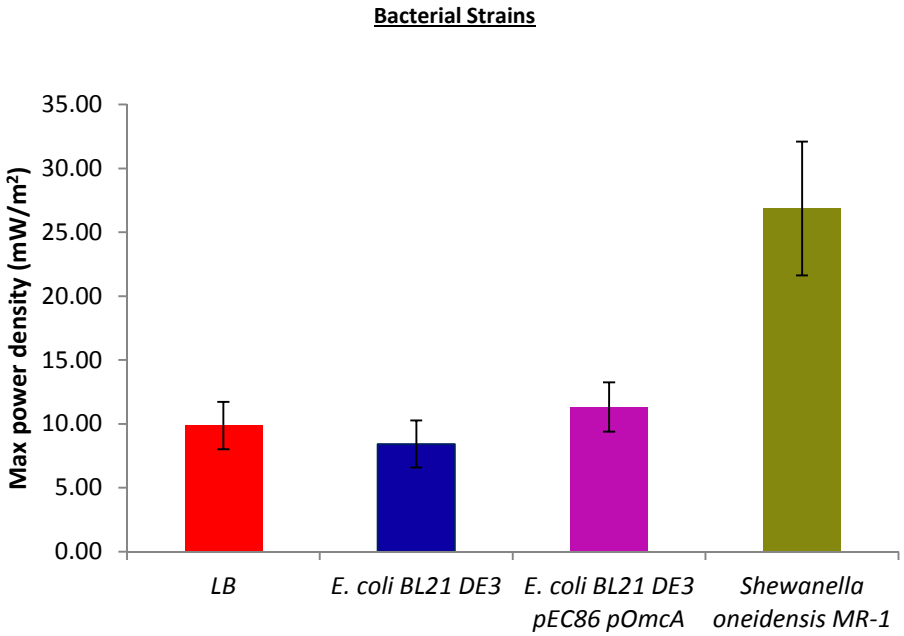

Figure 4.21- Initial in house replication of Cambridge results in Cambridge multichannel MFC. Results shown are averages with standard deviation from at least three biological replicates carried out within the University of Cambridge MFC. Differences between BL21 DE3 and BL21 DE3 pEC85 pOmcA were shown to not be statistically significant.

Although this result was carried out using power density instead of current density, the level of difference between empty media (LB), *E. coli* BL21 DE3 and the engineered strain is nowhere near where it is shown in the results obtained from Cambridge. The reasons behind this are uncertain. The biological setup was exactly the same as that used in Cambridge, but the results could not be repeated in Sheffield.

4.3.2 Expression of *S. oneidensis* MR-1 cytochromes in *E. coli*.

To introduce electrogenic activity into the host *E. coli* strain, a variety of plasmids were created in which cytochrome gene expression was under the regulation of a T7lac promoter as described previously.

The plasmids pACYCOmcA (OmcA), pRSFOmcA-MtrCAB (OmcA-MtrCAB), pACYCMtrDEF (MtrDEF) and pACYCMR-1 (MtrDEF, OmcA, MtrCAB) were created and tested. The use of an additional IPTG inducible plasmid, pRGK333 (Figure 4.22) containing cytochrome maturation genes (ccmABCDEFGH, denoted ccm), was required in combination with the recombinant *S. oneidensis* cytochromes, due to the lack of expression of the equivalent maturation genes within *E. coli* under aerobic growth conditions (252)**.** The need for anaerobic conditions was to ensure prevention of the use of oxygen, as the terminal electron acceptor, as this has a preferential redox potential over the anode. Although the anode is considered an anaerobic or more likely a microaerobic environment, which is conducive to the expression of the native *E. coli ccm* genes, the inducible basing of the gene set allowed for more controlled induction. This meant that in theory there would be no variation between the amount of *ccm* expression seen in each strain and replicate, which may not have been the case if it was based on how anoxic the anode was.

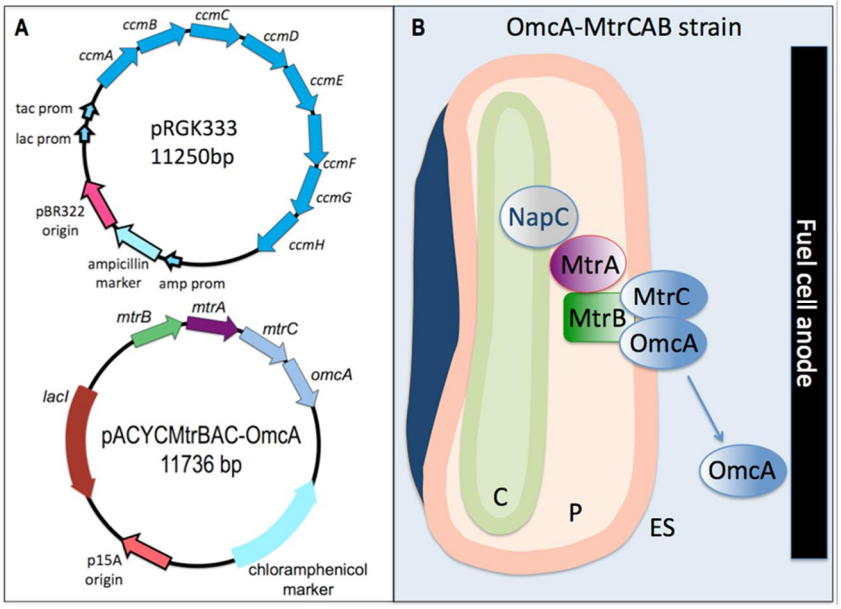

Figure 4.22 - (A) Two of the plasmids used in this chapter; pRGK333, an IPTG inducible E. coli cytochrome maturation protein over-expression plasmid (Feissner et al. 2006) and the Shewanella cytochrome expression plasmid pACYCMtrCAB-OmcA(B) Heterologously-synthesised decahaem cytochromes (MtrA-C and OmcA from Shewanella oneidensis MR-1) potentially involved in the transfer of electrons for the novel E. coli strains. (C refers to cytoplasm, P to periplasm, and ES to extracellular space).

To test the hypothesis that the more engineered strain, with a larger number of cytochromes would generate more current, the expression of the target protein was firstly attempted. In order to determine successful expression of the desired cytochromes, the cells needed to be tested for the presence of the proteins. The chosen methodology for this was the purification of the proteins from the cells followed by SDS-PAGE and in gel digestion (full methods detailed in chapter 3). Table 4.3 shows the identification of the expressed proteins within their relevant strains.

Table 4.3 – Analysis of engineered E. coli strains with the portable electron transporter assembly. The proteins identified are from the Mtr operon of S. oneidensis MR-1 through the use of Auto MS(n) and/or HPLC-ESI-pSRM (pseudo-selective reaction monitoring – see text) MS/MS, after resolving protein extractions via 1D SDS-PAGE. A Phenyx AC score of at least 5.0 was considered an unambiguous identification. Brackets indicate the number of unique peptides from the total number identified.

Mtr plasmid within *E. coli* strain	Expressed proteins	Fraction identified	Phenyx AC score	Coverage %	Number of peptides
pACYCOmcA	OmcA	Soluble	23.77	5	6 (3)
	OmcA	Insoluble	23.26	5	8 (3)
	OmcA	Insoluble	14.47	3	3 (2)
pACYCOmcA-MtrCAB	MtrC	Insoluble	13.75	3	3 (2)
	MtrA	Soluble	5.77	4	1 (1)
	MtrA	Insoluble	7.36	3	2 (1)
	MtrB	Soluble	11.23	4	2 (2)
	MtrB	Insoluble	8.37	1	3 (1)
	OmcA	Soluble	12.45	3	3 (2)
	OmcA	Insoluble	10.69	3	3 (2)

The following peptides were identified from OmcA:

OmcA

Identified peptides:

SNVVTGIALGR	VTYSADATQR	GYQWQAYINAK
GFALSNSK	FTNATVDAGK	GGYGVEDVVATPCSTDTR
TFTIDSTNSNLK	FGIAQLTPVK	EFISDPSAYTK

These peptides map onto the target protein as follows:

>gi|24347602|gb|AAN54832.1|AE015622_1 decahaem cytochrome c [*Shewanella* oneidensis MR-1]

MMKRFNFNTATKAMLGAGLLSLLLTGCGGSDGKDGEDGKPGVVGVNINSTSTLKAK**FTNATV DAGK**VTVNFTLENANGVAVLGLTKDHDLR**FGIAQLTPVK**EKVGETEADR**GYQWQAYINAK**KE PGTVPSGVDNLNPSTQFQANVESANKCDTCLVDHGDGSYSYTYQVNVANVTEPVK**VTYSADA**

TQRATMELELPQLAANAHFDWQPSTGKTEGIQTRNVVSIQACYTCHQPESLALHGGRRIDIEN
CASCHTATSGDPESGNSIEFTYMIHAIHKGGERHTFDATGAQVPAPYKIIGYGGKVIDYGKVHYP
QKPAADCAACHVEGAGAPANADLFKADLSNQACIGCHTEKPSAHHSSTDCMACHNATKPYG
GTGSAAKRHGDVMKAYNDSLGYKAKFSNIGIKNNALTFDVQILDNKDQPIGK**EFISDPSAYTK**S
SIYFSWGIDKDYPAYTAGSRYSDR**GFALSNSK**VSTYNEATK**TFTIDSTNSNLK**LPADLTGMNVEL
YAGVATCFNK**GGYGVEDVVATPCSTDTR**YAYIQDQPFRFKWNGTDTNSAAEKRRAIIDTAKCS
GCHNKEIVHYDNGVNCQACHTPDKGLKTDNTYPGTKVPTSFAWKAHESEGHYLKYAGVQSGT
VLKTDCATCHTADK**SNVVTGIALGR**SPERAWLYGDIKNNGAVIWVSSDAGACLSCHQKYLSDA
AKSHIETNGGILNGTSAADVQTRASESCATCHTPSQLMEAHGN

The numerous peptides detected in OmcA, MtrA, B and C provided the proof for the presence of these proteins in the strains they were extracted from. Apart from MtrC in the strain BL21 DE3 pRGK333 pACYCOmcA-MtrCAB, all the other *Shewanella* proteins were identified both in the soluble and insoluble fractions. This could suggest that the proteins were being incorrectly localised with a certain percentage appearing in the cytoplasm instead of the membrane. This does not mean that any proteins in the cytoplasm would be correctly folded or functional due to the sec signal sequence on the Mtr proteins, which transports unfolded proteins to the periplasm and also the requirement of the *ccm* machinery to insert the haem groups. The identification of these proteins in unexpected cellular fractions could have been due to the lack of specificity yielded by the protein extraction method used. Ultracentrifugation would most likely provide a better division of subcellular compartments.

4.3.3 Current generation from *E. coli* expressing *S. oneidensis c*-type cytochromes within a microfluidic MFC.

A microfludic-scale MFC (μMFC) (shown in Figure 4.20) was chosen due to its many advantages: easy assembly, high power density per unit area, and utility for high throughput analysis of a wide number of strains (253). The main disadvantage of the μMFC is that long-term growth is infeasible. In order to determine whether the *E. coli* strains expressing *S. oneidensis* cytochromes could produce current, the bacterial strains were each tested by carrying out a polarisation curve within the μMFC. A longer

term analysis was carried out using a sedimentary fuel cell in which the negative redox potential generated by the bacterial culture was measured over 15 h (900 min) (as detailed in methods chapter section 3.4.3). Following proteomic analysis of the strains and initial MFC test using the microfluidic Cambridge MFCs was carried out in Sheffield. The results of this are shown in Figure 4.23 with the values of the empty media subtracted (-10mW/m^2) in Figure 4.24 to make it determine the difference in power density between the engineered strains and the most basic control.

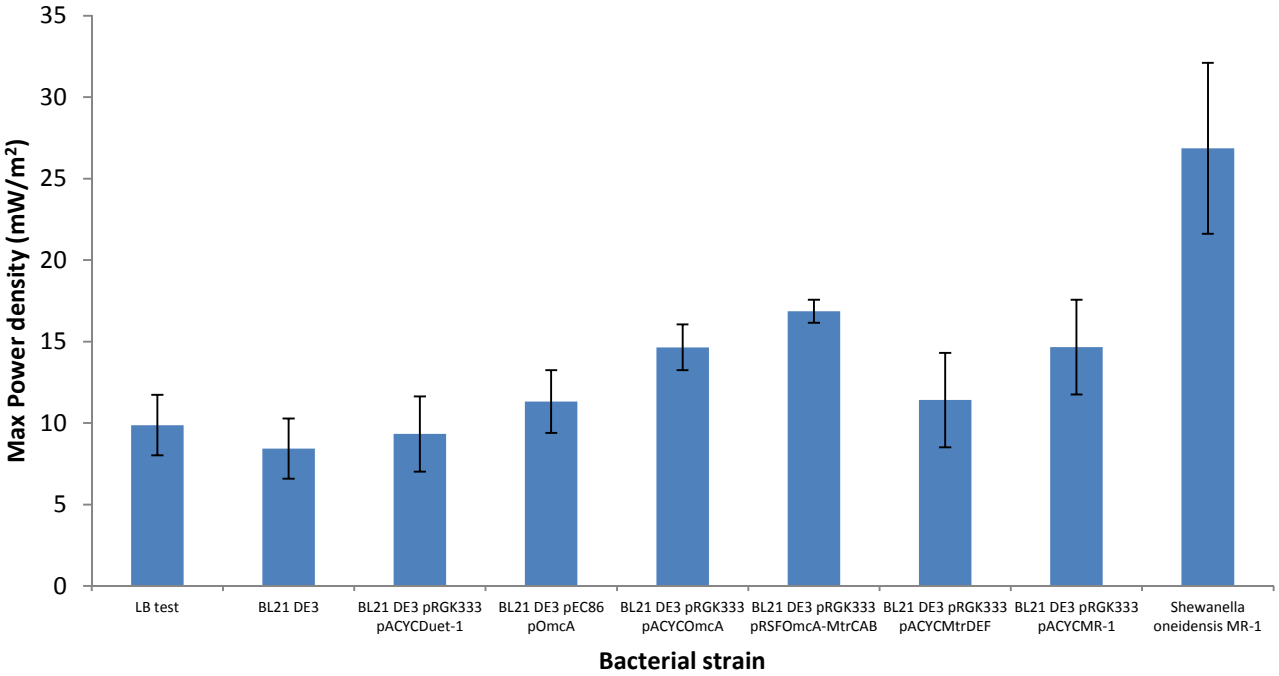

Figure 4.23 – Max power density obtained from a variety of different strains and standards within the Cambridge MFC at Sheffield. Results shown are averages with standard deviation from at least three biological replicates carried out within the University of Cambridge MFC. Only the result between the highest maximum power density strains (BL21 DE3 pRGK333 pRSF-OmcA-MtrCAB) and the control (BL21 DE3 pRGK333 pACYCDuet-1) generated a statistically significant P-value (0.0085).

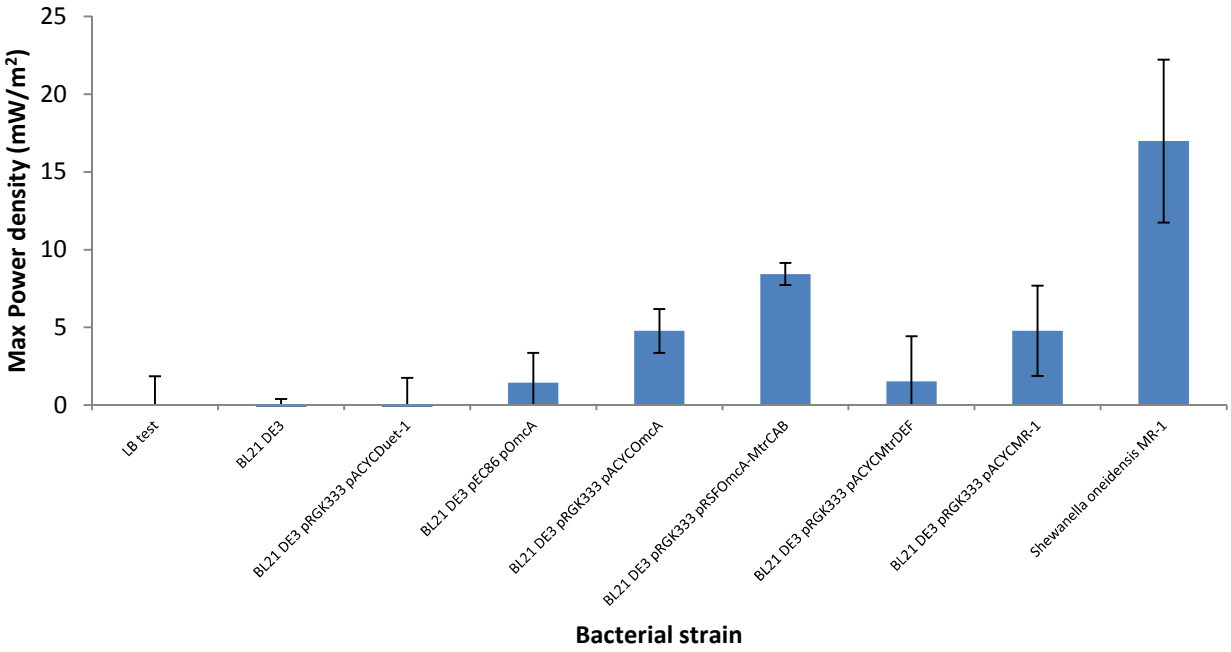

Figure 4.24 – Max power density obtained from a variety of different strains and standards within Cambridge MFC with LB result subtracted. Results shown are averages with standard deviation from at least three biological replicates carried out within the University of Cambridge MFC. The difference between BL21 DE3 pRGK333 pRSFOmcA-MtrCAB and BL21 DE3 pRGK333 pACYCDuet-1 considered to be statistically significant (p-value = 0.01). The difference between BL21 DE3 pRGK333 pACYCOmcA and BL21 D3 pRGK333 pACYCDuet-1 was also deemed to be significant (p-value=0.02)

The results shown in Figure 4.24 demonstrated that although all the engineered strains appeared to generate a greater power density than the other controls (BL21 DE3 and BL21 DE3 pRGK333 pACYCDuet-1) this was not to a significant level (unpaired *t*-test compared to BL21 DE3 pRGK333 pACYCDuet-1 – (pEC86 OmcA, *p*-value = 0.29), (pRGK333 pACYCMtrDEF, *p*-value = 0.76), (pRGK333 pACYCMR-1, *p*-value = 0.13)) within this MFC. It was decided at this point that only BL21 DE3 pRGK333 pACYCOmcA and BL21 DE3 pRGK333 pRSFOmcA-MtrCAB should continue to be tested as both of these were considered significant when compared to BL21 DE3 pRGK333 pACYCDuet-1 (pRGK333 pACYCOmcA, *p*-value = 0.02.) and (pRGK333 pRSFOmcA-MtrCAB, *p*-value = 0.01).

All cultures were diluted to an OD600 of 1.0. They were then replenished with a carbon source (in the form of 5 mM sodium lactate); fresh antibiotics and IPTG (0.5 mM) were added before being loaded into the anode chamber of the μMFC. A polarisation curve was generated by varying the load applied to all the channels of the μMFC (full methods in Chapter section 3.4.2). Each strain had 6 replicates carried out simultaneously within the different channels of the μMFC. As shown in Figure 4.25, the engineered strain containing pRSFOmcA-MtrCAB was capable of generating power within the μMFC, with a power output of 17 mW/m^{-2}. This strain had a power output 6.4 mW m^{-2} higher than the control bearing the empty parent plasmid pACYCDuet-1 in combination with the overexpressed cytochrome maturation genes in pRGK333. The strain bearing pRSFOmcA-MtrCAB also produced a power output 5 mW m^{-2} higher than pACYCOmcA alongside the ccm genes. This demonstrates the ability of a "more complete" extracellular electron pathway to allow for the greater power generation. The functional interaction between a more complete electrogenic pathway in the form of OmcA-MtrCAB appeared to be key in allowing *E. coli* to produce current more efficiently. The initial results within the Cambridge MFC did however demonstrate that this is a balance and that there can potentially be too many cytochromes leading to redundancy in the system and metabolic burden. The length of the transcript in pACYCMR-1, which contained MtrDEF-OmcA-MtrCAB, may have been too long to provide an adequate level of the desired protein. The lack of activity of MtrD, E and F within *E. coli* suggested that although these proteins are highly similar to MtrC, A and B, they do not appear to be able to provide the same power generation capability. It is hard to determine why this is without further analysis. The native electron donator NapC may not be able to interact with MtrD to the same extent as it does with MtrA. Admittedly there was no OmcA or a suitable alternative in this strain, which may have also impacted on the results.

Previous studies on Fe (III) reduction by *E. coli* strains revealed that expression of MtrC, A, and B cytochromes in *E. coli* results in an engineered strain that can reduce metal ions and solid metal oxides 8× and 4× faster, respectively, than its parental strain (125). Before the work presented in this chapter and that demonstrated by Goldbeck et al

(124), it was unclear whether cytochrome-containing *E. coli* strains would produce current in an MFC, especially given the observation that for *Pelobacter carbinolicus,* the capacity for Fe (III) oxide reduction does not necessarily demonstrate an ability to transfer electrons to fuel cell anodes (122). It is also not clear how similar (a) cytochromes *in situ* in *S. oneidensis*, with or without the presence of other cytochromes, (b) isolated cytochromes tested *in vitro*, and (c) cytochromes expressed in *E. coli*, are to each other and whether it is possible to draw generic functional conclusions. Gram negative bacteria are known to respond to stress conditions by shedding membrane vesicles (254) and in the case of an OmcA-only *E. coli* strain it has been shown that these vesicles only carry OmcA molecules (120). Analysis of both the OmcA-only and OmcA-MtrCAB cluster bacterial samples showed OmcA was always present in the supernatant. It is possible that vesicle-bound OmcA proteins are involved in electron transport maybe via bound flavins (255)**,** and that the vesicles act as some sort of transport system to the anode surface.

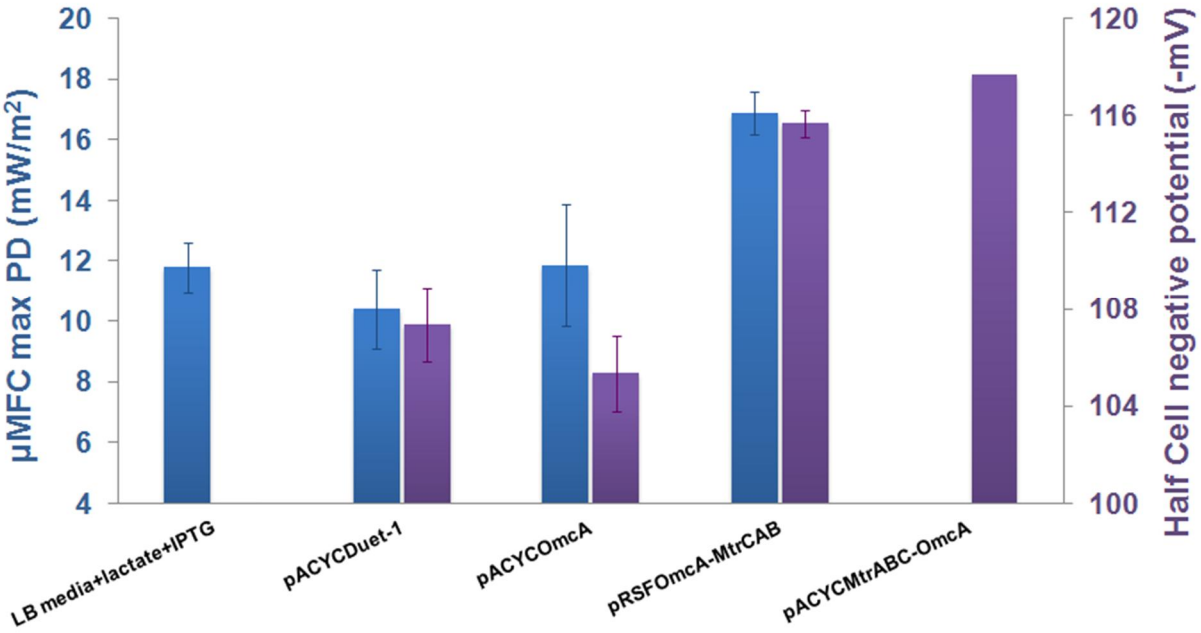

Figure 4.25 - Maximum power density (mW/m²) attained within the microfluidic microbial fuel cell (µMFC) (blue data - left axis). Half cell results are presented as the negative potential obtained at 900 mins against the counter electrode (purple data - right axis) (1) Growth medium only - LB + lactate + 0.5mM IPTG (µMFC=11.8 mW/m² +/- 0.8 mW/m²). (2) E. coli expressing the plasmids pRGK333 and pACYCDuet-1(µMFC =10.7 mW/m² +/- 1.1 mW/m²) (Half cell = 107.4 mV +/- 2.0 mV), (3) pRGK333 and pACYCOmcA (µMFC = 12.0 mW/m² +/- 2.5 mW/m²) (Half cell = 105.7 mV +/- 1.8 mV) (4) pRGK333 and pRSFOmcA-MtrCAB (µMFC = 17.0 mW/m²+/- 0.6 mW/m²) (Half cell =115.8 mV +/- 0.8 mV) and (5) pRGK333 and pACYCMtrABC-OmcA (Half cell = 117.9 mV +/- 0 mV). T

4.3.4 Negative potential within a sedimentary half cell

To verify the results and test the capability of the electrogenic strains within different devices, we employed a sedimentary half cell (Figure 4.26). This provided an opportunity for a longer term analysis in which the carbon (working) electrode was placed in the base of the sedimentary half cell to allow the transfer of current from planktonic cells, sedimented bacteria and/or from bacterial biofilms. In combination with an Ag/AgCl red rod reference electrode, the negative potential from the reduction of the working electrode was calculated. The results clearly show a more negative potential in strains expressing *S. oneidensis c*-type cytochromes following a 15h growth period within the sedimentary half cell (Figure 4.27). Both the pACYC and pRSF derivatives of OmcA-MtrCAB gave a higher electrogenic potential than an empty plasmid (pACYCDuet-1).

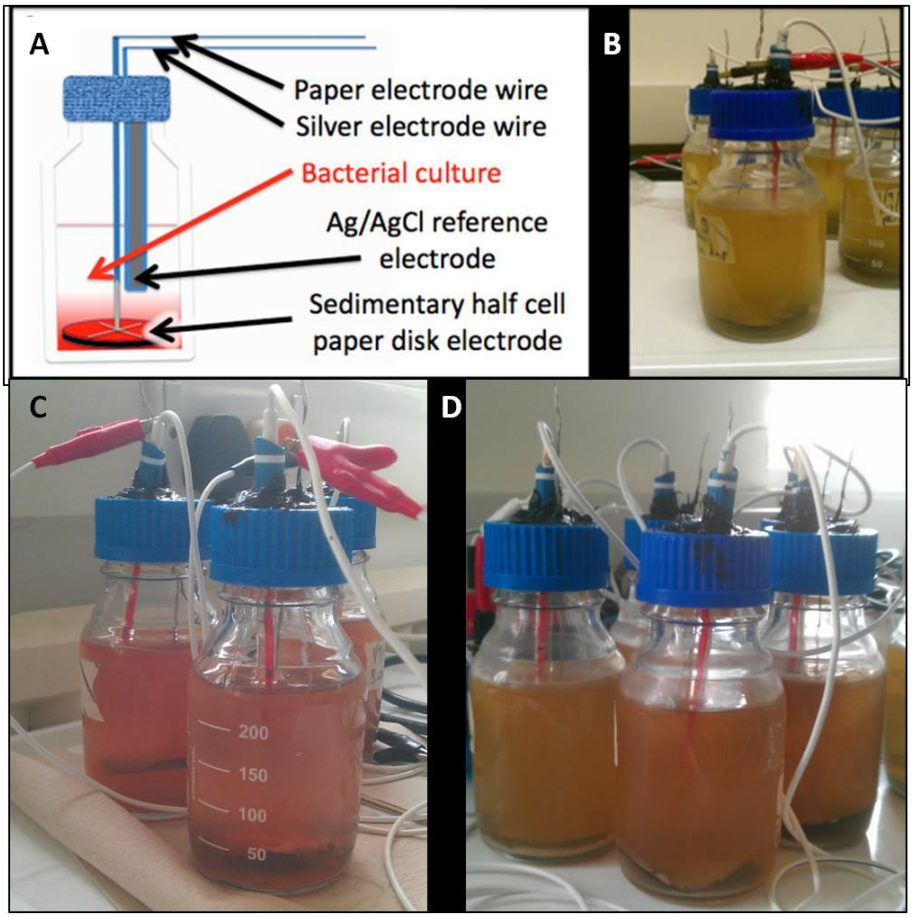

***Figure 4.26 - Schematic diagram and photographs of the sedimentary half cell (HC). The circular anodes are arranged at the base of the cell to allow potentially electrogenic bacteria to form a layer or a biofilm. A) Schematic of half cell setup B) Photograph of E. coli* BL21 DE3 in HC C) Photograph of *S. oneidensis* MR-1 *in* HC *(D) Photograph of engineered E. coli* strain pRGK333 pACYCOmcA.**

The engineered strains pACYCOmcA and pACYCOmcA-MtrCAB were also compared over an 8 day period within sedimentary half cells containing sparged M9 minimal media. The results (Figure 4.25) presented a difference (unpaired *t*-test, *p*-value = 0.001) in the potential observed between pACYCOmcA-MtrCAB and pACYCOmcA with average readings of -207 mV and -176 mV respectively. This further demonstrates the ability of the engineered strain to interact with a working electrode over a substantial period of time within nitrogen sparged, minimal media with a defined carbon source. It

should be noted that the half cell tests were done to provide extra validation of the setup with the potential to be used as a screen but MFC's are still required to provide more detailed information about the strains such as power density.

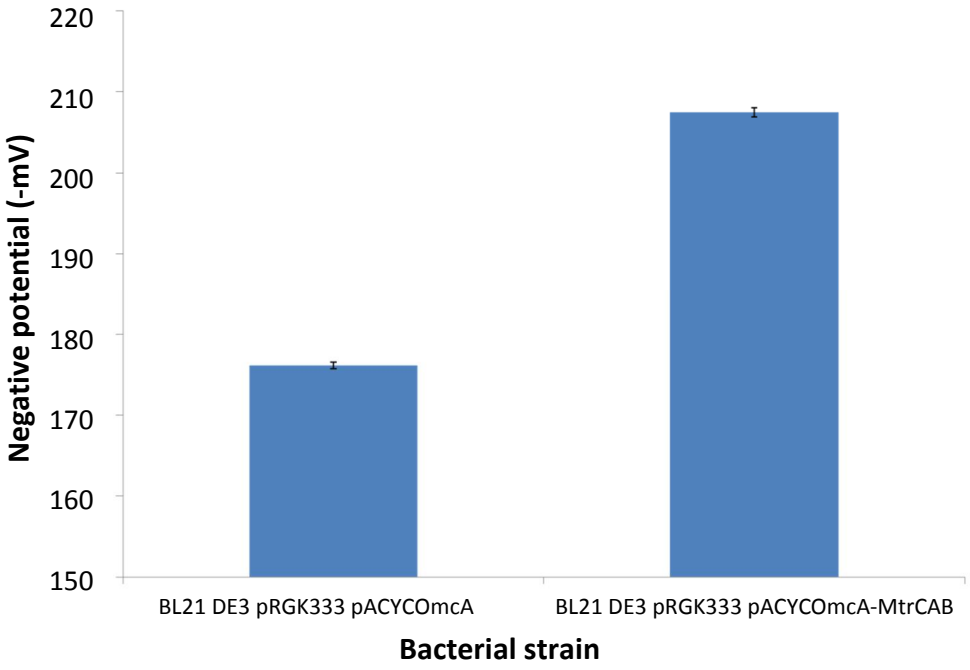

Figure 4.27 Results from an 8-day half cell run in minimal media with three biological replicates of each. Average negative potential is shown (-mV) along with standard deviation. The result were shown to be statistically significant (p-value=0.001)

4.4 Discussion and Conclusions

The results presented in this chapter show that transfer of electrogenic activity into an organism not naturally capable of such an ability, is possible. The use of OmcA, MtrC, A and B proteins from *S. oneidensis* MR-1 alongside overexpressed cytochrome maturation genes proved to be the more successful method to do this within this in this case. The aforementioned Goldbeck paper (124), although utilising largely the same genetic elements (MtrCAB from *S. oneidensis* MR-1) as those used in this chapter, took a different, synthetic biology approach to the experiment. Goldbeck et al (124) made use of a promoter library which provided an opportunity to focus on the

greatest cellular balance between overexpressed recombinant protein and a healthy, functional cell, capable of generating ~30-fold greater maximal current per cfu than the cytochrome maturation gene only control strain.

This chapter demonstrates the challenges faced by synthetic biologists. The molecular/synthetic biology community have moved past the point of recombinant expression of single non-native proteins and ventured into non-native recombinant pathways. It is to be expected that significant challenges would be faced in this quest, especially when the overexpression of relatively large pathways is attempted simultaneously. Complexity was added due to the fact that all the proteins chosen to work with were membrane proteins, many with multiple haem groups. The option for codon optimisation of the pathways for enhanced expression was limited due to the large financial investment in producing constructs of such considerable size that may well not provide any greater yield. The BioBrick style approach towards the challenge that Goldbeck et al (124) took in regard to the promoter variation was an efficient way of adapting towards the challenges of the project. An interesting conclusion from this study was the importance of minimal perturbation to cellular morphology when transferring electrons extracellularly. The choice of basing the Mtr system with the Duet-1 series of plasmids from Novagen provided downstream flexibility in the fact that these plasmids have two multiple cloning sites. In the event of further genes being identified that could enhance the power density, these would have then been inserted and attempted. This did however put the genes under the control of the notoriously active T7 viral promoter. This promoter is designed for maximum expression of the target protein (typically a single target protein) (256,257) with yields of that protein reaching up to 50% of total cell protein (258,259)**.**

The challenges faced in the synthetic biology aspects of the project were paired with equal challenges with testing apparatus. Although microbial fuel cells have seen considerable development over the past 10 years, they are still far from a “plug and play” device. A great deal of electrochemistry knowledge is required in order to make sense of the results obtained and even more in order to be able to troubleshoot. The

demands of the project in terms of the high throughput approach to determining the genetic variants that lead to an increase in power generation due to the heavy industrial basis of the project caused issues with the initial MFC setup.

With all said the aforementioned challenges, the expression of two large plasmid systems coding for two separate membrane localised pathways within *E. coli* did demonstrate a change in the electrogenic activity between engineered strains and wild type *E. coli* across multiple testing devices. The increase in power generation noted between wild type and the highest output engineered strain was approximately 60%. This was 64% of the *S. oneidensis* value (which produced an average power density of 26.8 mW/m^2) and showed that there was still room for improvement in order to be able to reach the levels seen in the native organism. It must be noted that the result generated from the *Shewanella* will be skewed from the expected values from *S. oneidensis* MR-1 due to the aerobic growth of the MR-1 culture and replacement of the media before use in the MFC. Aerobic growth would have prevented full expression of the *c*-type cytochromes normally utilised within an anaerobic environment and the replacement of the media would have removed any flavins. These flavins are *Shewanella*'s dominant method of extracellular electron transfer (104) and their removal would drastically decrease any power reading obtained.

Limited proteomic work had been carried out between *S. oneidensis* MR-1 under different environmental conditions, especially with regard to the proteomic changes noted when adapted to survival within an MFC was carried out. With this in mind an investigation into a comparison between the proteomic profiles of *Shewanella* under standard lab conditions and *Shewanella* within a MFC. The results obtained from this study were intended to be used to identify heavily upregulated proteins and pathways within *Shewanella* that could then be used for further genetic engineering in *E. coli.* As the reason behind the low increase in power generation was unknown, pairing additional genetic components with the already established Mtr pathway may then yield a greater power output. The reasoning behind this being that there may be other components present in *Shewanella* that allow it to generate higher current, which

could be detected using quantitative proteomics. Issues relating to the substantially different regulatory mechanisms in *Shewanella* compared to *E. coli* (260) would have to be carefully considered. Details of this proteomic analysis can be found in chapter 5.

As stated previously, the reason behind the low power output was complex. Further thought as to the cause of this issue was that it could have been due to the high level of metabolic burden imposed upon the cells. The current setup was 2 large plasmids, with one carrying native *E. coli* genes, in the form of cytochrome maturation genes, (11,250 bp) and the other consisting of varieties of the Mtr pathway (up to 16,994 for pACYCMR-1). A method to move away from this was considered, with further analysis as to the thought process of why this should occur, and is detailed in chapter 6.

Chapter 5 - Quantitative proteomic analysis of *Shewanella oneidensis* MR-1 within an MFC compared to microaerobic chemostatic growth

This chapter was done in collaboration with Dr. Greg. J. S. Fowler, Dr. Ana. G. Pereira-Medrano, Dr. Trong Khoa Pham, Dr Pablo Ledezma, Dr Ioannis A. Ieropoulos and was supervised by Prof. Phillip C. Wright

5.1 Introduction

As detailed in chapter 2, the use of model organisms such as *Shewanella* within BESs is well documented (96,261–264) and various bacterial biochemical pathways have been proposed to explain the mechanisms through which MFCs are capable of producing electricity (265,266). Direct electron transfer to an MFC anode has been widely studied in dissimilatory metal reducing bacteria such as *Shewanella oneidensis* MR-1 (the bacterium used in this chapter) and *Geobacter sulfurreducens*. Several reviews discuss the putative mechanisms of direct transfer, typically involving at least a series of periplasmic and outer membrane complexes in these species (266–268). Primary bacterial metabolites, such as sulphur species (269), and iron oxides have also been found to conduct electrons to electrodes (270) respectively, whilst electron shuttles have been shown to be produced by some organisms as secondary metabolites, such as flavins by *S. oneidensis* MR-1 and *Shewanella sp*. MR-4 (104,136) and phenazines by *Pseudomonas aeruginosa* KRP1 (271). The use of "omics" studies has previously demonstrated their ability to not only provide an understanding of the shift of the metabolism of an organism towards a situation, but also towards forward engineering (272).

A number of transcriptomic and proteomic studies have been carried out on *S. oneidensis*, including the effect of chromate challenge (273,274), the role of the fur

regulon (275,276) and investigations into the membrane and biofilm composition (277–280). Most recently, a transcriptional analysis of *S. oneidensis* with an electrode compared to Fe (III) citrate or oxygen as terminal electron acceptor, has been published (281). Although advances have been made in understanding anodic electron transfer mechanisms by the terminal cytochromes of exoelectrogenic bacteria (102,282), related non-cytochrome outer membrane biochemical mechanisms used by electricity-producing organisms are still poorly understood. The current understanding of fundamental mechanisms is largely due to extensive bioelectrochemical and biophysical studies, genomics and some proteomics studies. The subcellular proteome of *S. oneidensis* MR-1 has been qualitatively mapped using LC-MS/MS (277), but quantitative proteomics has yet to play a major role in the characterisation of the extracellular electron transfer pathways (215). Recent work has shown the first demonstration of control and measurement of specific growth rates in MFCs and the maximum specific growth rate for *S. oneidensis* biofilms, and that operation at maximum specific growth rate returns maximum electrical power output (212).

In this chapter, quantitative proteomics techniques have been employed to understand more about the *S. oneidensis* electrogenic behaviour when operating under relevant current inducing conditions at the anode in an MFC. The results from chapter 4 revealed that a greater knowledge of the mechanisms of exoelectrogenic activity was required and thus, by developing a greater understanding of the protein profile of a DMRB within an MFC compared to microaerobic growth, it may be possible to apply this knowledge to the enhancement of the engineered *E. coli* strain. Whilst a quantitative proteomic analysis of the engineered *E. coli* strain BL21 DE3 pRGK333 pRSFMtrOmcA-CAB may have provided information as to where bottlenecks lie within the metabolism of the organism, this was not considered the highest priority. The reasoning behind this was that *S. oneidensis* MR-1 is a well studied organism, especially in regards to extracellular electron transport but no quantitative proteomics had been carried out at this point. This presented an opportunity to conduct highly informative research for the DMRB and MFC community. Although engineered *E. coli* was producing a statistically significant amount of power when compared to BL21 DE3

and the control strain BL21 DE3 pRGK333 pACYCDuet-1, it was not considered sufficient to deem this the most useful experiment at this point in time. Instead a more targeted analysis of the interacting partners of the recombinant Mtr pathway within *E. coli* was considered (as detailed in chapter 6). Quantitative proteomics of engineered *E. coli* was still considered for later research following analysis of *S. oneidensis*, with the potential for any information obtained from the proteomic analysis of MR-1 to be applied to further increase power generation in *E. coli*. The basing of the Mtr pathway on the chromosome of BL21 DE3 (discussed in chapter 6) was done with the aim of reducing the metabolic burden and increasing electrogenic activity. This would then be a more stable basing of the genetic material, where less cellular energy was being diverted to plasmid maintenance, which could otherwise create a proteomic skew. A proteomic analysis of a further engineered *E. coli* was deemed to be the most valuable after these two key developments.

iTRAQ (and other prominently applied silent isotope incorporation techniques) remains one of the most robust and easy-to-use techniques to be applied in quantitative proteomics (283). Previous work in an MFC indicates that even in a *Shewanella oneidensis* MR-1 mutant that has had OmcA and MtrC knocked out, the bacterium still produces approximately one seventh of the current of WT *S. oneidensis*, and has approximately one third of the ability to reduce iron (III) species to iron (II) species. (109). This evidence is not wholly by the literature as at least one study identifies the Mtr pathway as being essential (284). This suggests that these decahaem proteins may not be the only route for electrons producing current at an MFC anode. Following this information, iTRAQ proteomics was carried out for the first time to try and understand more about the non-cytochrome *S. oneidensis* MR-1 electrogenic behaviour, when operating under relevant current inducing conditions at the anode of an MFC. Full details of the materials and methods used in this chapter can be found in chapter 3.

Before discussing the results obtained from this iTRAQ experiment it should be noted that iTRAQ analysis can under-estimate the degree of fold change (283,285,286). This

results from technical issues, mainly due to the so called mixed MS/MS, which results when two or more precursor (nearly isobaric) ions with similar mass/charge and retention time during HPLC, prior to MS analysis', are selected for fragmentation. The net result is augmented iTRAQ reporter intensities with compression of the ratio for selected peptides and thus underestimation (283,287,288). Whilst the fold change may be underestimated, the direction of change i.e. up or down regulated, is correct (289).

5.2 Results and discussion

5.2.1 Bacterial growth within the UWE MFC and protein extraction

The first step towards making a comparison of the cellular proteins produced from anode-associated cells in an MFC, with those produced in planktonic conditions was to grow cells of *S. oneidensis* MR-1 both in an MFC set up and in flasks. Accordingly a pre-culture of *S. oneidensis*, grown microaerobically in LB, was used to inoculate replicate cultures in lactate minimal medium (see materials and methods section 3.4.1.1 for details). These cultures were grown either microaerobically in flasks or anaerobically in MFCs, such that all cultures reached the late exponential growth phase.

Following the initial 3 week growth period where a stable biofilm was allowed to develop, the MFCs then had a load applied to them with the resulting power output shown in Figure 5.1. The power outputs stabilised until the point in which the flow rate of the growth medium within the MFCs was increased. This happened after 10,000 mins, which led to an increase in power seen in Figure 5.1. The increase in flow rate allowed for a greater circulation of nutrients, which in turn allowed higher metabolic activity and movement of endogenous mediators through the media. All these elements combined yielded a near instantaneous 4 fold power increase from an average of 15 μW to 60 μW.

At the end of the appropriate growth period, *S. oneidensis* MR-1 cells were harvested from the liquid phase of the microaerobic growth vessels and from the electrode biofilm of the MFCs. A comparison of protein abundances in cells that use oxygen as a

terminal electron acceptor (aerobic cells) versus cells, which can use the carbon anode as an electron acceptor (anode bound cells) was then carried out.

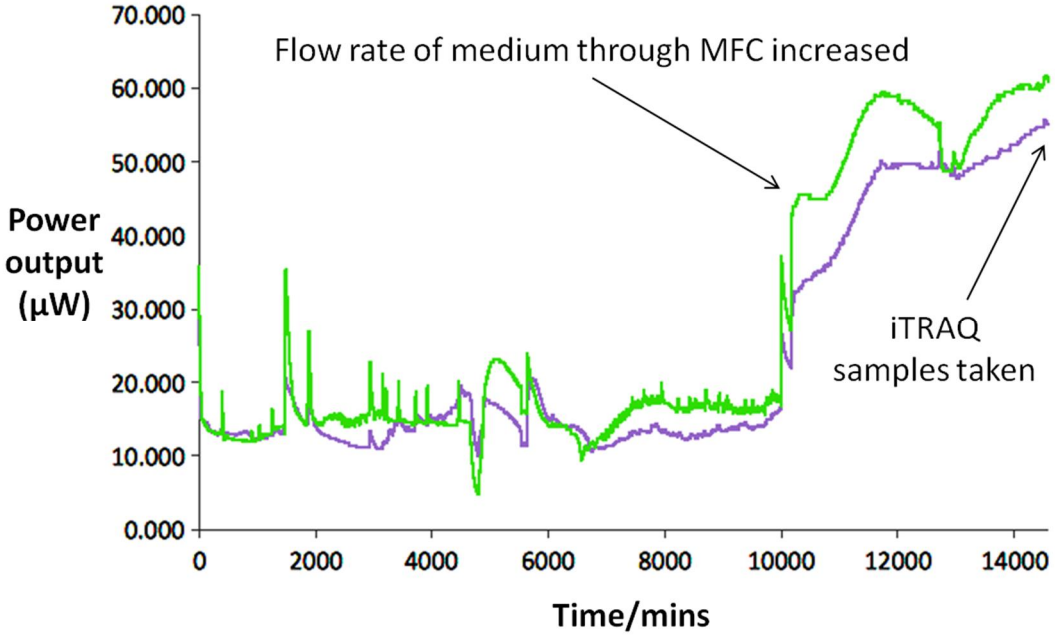

Figure 5.1 The production of electrons in the form of power output (in µW) versus time (in min) recorded from Shewanella oneidensis MR-1 attached to the anodes of microbial fuel cells (MFC) (data generated from 2 MFCs). Following the initial 3 week growth period (before time = 0 mins) where a stable biofilm was allowed to develop, the MFCs then had a load applied to them, with the resulting power output shown in the figure. After 10,000 mins the flow rate of the medium in the MFCs cells was increased, which led to a near instantaneous 3 fold power increase from an average of 15 µW to 57 µW. The increase in flow rate allowed for a greater circulation of nutrients, which in turn allowed higher metabolic activity and movement of endogenous mediators through the media.

5.2.2 Data mining: identification and quantification of differential protein abundance

The method used to quantify the differential abundance of bacterial proteins in the MFCs compared to bacteria grown in flasks was iTRAQ, as it has major advantages over traditional gel-based quantitative approaches, not least in reproducibility, since it

produces a relative quantification for each identified peptide (225). This section describes the quantitation methods used, the number of proteins detected by iTRAQ, and the distribution of proteins between soluble and insoluble fractions, prior to analysis of which proteins were significantly associated with growth on the anode.

The relative quantification of proteins from the anaerobic cells taken from the MFC anode versus microaerobically grown cells was carried out using iTRAQ labels. These iTRAQ sets were used to carry out different analyses to include the soluble and insoluble sub-proteomes for each phenotype (Table 5.1). As described in materials and methods section 3.3.9, MS/MS data interpretation was performed using Phenyx peptide identification, and a quantitative data analysis algorithm using in-house developed Mathematica scripts.

Table 5.1. - Summary of iTRAQ experiments

iTRAQ experiment number and description[a]	**Type of sub-proteome,** μg **per sample, iTRAQ kit used**	**Phenotype 1 – Labels of biological replicates for microaerobic planktonic *S. oneidensis* cells**[b]	**Phenotype 2 – Labels of biological replicates for MFC anodic *S. oneidensis* cells**[c]	**Biological comparison by pair**
iTRAQ 1 Microaerobic planktonic *S. oneidensis* MR-1 vs anaerobic anodic *S. oneidensis* MR-1	Soluble proteins 100 μg 4 iTRAQ labels	Aerobic –115, 116	Anodic – 119, 121	119:115, 121:115, and 119:116, 121:116
iTRAQ 2 Microaerobic planktonic *S. oneidensis* MR-1 vs	Insoluble proteins 100 μg	Aerobic – 115, 116	Anodic – 119, 121	119:115, 121:115, and 119:116, 121:116

anaerobic anodic *S. oneidensis* MR-1	4 iTRAQ labels			

a. Two biological replicates were used for each phenotype. Biological comparisons for each pair were carried out as indicated, and determination of differential expression was evaluated via *t*-tests, as described in methods section 3.3.10, MS and MS/MS level measurements for QStarXL instrument Survey scans were acquired from 350 to 1,800 m/z, and MS/MS scans from 65 to 1,800 m/z. The spectrometer sequentially conducted MS/MS on the precursor ions (+2 and +3 charge state) detected in the full scan. MS profile data was acquired using Analyst QS 2.0 (Applied Biosystems ABI). Profile data was stored in wiff format.

b. Phenotype 1 are microaerobic planktonic cells culture.

c. Phenotype 2 are all anaerobic anodic biofilm cells cultured from the MFC.

Using Phenyx and a robust in-house statistical approach, 2090 and 2727 peptide spectral matches (PSM) were detected from the anaerobic MFC vs microaerobic cells. (iTRAQ 1 for soluble sub-proteome and iTRAQ 2 for the insoluble, respectively).

Combined datasets from the soluble and insoluble sub-proteomes of MFC cells vs microaerobic planktonic cells comparison (iTRAQs 1 and 2, respectively) identified a total of 170 unique proteins, of which 92 are common to both sub-proteomes, whilst 42 and 36 were only identified in the insoluble and soluble sub-proteomes, respectively. The predicted protein functions for the identified proteins are shown in Figure 5.2, whilst a schematic showing the subcellular localisation of some of the quantified proteins is shown in Figure 5.3. There were 8 and 11 predicted membrane proteins (including cytoplasmic membrane, outer membrane and periplasmic proteins) identified in insoluble and soluble fractions, respectively, whilst 3 regulated membrane proteins were common to iTRAQs 1 and 2 (Details in Appendix). A high proportion of predicted regulated cytoplasmic proteins were found in the insoluble fractions (62% of regulated proteins), many of which were ribosomal proteins (cytoplasmic proteins)

possibly due to the attachment of these (nominally cytoplasmic) proteins to the membrane via nascent polypeptide chains (214,290). It is clear that separate measurement of the insoluble and soluble sub-proteomes increased the total number of identified and quantified membrane and cytoplasmic proteins.

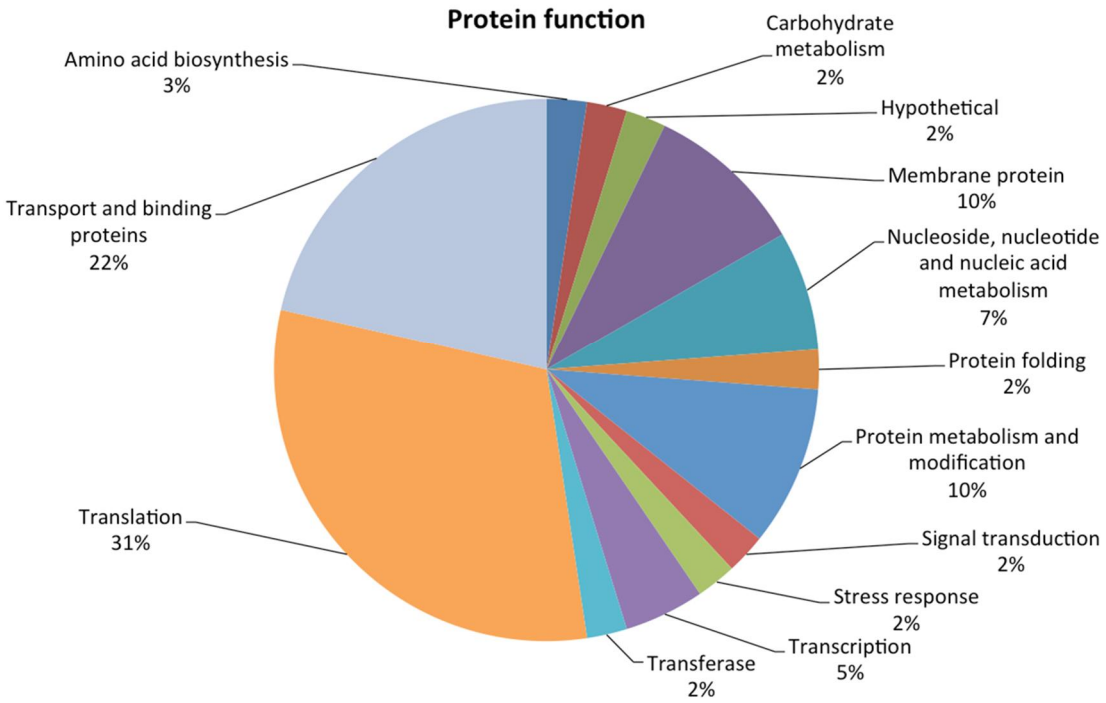

Figure 5.2 Analysis from iTRAQ data of the functions of the identified proteins from Shewanella oneidensis MR-1 in the microbial fuel cell under fast perfusion (62.5 mL.h-1) conditions. Combined datasets from the soluble and insoluble sub-proteomes of anaerobic HC vs microaerobic planktonic cells comparison (iTRAQs 1 and 2, respectively) identified a total of 170 unique proteins, of which 92 are common to both sub-proteomes, whilst 42 and 36 were only identified in the insoluble and soluble sub-proteomes, respectively.

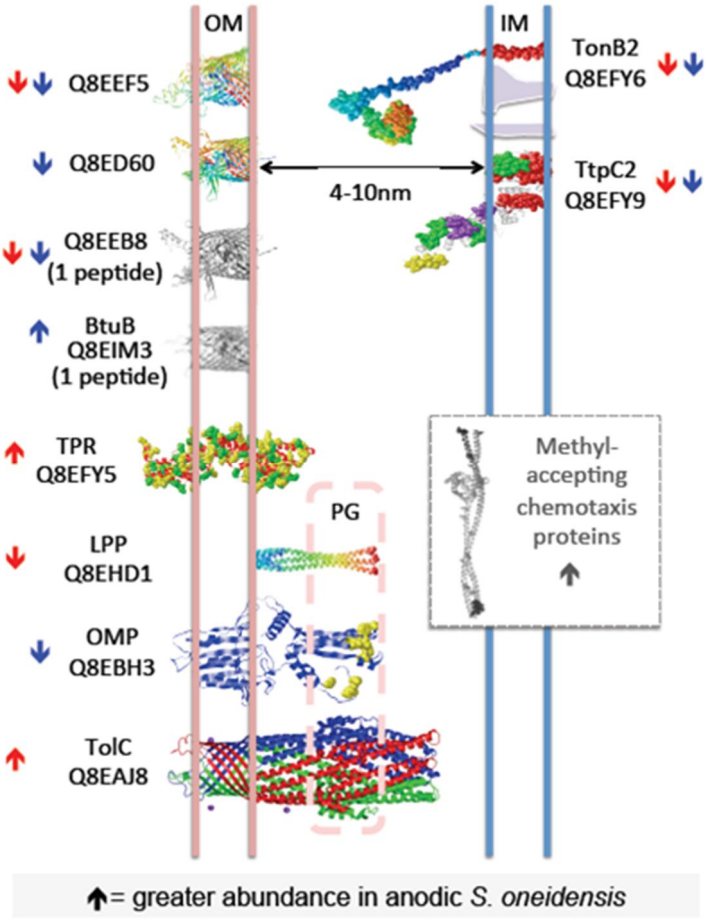

Figure 5.3 A schematic diagram showing the subcellular locations of selected membrane protein "hits" from the iTRAQ and 2D-LC MS/MS experiments. Membrane proteins are represented as RasMol drawings made using PDB coordinates generated using from the relevant protein sequence by the I_TASSER software suite* (291)*. Structures in grey represent an iTRAQ result from either only one unique peptide (Q8EB8 and Q8EIM3) or from a peptide unique to a class of proteins rather than one protein within that class (methyl-accepting chemotaxis proteins) (see Table 5.2). OM= outer membrane, IM= inner membrane PG = peptidoglycan layer/cell wall. An upward arrow indicates a protein that is overall more abundant in anodic electron-producing Shewanella oneidensis MR-1 than the planktonic equivalent. Red arrows represent results from the "insoluble" fraction whilst

blue arrows represent results from the "soluble" fraction. Figure developed by Dr Greg Fowler.

5.2.3 The TolC efflux pump (Q8EAJ8/SO_3904)

The iTRAQ results indicate that TolC (Q8EAJ8/SO_3904) protein is statistically increased in abundance, in the insoluble fraction prepared from *S. oneidensis* cells, producing electricity at an anode than in planktonic cells (Table 5.2). It has been noted previously that the TolC-dependent efflux system of MR-1 is required for protection against toxic levels of redox active compounds (292), and it has been suggested that this may provide direct evidence linking efflux pumps with the reduction of insoluble electron acceptors (106). TolC proteins can form part of a type 1 secretion system or be part of an efflux pump complex, creating a continuous, solvent-accessible conduit (293): structurally, TolC itself is a channel over 14 nm long that spans both the outer membrane and periplasmic space (see, for example, the Protein Data Bank (PDB) archive rcsb.com). The periplasmic or proximal end of the tunnel is sealed by sets of coiled helices. In *E. coli*, TolC is involved in the export of enterobactin, which, once it has bound iron to become ferric enterobactin, is imported by the cell (294). TolC may form part of the putative type I secretion from *G. sulfurreducens*, another electrogenic bacterium, whose function may include exporting some outer membrane proteins which are important in cell–anode interactions (295). These observations, combined with the iTRAQ results seen in this chapter, suggest that TolC may also have an indirect role in the transfer of electrons to an anode.

Table 5.2 Selected iTRAQ abundance trends for Shewanella oneidensis MR-1 membrane proteins in cells at the anode of an anaerobic MFC (compared to those from a microaerobic planktonic culture)

Uniprot Name_SHEON	**NCBI identification**	**iTRAQ distinct peptide hits**	**Soluble fraction abundance[a.]**	**Insoluble fraction abundance[a.]**	**Subcellular location[b.]**	**p-value[c.]**
Outer membrane proteins						
Q8EAJ8 (SO_3904) AE015823_1	TolC	TIVDVLNR ALNVLDTNR	-	**Increase**	OM	$7.58e^{-4}$
Q8EFY5 (SO_1829) AE015626_10	TPR	LYADLLLQEK QAVEADILGGTDHAATLR LAQLMAQK MLGNFYAEK YSEAIPVLEK	-	**Increase**	OM	$1.36e^{-2}$
Q8EHD1 (SO_1295) AE015573_9	Lpp	AAAMDAQAEAK AAAMDAQAEAKR RANDRLDNVASR ANDRLDNVASR LDNVASR VDQLSADVSSLK	-	Decrease	OM	$1.31e^{-11}$
Q8EBH3 (SO_3545) AE015790_7	OMP	GATLGLVGVWPLGNR RIEAIVTTTEK VTSNGYGITKPLVAGNSK	-	Decrease	OM	$1.18e^{-3}$

		VDSVGCTLYENVK				
Outer membrane TonB receptors						
Q8EIM3 (SO_0815) AE015526_2	BtuB	VDEHLVVIGR (unique) [d.]	**Increase**	-	OM	1.44e-3
Q8ED60 (SO_2907) AE015729_7	ArgR-reg TonBR	YEALDNLVLR VVFAGYK ITDELEWFGQAIVMR TFDGLAFDAK GNPACEDTQYLR	Decrease	-	OM	2.63e-3
Q8EEF5 (SO_2427) AE015683_8	ArgR-reg TonBR	IYNQDTDTWR LTGEFALR MNDVGPR VIDANGNWVK TIYGGVTVK QDMETASPVTVIDAAAIK TLVLIDGR TLVLIDGRR	Decrease	Decrease	OM	1.40e-11 1.73e-2
Q8EEB8 (SO_2469) AE015688_6	TonBR	TLVLIDGR (unique) [d.]	Decrease	-	OM	2.74e-5
TonB2 system						
Q8EFY6 (SO_1828)	**TonB2**	IEPQYPIAAAR DGDATPIVR	Decrease	Decrease	-	6.90e-4

AE015626_9		FTINELGGVEDVEVIQAEPK				$1.38e^{-2}$
Q8EFY7 (SO_1827) AE015626_8	**ExbD2**	NGIIMMENR (unique) [d.]	Decrease	-	IM	$7.18\ e^{-3}$
Q8EFY9 (SO_1825) AE015626_6	**TtpC2**	EQEFQAER ETPALEAR FIADLGAR TIDQLLQQVK VGAYNLTAEGK GVLLNIYTNK TAQGDLGEMFGVVK GEAGDFAGK GKDLNQAFLDNER SITQILEEQSAGIIAAHAEK NVDKPGNNALGR DKFIADLGAR FQGSVTAIDGSVK	Decrease	Decrease	IM	$4.96e^{-9}$ $3.51e^{-10}$
Q8EFZ0 (SO_1824) AE015626_5	DUF3450	LILDAYSIER LLNTAEVTLAEK VALYAQSLDQK QGVVPLMFK GWDKLEDSYLR EVLVDFFNLGR	Decrease	Decrease	-	$2.82e^{-11}$ $3.72e^{-6}$

		MVESLEQFVQLDLPFNSEVR TGWMYNPQTK LLNTAEVTLAEK QGALDLFALPIPAAETAQ SMDAIQNDINGVDKLR				
Methyl-accepting chemotaxis proteins						
24 possible *S. oneidensis* Methyl-accepting chemotaxis proteins *	Methyl-accepting chemotaxis proteins (MACP)	GFAVVADEVR *	**Increase**	**Increase**	IM	$8.66e^{-10}$ $1.11e^{-16}$

a. "Increase" represents a greater abundance for that protein in anodic *S. oneidensis*.

b. Tang et al., 2007 Profiling the Membrane Proteome (278) and InterPro, OM = outer membrane, IM = inner membrane.

c. The p-values are included (see appendix for more details) to give an indication of statistical significance.

d. Peptides labelled “unique” are only found in that particular protein in the *S. oneidensis* proteome, and since these results only represent one peptide in an iTRAQ run, they are included merely because they appear suggestive rather than because they provide conclusive proof.

* Peptide GFAVVADEVR is found in 24 different *S. oneidensis* methyl-accepting chemotaxis proteins (MACP) and the iTRAQ data is included not as definitive data but merely as a possible clue to what may be different between anodic and planktonic cells. Q8EA56, Q8ECT0, Q8E837, Q8EBE2, Q8EJ84, Q8E939, Q8EC62, Q8EI62, Q8EGZ8,

Q8EEX1, Q8EFA2, Q8EHS3, Q8EHE5, Q8EB90, Q8EAL2, Q8E928, Q8E8M8, Q8E8U9, Q8EHZ8, Q8EBU5, Q8EF69, Q8EAQ8, Q8EH45, Q8EJG7

5.2.4 The TonB2 system

The iTRAQ results indicate that TonB2 (Q8EFY6/SO_1828), ExbD2 (Q8EFY7/SO_1827), TtpC2 - the (Q8EFY9/SO_1825/AE015626_6) TonB2 complex-associated transport protein and DUF3450 (Q8EFZ0/SO_1824) are statistically less abundant in anaerobic cells from the MFC anode than in microaerobic planktonic *S. oneidensis* MR-1 cells (Table 5.2). The genes coding for the TonB2 system of *S. oneidensis* all lie on the same operon (AE015626_5/AAN54876.1 - AE15626_9/AAN54880.1, 1917616-1921206) as shown in Figure 5.4.

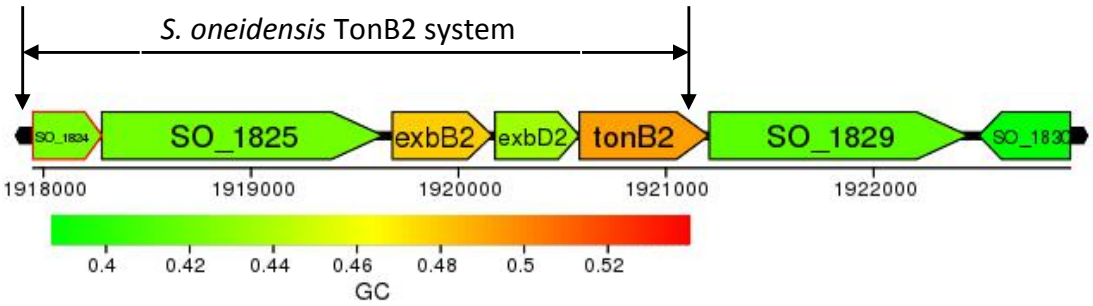

Figure 5.4 - TonB2 system genes located within the S. oneidensis MR-1 genome. SO numbers equate as follows; SO1829=DUF3450, SO1825=TtpC2, exbB2 = SO1826, exbD2=SO1827, TonB2=SO1828

The TonB family of proteins are generally thought to be required, amongst other things for the energy dependent active transport of iron bound substrates across the outer membrane of gram-negative bacteria (296–301).

In order to highlight the functions of the TonB2 and related systems in *S. oneidensis,* it was thought useful to compare them with those of the gram negative gammaproteobacteria *Vibrio* (which although not defined as a DMRB, has multiple decahaem *c*-type cytochromes. There are examples of other similar uncharacterised proteins within other *Shewanella* species but the high sequence homology and level of investigation into this protein in *Vibrio* made it a suitable choice for comparison. Further reasons will become clearer throughout the chapter). This parallels a similar

comparison between the TonB2 systems of *V. anguillarum* and *Escherichia coli* (302). A number of bacteria, including the *Vibrio* bacteria (*V. anguillarum*, *V. vulnificus* and *V. cholerae*) and *S. oneidensis,* contain a second TonB system termed the TrpC2-TonB2 system and in this way differ from, for example, *E. coli*, which only contains the single TonB1 system. The TtpC2-TonB2 system has shown uptake specificity to certain iron-bound substrates in both *V. anguillarum* and *V. cholerae* [(301) and, unlike the TonB1 system, the TtpC2-TonB2 system consists of four proteins: TonB2, ExbD2, ExbB2, and TtpC. TtpC2 and TonB2 are required for the uptake of endogenously produced ferric-siderophores (300). In *Vibrio anguillarum* the TonB2 protein, the protein most comparable to *S. oneidensis* TonB2, is essential for the uptake of the indigenous siderophore anguibactin (302). Siderophores are naturally secreted iron carriers with a high specificity and affinity towards ferric iron (303,304). Gram-negative bacteria take up ferric-siderophore complexes via TonB outer membrane receptors, by energy-transducing TonB systems. Further bioinformatic examination of TonB2 and TtpC2 (Discussed further at the end of this section) suggests similarities with *Vibrio* TonB2 systems, which are associated with endogenously produced ferric-siderophores, exogenous siderophore aerobactin and anguibactin transport, for example.

DUF3450 (Q8EFZ0/ SO_1824) (shown in Figure 5.4) is one of a family of functionally uncharacterised proteins that are found in bacteria and eukaryotes. DUF3450 (PF11932) is a protein family of unknown function with 253 members from 168 bacterial species including many of the *Shewanella* and *Vibrio* Gammaproteobacteria, and is represented in this chapter by Q8EFZ0 from *S. oneidensis* (see, for example, http:/pfam.sanger.ac.uk/family/DUF3450). It has already been noted in this chapter that DUF3450 lies on the same operon as the TonB2 system and therefore it has been posited that it is involved with the TonB2 system (300). DUF3450 (Q8EFZ0) is described as a “TonB2 energy transduction system periplasmic component” in its entry in the NCBI database (http:/www.ncbi.nlm.nih.gov/protein/NP_717432) and this study gives some new quantitative experimental evidence that DUF3450 is connected with the TonB2 system as the abundance for this protein seems to mirror that of the TonB2 and ExbD2, namely, being less abundant in anodic than planktonic *S. oneidensis* cells. This

is the first known example of a potential role for DUF3450, with a potential role in the TonB2 system.

5.2.5 The *Shewanella oneidensis* MR-1 TonB2 system

A BLAST comparison (discussed later in the chapter) indicates that the loop 3 in the *V. anguillarum* TonB2 associated with anguibactin transport (302) aligns well (70% identity) with a similar region in the *S. oneidensis* TonB2;

F7YJ70_VIBA7: 179 WKYQPQIVDGKAIEQPGQTV 198

Q8EFY6_SHEON: 177 WKYKPKIVDGKPLKQPGMTV 196

The TonB2 system in both *V. anguillarum* and *V. cholerae* shows uptake specificity to certain endogenously produced ferric-siderophores, TtpC2 and TonB being required for their uptake (300,301). TtpC2 is essential for the uptake of endogenous siderophores. Examples include the pathogenic bacterium *V. vulnificus* vulnibactin and a hydroxamate compound, an exogenous siderophore aerobactin (300) as well as enterobactin, vibriobactin and hemin in *V. cholerae*, vulnibactin in *V. vulnificus* and likely, vibrioferrin in *V. parahaemolyticus* and *V. alginolyticus* (305).

In *S. oneidensis* an affinity labelling study has co-localised TtpC2, ExbB2 and ExbD2 to the inner membrane (278), whilst in a recent study TtpC2 was found to be co-purified with the decahaem cytochrome MtrC (306). Furthermore according to a BLASTN search and the KEGG Ortholog Clusters databases, the C-terminus (amino acids 325-425) of TtcP2 is orthologous to ExbB, whilst BLASTP of this section of TtcP2 against a *Vibrio* database most closely resembles TolR (57-61%) (Q8DDW2 _VIBVU, Q7MPW4 _VIBVY, Q7MDW7_VIBVY, F7YJ67_VIBA7). TolR is anchored to the inner membrane by a single transmembrane (TM) segment, extends into the periplasm and is homologous to ExbD. The TM domains of TolQ and TolR present structural and functional homologies, not only to ExbB and ExbD of the TonB system, but also with MotA and MotB of the flagellar motor (307). In *E. coli*, for example, TolQ is involved in the TonB-independent uptake of group A channel-forming colicins. The MotA/TolQ/ExbB proton channel family groups together integral membrane proteins that appear to be involved

in translocation of proteins across the outer membrane, and TtpC2 may be fulfilling an analogous role in the *S. oneidensis* TonB2 system.

For DUF3450 (Q8EFZ0/SO1824) a BLAST search against the protein databases shows that it has sequential similarities to a type of protein described as a "TonB system biopolymer transport component" particularly in the *Vibrio* bacteria (alignment not shown). The results from some online protein modelling programs (www.expasy.ch) such as TMpred, HMMTOP, TMHMM, SOSUI and SAPS indicate that DUF3450 is a soluble protein with high alpha helical content, no transmembrane spanning regions, and no hydrophobic or charged patches. Coiled-coil prediction software COILS indicated a high probability of a coiled-coil region between approximately Arg101 and Tyr130. Annotated coiled coil motifs are not especially common in the proteome of *S. oneidensis* and the handful that are there, belong to either chemotaxis related proteins or proteins that bind zinc ions (see for example in the Uniprot database *S. oneidensis* proteins Q8EF63, Q8EEQ2, Q8EC93, Q8EDR9, Q8EFG8, Q8EIG5, Q8EFV4, Q8EE83). Moreover, it is worth noting that the DUF3450 protein (Q8EFZ0/SO_1824) featured in this study (coded by the same operon as the TonB2 proteins) uniquely lacks an approximately 16 amino-acid N-terminal sequence that is found in other DUF3450 proteins from both the Shewanellaceae family and from the *Vibrio* bacteria; an example is MSKVSNRTKIATALVGVLALASSNLVVADPLTDVQKADS from the DUF3450 protein (A6WLT1_SHEB8) of *Shewanella baltica* (strain OS185).

5.2.6 TPR (tetratricopeptide repeat) protein Q8EFY5/SO1829 (AE015626_10)

The STRING annotation for TPR (http:/string-db.org) indicates a "co-occurrence" and a "neighbourhood" quality but not a "gene fusion" for TPR with the TonB2 system, Q8EFY6 (SO1828) - Q8EFZ0 (SO_1824) (Table 5.2), as well as with two other TPR domain-containing proteins (Q8EIS8/SO_0757, Q8EGP6/SO_1552), and a hypothetical protein (Q8EKN7/SO_0055), which when compared to the general proteome with BLASTP also shows similarity to TPR domain-containing proteins. However, sequence comparison of TPR with the three other putative TPR domain-containing proteins using

BLASTP shows that they have little in common and this seemed to be mirrored in the iTRAQ study results. The STRING entry also indicates a similar connection for TPR to a fimbrial biogenesis protein (Q8EC30/SO_3314) and an NlpI lipoprotein (Q8EHL0/SO_1210). Since this family of proteins (TPR) is of unknown function, it was thought sensible to look at whether structural data could be modelled. Examination of the protein sequence and modelling using the I-TASSER software suite (291) shows, in Figure 5.5 that Q8EFY5/SO_1829 TPR has an unusually high number of charged residues (106 R,K,D,E out of 415, shown in red and blue) with a number of hydrophobic alpha-helical regions (shown in green in Figure 5.5).

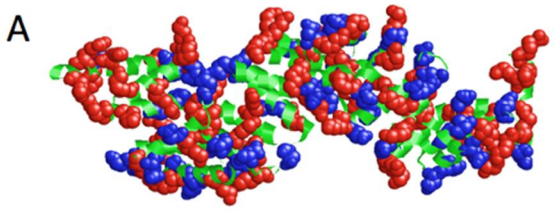

B

Protein Sequence Q8EFY5/SO1829 TPR (KR=+ve, DE=-ve)

MRNAHKIAVALLLSLCGGSLSVSSAIAAEKCAVDTRQSKAVGESSAKKVQKSF
EAYSNGQLDEAIAILLEANPKNDFDKAYVGRMLGNFYAEKGKMDTAIKYLKQA
VEADILGGTDHAATLRLYADLLLQEKQFKEAIPYYYKWMEFTCKTDSQMYRRI
GIAYSELKQWDKVIEVADKGLSLAESPDKGLYQMKLTSYFNQKKYKNAVGVLE
TMVPLFPDDGRLWVQLAQFYLMIEDYDNALATYDLAYRNGFLDTGANITRLAQ
LMAQKGAPYQAAKVFEKHMKSGLITQDVKSYEILAGFYQNAKEFKEAAELYGK
AAAISNDGKLYLKQGRLLSLEEKYSEAIPVLEKAISLGIEHPGEANFELALAH
LSLKQYKSAYNRAVLAAKDKKTEKSANSYISYIKEKARMHNVTL

Predicted Secondary Structure (H=alpha-helix, C=coil)

CCHHHHHHHHHHHHHHHCCHHHHHHHHHHHHHHHHHHCHHHHHHHHHH
HHHHCCCHHHHHHHHHHHCCCCHHHHHHHHHHHHHHCCCHHHHHHHHHH
HHCCCCCCCHHHHHHHHHHHHHHCCCHHHHHHHHHHHHCCCCCHHHHHHH
HHHHHHCCCHHHHHHHHHHHHHCCCCCHHHHHHHHHHHHHCCCHHHHHHH
HHHHHCCCCHHHHHHHHHHHHCCCHHHHHHHHHHHHHCCCCCHHHHHHHH
HHHHCCCHHHHHHHHHHHHHHCCCCCCHHHHHHHHHHHHCCCHHHHHHHH
HHCCCCCHHHHHHHHHHHHCCCHHHHHHHHHHHHHCCCCCHHHHHHHHHH
HHCCCHHHHHHHHHHHHHCCCCCHHHHHHHHHHHHHHHCCCC

Predicted Solvent Accessibility; 0 (buried residue) to 9 (highly exposed)

633221000000000012021530243352334244244134301410330241164731630140045017363232020020000002327316301600430061333436311200200020033273163016003300613374213001100200331631630150043004134623301000000003326316401600430013000200342631630150033016352642241022002003526314300410340073433462040010002003316416301600430071374040001002003427316401600430061337332301110020133163164016104401724443630430140044136347367

Figure 5.5 - Modelling of the Shewanella oneidensis MR-1 protein of unknown function Q8EFY5/SO_1829 TPR using the I-TASSER software suite (308) shows that this outer membrane protein has an unusual combination of a high number of charged residues (106 R,K,D,E out of 415, shown in red and blue) with a number of hydrophobic alpha-helical regions (shown in green). These observations suggest that Q8EFY5/SO_1829 TPR could form part of an amphiphilic membrane spanning protein, possibly lined with positive arginine and lysine residues. This may explain its up-regulation/increased abundance during electron transfer to an anode (Table 5.2).

In direct contrast to the other putative members of the TonB2 gene cluster, the iTRAQ results indicate that the TPR protein (Q8EFY5/SO_1829) is statistically increased in abundance in the insoluble fraction in *S. oneidensis* cells that are at an anode producing electricity compared to planktonic cells that are not (Table 5.2). This type of TPR protein seems, judging from BLAST searches (Discussed previously in this chapter), to be mainly found in Gammaproteobacteria, especially the *Vibrio* and *Shewanellaceae* families. In the most recently updated version of the *S. oneidensis* proteome, the TPR protein is described as a putative Zn-dependent protease associated with a TonB2 energy transduction system and containing a tetratricopeptide repeat (TPR) domain. This TPR protein, which is "geographically" near to the TonB2 gene cluster on the *S. oneidensis* genome, appears not to be co-transcribed or co-regulated with the other putative TonB2 operon members (discussed previously in this chapter). It has been confirmed that TPR is an outer membrane-located protein (278), (Table 5.1), unlike the other component proteins of the TonB2 system. These observations suggest that Q8EFY5/SO_1829 TPR could form an amphiphilic membrane spanning protein, possibly lined with positive arginine and lysine residues (Figure 5.5) and thereby may explain its up-regulation/increased abundance during electron transfer to an anode.

5.2.7 The TonB-receptors, iTRAQ data and bioinformatics

Two TonB-receptors were observed by iTRAQ to be more abundant in planktonic than anodic *S. oneidensis*; (namely Q8ED60/SO_2907) and Q8EEF5/SO_2427) (Table 5.2). An NCBI BLAST comparison of the TonB-like proteins coded by the various operons in *Vibrio vulnificus* (strain CMCP6) with the *S. oneidensis* proteome was carried out to see if more light could be shed on these *S. oneidensis* TonB receptors (Table 5.3). As would have probably been expected, the TonB1 of *S. oneidensis* most resembles the TonB1 system in *V. vulnificus*, namely Q8D3S3-Q8D3S7. The TonB2 system of *S. oneidensis* resembles both the TonB2 and TonB3 system in *V. vulnificus*, namely Q8D705-Q8D710 and Q8DDV8-Q8DDW3. With respect to the potentially associated TonB receptors, the *V. vulnificus* TonB3 system also has associated with it a protein Q8DDW4 (VV1_0842)

(described as a TonB-dependent receptor or an outer membrane receptor for ferrienterochelin and colicins). Despite the fact that this gene coding for Q8DDW4 - according to the operon predictor from the UCSC Genome Browser (http:/microbes.ucsc.edu, vibrVuln_CMCP6_1) - may not be on the same operon in the genome of *V. vulnificus* as those for Q8DDV8-Q8DDW3, nonetheless lies in the same 5' to 3' orientation close to the operon. Interestingly, a BLAST study showed that three of the TonB proteins that showed up in the iTRAQ study were the closest (if not very good) fits to the aforementioned *V. vulnificus* Q8DDW4 from the *S. oneidensis* proteome, namely, Q8EEB8/SO_1822 (28%), Q8ED60/SO_2907 (28%) and Q8EEF5/SO_2427 (24%) (Table 5.3). Two nearby proteins in the *S. oneidensis* proteome, a TonB receptor-like protein Q8EFY2/ SO_1822 (Table 5.3) and a putative outer membrane porin, Q8EFZ3_SHEON/ SO_1821 are not predicted to lie in the same operon as the *S. oneidensis* TonB2 protein genes. (The area of genome once attributed to Q8EFZ1_SHEON/ SO_1823 is probably not a coding region as this has been removed from the latest genome annotation.) Given that from the BLAST search it is not possible to narrow down which TonB receptor is interacting with the *S. oneidensis* TonB2 system, the question remained as to whether any further light be shed by the iTRAQ results. As discussed previously, the TonB2 system proteins are in general statistically more abundant in the planktonic cells compared to the anodic *S. oneidensis* cells (Table 5.2). The TonB receptor that most closely fits this downregulation trend is Q8EEF5/S0_2427, which is described in the NCBI database as an ArgR-regulated TonB-dependent receptor and if this is indeed the role played by this protein, then the results suggest that, in the absence of an electron-accepting electrode, a siderophore transport mechanism is brought more into play by *S. oneidensis*. It also suggests that the TonB2 system in *S. oneidensis* can play a similar physiological role to the TonB3 system in *V. vulnificus*. For the other two TonB receptors, BtuB (Q8EIM3/SO_0815) and Q8EEB8 (SO_2469), only one peptide was observed by iTRAQ for BtuB (Q8EIM3/SO_0815) namely VDEHLVVIGR (although it was identified 39 times), and this was found to be more abundant in anodic than planktonic cells (Table 5.2). Similarly, only one peptide (identified 13 times) was

observed by iTRAQ for TonB-receptor Q8EEB8 (SO_2469), namely TLVLIDGR, and this was observed to be less abundant in anodic than planktonic cells.

Table 5.3 - BLAST comparison of the proteins coded by the TonB systems operon from Shewanella oneidensis MR-1 with similar operons from Vibrio bacteria.

(a) BLAST comparison of the proteins coded by the TonB2 system operon from *Shewanella oneidensis* MR-1 with similar operons from other gammaproteobacteria.

Shewanella oneidensis UniProt submitted name	Protein	*Vibrio vulnificus* (CMCP6)	*Vibrio cholerae* (M66-2)	*Vibrio anguillarum* (ATCC 68554/775)	*Shewanella baltica* (OS155)	*Ferrimonas balearica* (DSM 9799)	*Pseudoaltero-monas atlantica* (T6c)
Q8EFY5	**TPR**	Q8DDV8, (24%*) Q8D710, (23%)	C3LMM2, (26%)	F7YJ71, (28%)	A3D344, (83%)	E1SW90, (46%)	Q15RJ5, (63%)
Q8EFY6	**TonB2**	Q8DDV9, (29%) Q8D709, (25%)	C3LMM3, (35%)	F7YJ70, (33%)	A3D343, (77%)	E1SW89, (57%)	Q15RJ4, (48%)
Q8EFY7	**ExbD2**	Q8DDW0, (51%) Q8D708, (48%)	C3LMM4, (49%)	F7YJ69, (50%)	A3D342, (94%)	E1SW88, (76%)	Q15RJ3, (54%)
Q8EFY8	**ExbB2**	Q8D707, (51%) Q8DDW1, (44%)	C3LMM5, (53%)	F7YJ68, (54%)	A3D341, (88%)	E1SW87, (69%)	Q15RJ2, (70%)

Q8EFY9	**TtpC2**	Q8DDW2, (40%) Q8D706, (33%)	C3LMM6, (36%)	F7YJ67, (34%)	A3D340, (83%)	E1SW86, (51%)	Q15RJ1, (46%)
Q8EFZ0	DUF3450	Q8DDW3, (38%) Q8D705, (29%)	C3LMM7, (36%)	F7YJ66, (29%)	A3D339, (93%)	E1SW85, (51%)	Q15RJ0, (47%)

*Identity to *S. oneidensis*

(b) BLAST comparison of the TonB-like system operons from *Vibrio vulnificus* (strain CMCP6) with proteins coded by various operons in *Shewanella oneidensis* MR-1

V. vulnificus TonB1 *	Q8D3S3 VV2_1614 TonB	Q8D3S4 VV2_1613 ExbB	Q8D3S5 VV2_1612 ExbD1	Q8D3S6 VV2_1611 Periplasmic hemin-binding protein HutB	Q8D3S7 VV2_1610 Hemin ABC transporter, permease protein HutC	Q8D3S8 VV2_1609 Hemin import ATP-binding protein HmuV/HutD
Nearest BLAST identity in *S. oneidensis*	Q8EB64 SO_3670 TonB1, 38%	Q8EB63 SO_3671 ExbB1, 37%	Q8EB62 SO_3672 ExbD1, 42%	Q8EB61 SO_3673 Hemin ABC transporter HmuT, 43%	Q8EB60 SO_3674 Hemin ABC transporter, permease protein 44%	Q8EB59 HMUV_SHEON SO_3675 Hemin import ATP-binding protein HmuV 48%

V. vulnificus TonB2 *	Q8D710 VV2_0359 TPR domain protein, putative	Q8D709 VV2_0360 Periplasmic protein	Q8D708 VV2_0361 ExbD/TolR	Q8D707 VV2_0362 ExbB	Q8D706 VV2_0363 MotA/TolQ/ExbB “TtpC2”	Q8D705 VV2_0364 TonB system biopolymer

	component of TonB system	TonB (tonB2)				transport component DUF3450
Nearest BLAST identity in *S. oneidensis*	Q8EFY5 SO1829 TPR, 25%	Q8EFY6 SO1828 TonB2, 33%	Q8EFY7 SO1827 ExbD2, 48%	Q8EFY8 SO1826 ExbB2, 51%	Q8EFY9 SO1825 TtpC2, 35%	Q8EFZ0 SO1824 DUF3450, 29%

V. vulnificus TonB3 *	Q8DDV8 VV1_0848 TPR	Q8DDV9 VV1_0847 TonB	Q8DDW0 VV1_0846 ExbD/TolR	Q8DDW1 VV1_0845 ExbB	Q8DDW2 VV1_0844 TolR "TtpC3"	Q8DDW3 VV1_0843 TonB system biopolymer transport component DUF3450	** Q8DDW4 VV1_0842 TonB-dependent receptor; Outer membrane receptor for ferrienterochelin and colicins
Nearest BLAST identity in *S. oneidensis*	Q8EFY5 SO1829 TPR, 24%	Q8EFY6 SO1828 TonB2, 45%	Q8EFY7 SO1827 ExbD2, 51%	Q8EFY8 SO1826 ExbB2, 37%	Q8EFY9 SO1825 TtpC2, 41%	Q8EFZ0 SO1824 DUF3450, 38%	Q8EFZ2 SO_1822, 24% Q8EEB8 SO_1822, 28% Q8ED60 SO_2907, 28% Q8EEF5 SO_2427, 24%

* The nomenclature for the TonB systems of *V. vulnificus* is taken from Kustusch *et al*., 2012 [34].

** according to the operon predictor from the UCSC Genome Browser (http://microbes.ucsc.edu, vibrVuln_CMCP6_1) the gene coding for Q8DDW4 may not be on the same operon in the genome of *Vibrio vulnificus* CMCP6 as those for Q8DDV8-Q8DDW3, despite being in the same 5' to 3' orientation.

5.2.8 Outer membrane porin (OMP) Q8EBH3/SO_3545 and Lpp murein lipoprotein (Q8EHD1/SO_1295)

The iTRAQ results indicate that outer membrane porin (OMP) Q8EBH3/SO_3545 protein is statistically increased in abundance in the insoluble fraction prepared from planktonic *S. oneidensis* cells compared to anaerobic cells producing electricity at an anode (Table 5.2). This OMP belongs to the "Outer membrane protein, OmpA/MotB, C-terminal (IPR006665)" family. In contrast, various authors have determined that OmpA is overexpressed in *E. coli* biofilms compared to planktonic cells in different oxidation states (164,309).The reason for the up-regulation of OmpA in biofilms is not yet fully known, but it could be that it facilitates the transport of extracellular polymeric substances (EPS) formed during biofilm maturation (164).

```
PAL_ECOLI   IVYFDLDKYDIRSDFAQMLDAHANFLRSNPSYKVTVEGHADERGTPEYNI 119

PAL_SHIFL   IVYFDLDKYDIRSDFAQMLDAHANFLRSNPSYKVTVEGHADERGTPEYNI 119

Q8EBH3      SIQFANDSAVVKKEYYKDIERLANYMNKNPEFTVEIAGHASNVGKPEYNM 300

                 : *  *.  ::.:: : ::  **::..**.::* : ***.: *.****:

PAL_ECOLI   SLGERRANAVKMYLQGK-GVSADQISIVSYGKEKPAVLGHDEAAYSKNRR 168

PAL_SHIFL   SLGERRANAVKMYLQGK-GVSADQISIVSYGKEKPAVLGHDEAAYSKNRR 168

Q8EBH3      VLSDKRADAVAKILVEKYGISQSRVTSNGYGITKPLVAGNSKEAHAANRR 350

                 *.::**:**   *  * *:* .:::  .**  ** * *:.: *:: ***
```

Figure 5.6 - CLUSTALW2 alignment of the c-terminus of OMP (Q8EBH3) with the peptidoglycan(PG)-associated lipoproteins of Escherichia coli (strain K12) PAL_ECOLI and Shigella flexneri PAL_SHIFL indicates that they share similar peptidoglycan binding motifs (cd07185: OmpA_C-like conserved domain, NCBI, shown underlined

These OmpA_C-like conserved domains have been shown to non-covalently interact with peptidoglycan layer (PG). Furthermore, a role for OM-peptidoglycan links in vesiculation has been suggested since deleting or truncating OmpA, an abundant protein linking the OM and PG, results in increased vesiculation in *E. coli*, *Salmonella*, and *Vibrio cholerae* (310,311).The abundance of OMP seems to correlate with that of Lpp murein lipoprotein (Q8EHD1/SO_1295), which may be more than a coincidence.

The iTRAQ results show that Lpp murein lipoprotein (Q8EHD1/SO1295, Braun's lipoprotein) is statistically decreased in abundance in the insoluble fraction of *S. oneidensis* cells producing electricity at an anode compared to planktonic *S. oneidensis* cells (Table 5.2). Lpp is one of the most abundant proteins in *E. coli* (312) and therefore may be equally abundant in *S. oneidensis*; recent studies have shown that Lpp can span the OM despite the lack of an obvious transmembrane segment (313). Lpp can occupy two separate and distinct subcellular locations: the “free” state is thought to be an integral outer membrane protein whose C-terminus is exposed on the cell surface (i.e. mostly in the outer membrane “insoluble” environment), whilst the “bound” form of the protein is tethered to the outer membrane (OM) by its N-terminal lipid moiety and covalently attached to the PG by its C-terminal lysine residue (i.e. mostly in the periplasmic “soluble” environment). The iTRAQ results show a statistically significant drop in abundance in the insoluble fraction in anodic cells that could suggest that the Lpp is in its “bound” form within planktonic *S. oneidensis*. Since "bound" Lpp is associated with a reduction in outer membrane vesicle (OMV) formation (254), perhaps OMV's do not form an important part of the mechanism of cell-anode electron transfer. Similarly since "bound" Lpp forms a tether which helps maintain the structural integrity of the cell (313), it maybe is found in less abundance at anode cells to allow the relaxation of a particular cell shape; for example, a more elongated cell shape can lead to increased current densities (314).

5.2.9 The OmcA and MtrA-F decahaem cytochrome system

Previous work in an MFC indicates that even in a *Shewanella oneidensis* MR-1 mutant that has had OmcA and MtrC knocked out, the bacterium still produces about

approximately one seventh of the current of WT *S. oneidensis*, and has approximately one third of the ability to reduce iron (III) species to iron (II) species (109). Another study carried out by Coursolle et al (315) further states the impact on *S. oneidensis* mutants that are deficient in Mtr proteins with an even greater reduction in activity noted from a double OmcA/MtrC knockout. A large body of evidence points towards the importance of the Mtr pathway and the interaction with soluble mediators (315) in the form of FMN following processing by UshA (316) and bfe (104). Up to 75% of the extracellular electron transfer capabilities of *S. oneidensis* are believed to be from the interaction of mediators with the Mtr pathway, whilst the other portion is likely largely due to direct contact. The results from chapter 4, with the overexpression of OmcA, MtrC, A and B leads towards the conclusion that direct contact is capable of generating current without the presence of mediators. This does not however mean that these decahaem proteins are the only important proteins allowing for this power generation to occur. A number of membrane proteins associated with electron transfer, most notably MtrC/OmcB and OmcA from the decahaem cytochromes electron transport system did not show up on the list of proteins found in the present iTRAQ work; comparison with the literature suggests that for some "-omics" studies the abundance of these *S. oneidensis* decahaem cytochrome proteins is not high enough (Table 5.4). Briefly, in previous studies, cytochromes were not detected in the collection of proteins identified using proteomic or transcriptomic techniques, and other proteomic studies using 2-D gel electrophoresis have also failed to identify these proteins (Table 5.4).

Table 5.4 - Summary of "-omics" literature related to the OmcA and MtrA-F decahaem cytochromes of Shewanella oneidensis

Paper	"Challenge"	Which -omic, i.e. *italics= proteins*	*OmcA* or *MtrA-F* detected?	fold change/ difference	Growth conditions
Beliaev 2002 (317)	Different terminal	global mRNA patterns	*OmcA* *MtrA* *MtrB*	2-5 1.8-5 1.4-4.7	For anaerobic growth, anaerobically

	electron acceptors		No *MtrC*		prepared LB broth supplemented with sodium lactate (20 mM) as an electron donor and the following electron acceptors: 20 mM sodium fumarate, 10 mM ferric citrate, or 5 mM sodium nitrate.
Beliaev 2002 (318)	*etrA* (fur) mutant	global mRNA patterns	No	-	Myers and Myers 1993 (319), defined minimal medium supplemented with 15 mM lactate and vitamin-free Casamino acids. 24 mM fumarate was added to the medium as the electron acceptor.
Beliaev 2005 (106)	Metal ions, different terminal electron acceptors	global mRNA patterns	*MtrCAB* operon, No *OmcA*	2- to 8- fold decrease in mRNA levels under metal-reducing conditions	Anaerobic minimal medium containing 15 mM sodium fumarate and 20 mM sodium lactate.
Brown 2006 (273)	Chromate stress	Transcriptomics Table IV *Proteomics Table VII*	omcA mtrA mtrC *OmcA* *MtrA* *MtrB* *MtrC*	1.2-8 1-6 1-5 *53.5/26.7=2* *From "9" to "0"* *48.5/25.7=1.8* *55.1/25=2.2*	Both transcriptomic and proteomic analyses and was propagated in Luria-Bertani (LB)1 medium (pH 7.2) at 30 °C under aerobic conditions

Cao 2011 (280)	? loosely versus tightly bound EPS	*Used number of peptides as measure of protein abundance?*	*OmcA* *MtrB* *MtrC* *No MtrA*	*No change* *2.9* *8.2*	Modified M1 medium containing 3.00 mM PIPES, 7.50 mM NaOH, 28.04 mM NH4Cl, 1.34 mM KCl, 4.35 mM NaH2PO4 and 0.70mM CaCl2 supplemented with trace amounts of minerals, vitamins and amino acids under anaerobic conditions
Chourey 2006 (320)	Chromate stress	RNA isolation, microarray	No	-	LB medium containing either 0 or 0.3 mM potassium chromate
Cruz-Garcia 2011 (321)	Grown on lactate and nitrate relative to the wild type	Total RNA global expression, microarray	*OmcA* *MtrA* *MtrB* *MtrC*	0.3 0.25 0.22 0.3	Anaerobically in 3 mM KNO3 in HEPES medium with 20 mM sodium pyruvate as the electron donor and dimethyl sulfoxide (DMSO; 1 mM), fumarate (10 mM) or nitrate (2 mM) as electron acceptors.
De Vriendt 2005 (322)	Sessile and planktonic	*Darkness of 2D gel spots*	No	-	Silicone tubing containing LB medium
De Windt 2006 (323)	*aggA* mutant	Total RNA global expression, microarray	*MtrB* *No OmcA, MtrA, MtrC*	1.6-4.3 *0.185/0.08=2.3*	Test tubes containing 10 ml LB medium and propagated using

		Darkness of 2D gel spots			increasing concentrations of rifampicin
Elias 2008 (324)	Controlled batch or continuous culture in bioreactors versus shake flasks	*Darkness of 2D gel spots*	*OmcA* *MtrA* *MtrB* *MtrC*	*1.9* *5.5* *2.0* *2.1*	Aerobically in defined medium (Elias et al. 2005), 18 mM lactate, PIPES concentration 3-30 mM
Fang 2006 (325)	Transitioned from aerobic to suboxic conditions	*Differential quantitative analysis using the AMT tag*	*OmcA* *MtrA* *MtrC*	*4.3-7.1* *No and 5.5* *3.7-4.5* *Suppl. Table 3*	Defined medium - 0.907 g/liter PIPES, 0.3 g/liter NaOH, 1.5 g/liter NH4Cl, 0.1 g/liter KCl, 0.6 g/liter NaH2PO4, 0.213 g/liter Na2SO4, and 16.85 g/liter DL-lactate as well as vitamins, minerals, and amino acids. The cultures used O2 as the terminal electron acceptor.
Gao 2006 (326)	Cold shock	RNA isolation, microarray	No	-	LB medium, aerobic
Gao 2008 (279)	*arcA* deletion, aeorbic versus anaerobic	RNA isolation, microarray, RT-PCR	*OmcA* *MtrC* No *MtrB,* *MtrA*	0.35-1.08 0.43-1.17 Suppl. Table	M1 defined medium containing 0.02% (w/v) of vitamin-free Casamino Acids and 15 mM lactate under aerobic or anaerobic
Gödeke 2012 (327)	Surface-associated growth	RNA isolation, microarray, RT-PCR	*MtrB* *MtrC*	-1.24 -1.08	LM medium [72] without antibiotics containing 0.5 mM

	between 15 and 60 minutes after attachment		No *OmcA, MtrA*	log2 fold change Suppl. Table	lactate. FeCl2 and FeCl3 were used at a concentration of 20–100 mM.
Leaphart 2006 (328)	Acidic and Alkaline pH	Transcriptome microarray analysis, RT-PCR	*MtrA, MtrC* No *OmcA, MtrB*	pH10/pH7 0.44 pH7/pH10 2.26 pH10/pH7 0.57 pH7/pH10 1.73 Suppl. Table	Specialised minimal medium, aerobically
Liang 2012 (329)	Pellicle cells relative to planktonic cells	Transcriptome microarray experiments	No	-	LB in beakers
Liu 2005 (330)	Elevated salt conditions	Transcriptome microarray experiments	No	-	MR2A medium containing different amounts of NaCl
Mclean 2008 (331)	O2-limited versus aerobic aggregated cells	Transcriptome microarray experiments	*MtrD* *MtrE* *MtrF* No *MtrCAB, OmcA*	3.32 2.39 3.32 log2 fold change	30°C in tryptic soy broth (TSB, pH 7.4) or M1 minimal medium (pH 7.0) that contained 3 mM PIPES, 2.8 mM NH4Cl, 0.4 mM NaH2PO4, 3 mM NaCl, 0.1 mM KCl, 1 mM Na2SeO4, 10 mM L-arginine hydrochloride, 13 mM L-glutamate, 19 mM L-serine and 10 ml each of 10¥ Wolfe's vitamin and 10¥ mineral solutions, plus 6-30

					mM D, L-sodium lactate.
Rosenbaum 2012 (281)	Anode versus iron salts oxygen	Transcriptome microarray analysis, RT-PCR	*MtrB* *MtrA* *MtrC* *OmcA*	2.96 2.16 1.93 3.27	The medium for all experiments was prepared according to Myers and Nealson and was modified by adding 1.27 mM K2HPO4, 0.73 mM KH2PO4, 125 mM NaCl, 5 mM HEPES, 0.5 g/L yeast extract, 0.5 g/L tryptone, and 5 g/L sodium ß-glycerophosphate (no addition of amino acids as in the original medium recipe). The pH was adjusted to 7.2. After autoclaving, sodium L-lactate was added to final concentrations of 20 mM. In iron respiration experiments 50 mM iron(III) citrate as the electron acceptor.
Ruebush 2006 (332)	Soluble and Insoluble Iron Forms, Aerobic and Anaerobic Conditions	*Darkness of 2D gel spots, Western blots*	*OmcA* *MtrC/OmcB* *MtrB* *MtrA* *CymA*	*Various, not all detected in all conditions, already discussed in paper.*	Defined minimal medium as per Myers and Nealson with the following modifications: 30 mM D,L-lactate, 4

					mM sodium phosphate, and 10 mM HEPES (pH 7.4) with 50 mM ferric citrate or 25 mM fumarate in 4-liter flasks under N2 at 30°C.
Thompson 2007 (333)	Chromate stress	*Label free quantitation, LC-MS/MS analysis.*	*MtrB* *OmcA* *OmcB/MtrC* *No MtrA*	*1mM downreg* *0.5mM downreg* *0.3mM downreg* *1M downreg* *0.5mM No* *0.3mM No* *1M downreg* *0.5mM No* *0.3mM No*	LB plus potassium chromate
Vanrobaeys 2003 (334)	Growth on fumarate compared to growth on Fe2O3	*Darkness of 2D gel spots*	*No*	-	Anaerobically prepared LB broth supplemented with lactic acid (20 mM) as an electron donor and either one of the electron acceptors 20 mM sodium fumarate or 1.6 g/L ferric oxide (Fe2O3)
Wan 2004 (275)	Fur mutant, aeorbic versus anaerobic with 20 mM fumurate	Transcriptome microarray analysis, RT-PCR	*OmcA* *MtrC* *MtrB* *MtrA*	5.9- and 4.8-fold 5.3- and 4-fold No 4.5- and 2.7-fold	LB medium in the presence of 20 mM lactate at 30°C under aerobic or anaerobic (with 20 mM fumurate as the

					electron acceptor) conditions.
Wang 2010 (335)	Grown with azo compound or Fe (III) citrate	*Darkness of 2D gel spots*	*No*	-	In anaerobic cultivation, strain S12 grew in defined medium (pH7.4) as described by Hong et al. (2007) with minor modifications: 10 mM succinate, 12 mM formate, 5.7 mM Na2HPO4, 3.3 mM KH2PO4, 18.0 mM NH4Cl, 1.01 mM MgSO4, L- cysteine (20 mg/L), 1% vitamin solution, and mineral solution

The only study similar to the present work, is one in which the transcriptome of *S. oneidensis* producing current at an electrode, was compared to the transcriptome of *S. oneidensis* using Fe (III) citrate or oxygen as a terminal electron acceptor (336). In that work, genes for *OmcA*, *MtrA*, *MtrB* and *MtrC* were shown to be upregulated at an electrode compared to those using Fe (III) citrate (which is membrane permeable) or oxygen as an electron acceptor. However this does not provide any information as to the likely final abundance of protein that might be expected in a proteomic study. This is often due to the lack of 1:1 correlation between mRNA levels and protein levels (337,338). The number of OmcA molecules per bacterial cell is about 2000-2500 (339), a number probably similar to that for the TonB1 system proteins (ExbB1 = 2463+/- 522 in *E. coli* (340)), but neither - despite their apparent abundance - gave peptides that were identified using this particular mass spectrometry technique.

5.3 Conclusions

In the present work, iTRAQ techniques were used to investigate changes in the soluble and insoluble sub-proteomes of a functioning exoelectrogen. We identified 75 differentially expressed proteins in the Gammaproteobacterium *Shewanella oneidensis* MR-1 during anaerobic growth on an insoluble electrode in a microbial fuel cell. For *S. oneidensis* under these conditions whilst producing current at an electrode, the efflux protein channel TolC (Q8EAJ8/SO_3904) and the putative amphiphilic channel-forming Q8EFY5 (SO_1829) tetratricopeptide repeat (TPR) protein, are more abundant than in equivalent microaerobic planktonic cells. Under the same circumstances, systems involved with iron respiration such as the TonB2 system and TonB receptors are less abundant, suggesting that this is a competing system for energy transfer that is taken "off line". Proteins that interact with the peptidoglycan layer and that may have a role in overall cell shape or the formation of outer membrane vesicles such as Q8EBH3 (SO_3545) outer membrane porin (OMP) and Lpp murein lipoprotein (Q8EHD1/SO_1295) are more abundant in planktonic microaerobic *S. oneidensis* cells than anodic electrogenic cells, and future work may be able to tell what these potential changes in cell morphology, if they are present, signify.

This chapter illustrates that different mechanisms may come into play for transfer of electrons to an anode by *S. oneidensis* depending on the degree of oxygenation of the growth medium. For example in an anaerobic study, such as the transcriptomic study by Rosenbaum and co-workers (336), not only are the mRNA levels for the MtrCAB-OmcA decahaem cytochrome system upregulated in electrogenic anodic respiration *S. oneidensis* (versus Fe(III) respiration), but also the TonB2 system (SO1824-1928) and the putative TonB receptors Q8EEF5/SO_2427 and Q8ED60/SO_2907. This seems to be in contrast to the present study, where some of the same proteins are less abundant in anaerobic anodic cells. This again points towards the lack of correlation between mRNA levels and protein quantification as a possible explanation for this. There is the need to consider that the relative abundance of mRNA and protein for each of these differentially regulated elements is incredibly dependent upon the exact circumstances under which the comparison is being carried out. It makes it very difficult to draw

comparisons between the mRNA and proteomic level studies discussed and can only be considered suggestive of differences at this point in time.

With respect to electron transport mechanisms that can operate in the absence of a high abundance of the *S. oneidensis* decahaem cytochromes, a recent study by Bücking and co-workers (341) demonstrated a membrane cytochrome-independent electron transport chain (MtrA-minus and MtrB-minus) to ferric iron, manganese oxides, and humic acid analogues, operating in *S. oneidensis*. Qian and co-workers have proposed an outer membrane cytochrome-independent iron chelate uptake mechanism catalyzed by TonB receptor Q8ED60 (SO_2907), with subsequent periplasmic ferric iron reduction (342). Bücking et al (341) note that these results would certainly challenge the assumption that Fe (III) citrate can be used as a model substance to study extracellular respiration.

This chapter provides the first demonstration of quantitative proteomics carried out on *Shewanella oneidensis* MR-1 within an MFC, delivering an insight into the regulation of pathways under these conditions compared to microaerobic growth. The identification of upregulated targets within the anode bound cells in the MFC, points towards a target that needs further validation to determine if it has any role in activity. Although the analysis did not identify any obvious targets to transfer into an engineered *E. coli* strain, the validation of the activity of these proteins within *Shewanella* may more clearly demonstrate their activity. This work may however be better suited towards forward engineering *Shewanella* to enable it to better survive and produce current in the environment within the MFC. Further analysis of engineered *E. coli* strains through either interaction work, or global proteomic analysis, may be paired with this *Shewanella* analysis in order to direct future work.

Chapter 6 – Chromosomal insertion of an electrogenic pathway and Interaction studies of plasmid based electrogenic system

This work was carried out with initial assistance from Dr Graham Stafford with the supervision of Professor Phil Wright

6.0 Introduction

This chapter is broken down into two distinct sections detailing chromosomal insertion work carried out at the start of the chapter in section 6.1 and interaction work carried out in section 6.2.

6.1 Chromosomal insertion of an electrogenic pathway

6.1.1 Introduction

Following on from the demonstration in chapter 4 that current generation is possible using plasmid based expression of an extracellular electron transfer pathway, the decision then had to be made as to what steps could be taken to further increase output.

- Would this be a case of metabolic engineering and pathway tuning to streamline the transfer of energy?
- Inserting further genetic elements?
- Or reducing the metabolic burden on the system?

It was decided that the path to follow that would yield the greatest “bang for our buck” was most to remove reliance on the dual plasmid based system.

Chromosomal insertion was considered over the other options due the fact that as chapter 4 discussed, the use of a non-native Mtr pathway was based within a 4 kb pACYCDuet-1 plasmid. The overall size of this plasmid for the different constructs varied from 6 to 17 kb and this was only considering the Mtr pathway. A further plasmid was also required for the IPTG inducible overexpression of the cytochrome maturation genes in the form of the 12 kb plasmid, pRGK333. Metabolic burden due to plasmid based expression is well documented (343–348) with physiological effects noted including up to 18% of total cell protein being required for antibiotic resistance (343) and 26% decrease in growth rates between plasmid and non plasmid systems (345). Increasing the metabolic burden can also decrease the chance of plasmid retention (344) which, when a system is being used for long term analysis, is of even greater concern.

If a purely metabolic engineering pathway had been chosen, then this would have meant either manipulation of the host organism genome or overexpression of a (metabolic) bottleneck. Both of these would firstly require a study (potentially quantitative proteomics) into how the wild type host cells (or empty plasmid bearing cells) compared to the engineered (plasmid bearing) strain, which is a significant piece of work in itself. If the genome modification option was chosen, then this presents further challenges compared to standard cloning. If a more standard cloning option was chosen, then the option is either to base an upregulated gene on a new plasmid (making a highly undesirable 3 plasmid system) or add to the already very large plasmids (difficult due to cloning limitations with such a large plasmid).

Due to the aforementioned stated reasons, it was decided that basing the *S. oneidensis* MR-1 Mtr genes and overexpressed cytochrome maturation genes on the chromosome was the most logical choice. Once this system was chromosomally based, it would yield the following potential outcomes:

1. Greater power output than a plasmid based system

2. No change in power output compared to the plasmid based system
3. Decrease in power output compared to the plasmid based system

Result number 1 presents the obvious advantage that a greater power output is achieved from the system being chromosomally based and therefore showing the impact of plasmid maintenance. It provides opportunities to base other potentially useful genes on plasmids.

Result number 2, where the power output is the same would mean that although there is no increase in power output, the cells are still now plasmid free. Although this may not have removed any metabolic burden, it frees up space for new plasmids that may allow for power increases that could not easily be done with the current 2 plasmid system.

Result number 3 is the worst circumstance, but as long as the cells are still alive, then there is no real reason why the cells would be producing less power. It could be due to reduced transcript levels due to a single DNA copy of the genes being based on the genome compared to multiple plasmid copies. This would not be a failure of the chromosomal insertion, but would instead be a question of rebalancing the overall transcript levels generated by the genome based system through promoter tuning. If the transcript strength was determined to be the same as that seen in the plasmid based system (through a comparison by q-PCR), then theoretically there is no reason why the system should not generate the same power output as the plasmid based system. Once this has been done the cell system still has at least the advantages of result number 2.

This thesis was based on an attempt to generate electricity through the use of an organism that was previously incapable or at the very most, poorly capable of this ability. Following demonstration of this through a plasmid based system, maximising electrical output was the ultimate aim of this chapter through the reduction in the metabolic burden of the cells.

6.1.2 Experimental thought process

The details presented here are specific to this chapter and necessary to explain the various iterations that were worked through, as the process went on in order to try and attain a functional chromosomal insertion method.

6.1.2.1 Chosen organism

As discussed in chapter 4, the choice of the host cell for the introduction of a non-native extracellular electron transport pathway for interaction with an electrode was based on a variety of reasons. *E. coli* was the chosen species due to its well documented history as a model organism for genetic engineering (349–351) and also due to previous research that had been conducted showing that heterologous expression of *Shewanella c*-type cytochromes allowed for the reduction of soluble and insoluble iron (248,249). During the course of these studies it was discovered that in order to be able to express the membrane based *c*-type cytochromes, a type II secretion system was required (249).

Due to the use of a T7 based expression system, the BL21 variant, BL21 (DE3) was chosen as this has the prophage DE3. This provides a chromosomally based, stable integration of T7 RNA polymerase under the control of the *lac*UV5 promoter, allowing for production of transcript of T7 regulated genes following induction by IPTG (258).

6.1.2.2 Chromosomal insertion techniques

Choice of genetic manipulation

There is a variety of different methods that can be used to insert genetic fragments into a chromosome of a desired organism, all with varying degrees of success, size limitations and localisation options. A selection of these is shown in Table 6.1.

Table 6.1 – Comparison of a variety of chromosomal insertion methods

Chromosomal insertion method	**Recombination**	**Attenuation transposition**	**Mosaic (random) transposition**
Success rate	Up to 90 % (352)	79% average (up to 97%) (217)	50% (353) Up to 90% (354)
Insertion size limits	10 kb demonstrated (352)	7 kb demonstrated and ~14 kb theoretical (217)	10 kb demonstrated (353)
Localisation options	Site specific recombination, theoretically at any point	Targets highly conserved specific region (*attTn7*) – immediately downstream (3' end) of *glmS* gene	Random integration into the genome
Highly cited example system	Datsenko and Wanner's Lambda red recombination – pKD46 based system (210)	Tn7 - pGRG36 based system (217)	Mini Tn5 – pUJ based system (354)

A more detailed analysis of two of the methods described in Table 6.1 is carried out in sections 6.1.2.2.1 to 6.1.5 with descriptions of the pros and cons of different methods, leading to their eventual use within this chapter.

6.1.2.2.1 Lambda red recombination

This is a homologous recombination technique whereby PCR primers can be designed to provide the homology that permits "one-step" gene knockouts and if designed properly, can be tailored for "three-step" gene insertion. This method, although not

initially discovered, was highly popularised by Datsenko and Wanner in 2000 (210) with the paper being cited over 6000 times as of 2014.

The protocol can be used for either site specific deletion of a gene, gene cluster or with a little more work, the insertion of a gene or gene cluster. Due to the flexibility of the system, a researcher feeling bold enough can even manage a simultaneous deletion of a genetic element and replacement within the same experiment. Recombination can occur with as little as 35 bp homology on either side of the desired site of modification (355,356) and has been used as the sole method to create a library collection of single knockout *E. coli* K-12 variants (357).

The system is strongly based around solid work with PCR with this being especially true for insertion work. Full description of the exact methods can be found in the materials and methods section 3.2.7 – this discussion point is being used to confer the simplicity (or not so as is shown to be the case) of the techniques to get either method to work.

This site specific system makes use of the yeast homologous recombination machinery neatly packaged away within a set of plasmids as shown in Table 6.2 below

Table 6.2 – Details of Datsenko and Wanner lambda red recombination plasmids

Plasmid name	**Genetic elements contained**	**Role in the process**
pKD46	*Beta, Gam, Exo* (355)	Arabinose inducible recombination machinery. • Gam - protein to prevent degradation of linear DNA. • Exo – 5’ to 3’ dsDNA lambda exonuclease.

		• Beta- protein to aid in insertion of linear DNA (355)
pKD3, pKD4, pKD13, pKD32	Flippase recognition target (FRT) flanked resistance cassette. Kan for pKD3 and pKD13 and Cm res for pKD4 and pKD32	For insertion of FRT flanked, removable selection marker
pCP20	FLP recombinase (358)	Allows removal of FRT flanked resistance cassette

For deletions to occur, the following steps must be followed (illustrated in Figure 6.1):

1. A set of primers need to be designed that will amplify the desired FRT flanked resistance cassette (either Cm or Kan) with 5' regions that are homologous for the region flanking the desired deletion point. These can be designed to be base sensitive to allow for very precise deletion (and insertion of selection marker) of DNA regions.
2. Once the resistance cassette has been amplified with the flanking regions for the desired deletion target, the strain in which the deletion is to occur needs to be transformed with the temperature sensitive plasmid pKD46. This plasmid contains the recombination machinery, Bet, Gam and Exo. Gam inhibits the host RecBCD exonuclease V (359) so that Bet and Exo can gain access to DNA ends to promote recombination. This plasmid is selected for by ampicillin and then induced in a fresh culture with 1 mM arabinose to express the plasmid proteins to allow for recombination. Purified dsDNA of the FRT flanked resistance cassette is then electroporated into a washed, desalted aliquot of the induced pKD46 containing target cells. Outgrowth is done in suitable media such as LB and cells are then plated out on selective plates, dependant on the choice of FRT flanked resistance cassette. Colonies that grow on the selective

plate are deemed to be positive but are the deletion event can be confirmed in a variety of ways including western blots against a control to see if the target protein is no longer present. An example of the layout can be seen in Figure 6.1.

Step 1. PCR amplify FRT flanked resistance cassette

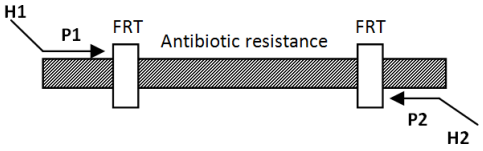

Step 2. Transform strain expressing λ Red recombinase

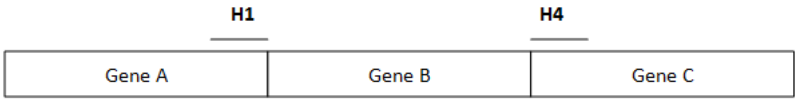

Step 3. Select antibiotic resistant transformants

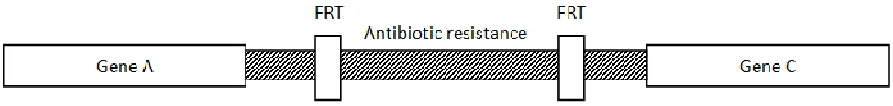

Step 4. Eliminate resistance cassette using FLP recombinase

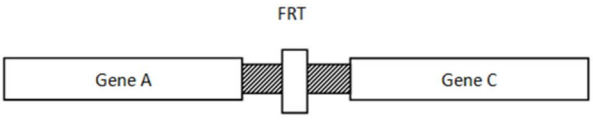

Figure 6.1 - 4-step procedure for site specific gene knockout using lambda red recombination. Modified from Datsenko and Wanner (210)

In order for an insertion event to occur, two additional PCR steps are required at the beginning which can be considered a step 1 and step 1.5 in relation to Figure 6.1. The gene(s) to be inserted need to be amplified and fused to the antibiotic resistance cassette. For the duration of this explanation it will be assumed that the resistance

cassette is to be attached upstream of the genes of interest. In practice, the localisation of the resistance cassette in regard to the gene(s) of interest doesn't matter.

1. The first step for the insertion event involves modification of the primer design whereby the first chromosomally homologous region (H1) at the 5' of primer 1 remains the same but primer 2, shown at the 3' end in step 1 in Figure 6.1 retains priming site P2 but H2 changes from being homologous to the region of chromosomal insert to being a flanking region homologous to a flanking region of the gene of interest (H3).
2. The gene of interest then has primers that are designed for it amplification but also have homologous ends that permit fusion to the resistance cassette at the 5' and are homologous to the desired region of insert at the 3'.
3. Once both these targets have been amplified the two PCR fragments must then be fused together which is done through the use of PCR overlap. This is typically done by adding in the two PCR products as the templates, relying on H2 and H3's complementarity to each other for the fusing of the two regions. P1 and P4 are then used to amplify the completed construct which then results in a product with internal homologies linked but still with terminal flanking regions that are homologous to the chromosome.
4. A strain expressing the lambda red recombinase system based on pKD46 is electroporated with the fused linear DNA from step 3. Outgrowth and selective plating of the cells is then done.
5. Cells demonstrating antibiotic resistance to the inserted cassette are deemed to be successful insertions but further verification is done by PCR, sequencing or western blots.
6. The resistance cassette is then removed through the use of a curing plasmid named pCP20 that expresses a Flippase for recognition and removal of the FRT flanked cassette.

Step 1. PCR amplify FRT flanked resistance cassette

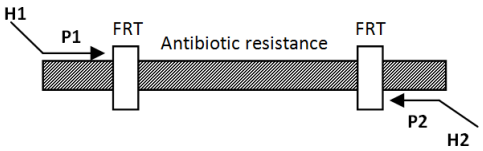

Step 2. PCR amplify gene of interest

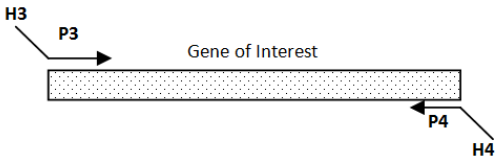

Step 3. Overlap PCR

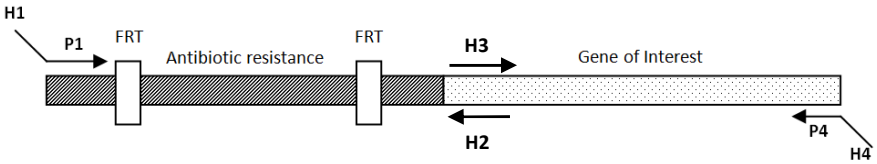

Step 4. Electroporate overlap DNA into strain expressing λ Red recombinase

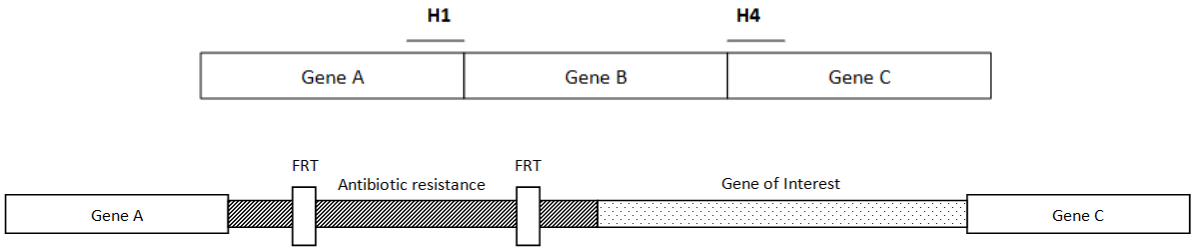

Step 5. Select antibiotic resistant transformants

Step 6. Eliminate resistance cassette using FLP expression plasmid

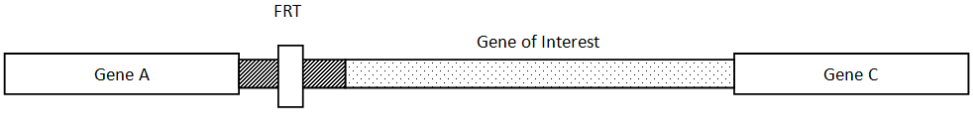

Figure 6.2 - Example of the steps needed in order to be able to insert a genetic element into a genome using lambda red recombination

6.1.2.2.2 Transposon based insertion

An alternative to the lambda red recombination method for chromosomal insertion is transposon based insertion. Whereas recombination is a highly flexible technique in terms of the site of modification and the type of modification (deletion, base swapping or insertion), a transposon based method is purely focussed on insertion and is localised towards a single site. The chosen method for further investigation is Tn7 based attenuation with a basis around a paper from McKenzie and Craig (217) with details of the plasmid used shown in Table 6.3**.**

Table 6.3 Details of Tn7 attenuation chromosomal insertion plasmid

Plasmid name	**Genetic elements contained**	**Role in the process**
pGRG36	*TnsA,B,C and D* (217,360)	• *TnsA* - works together with TnsB to form a transposase – recognising, breaking and joining transposon • *TnsB* – member of retroviral integrase family – works with *TnsA* to form transposase • *TnsC* – double stranded DNA binding protein and regulator. Required for activity of *TnsAB* complex • *TnsD* – Target selection protein

This system makes use of a single 12kb plasmid (pGRG36) whereby the GOI is inserted into the MCS which is flanked by two Tn7 recognition arms. Once in there, the plasmid is then transferred into the desired host strain, induced with arabinose and plated out on selection free media. This in theory turns chromosomal insertion into a cloning experiment followed by a transformation and induction. The plasmid contains numbers transposase proteins that are required for identification, regulation, DNA cleavage and insertion (as detailed in table 5.3). A full description of the methods used can be found in chapter 3.2.28.

This system has been used for the insertion of a variety of different genetic elements with sizes up to 7.1 kb being demonstrated for insertion and a theoretical size limit of 14 kb (217) making it a viable option for the insertion of potentially the entire Mtr operon (MtrD, E, F, OmcA, MtrC, A and B) if required.

Once the GOI is cloned into pGRG36, the same plasmid can be taken to a wide variety of different strains, not just *E. coli* but other gram negative species, due to the highly conserved nature of the Tn7 recognition sequence (361–364).

6.1.2.3 Method overview

Following an overview of the available methods a final table stating the clear advantage and disadvantages of each can be seen in Table 6.4.

Table 6.4 - Comparison of the two chromosomal insertion methods

Method of insertion	**Advantage**	**Disadvantage**
Lambda red recombination	• Site specific insertion • Resistance selection marker • Multiple insertion/deletion events can be done in one strain	• Linear dsDNA • Overlap PCR to join resistance cassette and GOI

		• Must be optimised and repeated for every experiment • Multiple plasmids needed • Limited transfer to organisms outside of *E. coli*
Transposon	• Single plasmid system • Standard cloning into MCS of plasmid before insertion • Allows for large quantity of DNA to be made • Attenuation site is highly conserved within many prokaryotic species • Allows for chromosomal insert into many strains (other than *E. coli* due to highly conserved AttTn7 region) using same plasmid	• Single insertion into strain. Once the site is used then you can't use it again • No selection marker • Large plasmid (12kb) made larger with insert. • Very low copy number • Very limited MCS

The advantages of the lambda red recombination system make it a very appealing method for insertion although the number of steps involved, the complications in designs and multiple plasmid systems mean that you need to be very comfortable in your molecular biology skills before attempting. The attenuation system, although slightly limited, provides the opportunity for a standard cloning experiment to turn into a chromosomally based system – although at a fixed location.

6.1.3 Results and Discussion

6.1.3.1 Lambda red recombination for upregulation of native cytochrome maturation genes

In an attempt to move away from the large dual plasmid system detailed in chapter 4, the overexpressed cytochrome maturation genes found on pRGK333, which are native to *E. coli*, but not under aerobic conditions, were to be chromosomally upregulated. This meant that instead of having to try and insert all the genes present on the large plasmid, the genes that were already present were to be tuned to more appropriately fit the task at hand. This required a much smaller insertion than the chromosomal basing of the full Mtr pathway and presented a good test of the lambda red recombination system.

The options for this were a high level constitutive based expression system for continual protein expression of these genes using the promoter for the native *hupA* gene (365–368) and also a tuneable or at least an inducible system using the arabinose promoter (369). These promoters were then to be inserted upstream of the respective Ccm genes and an option to include the further upstream genes NapB and NapC was included due to their alleged roles in donating electrons to a recombinant Mtr pathway within *E. coli*.

In order to do this, the respective promoters needed to be amplified with ends permitting attachment to the FRT flanked resistance cassette. The initial amplification of the HupA promoter for use with Ccm A-H and for NapB, C and CcmA-H is shown in Figure 6.3.

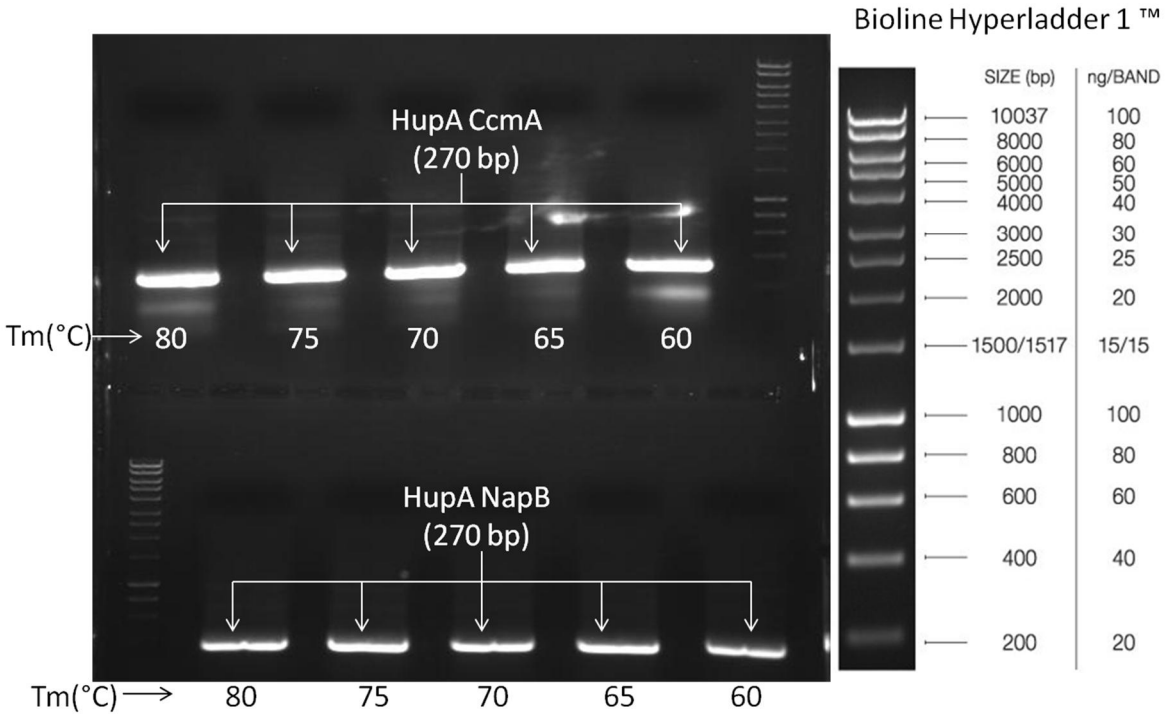

Figure 6.3 - Amplification of the HupA promoter for constitutive expression of CcmA-H and NapB, C, CcmA-H

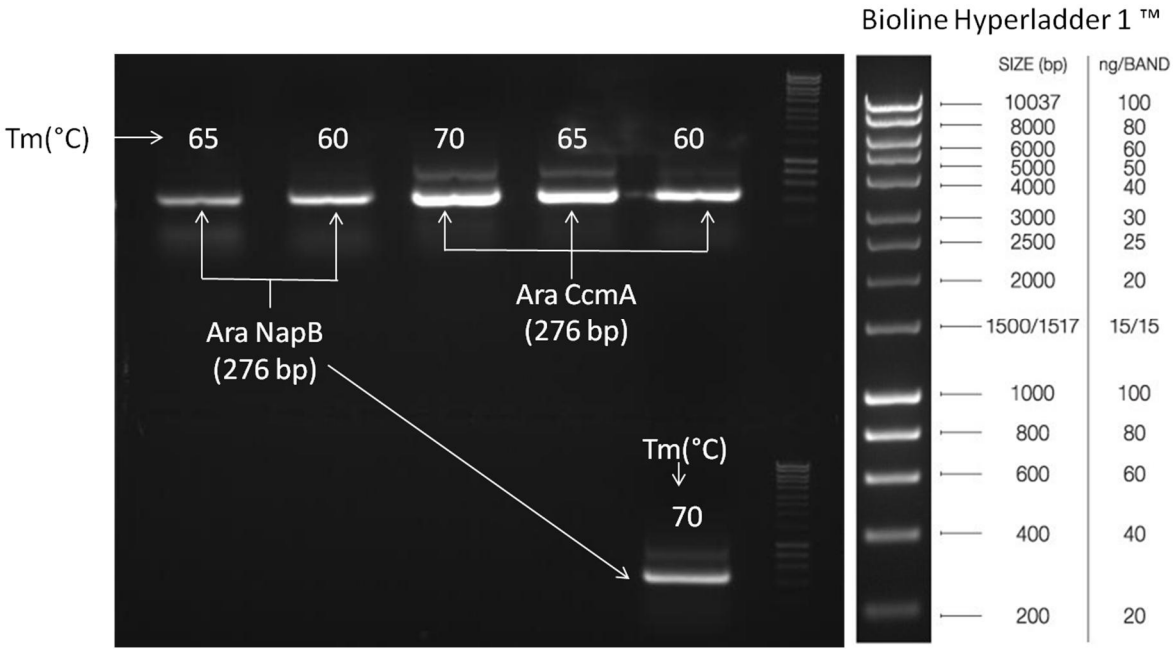

Figure 6.4 - Amplification of the arabinose promoter for inducible expression of CcmA-H and NapB, C, CcmA-H

The results show clear bands of the desired size for the amplified *HupA* and arabinose promoter, which could then be used to attach to the FRT flanked resistance cassette. Each of the amplified DNA sequences had a complementary DNA region to the element that it was to be attached to.

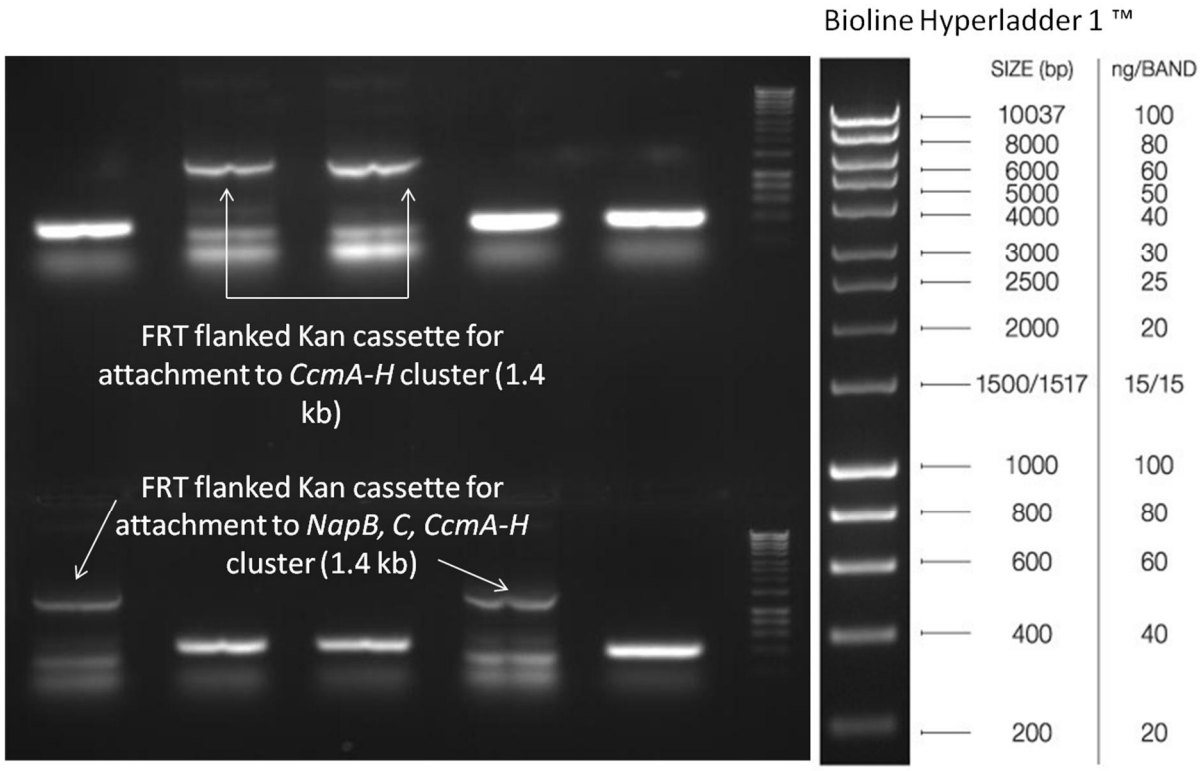

Figure 6.5 - Successful amplification of FRT flanked Kan cassette for attachment to respective promoter systems

Now that both the FRT flanked cassette and promoter systems had been amplified, the procedure to attach the two separate genetic sections needed to be carried out. The results of this overlap are shown in Figure 6.6.

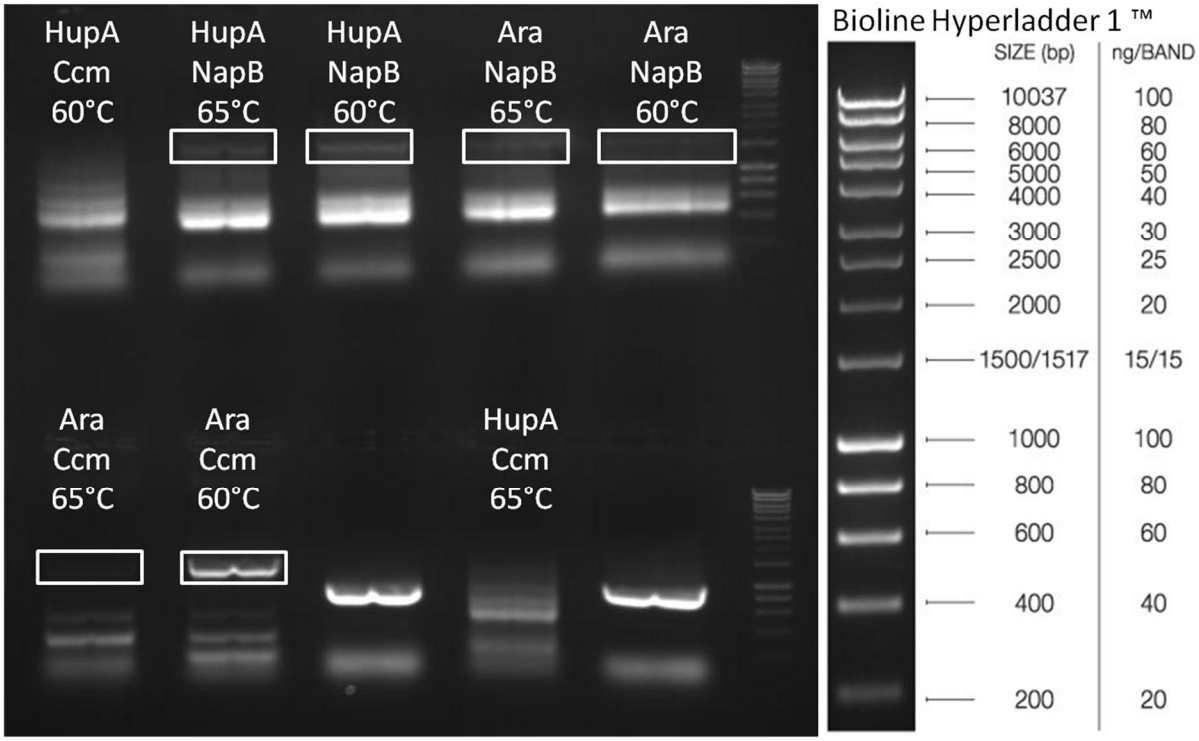

Figure 6.6 - Overlap PCR joining promoter regions to FRT flanked Kan cassette

Figure 6.6 shows the attempted overlap of the sections that resulted in low level amplification of bands around 1.5 kb. This was done using the same protocol to amplify the promoter section and the resistance cassette separately but used a longer extension time and appeared not to have worked. The protocol for the initial amplifications were optimised to provide the best possible yields as shown in Figure 6.7.

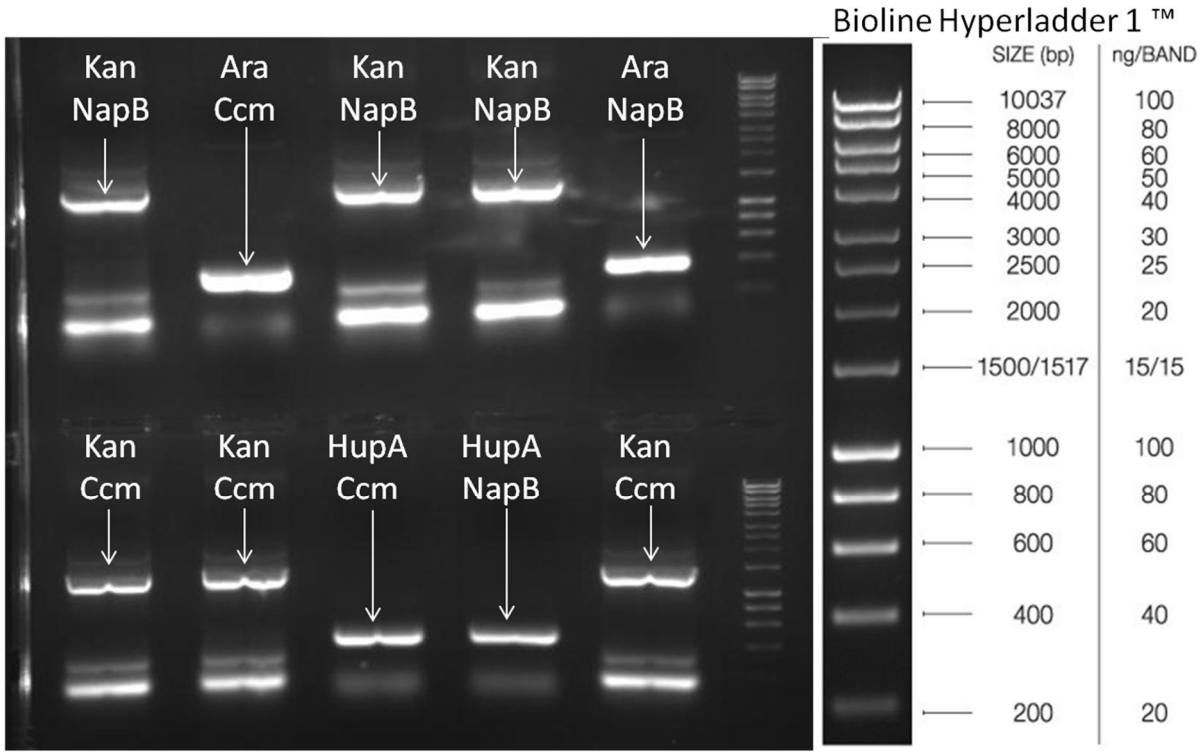

Figure 6.7 - Optimised PCR protocol for amplification of promoters and FRT Kan

Following the optimised amplification of the initial DNA elements, there was now a greater concentration of each of the components and potentially a greater chance of the overlap procedure working. The results of the overlap are shown in Figure 6.8.

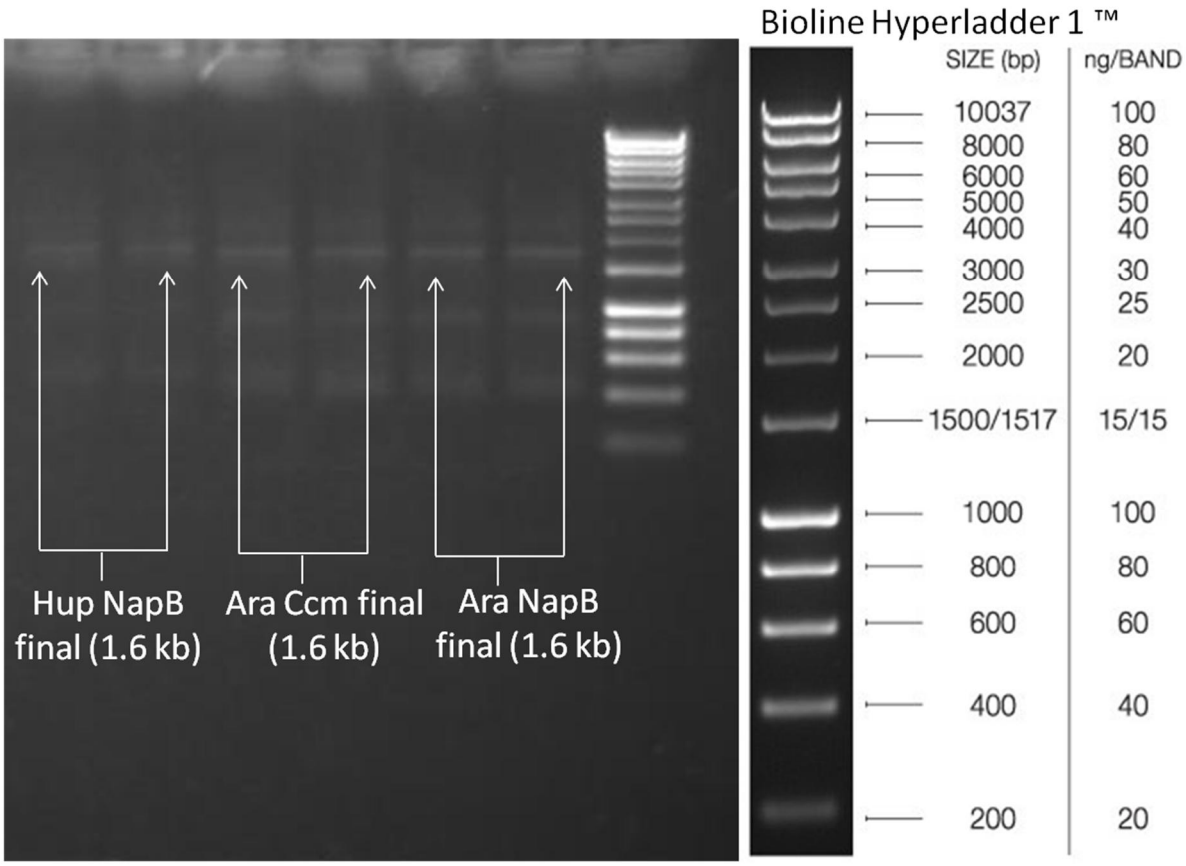

Figure 6.8 - Overlap PCR joining defined promoters to FRT flanked resistance cassette

The results show that the bands appear to be the correct size at 1.6 kb but are very faint even before full purification to remove other bands. The bands post purification are shown in Figure 6.9.

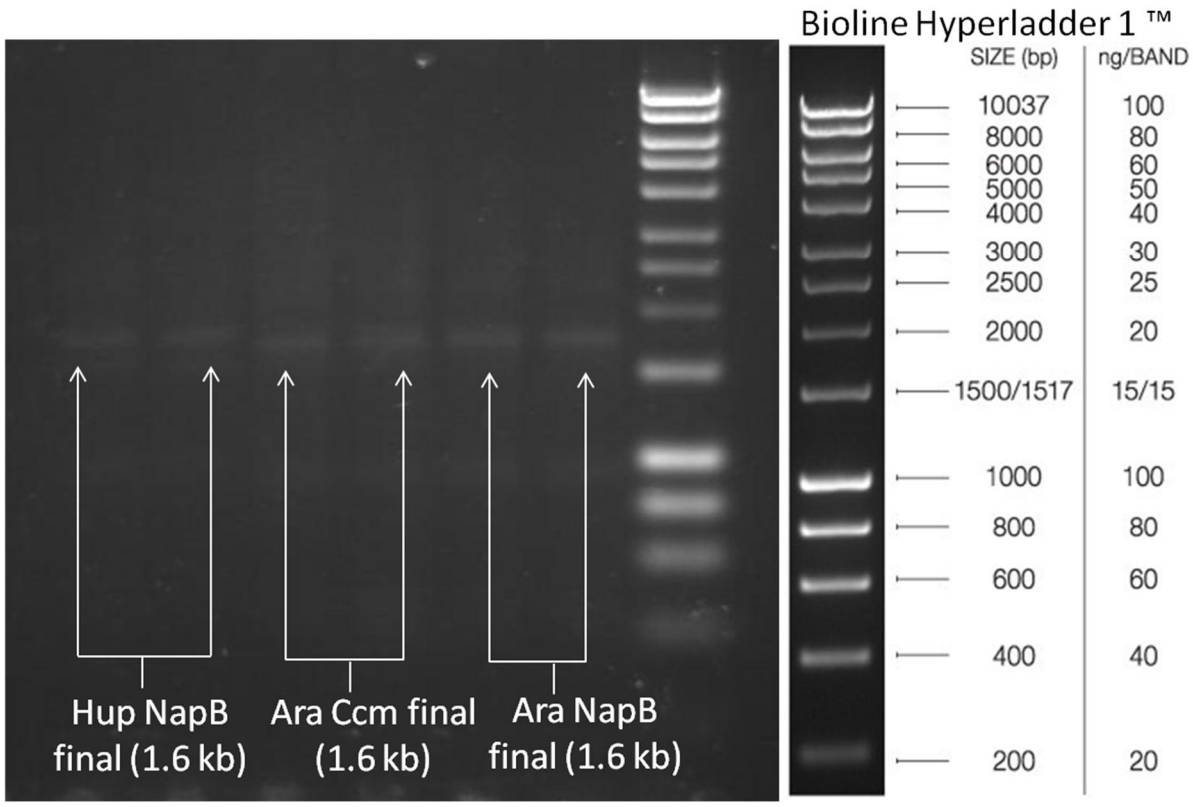

Figure 6.9 - Gel purified joined promoter and FRT flanked resistance cassette

An electroporation into BL21 DE3 expressing the recombinase machinery (pKD46) was done using 10 µL of each of these samples in 100 µL aliquots of electrocompetent cells, but no positive colonies appeared on any of the plates. The procedure needed to be optimised further in order to be able to get a quantity that could be used for a successful insertion.

Balancing the molar ratios of the different DNA elements was attempted in order to try and aid the overlap procedure. This meant that instead of using equal volumes of the promoter and Kan cassette, the size and concentration of the different components was taken into account to provide a better balance of each. The results of this are shown in Figure 6.10.

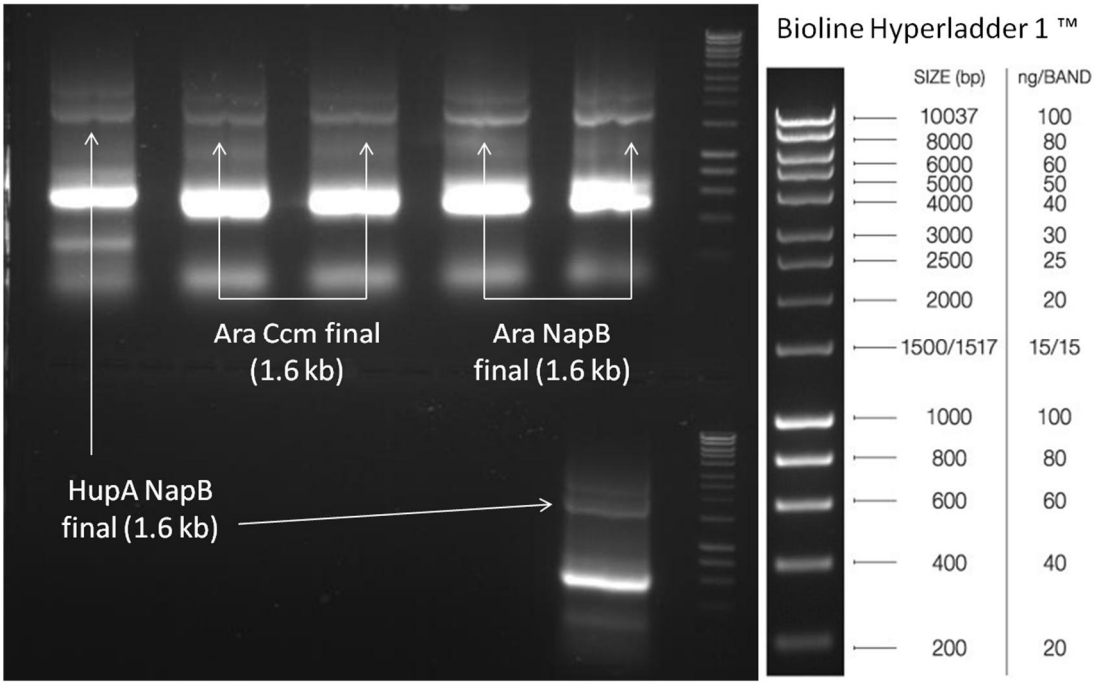

Figure 6.10 - Increased concentration of promoter joined to FRT flanked cassette using molar ratio technique

The modification of the procedure appeared to produce a greater yield in the final DNA product when compared to Figure 6.8. A large, unwanted band was still amplified at roughly 500 bp. Due to the high level of unwanted DNA bands, the product still had to be purified before it could be used for recombination. The post purification concentrations of the samples are shown in Figure 6.11.

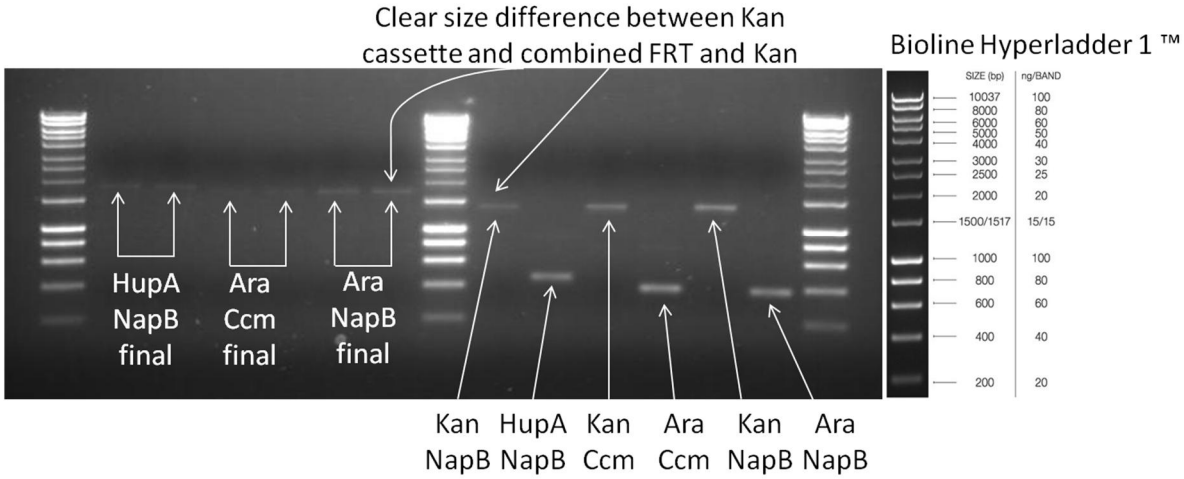

Figure 6.11 - Gel purified promoter, Kan cassette and combined samples

The purified samples were still of a very low concentration that again did not yield any colonies when electroporated into cells expressing recombination machinery. As the concentration of the overlap PCR product could not be increased, the obtained final product was then used as a template to allow for amplification of this using a simple PCR technique. The results of this are shown in Figure 6.12.

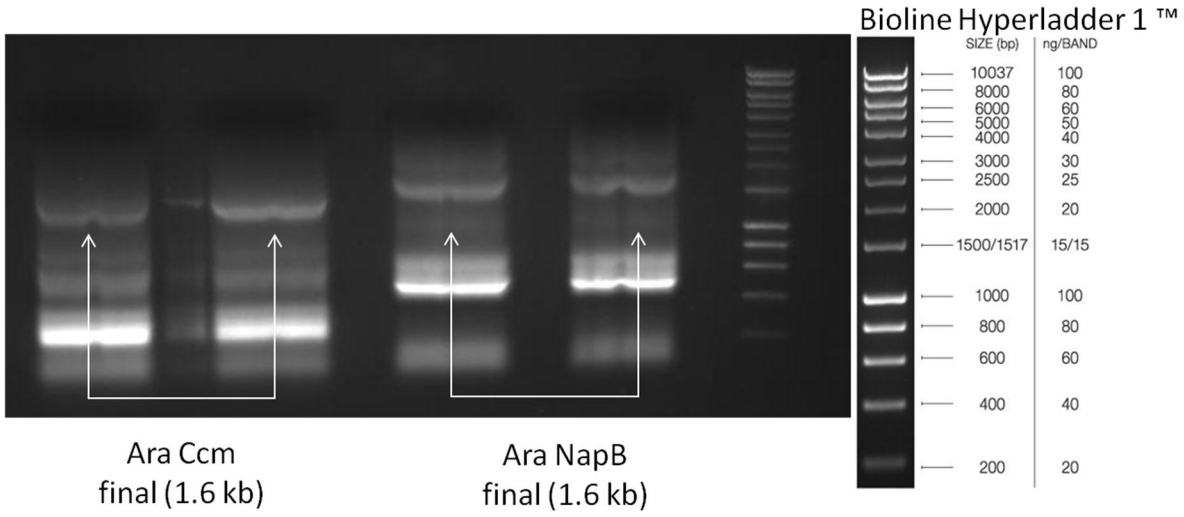

Figure 6.12 - Attempted amplification of the final overlapped PCR and Kan cassette using the product from Figure 6.11 as a template

The results from this attempted amplification show that the yield is roughly the same as was previously acquired with multiple bands also being amplified as well. As the use of the template instead of the two separate fractions appeared not to make a difference, an adaptation of the old method was instead attempted. This one made use of a high temperature initial denaturation. A variety of conditions were attempted with the high denaturation and 1:1 molar ratio of different DNA elements kept as a constant. The results of this setup are shown in Figure 6.13.

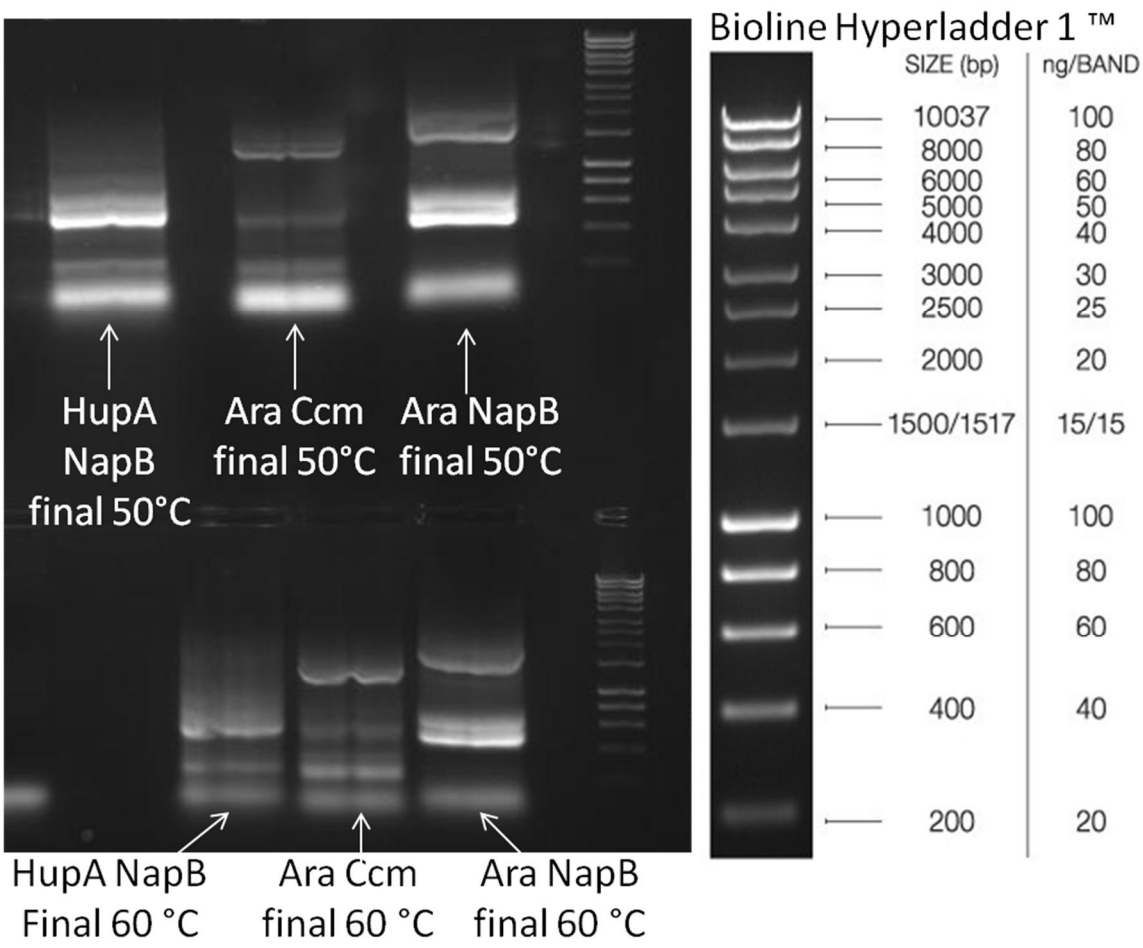

Figure 6.13 - Overlap PCR for combination of promoter with Kan cassette using modified protocol

The results of this experiment provided very similar results to those seen before with little, if any increase in the desired final PCR product. Due to the large number of attempts at this method, with little no real sign of improvement, alternative methods were sought. This is discussed further at the end of this section.

6.1.3.2 Lambda red recombination for chromosomal insertion of Mtr genes

This was attempted simultaneously with the chromosomal upregulation of the cytochrome maturation genes.

In order to try and ensure good production of transcript, it was decided that the Mtr cluster should be inserted near the origin of replication on the BL21 (DE3) genome. It

also had to be done at a point that wouldn't interfere with any genes or operons. In order to do this, the genome of BL21 (DE3) was viewed on Xbase (http://www.xbase.ac.uk/) starting from the origin of replication. The genes closest to the origin were then reviewed in order to try and identify operons. Immediately downstream of the origin of replication is *thrL, thrA, thrB* and *thrC* which is then followed by *yaaX* (shown in Figure 6.14). This appears to show a 4 gene cluster at the start of the genome which is then followed by an unconnected *yaaX* gene. It was decided that the cluster could be inserted at this point.

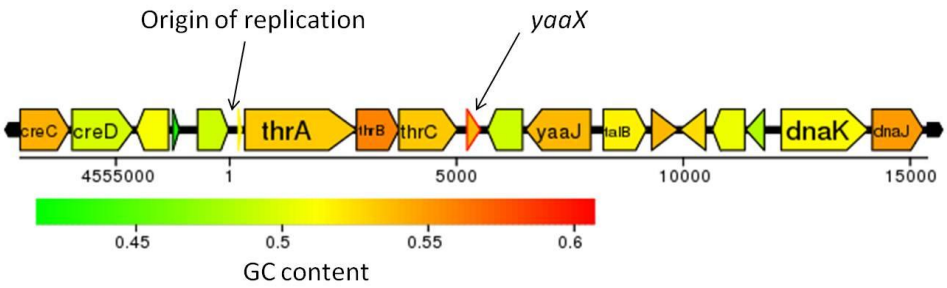

Figure 6.14 – Genome view of yaaX location near the origin of replication in the BL21 (DE3) genome

In order to make sure that the insert would not interfere with the *yaaX* including any regulatory elements, this had to be inserted sufficiently upstream of the *yaaX* start codon.

The primers were designed to have 40% of the primer available for amplification of the GOI with 60% homologous to the region the insertion was to occur (upstream of *yaaX*).

Amplification of the various Mtr gene sets were divided up as follows:

- OmcA
- MtrA, B and OmcA (MtrABO)
- MtrC, A and B (MtrCAB)
- MtrC, A, B and OmcA (MtrCABO)

In order to ensure proper regulation of the inserted genes, the same regulation system utilised within the plasmid system (lac inducible T7 promoter) was chosen to be amplified. Due to the high level of activity exhibited by the T7 RNA polymerase, it was essential that a T7 terminator was placed downstream of the GOI. Due to the fact that all Mtr clusters were cloned into MCS1 of pACYCDuet-1 and the same upstream and downstream elements of the plasmid were required from each plasmid, only a single set of primers was required to amplify all the different Mtr fractions. The primers were however modified to such an extent that correct binding to the Mtr sequence was not guaranteed due to the fact that a large percentage of the primer was not homologous to the target sequence. This however proved not to be an issue as can be seen with the amplification of the gene sets in Figure 6.15.

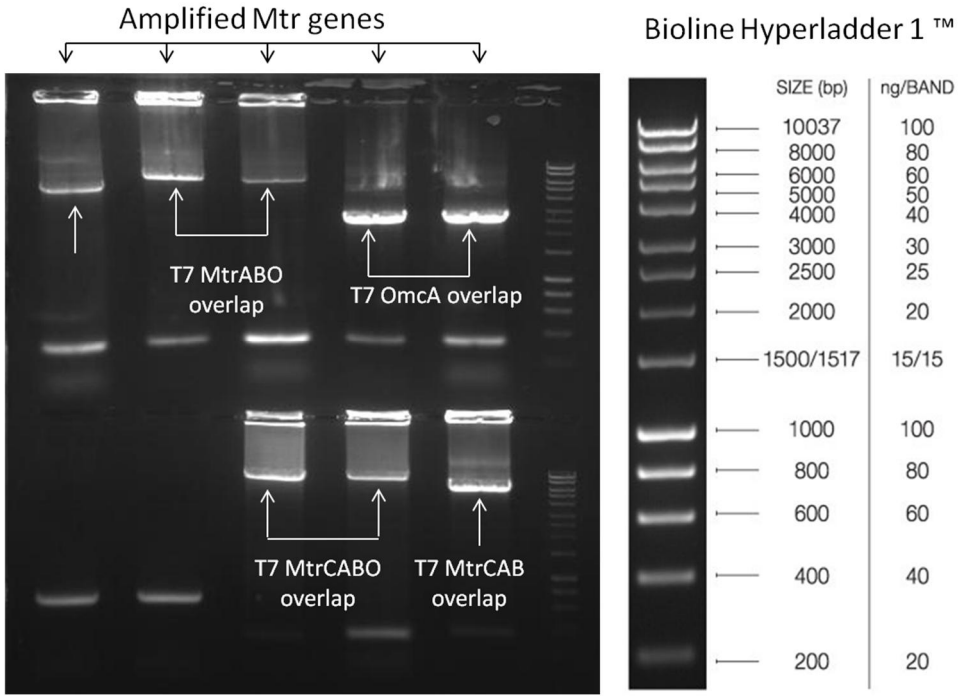

Figure 6.15 - Amplification of Mtr gene fragments with flanking ends overlap with FRT flanked Kan cassette

Following this successful amplification, the FRT flanked Kan cassette from pKD13 was the amplified as shown in Figure 6.16.

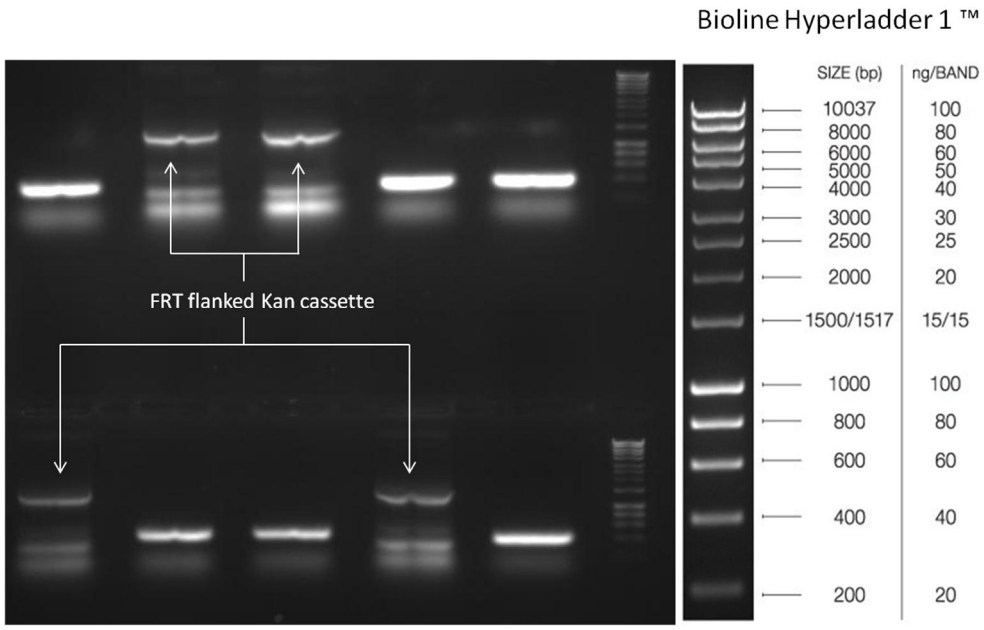

Figure 6.16 - Amplification of FRT flanked Kan cassette to be overlapped with Mtr fractions

Now that both the Mtr fraction and FRT flanked resistance cassette had been amplified, these two individual elements needed to be combined into a single dsDNA element to allow for site directed insert into the genome of BL21 (DE3). In order to ease the explanation of this, the reader is directed towards Figure 6.2 for further details**.** The two PCR products were added together into a single reaction along with primers for the 5' and 3' end of the eventual full sequence. The overlap of the two DNA sections together was in theory to be done through the homologous region in the middle of the two sections. Due to the multiple DNA binding events that were occurring within a sample, it was difficult to predict the best conditions for proper overlap to occur and so a range of temperatures were attempted. The result from this can be seen in Figure 6.17.

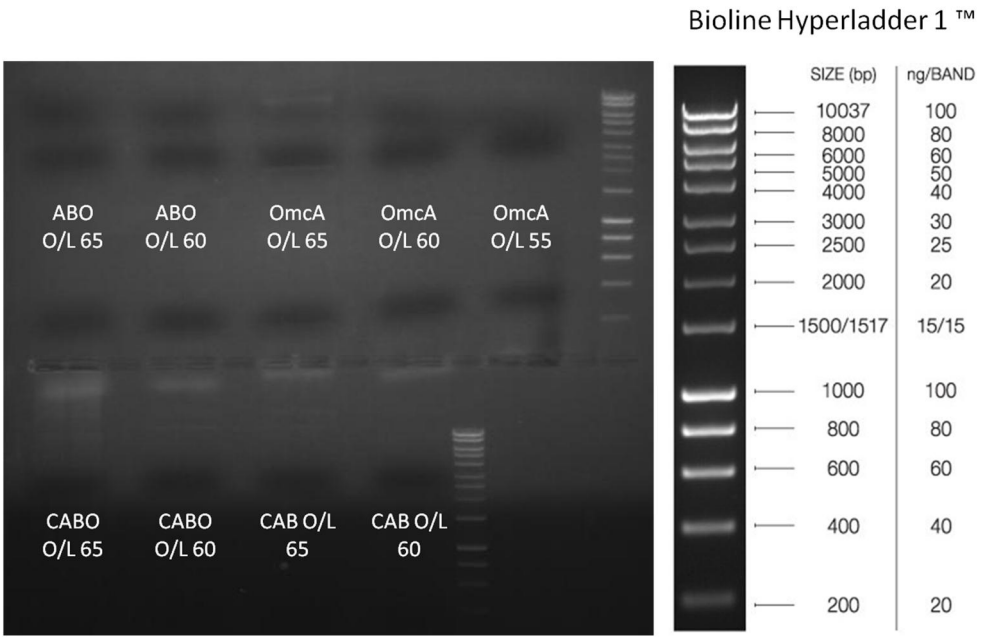

Figure 6.17 - Attempted overlap PCR for attachment of Mtr fragment to FRT flanked Kan cassette

The results above show that the PCR overlap didn't work across the range of temperatures chosen.

The results of these experiments demonstrated the difficulties of joining different DNA elements together in order to form single linear dsDNA fragments for insertion into the chromosome. This may have been down to issues with the length of the primers being used in the amplification of the Mtr gene cluster, FRT flanked resistance cassette and the promoter regions. The overlapping region between the two constructs may have been too small to allow for effective joining of the sections, but as there are no defined laws for this it is hard to properly estimate the correct amount of overlap. In order to get the overlap to work, the primers used could have been modified to increase the efficiency of the overlap but this would have led to very large primers and potentially increased the chance of secondary structures and unspecific binding. Even with new primers, the protocol would have to be essentially started from scratch, with the potential need for optimisation of all the amplification procedures that may well have yielded the same result. In the knowledge of the challenges accompanied by this method, alternatives were sought.

As the PCR required to amplify the Mtr fractions had already been demonstrated to work very successfully and the overlap was proving so troublesome, alternatives were looked for. A method that turned the issue into more of a cloning based one, compared to a complex overlap procedure was found with attenuation. This setup relied upon the cloning of the GOI into the MCS of the attenuation plasmid pGRG36 as detailed by McKenzie and Craig (217). This system was limited however by the fact that it was directed towards a specific region within the genome also meaning that further insertions, although not impossible, were supposedly done at a much lower (60-fold lower) efficiency using this system (219).

6.1.3.3 Tn7 based transposition

For the insertion of the Mtr gene elements into the genome using a Tn7 based system the genes needed to be cloned into the MCS of pGRG36 and then transformed into a desired host. Due to the limited MCS present in pGRG36 and the large size of the Mtr gene cluster (and resulting restriction sites naturally present within it), only the SmaI one site was suitable for insertion of the clusters. In order to try and ease the cloning of this blunt ended element it was decided that 5'phosphorylated primers should be utilised in order to try and increase the efficiency of the ligations. Using these primers would mean that any DNA amplified with these primers would by default have a 5' phosphate group that would be readily available for ligation instead of having to add this group through the use of a kinase or an equally complicated method.

Due to the fact that the PCR primers for the amplification of the Mtr fragments could be made directly homologous to the cloned Mtr constructs, no issues were expected with the amplification. This proved to be right as shown in Figure 6.18.

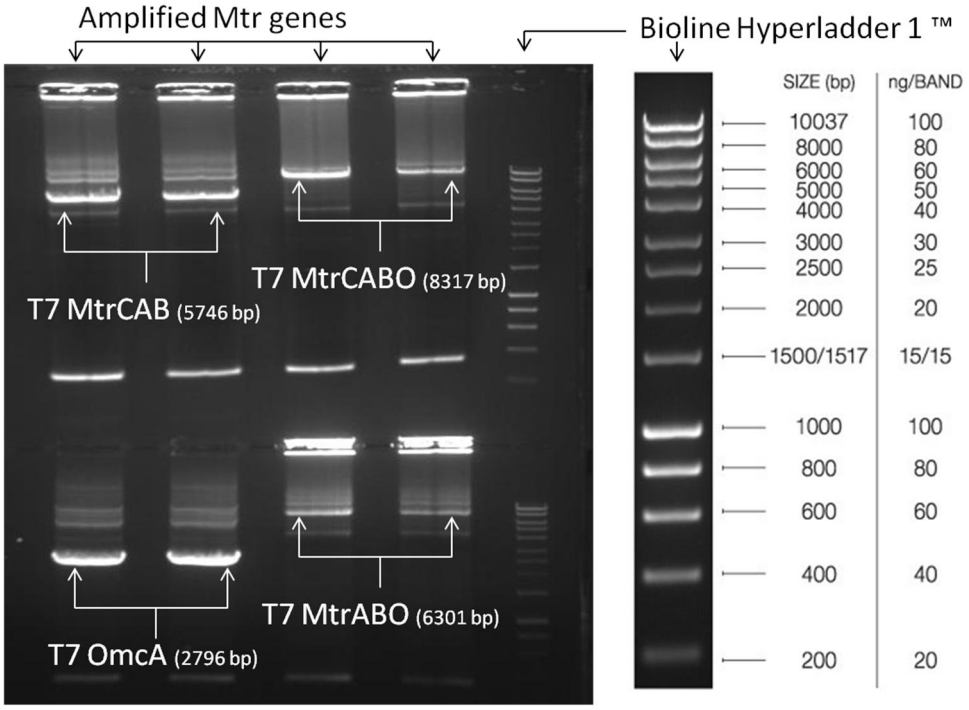

Figure 6.18 - Amplification of the Mtr fractions with 5' phosphorylated primers

The results show clear amplification of the desired fragments. The samples then needed to be prepared for ligation as shown below.

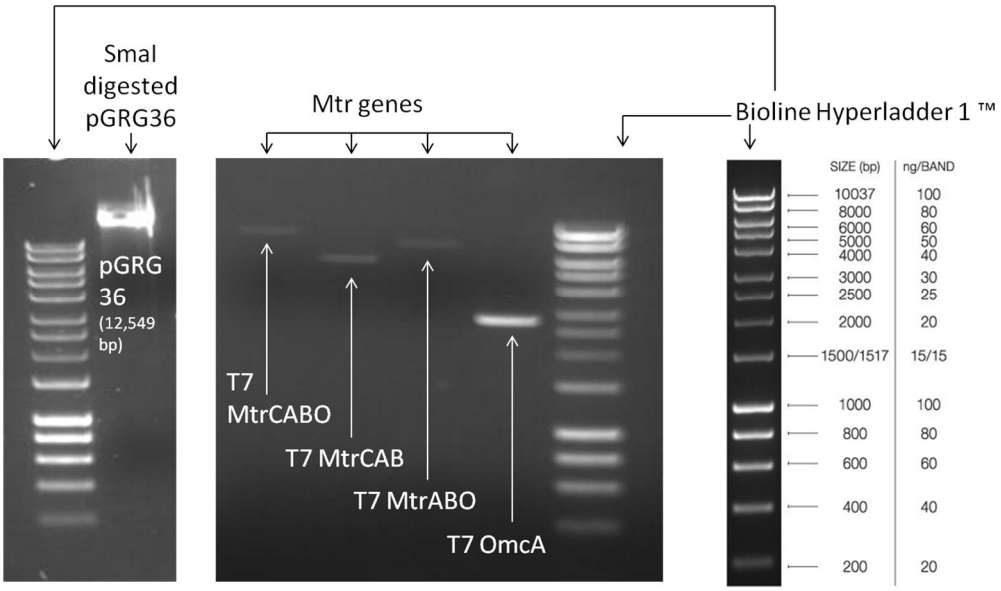

Figure 6.19 - Pre-ligation concentrations of Mtr fractions and pGRG36

Following ligation and successful transformation, the colonies were screened through the preparation of maxipreps and sending for DNA sequencing. For cloning purposes, DH5alpha library cloning efficiency was used as this has a EndA1 mutation resulting in decreased nuclease activity (370) making it a good choice for this procedure. The resulting miniprep DNA is shown in Figure 6.20.

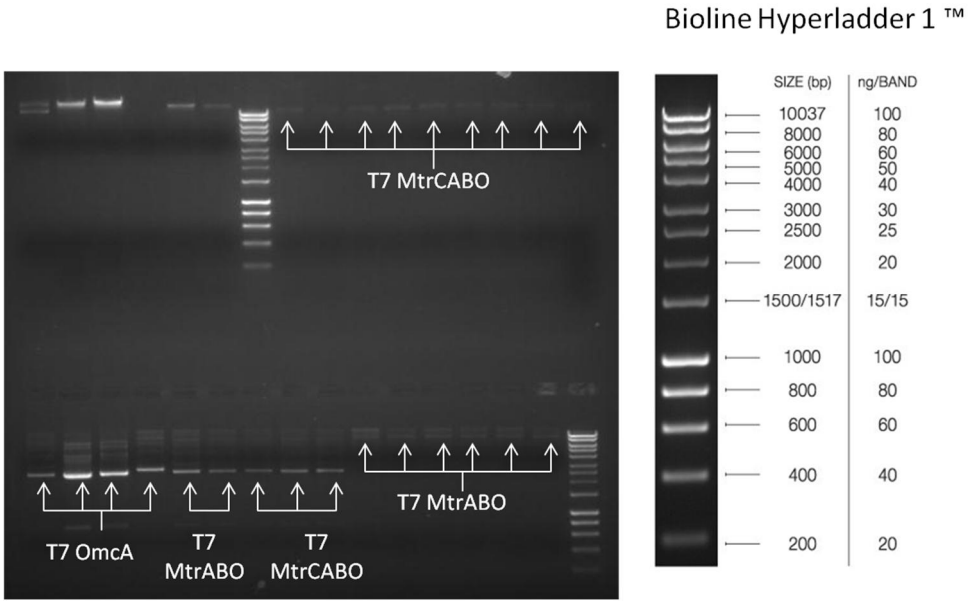

Figure 6.20 - Colony screening of pGRG36 clones following miniprep

The DNA sequencing for these constructs came back as a failure. At first it was presumed to have been a poor batch of sequencing as all of the pGRG36 insert screens failed. Other samples that had been sent up at the same time had however worked perfectly. The low yield of DNA shown in Figure 6.20 could have been the cause of lack of sequencing data and so a PCR amplification screen of the constructs was attempted as described by McKenzie and Craig (217). The results of this are shown in Figure 6.21.

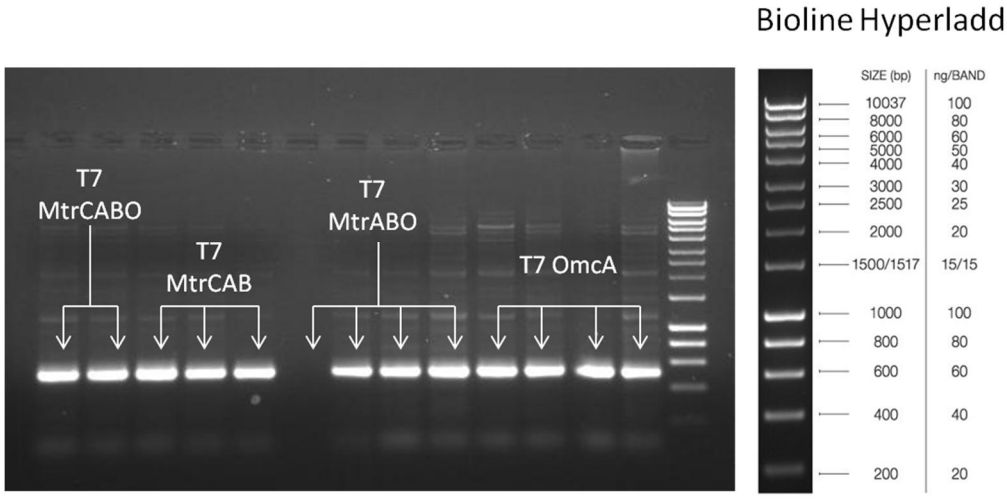

Figure 6.21 - PCR screen of miniprep DNA following inconclusive sequencing results

Using primers to amplify either side of the attenuation flanking arms, it provides a clear distinction between samples with an insert in the MCS of pGRG36 and those without. From immediately upstream of the Tn7 right arm to immediately downstream of the Tn7 left arm with no insert provides a product of 526 bp. The insertion of any genes within the MCS using the blunt end SmaI site would therefore yield the size of the gene (s) plus this 526 bp. As can be seen in Figure 6.21, all the screened colonies have inserts at the undesired size of 526 bp.

The issues with pGRG36 included a limited MCS, blunt end cloning, very low copy number of plasmid and very large sized plasmid that may have been a cause of why the ligations weren't working. Subsequently, it was decided that a work around for some of these issues should be attempted. A sensible and quick alternative was considered to be moving the attenuation recognition arms into a small, high copy number plasmid. Cloning into this alongside the larger pGRG36 (that still contained all the recombination machinery) in theory had the potential to help ease cloning issues. The chosen plasmid was pUC19 due to the fact that it was highly available, a very small plasmid, moderate sized MCS and was high copy number.

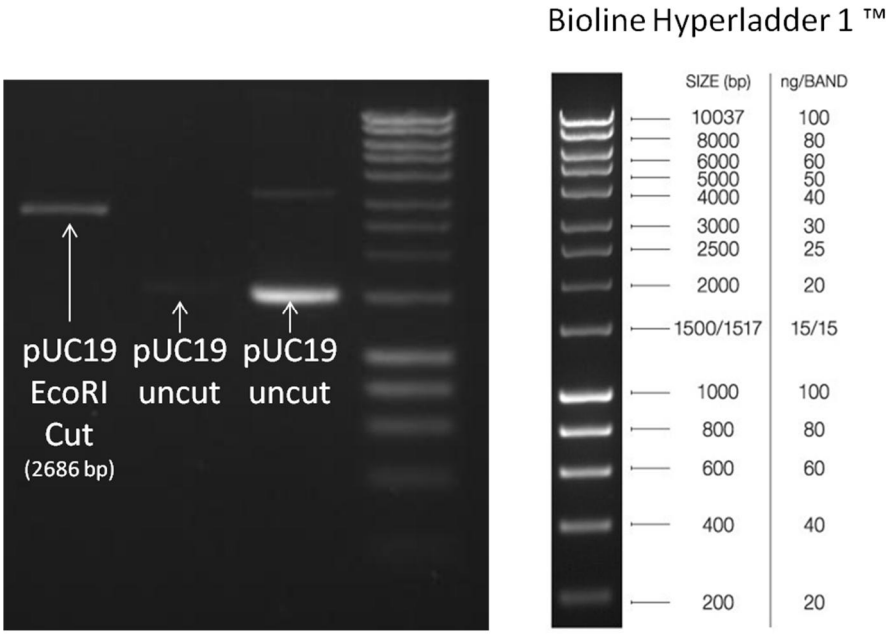

Figure 6.22 - pUC19 concentration analysis

A limiting factor with pUC19 was the fact that it carries Amp resistance which couldn't be used in parallel with pGRG36 as this also carried Amp resistance. In order to be able to change the resistance of pUC19, a recombination event was chosen as the simplest solution due to the ease of a single PCR and transformation allowing for simultaneous removal of the Amp cassette and replacement with the Cm cassette. The result of this can be seen in Figure 6.23.

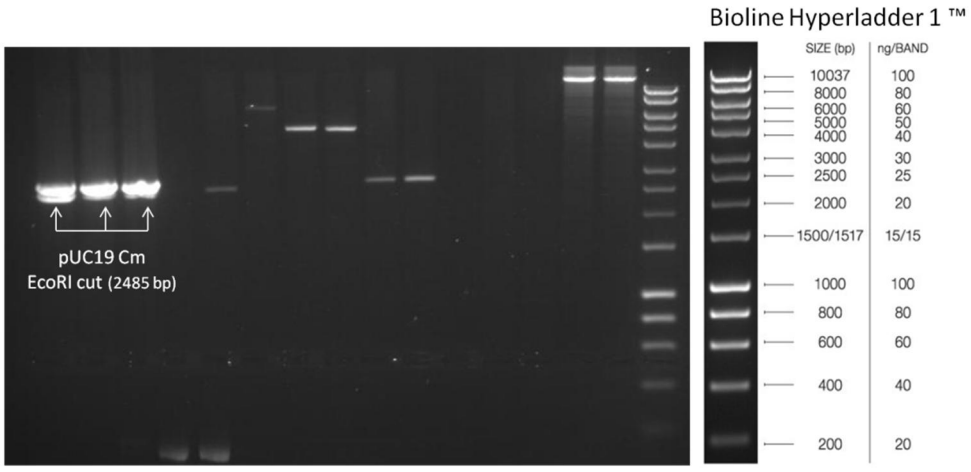

Figure 6.23 - pUC19 with Cm cassette inserted through recombination

In order to insert the attenuation recognition arms required for chromosomal insertion, the desired element from pGRG36 was simply amplified using PCR with the addition of restriction sites at the end that were compatible for insertion into the MCS of pUC19 (now with Cm). The insertion of the attenuation recognition sequence also included the MCS from pGRG36 including the previously used SmaI site. Results for this can be seen in Figure 6.24.

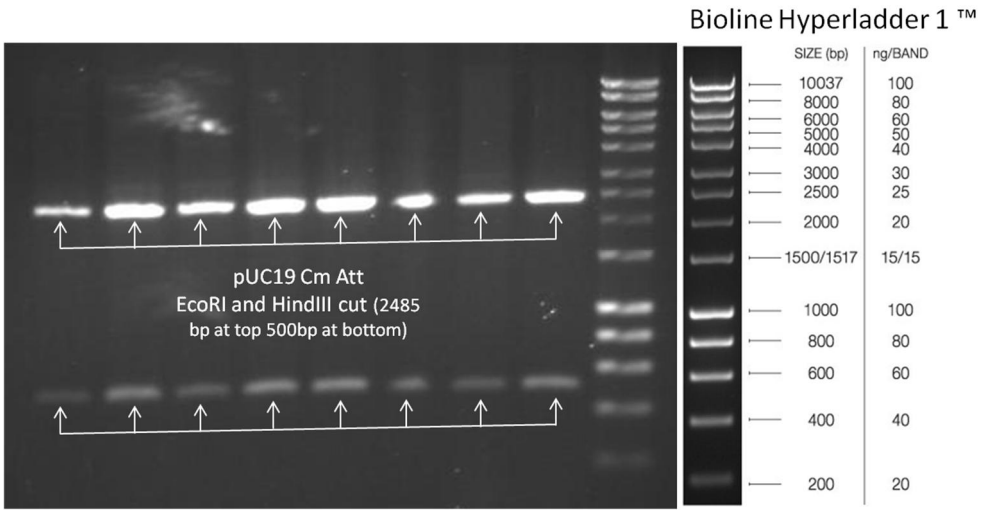

Figure 6.24 - Doubly digested pUC19Cm-Tn7 clones

Following the successful construction of pUC19Cm-Tn7, Mtr insertions into this plasmid were attempted as shown in Figure 6.25.

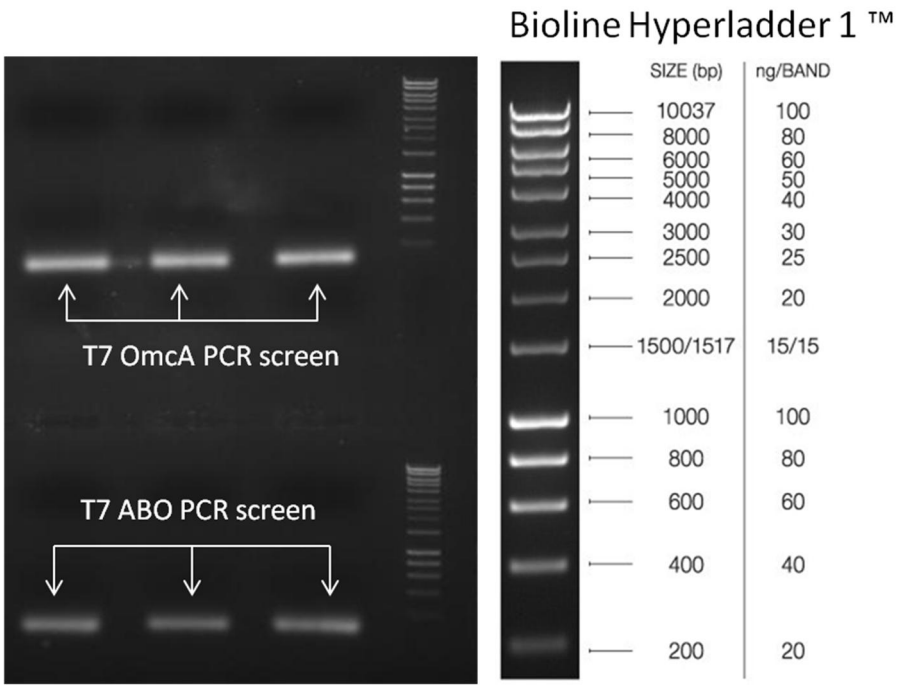

Figure 6.25 - PCR screen of insertions into pUC19Cm-Tn7

The insertion into pUC19Cm-Tn7 yielded no positive clones. The reasons for this are hard to determine and allow for speculation:

- It could potentially be due to a much larger range of concentrations for ligations are required to increase the chances. 1:10 ratio of plasmid to insert is touted as the recommended setup for blunt ended cloning although this is likely to be highly case dependent.
- The chosen batch of competent cells were not competent enough leading to decreased efficiency and propagation of unsuccessfully ligated plasmids.
- The plasmid had not been properly desphosphorylated and ended up re-circularising instead of allowing for insertion of the Mtr fractions.
- The concentration of the Mtr fragments could have been too low and a larger concentration, especially per volume may be required.
- Accidental induction of the plasmid through the activation of the arabinose inducible promoter when using rich media could have potentially caused chromosomal insertion into the cloning strain but 0.4% glucose was added to prevent this occurring.

- The whole experiment relies largely on the guarantee that 5' phosphates are present and tightly bound to the primers. If this is not the case then it is impossible for the blunt ended cloning to occur.

6.1.4 Conclusions

The attempts to transfer the previously cloned *S. oneidensis* MR-1 Mtr genes onto the chromosome of BL21 DE3 using two significantly different methods have been shown to be significantly harder than expected.

The many advantages of the lambda red recombination method were heavily outweighed by the difficulty in trying to get large DNA fragments to overlap. The technique is remarkably straight forward for deletions and for switching resistance cassettes but outside of this, the technical challenges increase greatly. From later discussions with externally based colleagues, overlaps have had to extend to hundreds of base pairs in length in order to be able to overlap the desired elements. This may be the case but is a costly and further time consuming option. The benefits later offered by the attenuation method became increasingly appealing as time went on.

The transition to the attenuation method meant that a simple cloning experiment could potentially yield an easy method to insert the genes on the BL21 chromosome. This however also turned out to be a challenge due, potentially to the very large plasmid size, large insert size and low efficiencies of blunt end cloning. The development of a small plasmid for this system was believed to help this situation although from the limited experiments done with it, it still did not work. Given time and new 5'phosphorylated primers, this small plasmid system may well work and has the potential to be very useful in other projects, due to the ability to insert genetic material in other gram negative bacteria, such as *S. oneidensis*.

Genetic manipulation is rarely, if ever documented within B-type *E. coli* strains which seems highly unusual due to the positive capabilities of these strains for protein expression. This however may be purely coincidental. In this particular case a BL21 (DE3) strain was chosen due to the fact that as stated in chapter 3, the strain

possessed a functional type II secretion system but, it was also capable of high level, inducible protein expression.

The levels of efficiencies stated in papers for either gene knockouts or chromosomal insertions seem infeasibly high. There are a number of possible options for this. Either the inserts they were dealing with were particularly small which is largely, but not always seen to be the case (as seen in (352)), they were very selective with the information they provided (i.e. it worked very well for certain setups but was either untested or the data was not shown for other attempts) or there was incredibly bad luck/technique applied during molecular biology experiments. This high level of efficiency seems especially dubious for insertions carried out without a selection pressure. It is conceptually understandable to expect to see a relatively high level of successful mutants, when a selection pressure is applied, as the vast majority of unsuccessful transformants would die. Having no selection marker, as presented in the Tn7 attenuation method, was very appealing due to the lack of extra resistance advantage post-insertion. The ability of a molecular biology procedure to not only produce successful mutants, but perform this so successfully that on average 79% of colonies on the resulting selection free plate having insertions appears higher than expected.

Science continues to move at an incredible rate with new technologies being developed on a near daily basis. Genome manipulation tools are no exception to this as other genome editing tools are appearing all the time. Recent tools that have come onto the scene include TAL (transcription activator-like) effector nucleases, zinc finger nucleases, with the latest technique being CRISPR/Cas (clustered regularly interspaced short palindromic repeats) RNA modification. All of these techniques are showing remarkable promise but are designed for genome modification (deletions, mutations) and post transcriptional regulation instead of gene insertion (371–373). For the field of chromosomal insertion, there has been very limited progress in terms of technology, which for something that the literature considers to be able to remove metabolic

burden, therefore providing more streamlined cell lines, leading to greater yields and industry profits, seems unusual.

A recent paper demonstrating promise in this area has come from Enyeart et al (374) with a highly flexible plasmid system capable of insertions, deletions and inversions. The system has shown the capability of inserting a 12-kb insert, simultaneous deletions up to 120 kb and inversions up to 1.2 Mb. The system is also capable of working within *Shewanella oneidensis*, which provides an added incentive to work with a system that is also functional in multiple organisms of interest. This is due to the use of the cre-recombinase system that is supposedly suitable for universal organism genome tailoring use (375) in combination with mobile group II introns.

Another recent paper of interest is a claimed single step recombination demonstrated by St-Pierre et al (376). This paper combines steps from a technique known as conditional replication, integration, excision and retrieval (CRIM) to reduce the total time taken for an integration. This system makes use of a highly efficient integrase from phage 186 and selection through the toxic *ccdB* gene. The GOI still has to be cloned into the MCS of the plasmid, but post ligation is transformed directly into the desired host strain.

6.2 Interaction studies of plasmid based electrogenic system

6.2.1 Introduction

In order to try and improve the efficiency of the plasmid based electrogenic system, the way in which it was able to work as a heterologously expressed system needed to be established. In order for current to be generated from the system, the Mtr pathway from *S. oneidensis* MR-1 had to have been functionally interacting with the host metabolism to some extent. Work prior to this thesis has also demonstrated functional interaction of Mtr proteins within *E. coli* (105,107,120,125). A proposed mechanism of electron transfer is from the quinone pool to NapC, a tetrahaem cytochrome homologous to CymA in *S. oneidensis* to MtrA to MtrC, through the beta barrel sheath protein MtrB. This was however shown not to be the only method by which electrons can travel through this recombinant pathway as Jensen et al deleted NapC from *E. coli* and still demonstrated current generation although at a reduced rate (125). This suggests that either a portion of the overexpressed recombinant cytochromes within *E. coli* are incorrectly localised and somehow obtaining electrons from intracellular mechanisms or other electron donors to MtrA present.

In an attempt to try and determine interacting partners of the recombinant Mtr proteins, to help gain a better understanding of the system and potentially increase efficiency, an interaction study was decided to be carried out.

Before attempting this, it was necessary to determine the best approach. The following analysis of the experimental techniques for interaction work has since been published as part of an article in IUBMB life (377).

6.2.2 Experimental techniques for protein-protein interactions (PPIs)

This section broadly considers and discusses the major approaches used to determine PPIs: (i) Yeast two hybrid (Y2H), (ii) Tandem affinity purification (TAP-tag), (iii) Proximity ligation assay (PLA) and (iv) Chemical cross-linking.

6.2.2.1 Yeast two hybrid screening (Y2H)

The first publications for the use of a yeast two hybrid (Y2H) system provided information about the interaction of a single protein with its specific partners (378), whilst simultaneously yielding the cloned interacting partner (379). This technique has seen noteworthy success over the past decade, allowing for some of the most complex and complete interactomics studies to be carried out (380,381).

The technique makes use of two sub-units of a protein (GAL4) which, when combined provide a transcriptional activator for the expression of beta-galactosidase (378). The first step involves cloning the protein of interest into a plasmid that fuses the DNA binding domain of GAL4. A second plasmid codes the activating domain of GAL4, which is fused to either pre-selected proteins of interest or protein sequences encoded by a library of genomic DNA fragments (379). Only when two interacting proteins come into contact, following their heterologous expression does the complete GAL4 protein occur, subsequently leading to expression of beta galactosidase. This therefore permits detection of interacting proteins to occur through the use of a galactose selection system such as X-gal. In order for the system to function, the assay has to be carried out in a system where the screenable gene has been inactivated or does not natively exist. This is to ensure that a positive result is only noted when the two subunits of the fusion protein come into contact.

Although initially designed for function with yeast, the system has been modified for use within *E. coli* (382,383) permitting a greater ease of use without the need for yeast growth facilities. A more complete list of the Y2H variations can be found elsewhere (384).

Two hybrid studies have been shown to be the method of choice for many of the ambitious, high profile interaction studies involving *Saccharomyces cerevisiae* (385,386), a *Drosophila melanogaster* map (387) and even the human protein interactome (388). This is mainly due to the simplicity of the technique, the ability to scale up and the vast amount of information that is retrieved. For all the benefits of the technique, two hybrid screening does however suffer from a variety of flaws:

- The system was designed to study binary interactions, whereby only a single protein is ever seen interacting with another at any point in time.
- A large number of false positives are found, with reports of up to 70% noted previously (389).
- If the system is plasmid based then the proteins may be overexpressed which can lead to inaccurate interaction (390).
- The fusion portion of the protein has the potential to interfere with the function of the protein and could theoretically prevent proteins from interacting.
- The protein may not function in the correct manner if expressed in a recombinant host.

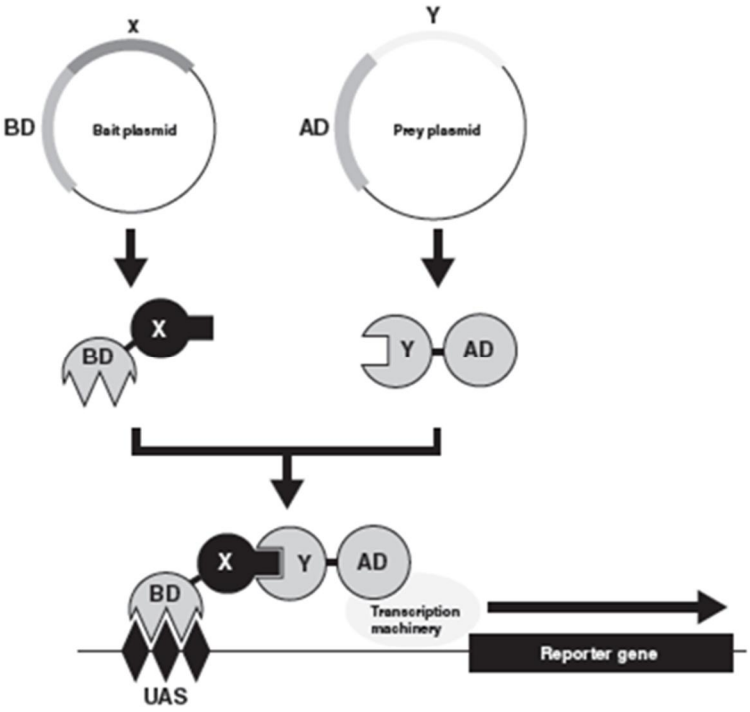

Figure 6.26 - An example of a yeast two hybrid (Y2H) setup. Modified from Causier (384)

6.2.2.2 Tandem Affinity Purification (TAP-tag)

Tandem affinity purification tag (TAP-tag) has seen significant use since it was first published over a decade ago (391,392). The method makes use of 2 simultaneous affinity tags expressed at either the C- or N- terminus of the desired protein. This technique initially relied on dimeric protein A followed by a tobacco etch virus (TEV) protease cleavage site and then calmodulin binding peptide (CBP) (Figure 6.27 provides an illustration). The technique is very open to modification and many different combinations of tandem tags have been developed since (393), allowing it to be tailored specifically to the protein interactions wanting to be studied. The method is similar to that seen in protein co-immunoprecipitation (Co-IP), although this method requires the use of a greater number of antibodies to target each specific protein.

The DNA sequence for the protein tags is inserted up- or downstream of the DNA sequence for the protein of interest to allow for native expression of the tagged target. This will allow for the most representative interaction with surrounding proteins, thereby limiting false positives that may otherwise occur due to overexpression. Following cellular disruption, the protein sample is loaded into a column containing either magnetic or agarose beads coated with anti protein A antibodies. The column is washed to remove contaminating proteins whilst still retaining interacting ones and the target protein. The protein A tag is cleaved from the antibody through the use of TEV protease and the protein of interest is eluted onto a calmodulin column where the secondary tag binds. The sample is washed again to remove any residual contaminants and then the proteins are eluted using ethylene glycol tetraacetic acid (EGTA). Samples are run through 1D SDS-PAGE gels against a protein sample from the wild type organism to allow for visualisation of proteins of interest. Bands present only in the positive sample are removed from the gel, enzymatically digested, typically with Trypsin, before being loaded onto a mass spectrometer for identification of the proteins.

The technique is relatively simple, requiring the chromosomal tagging (ideally) of proteins of interest but afterwards making use of the same antibody and column

components. Only one antibody is required unless a western blot of the target protein is desired following tandem purification. A large number of proteins can be successfully tagged and detected in the mass spec with reports of 86% successful tagging - confirmed by western blot, and 65% successful identification through mass spectrometry (394). A single tagged protein is able to pull down multiple interacting protein (391). The method has been used in large scale interactome studies in yeast (395) but has been shown to be susceptible to a high level false positives with one group reporting using the same method on the same samples but carried out by different researchers yielding less than 30% of the same interactions (396). It is highly recommended that any protein interactions that are detected should be confirmed through re-tagging the detected interaction protein to verify the detection of the initial target.

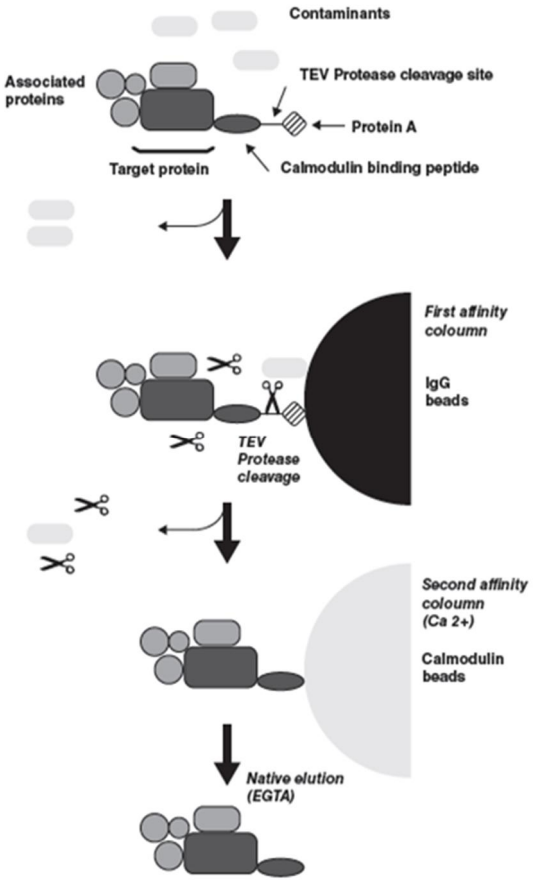

Figure 6.27 - An example of Tandem affinity purification tag (TAP-tag) setup. Modified from Rigaut et al (392)

6.2.2.3 Proximity ligation assay (PLA)

Proximity ligation assay (PLA), commercially known as Duolink is a novel technology for determining protein interactions in their native state (397) (Example illustrated in Figure 6.28).This allows for direct visualisation of the proteins within whole fixed cells or tissue sections, thereby preventing any erroneous data from cell lysis, cross contamination or imperfect subcellular fractionation. The system doesn't suffer from bias due to overexpression or functional modification of the proteins from the addition of an affinity tag.

The technique makes use of two primary antibodies, ideally from different organisms that are used against the target proteins. These are subsequently targeted by species specific secondary antibodies containing DNA linkers. When closer than 30 nm (depending on oligonucleotide length) (397) to an opposing oligonucleotide sequence on the opposite secondary antibody, the DNA is linked and ligated using a connector oligo and ligase. This creates a circular DNA sequence between the two adjacent antibodies. Using rolling circle amplification, the circular DNA sequence is amplified up to 1000 times (397,398). Addition of fluorescently labelled detector oligos permits the binding of multiple reporter molecules for a single event, thereby allowing low level interactions to be identified. Results are analysed and quantified using microscopy and Duolink software.

PLA is an incredibly powerful technique that allows for studies to be done on weak and transient interactions. Amplification of the signal is done by RCA so low levels of protein interaction can be detected. The major flaw in this method is that it can only be done when there is knowledge of the proteins to be targeted. It can provide useful information on interactions but no previously unknown targets will be detected. It is therefore incapable of doing large scale interaction studies or complete interactomics. The technique is highly suited to being used as a confirmatory measure of the interaction between proteins seen in any of the previously mentioned methods where false positives are much higher.

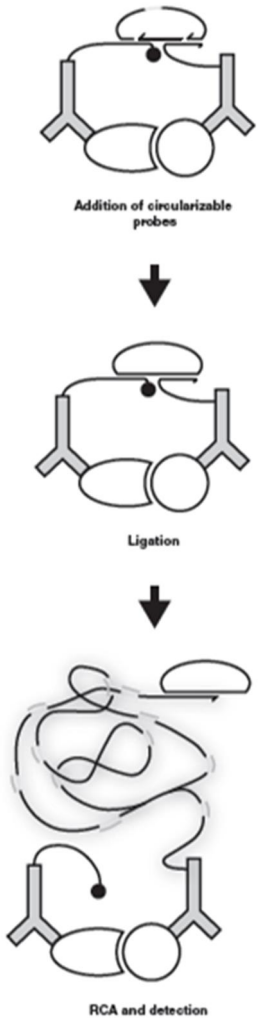

Figure 6.28 - An example of a proximity ligation assay (PLA) setup. Modified from Soderberg et al (397)

6.2.2.4 Chemical cross-linking

The use of chemical cross-linking allows for covalent clustering of nearby proteins through the use of a synthetic linker with the initial use of this technology being nearly 40 years ago (399). There are a wide variety of cross-linkers, allowing the technique to be used in a number of ways. A standard method is the introduction of the cross-linker molecule following the growth of the cell sample but before lysis. The cross-linker permeates the cell in order to link proteins and capture them in the configuration in which they act natively. The cross-linker will in this case be designed to have ends that are reactive to specific functional groups such as primary amines. Following lysis, the cross-linked proteins are purified and either detected using western blots or enzymatically digested and loaded onto a mass spectrometer (illustrated in Figure 6.29).

The development of photo-cross-linking has provided a method for rapid connection of cellular proteins that ensures linkers are distributed throughout the cells. The method makes use of inert photoactivatable amino acids, such as photo-methionine and photo-leucine (400), in the growth media which are then incorporated into mature proteins without affecting function. Application of ultraviolet light activates the molecules resulting in covalent cross-linking and allows for subsequent analysis as mentioned above.

Recent developments have seen a rise in the use of cross-linking coupled with mass spectrometry (401,402) permitting the identification of protein complexes. The linker

can be chosen to be of a specific length to determine provide information about distances between complexes, state the location of the cross-link and aid in structural understanding of multiprotein complexes (401).

The technique has many different available options that permit a wide range in the speed of processing and the quality of data that can be obtained. The linking of proteins *in vivo* increases the chances of detecting weakly interacting and transient partners (403).

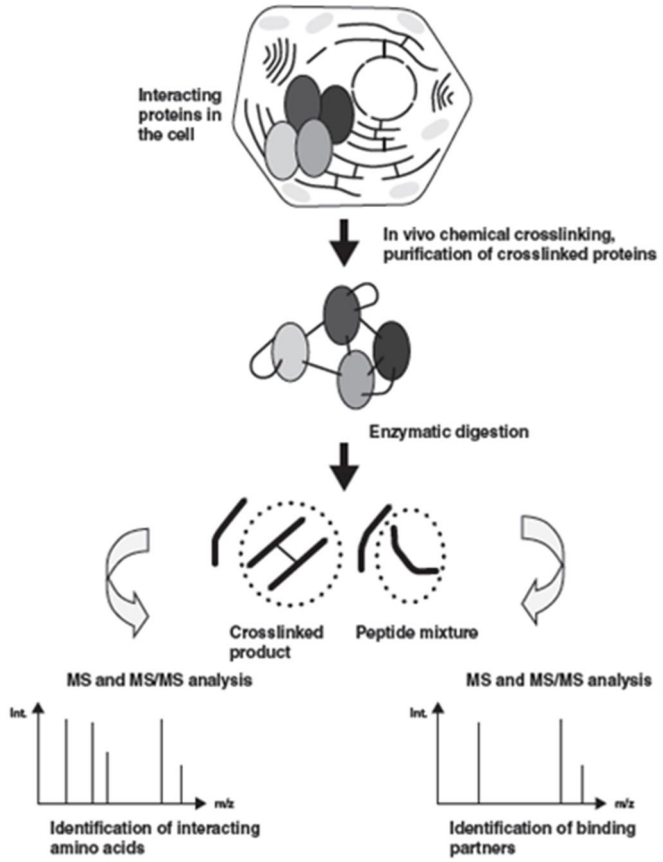

Figure 6.29 - An example of a chemical cross-linking setup. Modified from Sinz (403)

A large challenge in modern interactomics studies is the identification of interactions between metalloproteins. These proteins perform vital roles within cellular survival, with involvement in energy metabolism (404) and signal transduction (405). Roughly 30% of proteins within sequenced genomes predicted to contain a metal ion (406,407).

Determining the interacting partners of a particular metalloprotein, as with other proteins, can depend on the physiological function of the target. Interactions can range from stable complexes to incredibly transient interactions in the microsecond range (408) often seen with redox proteins (409). The use of coupled techniques such as *in vivo* cross-linking and subsequent tandem affinity purification helps to identify specific partners whilst also managing to remove decoys due to the dual purification (406). For a more detailed insight into interactions of metalloproteins, the reader is advised to view the following papers (406,408,409).

6.2.2.5 Closing statements - PPI Methods

A key component for the development of interactomics data is the use of mass spectrometers (410–412). The development in this field has made a dramatic impact on all aspects of the life sciences with interactomics being no-exception. Mass spectrometers allow for a far greater wealth of information to be obtained compared to western blots. *De novo* sequencing (413,414) structural analysis (415) and identification of interacting residues (401) are all possible.

There are many variations of methods that can be applied to attempt to achieve the best results from an interactomics study. If the identification of a large number of interactions is required, then use of Y2H or TAP-tagging is highly suited. However, these experiments are susceptible to high degrees of false positives that must be validated. Smaller scale studies involving the interaction between weakly interacting proteins and low abundance proteins are better suited to methods such as PLA or chemical cross-linking. Techniques are liable to bias, certain methods may determine the type of interaction that is found (396). The methods detailed above are not mutually exclusive, with examples of two being used in combination to provide greater detection methods (416).

With all this information in mind, it was decided that a directed approach towards to proteins of interest was needed which ruled out the use of a simple full cross-link although this still held potential. The system had to be able to work with a single known protein but not know any of the interacting species, meaning that PLA was

ruled out. This left the main choices between a Y2H and a TAP-tag study open for choice. The fact that TAP-tag allowed a defined tag to be integrated into the same plasmid based system currently used for previous electrogenic studies was particularly appealing. This meant that the cells could be used in a functioning current generation experiment and the desired protein then extracted to reveal the interacting partners. Due to the interest in metalloproteins and the recombinant nature of the system a combination of a simple cross-link of 1% formaldehyde (as previously demonstrated for the identification of MtrCAB, OmcA, CctA and CymA (237)) paired with tandem affinity purification was decided as the best option to attempt.

6.2.3 Experimental thought process

6.2.3.1 Reasoning for TAP-tag

Once the decision was made to use a combination of cross-linking and tandem affinity purification, the decision about which tandem affinity purification technique needed to be made. The initial TAP-tag setup, as described above, made use of a sequence of dimeric protein A, a TEV protease cleavage site and a CBP. This is quite a large protein sequence that adds around 20 kD onto the end of a protein sequence (and also confers to a large genetic element that needs to be attached). When trying to carry out an interaction study, the sequence of the target protein wants to be as close to the original as possible to avoid modifying the structure and disrupting normal interactions. The length of an affinity tag is a major consideration when carrying out single protein studies for the very same reason. As described above, it is the idea of tandem affinity purification, rather than the actual protein components that make it a useful technique. There have been many modifications of the TAP-tag setup so the criteria for choosing one had to be set as one that:

- Had a smaller tag than the TAP-tag, preferably under 10 kD
- Had been tested significantly
- Used common components

A match for all three of these was found in the form of the SPA-tag from the lab of Jack Greenblatt. This tag comprised of a CBP, TEV protease cleavage site and 3 x FLAG tag making the total tag size less than 8 kD (417). It had previously been used to carry out a highly cited interactomics study on *E. coli* (394) and as stated above, made use of a FLAG tag instead of protein A, which in a microbiology lab, is a lot more common.

6.2.3.2 Choice of genetic manipulation

For the SPA-tag to be able to function, it needed to be attached to the protein of interest. In order to do this, the 201 bp SPA-tag would need to be attached to the protein of interest. Due to the large size of the Mtr gene cluster and the compatible restriction sites available in pACYCDuet-1, the GOI's couldn't be cloned into the standard MCS and then have the SPA-tag inserted in frame with the current setup. Using a standard cloning method, the plasmid would need to be modified to add additional cloning sites, the inserted Mtr fraction would also have to be modified to allow for in frame insertion of the SPA-tag and the SPA-tag would need to have multiple restriction sites added. It was decided that the modifications to do the insertion this way would be overly laborious and that other options may provide a simpler solution.

The first method to be considered was Gibson assembly. This is a relatively new molecular/synthetic biology technique developed to help enable the generation of the first synthetic genome (100,418). It uses the homology of DNA elements to allow them to be joined together through the use of a T5' exonuclease, DNA polymerase and a ligase. The plan for this to be used was for the Mtr fraction to be amplified with a forward primer that was homologous to the start of the Mtr gene (s) whilst also being a reverse complement to the insertion point in the MCS of pACYCDuet-1. The plan for this was as follows:

1. Amplification of the SPA-tag from pJL148 using the specific primers making sure to leave the 3' of the specific Mtr sequence on the 5' of the amplified SPA-tag.
2. The next step had two options:

a. Amplify the Mtr region of interest using specific primers and use this product alongside PCR product from step 1 and amplify.
b. Use the product from step 1 alongside gDNA from *S. oneidensis* MR-1/pACYC plasmid containing insert to try and simultaneously amplify Mtr fragment and combine with the SPA-tag.

3. The final product would then contain both the Mtr section of interest and the SPA-tag. This would then need to be inserted into AscI and NotI digested pACYCDuet-1.

The second method that was considered for this was lambda red recombination. As this was being used in the chromosomal insertion work that was being carried out simultaneously, it seemed sensible to use the same setup to try and insert a sequence into different plasmids. The plan for this setup was essentially the same as the design for a gene knockout as shown in Figure 6.2. Instead of amplifying an FRT flanked resistance cassette with homologous arms to the region wanting to be deleted, the SPA tag was to be amplified with arms allowing for insertion at the end of the chosen Mtr gene. This would need to be designed carefully to be base perfect, ensuring in frame DNA insertion whilst simultaneously removing the final stop codon of the chosen Mtr protein.

For modification of the chosen Mtr plasmid the amplified SPA tag with homologous regions to the Mtr gene would merely need to be transformed into a cloning strain harbouring the desired Mtr plasmid and an induced pKD46. This, in theory would allow this to be a very quick procedure.

In order to have another option for the insertion of the SPA-tag, another simple modification method was considered. PCR overlap allows for simple modifications to be made within a plasmid sequence whilst simultaneously removing any of the original template plasmid (209). The full method for how to carry this out is detailed in methods section 3.2.6. A brief diagrammatic example of how this procedure was used is shown in Figure 6.30.

1. Amplify SPA-tag from pJL148 with 5’ region on FP (D1) complementary to the 3’ region of target gene and the 5’ of the RP (D2) designed to region downstream of the GOI.

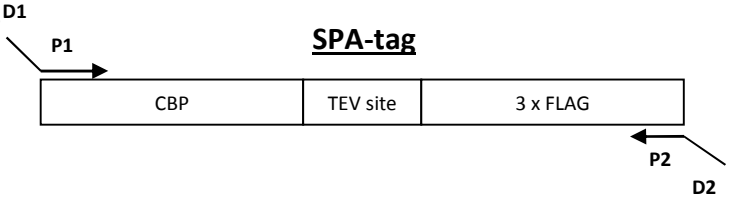

2. Combine amplified fragment from step 1 with desired template. Product from step 1 acts as FP and RP for second PCR reaction

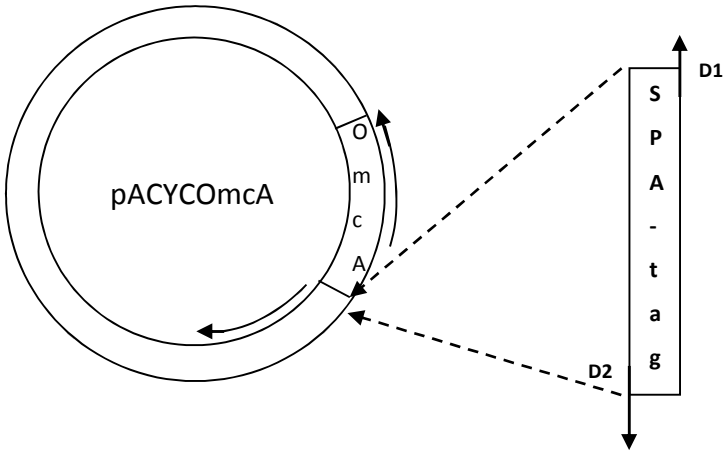

3. Add DpnI to digest original *dam* methylated template DNA leaving only nicked, recombinant unmethylated plasmid

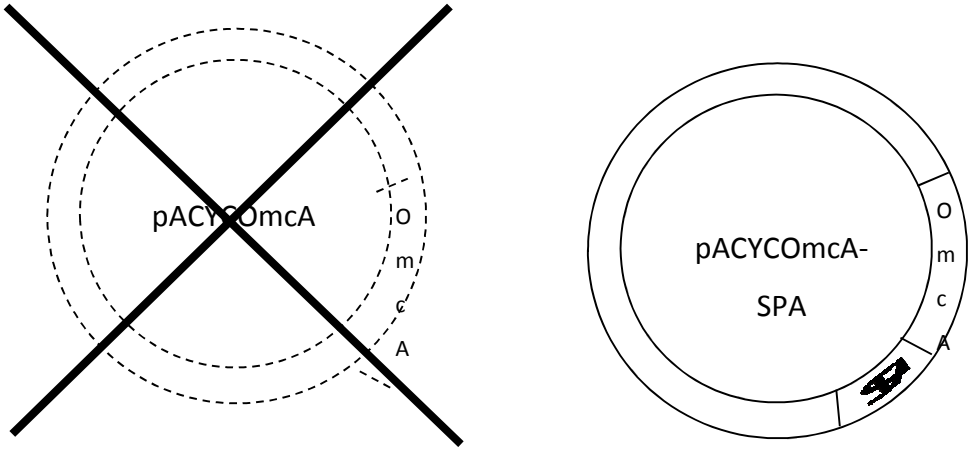

4. Transform recombinant plasmid into cloning strain such as DH5alpha to ligate nicked plasmid and allow for further replication
5. Extract plasmid and express in desired strain

Figure 6.30 - Diagrammatic representation of PCR-overlap method used to insert SPA-tag into Mtr plasmids

Using these two methods to try and simultaneously insert the SPA-tag had the advantage that the same primer sets could be used for both techniques.

6.2.4 Results and Discussion

6.2.4.1 Gibson assembly

The initial Gibson assembly PCR involved the amplification of the SPA-tag with modified primers that allowed for further combination of the genetic sequence with the desired Mtr region for further cloning into pACYCDuet-1. The initial amplification for this was tested with a wide range of annealing temperatures to try and determine the best option. The results are shown in Figure 6.31.

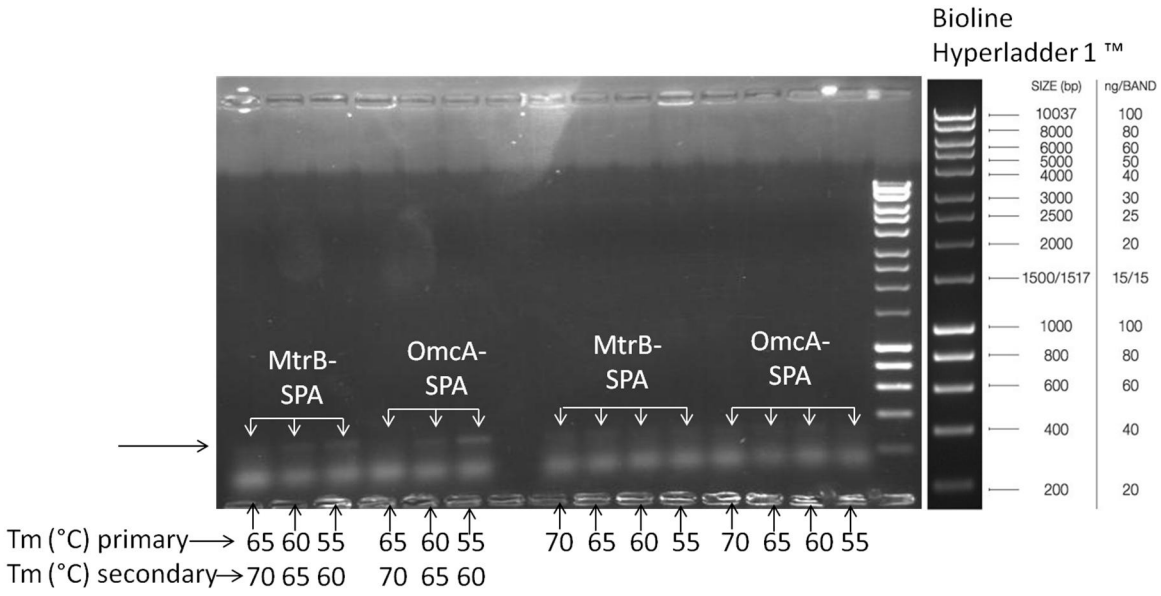

Figure 6.31 - Initial amplification of the SPA-tag using primers for Gibson assembly.

The gel shows a very poor amplification of the SPA-tag, at the size indicated by the arrow on the gel picture with the apparent banding beneath the indicated bands likely being unused dNTPs. This was across a wide range of annealing temperatures, making use of both primary and secondary annealing temperatures for some of the samples to account for the addition of extra nucleotides to the template. The poor amplification was most likely due to poor primer binding to the template, although this is unlikely to

have been caused from unspecific binding of the added homologous region as this would be expected to create a larger number of unspecific bands.

Due to the poor amplification of the SPA-tag using this technique, alternatives that had been designed for use in parallel were tested as described.

6.2.4.2 Lambda red recombination

Amplification of the SPA-tag using primers suitable for lambda red recombination was attempted with the results shown in Figure 6.32.

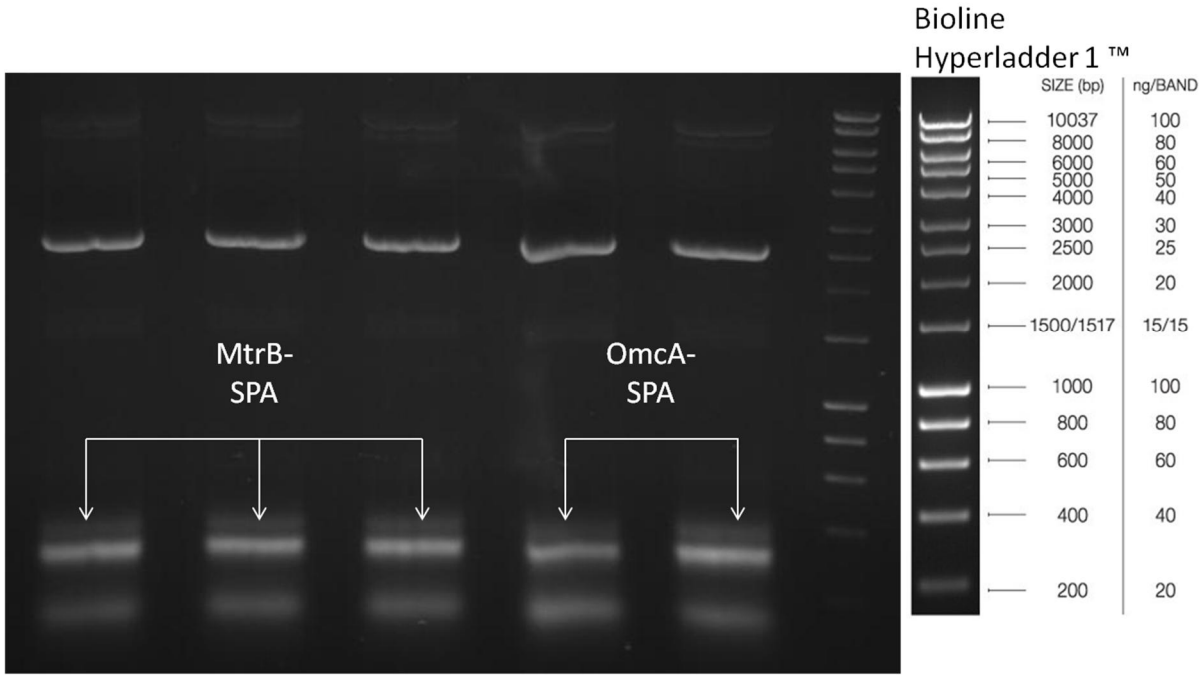

Figure 6.32 - Amplification of the SPA-tag for use in lambda red recombination

Figure 6.32 shows a much higher concentration of SPA-tag was obtained from this PCR compared to that used for the Gibson assembly PCR.

This sample was then gel purified ready for recombination with the resulting samples shown in Figure 6.33.

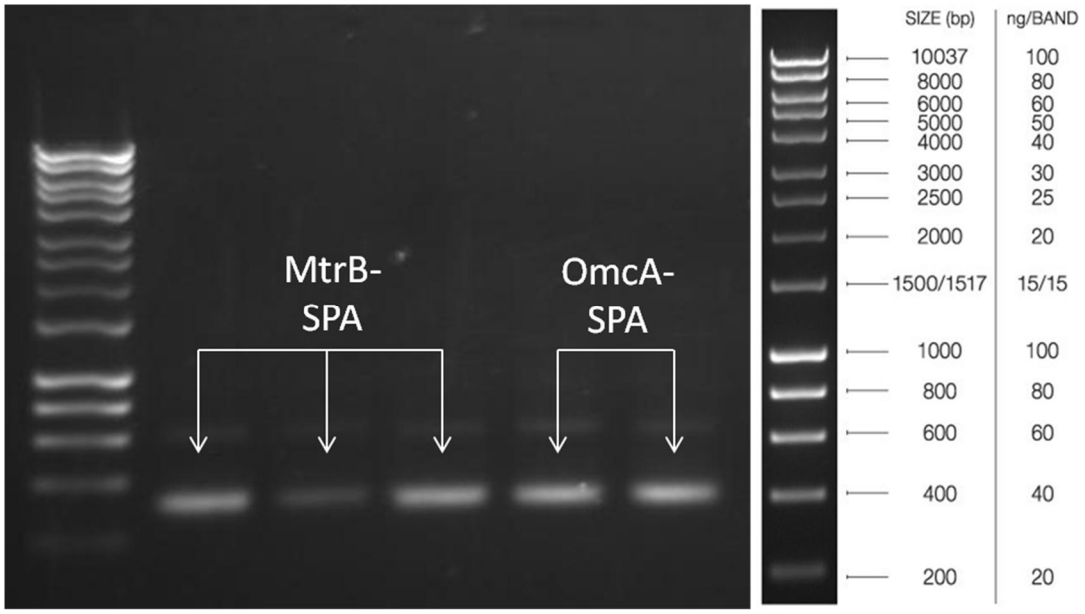

Figure 6.33 - Gel purified SPA-tag, ready for recombination into pACYCMtr plasmid

This purified sample was then ready for use within a strain expressing the lambda red recombination machinery (pKD46) and also containing the chosen pACYCMtr plasmid. The results of the subsequently plated out cells and colony screen are shown in Figure 6.34.

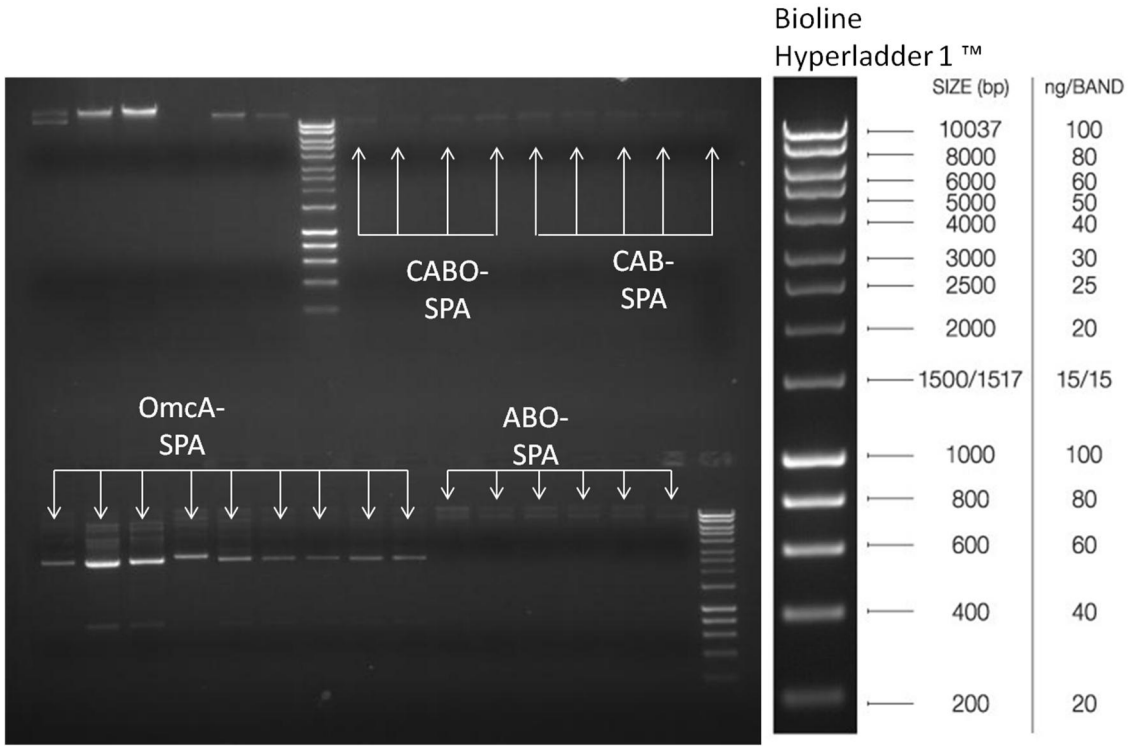

Figure 6.34 - Colony screening of potentially SPA-tagged pACYCMtr plasmids

Figure 6.34 shows that there is plasmid DNA present in all of the screened samples which were then sent on for sequencing. Unfortunately the samples came back showing that the plasmid was the original pACYCMtr template instead of samples that had been modified with the SPA-tag.

Although the amplification of the SPA-tag with homologous regions was successful, the following integration into the Mtr plasmid proved troublesome. This was potentially down to the fact that no further selection marker was added for the insertion of the SPA tag thereby preventing any additional requirement for the DNA sequence to be inserted. As another resistance cassette addition would have modified the current engineered cell setup, it was decided that a different method of modification should be attempted.

6.2.4.3 PCR overlap

Following the successful amplification of the SPA-tag for the lambda red recombination based insertion, it was known that the SPA tag amplified fine. As mentioned above, the primers used for lambda red recombination were also suitable for PCR overlap based insertion. The initial amplification of the SPA-tag cassette is shown in Figure 6.35.

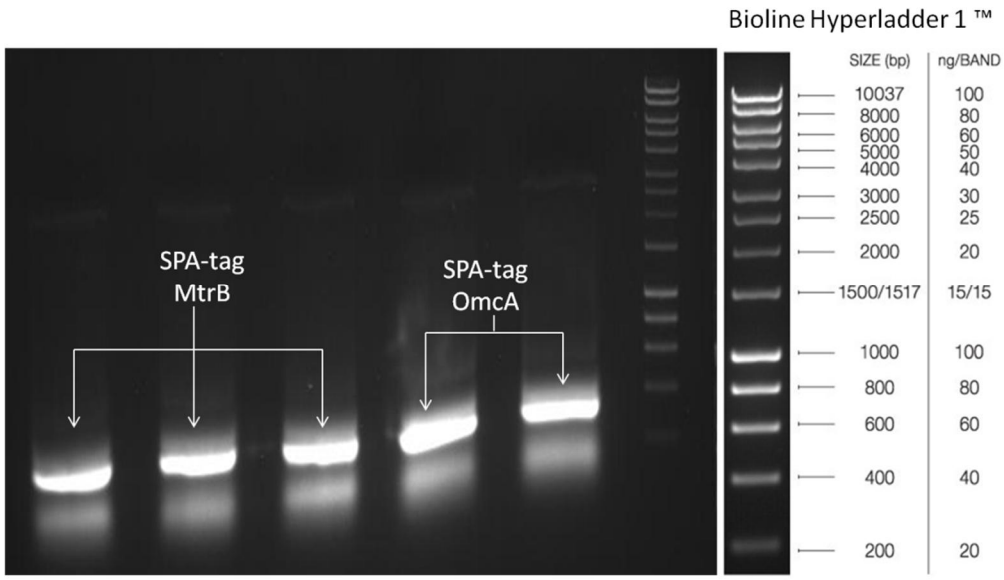

Figure 6.35 - SPA-tag amplification

Once this DNA fragment had been successfully amplified and purified it could then be used as essentially a forward and reverse primer for insertion into the chosen Mtr plasmid. The recombinant, amplified plasmid was then distinguished from the original pACYCMtr template, through the selective digestion of the original pACYCMtr plasmid with DpnI as shown in Figure 6.30.

Following transformation of the DpnI treated PCR mixture, the sample was transformed into DH5α and the resulting colonies screened for successful insertion. The results of this are shown in Figure 6.36.

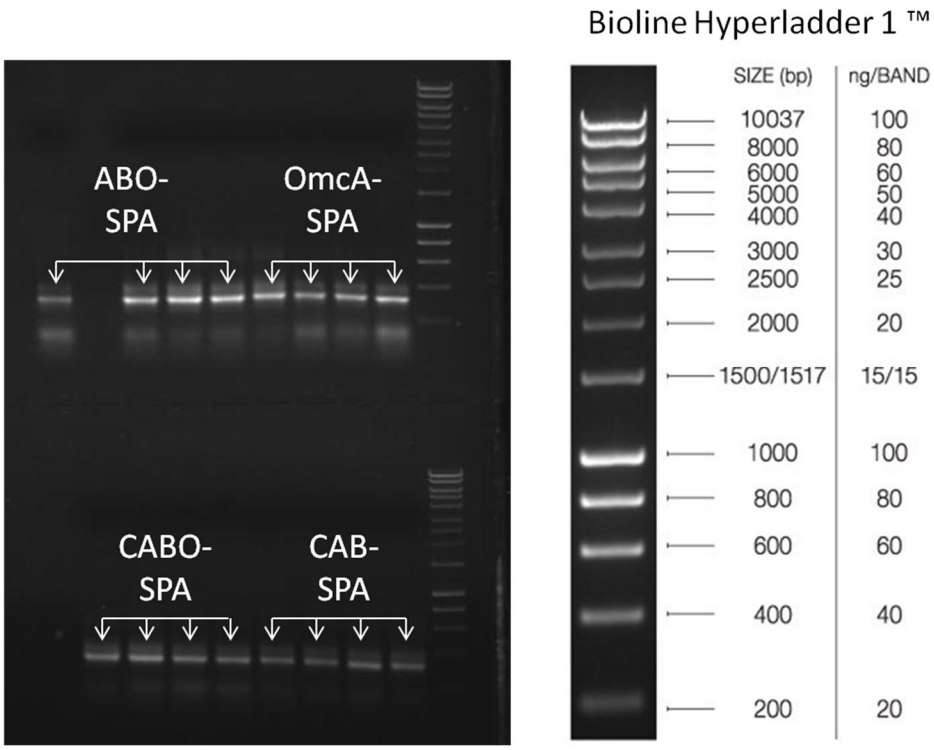

Figure 6.36 - SPA-tag screen. Identification of desired 300 bp band in all but one of the samples

Following on from the positive identification of bands of the correct size being amplified from all but one of the screened samples, a test SPA-tag pull down was attempted to trial the methodology before putting on a longer, current generating test run for full analysis. The full methodology for how this was carried out is detailed in methods section 3.2.29. The protein samples were added to protein A/G beads containing an anti-FLAG antibody. This allowed for the samples to be bound and permitted further release of the samples following TEV protease cleavage. The bead bound samples were washed with the released proteins being stored and loaded on the left hand side of Figure 6.37. The TEV protease was allowed to cleave the protease site overnight and the samples were then carried forward onto the next step. The beads with the remaining FLAG tag were kept, and the standard elution protocol for removal of bound sample was followed. This was then loaded onto a gel as shown in Figure 6.37.

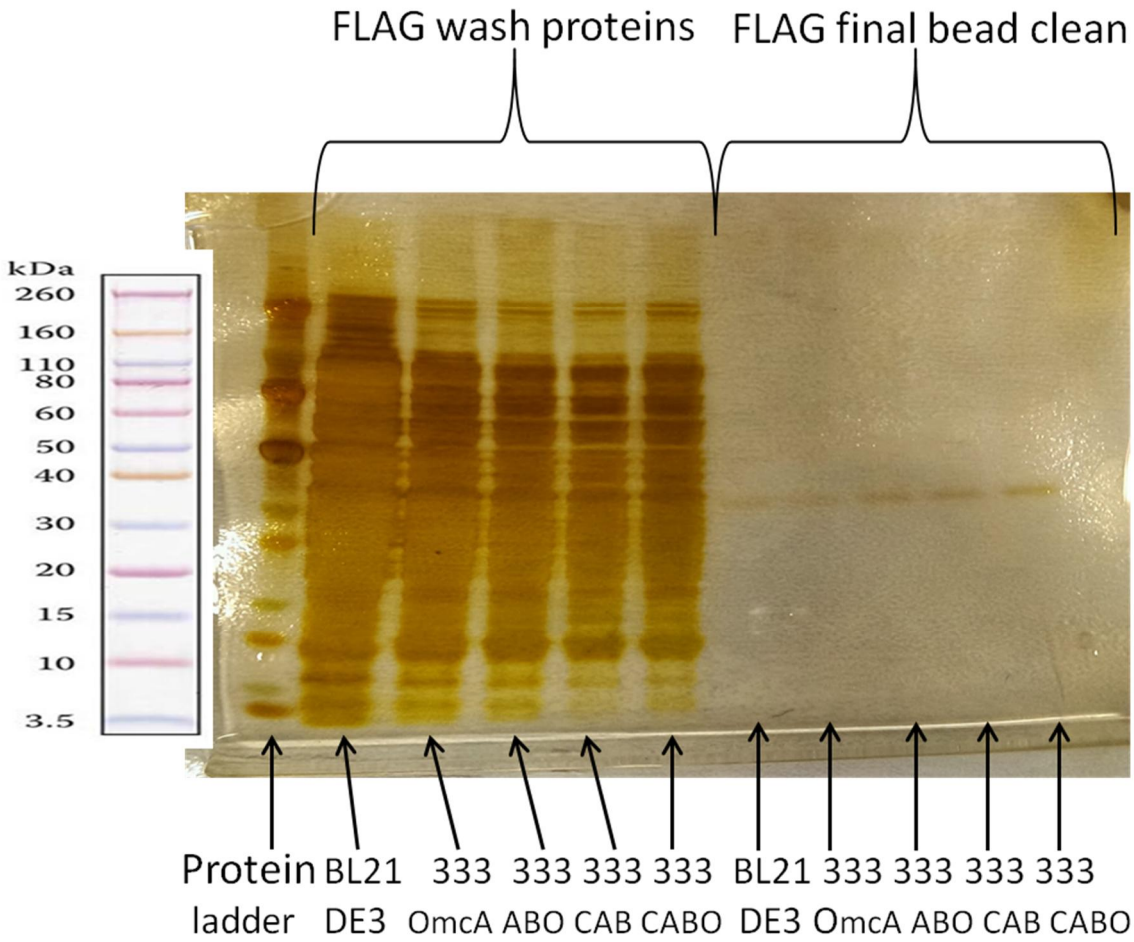

Figure 6.37 - Silver stained BL21 DE3 test samples following FLAG-tag pull down. Left hand side is the protein removed following the wash. Right hand side is remaining elution from beads following TEV protease cleavage of bound sample

Figure 6.37 shows proteins washed from the protein beads on the left hand side showing an expectedly high number of proteins due to the removal of the vast majority of the proteome. The right hand side of Figure 6.37 shows single bands at a weight of around 35 kD across all the samples. This is unusual as the only sample that should be eluted at this point is the 3xFLAG tag that was still bound to the protein A/G beads. This has a weight of 2.7 kD which is not visible on the gel.

Following TEV protease cleavage the removed samples were then taken on for a second stage of purification using CBP. The samples were again washed, with the removed protein removed from the second wash stored and then loaded on the left hand side of the gel shown in Figure 6.38. The sample containing the CBP tagged protein and interacting partners was then eluted from the protein A/G beads and the sample loaded onto the right hand side of the gel shown in Figure 6.38.

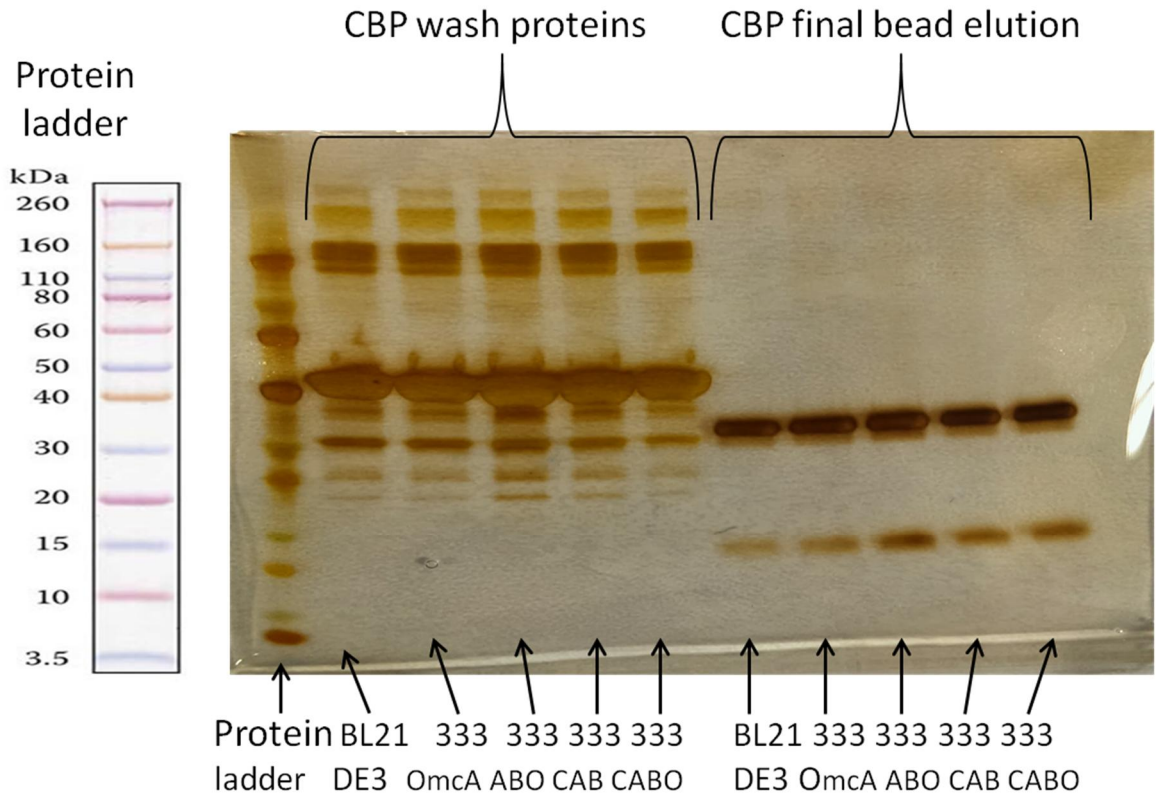

Figure 6.38 - Silver stained BL21 DE3 test samples following CBP pull down. Left hand side is the protein removed following the wash. Right hand side is the final elution of the CBP tagged proteins from the protein A/G beads

The results clearly show a reduced amount of contaminating proteins washed off from the beads following the second affinity binding using CBP after FLAG on the left hand side of the gel. The right hand side of the gel shows dark bands of eluted protein in all of the samples at sizes of around 30 kD and another smaller band at roughly 15 kD.

This is of concern due to the fact that the OmcA-SPA-tagged protein in BL21 DE3 pRGK333 pACYCOmcA shows exactly the same interacting partner as the other MtrB-SPA-tagged samples in BL21 DE3 pRGK333 pACYCMtrABO, CAB or CABO. This is however still possible. Of more concern is the fact that OmcA and MtrB are roughly 80 kD in size and yet there are no bands at this size. Of even greater concern again is the fact that the OmcA, ABO, CAB and CABO samples all yield exactly the same result as the control sample containing just BL21 DE3.

This seems extraordinary. It is not unusual for a single affinity purification step to co-purify host proteins along with the target protein (419,420) and potentially even outcompete the target protein if the tag happens to be folded within the protein. This is somewhat unlikely to occur with a FLAG tag due to the high specificity of the purification, especially compared to a His-tag (421). The chances of competing host proteins interfering with a single affinity can be considered a possibility, but for this to occur with a second high affinity tag following TEV protease cleavage and removal of protein but no elution, seems highly improbable. The fact that the same bands appeared in all of the samples presents a few possibilities:

- A native *E. coli* BL21 DE3 protein has both FLAG and CBP affinity with a TEV protease site between – highly unlikely to find BL21 DE3 only protein that has this highly engineered sequence present within it.
- Native BL21 DE3 proteins that have limited affinity for FLAG tag to prevent removal following a gentle wash but were eluted during TEV protease step due to buffer. This protein complex may then have had very high specificity for CBP, potentially outcompeting the low levels of recombinantly expressed, tagged Mtr protein.
- The samples were mixed up so that an engineered strain containing a recombinant, tagged Mtr protein was also loaded as a control – Unlikely due to the fact that if this were the case then the band for the protein would be seen at the correct size for the tagged protein (roughly 80 kD for OmcA/MtrB plus 3

kD for CBP) and any interacting partners. None of the samples show bands of the desired size.

- The protocol did not work – unlikely as the samples went through two stages of high affinity purification and still yielded high concentration bands at the end. The wash steps clearly worked as demonstrated with the near full proteome identified in Figure 6.37. The FLAG tag elution showed that the minimal proteins were still bound to the beads post TEV protease cleavage. The CBP wash loaded onto the gel shown in Figure 6.38 shows a potentially unexpectedly high level of proteins washed off, but this was of a vastly reduced complexity compared to the first step. The final eluted proteins from the CBP beads were tightly bound. The wash step may not have been harsh enough to remove all contaminating proteins, but it had to be kept relatively mild in order to retain the potential interacting partner proteins.
- The tagged Mtr proteins could have been digested to the extent that a tagged portion of the protein still bound to the beads but once run on a gel and stained, appeared the wrong size. This is unlikely due to the fact that all the samples have exactly the same size bands meaning that MtrB would have to have been digested/degraded to exactly the same size as OmcA. This also does not explain the presence of bands in the control sample. There is a chance that the equal digestion idea and incorrectly labelled samples have both occurred but this seems highly unlikely.
- The DNA sequence for the sample was incorrect. Although the band had come out the correct size from the diagnostic PCR, due to timescales, the test SPA-tag experiment was started as the sequencing was run. Before the sequencing data came back, a further SPA-tag PCR screen was run along with full controls including pJL148 (where the SPA-tag was originally amplified from) as a positive and the parent pACYCMtr plasmids (Duet-1, ABO, CAB and CABO) for negative controls. The results of this are shown in Figure 6.39.

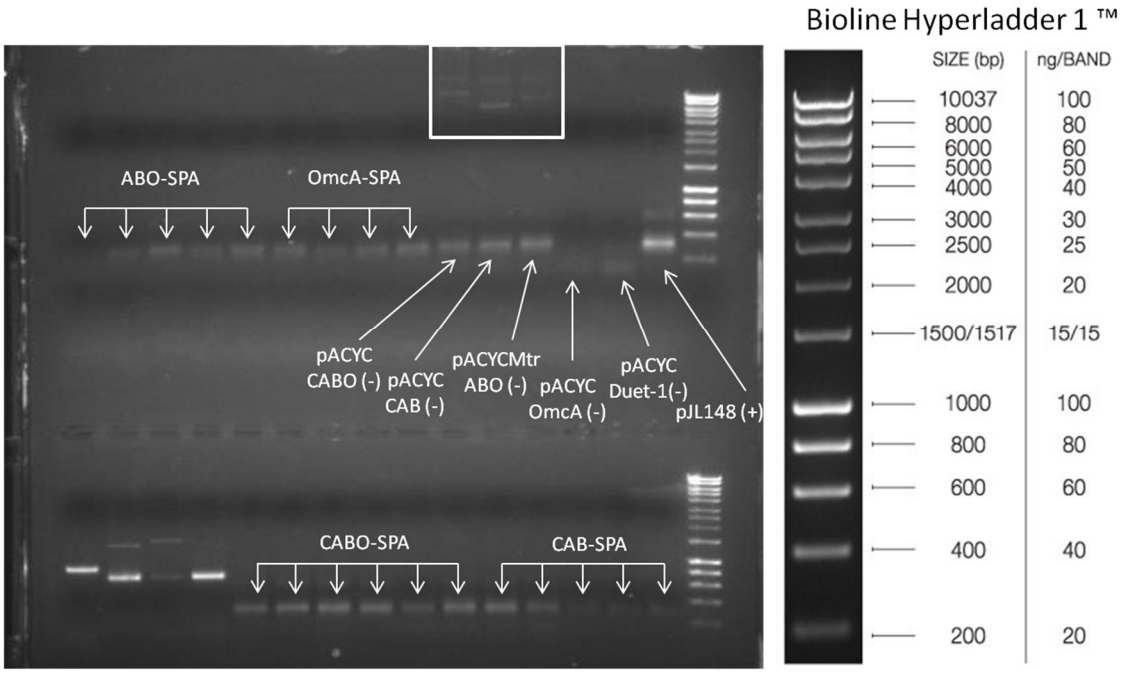

Figure 6.39 - SPA-tag screen with controls. Identification of band at the same size as desired in both positive and multiple negative controls

The gel in Figure 6.39 clearly shows that although there were bands of the correct size present in all but one of the tested SPA tag samples, there were also bands present within the negative controls.

6.2.5 Conclusions

The current plan was perhaps overly optimistic in scope, whilst also being overly eager to adopt new technologies that had not been thoroughly scrutinised such as Gibson assembly. The development of this technique (418) and the subsequently widely publicised use to create the greatest molecular/synthetic biology achievement to date with the generation of the first fully synthetic genome (100) and the more recent artificial yeast chromosome (422), made it appear an obvious choice for joining DNA sequences. Help in designing experiments using this technique has come from the vast increase in the number of computer tools available to help in the design and theoretical troubleshooting of cloning such as enhancements in SnapGene, release of Benchling and DNA 2.0's gene designer technology to name a few.

The attempted use of lambda red recombination without the use of an added selection marker appeared to prevent this insertion from occurring. Due to the design of the experiments, the same primers were able to be used for the PCR overlap technique. Understanding the correct process to undergo when carrying out a new technique always takes time and there have been a number of lessons learned during this.

6.3 Chapter conclusions

This chapter summarises the attempts to try and insert multiple genetic fragments onto the chromosome of a B-type *E. coli* strain and attempts to determine the interacting partners of a plasmid based Mtr system. The developments in the chromosomal insertion work, provide options to continue attempts with the development of the pUC19Cm-Tn7 plasmid. The insertion of the SPA-tag onto the Mtr based plasmids presented a greater challenge than expected, but the issues as with the methodology, has been demonstrated to be feasible, and further troubleshooting of the PCR overlap method are expected to yield useful information into interacting partners. The challenges posed by the overlap of DNA elements were a constant theme throughout the chapter and are an experiment to avoid if at all possible. Development of tools that prevent the use of these types of experiments are recommended.

Chapter 7 – Final Conclusions and Future Directions

At the closing point of this thesis, it presents an opportunity to consider the work that has been carried out during this endeavour. A variety of microbiology, molecular biology, proteomic and bioelectrochemistry techniques have been employed, in order to try and gain a greater understanding of the underlying mechanisms that allow for exoelectrogenic activity and options for engineering its improvement. The complexity of genetic systems means that they are usually far beyond a "plug and play" type analogy often espoused by the synthetic biology BioBrick community.

7.1 Microbial fuel cell evaluation

Something that became apparent throughout chapter 4 of this thesis was the difficulties and technical issues associated with microbial fuel cells, especially with regard to high-throughput strain evaluation. There is a huge variety of MFCs and BESs detailed in the literature but no single, commercially available, defined device(s) that are used as standards. Due to the complex nature of the interactions occurring within an MFC, especially with the level of exoelectrogenic activity change observed in this study for the *E. coli* strains, the device needs to be highly sensitive, reliable and reproducible, whilst still maintaining high-throughput capabilities.

7.2 Transferring electrogenic capabilities

A real focus of the thesis at the point of inception was to determine if the functional transfer of exoelectrogenic activity into a foreign organism was possible, the ultimate aim being to engineer a step change in current beyond wild-type behaviour. As the results from chapter 3 show, the transfer of a section of the Mtr proteins from *S. oneidensis* MR-1 into *E. coli* BL21 DE3 show this to be possible, although with a change (ca. 60%) in the observable power output.

As for the chosen methods for the transfer of electrogenic activity, these were scientifically sound from the literature available at the time (105,120). The continued research carried out into the mechanisms of extracellular electron transfer during the course of this thesis has led to the discovery that a great deal of the electrogenic activity seen in *Shewanella* is due to mediators (104,136,284,316,423). This is not to say that electrogenic activity is not possible without the use of mediators, and is far from limited to them through the broad range of organisms contained within the classification of DMRB, as discussed in chapter 1. The most clear cut example of this is the fact that the highly studied *Geobacter* genus not making use of mediators for extracellular electron transfer (104,424).

Whether the continuation of engineering *E. coli* is the best route to further pursue for the creation of a highly tuned electrogenic organism is up for debate. This project was executed as a synthetic biology challenge to attempt the integration of a ('useful') functional pathway within a MFC. The use of a mixed consortium during this or even in the future is out of the remit of this approach due to the incredibly high complexity of microbial communities. As to whether *E. coli* should be used as the chosen organism for further manipulation, this is again questionable. The use of a tried and tested DMRB such as *Shewanella* or *Geobacter* provides advantages and although they are not specifically evolved for life within an MFC, further directed evolution has been shown to be possible (114). Genetic manipulation of strains such as *Shewanella* and *Geobacter* could yield large improvements in current generation through metabolic engineering and overexpression of desired pathways. *E. coli* is not naturally evolved for survival within the anode chamber of an MFC and cannot, at this stage, even with the introduction of the Mtr pathway create a considerable amount of current. There are however significant advantages of using *E. coli* over other organisms. It is still the most widely (genetically) studied micro-organism with an extensive list of models, mutants and studies having been carried out on it. It should be considered an incredible achievement that any increase in power density was noted following the introduction of the Mtr pathway, as this shows the integration of a highly complex system with the host metabolism. Now that this has been shown, the possibilities for

further/completely different components from a variety of organisms can be introduced and screened for activity. The results from *E. coli* in chapter 4 then showed that more fundamental studies of electron transport in both *E. coli* and *Shewanella oneidensis* MR-1 were required, which was the thinking behind the two proteomics driven chapters, 5 and 6.

7.3 Quantitative proteomics of *Shewanella*

This study, detailed in chapter 5 was done to try and determine the proteomic changes within *Shewanella oneidensis* MR-1, when generating current within an MFC compared to aerobically grown cells. Although a large amount of work has been carried out on deciphering the exact proteins involved in electron transfer within *Shewanella,* there was very little done at a global proteomic level. Understanding how *Shewanella* adapts to survival within the anode had the potential to provide insight into how an engineered *E. coli* strain could be modified to increase power generation. An iTRAQ analysis into the proteomic shift in the highest power producing *E. coli* strain BL21 DE3 pRGK333 pRSFOmcA-MtrCAB was decided against a targeted interaction study, within this strain, as detailed in chapter 6. At the point of this study, a great deal of work had been conducted on the Mtr pathway and it had already been chosen for insertion into *E. coli*. The identification of the TolC as a potential component in the transfer of electrons extracellularly requires further testing in order to be verified as discussed in further work. This information was then carried forward for analysis with the interaction work in the Mtr gene expressing *E. coli* detailed in chapter 6.

7.4 Chromosomal insertion of the Mtr pathway

The issues of metabolic burden noted due to plasmid based systems detailed in the literature (343,345,347,425–427) needed to be addressed. This was due to the high level of metabolic burden placed upon the *E. coli* cells bearing the plasmids for the overexpression of the cytochrome maturation genes and the Mtr pathway. In order to remove the burden or at least determine if it was an issue, a method of basing the system on the genome of *E. coli* was needed. Though a variety of different methods

were attempted and new plasmids were developed, neither the overexpression of the native cytochrome maturation genes nor the chromosomal insertion of the Mtr genes was achieved in the time period. Table 6.4 in chapter 6 provides a concise overview of the pros and cons of the different genome manipulation tools that were evaluated. This evaluation had to be done as there is no kit based insertion system available that could be ordered and allow for guaranteed insertion. Analysis of the literature did not provide a defined, single tool that can be used in every situation for the basing of the different elements. There are significant challenges that must be overcome in order to integrate genetic material onto the chromosome of an organism. Choosing a commercial option such as paying for a company like Genebridges (http://www.genebridges.com) to carry out this insertion would not only be expensive but through discussion with the company, it appears they have experienced limitations with the insertion of genes in B-type strains. Plasmids were developed to aid in the chromosomal basing of genetic elements both in a fixed location and also at a chosen site.

7.5 Interaction of the Mtr pathway with the native *E. coli* host machinery

The transfer of electrogenic activity into *E. coli* (chapter 4) showed that it was possible for the electrogenic capability to be transferred although, this research, along with work in the same area from the group of Ajo-Franklin (124,125) does not indicate exactly how this is possible. In order to try and increase the level of power generated by the engineered strain, it was important to understand the partners that this recombinant system was interacting with. The use of a "SPA-tag" for tandem affinity purification of the genetically tagged proteins was attempted for identification of these. The exact localisation of the proteins within the engineered strain is not properly identified and due to the delicate nature of overexpressing recombinant proteins, it is highly unlikely that the system is arranged exactly as detailed in *Shewanella.* A portion of the complex decahaem cytochromes may well be in the correct orientation and ratio, to allow for correct extracellular electron transfer, but

there may well also be a large portion of charged recombinant cytochromes that are present within the media that are able to interact with the anode. There are indications of the methods that the host *E. coli* is able to interact with the Mtr pathway as shown by Jensen et al (125). The main hub of electron donation within *Shewanella* to the Mtr pathway is the tetrahaem *c*-type cytochrome CymA. This is very clearly demonstrated through a near complete knockout of current density of a knockout strain shown by Bretschger et al (109). The *E. coli* CymA homolog, NapC, was therefore posited to be a highly important in the transfer of electrons to the recombinant Mtr pathway (105,107). This theory was put to the test by Jensen et al where a NapC knockout within BL21 (DE3) was created and tested, in combination with and without cytochrome maturation genes and separately MtrA. This demonstrated that the cells were still able to reduce membrane soluble Fe (III) citrate without the presence of NapC. The ability of *E. coli* to provide a greater level of electron donation to the outer membrane than *Shewanella,* seems unlikely due to the high level of extracellular electron donation noted in the latter but not the former. It may well be due to the mislocalisation of overexpressed MtrA proteins. The use of subcellular fractionation could help to determine where recombinant proteins are being localised, but this technique is far from perfect. There can be “bleeding” from different cellular compartments leading to false positives. The use of the TAP-tag system described in chapter 6 allows for the discovery of interacting partners within the cell. The need for reciprocal tagging allows for the removal of false positives. The attempts to complete this within the time frame of this thesis were not successful as the use of the PCR overlap appeared to provide false positives. The SPA-tag setup used within this chapter has already been tested and a methodology for insertion created, making continuation of this work feasible.

7.6 Future work

7.6.1 Chromosomal insertion

Although developments were made in the generation of alternative chromosomal insertion plasmids that potentially allow for the bypassing of certain issues, the lack of

a complete insertion into the chromosome of a desired organism means that this is the future work that needs to be tackled.

As a limiting factor in the use of lambda red recombination is the overlap of the FRT flanked resistance cassette and the GOI. As shown in Figure 6.2 the resistance cassette has to be amplified from either pKD13 or pKD32 whereas the GOI is amplified separately (Step 1 in Figure 6.2). The 2 amplified genetic elements must then be connected to each other through a PCR reaction (step 3 in Figure 6.2). This means that they must have an overlapping section that is homologous (H2 complementary to H3), so that when the dsDNA is denatured, the two sections are complementary and have the potential to bind to each other and allow for amplification of the other element. There is a delicate balance when designing primers to ensure that the region of the primer specific to amplifying the first target e.g. GOI has enough of the primer that is specific to amplifying that target so that unspecific binding does not occur. It must, at the same time, have enough of a flanking region that is complementary to the DNA it is to be connected to e.g. an FRT flanked cassette. The larger the GOI is, the harder this can be as the primers will need to increase in size to be able to provide specific PCR of each of the reactions. This also becomes increasingly expensive, the PCR reactions less likely to work and the melting temperature of the primers continues to increase – all leading to the reactions being less likely to succeed.

In order to combat these challenges a plasmid could be designed that contains the pKD13 or pKD32 FRT flanked resistance cassettes (or newly designed flanked resistance cassettes) in a plasmid that contains an MCS next to (upstream or downstream) it. This means that the GOI could then be cloned into the plasmid and relatively simple primers could be designed, one to amplify from the resistance cassette end and another from the GOI end. This would only need ends that are homologous to the region where the insert is needed and would then create a linear dsDNA template needed for transformation into a strain bearing an induced pKD46 variant plasmid. This would therefore remove, what could be considered a major

limitation, of the current Datsenko and Wanner plasmid setup for chromosomal insertions.

In terms of the attenuation plasmid setup, the pUC19Cm-Tn7 plasmid still has the potential to be a very useful plasmid for fixed site insertion of genetic elements alongside pGRG36. This is still a two plasmid setup but presents an opportunity to clone the GOI into a very small plasmid for later insertion. The fact that Tn7 systems can be used within such a wide range of organisms makes it very appealing option that is still worth consideration for future work.

There are still a wide variety of opportunities that could be used to attempt to overexpress the cytochrome maturation genes and localise the heterologous Mtr pathway onto the chromosome to determine if metabolic burden is having an effect on the power output of the cells.

7.6.2 Interaction of the Mtr system with native *E. coli* proteins

In order to gain an understanding of how the Mtr pathway allows for current production within *E. coli*, either a new interaction method needs to be used, or a continuation of the SPA-tag work needs to be done. As the SPA-tag methodology has been established and trialled, albeit unsuccessfully so far, it still has the potential to be the quickest method and to deliver useful information. This is due to the fact that in theory, only two PCR reactions are required to insert the SPA-tag into desired plasmid.

In order to carry on with the SPA-tag experiments, the following things would need to be considered:

- Order fresh primers, amplify SPA tag and send for sequencing
- Use PCR overlap protocol for insertion of SPA-tag – send transformants for sequencing
- Test run of the SPA-tag protocol
- If unusual banding is discovered, gel bands should be cut, digested and run on the MS for analysis

    - If native BL21 proteins are detected then the sequence can be identified and a further investigation into how these proteins are being purified following TAP-tag can be made.
    - If the proteins are found to be digested/degraded Mtr proteins then this may suggest that either a higher concentration or a different protein inhibitor complex is needed.
- Once the issues with the test procedure have been resolved, then the testing of the strains in triplicate within a poised potential half cell can begin, with the cells ready for SPA-tag purification and MS analysis.

Analysis of the samples should provide details of the interacting partners of the Mtr proteins, which apart from helping to settle the debate about the proteins that donate electrons to this pathway within *E. coli*, they could also potentially provide the opportunity for upregulation of native machinery and remove bottlenecks. This work will then need to be carried out in *Shewanella* in order to visualise the difference between the interacting partners.

7.6.3 Post iTRAQ analysis and future potential

Following the quantitative proteomic analysis of *S. oneidensis* MR-1, the most logical way to test if any of the theories put forward in the thesis are true is through the creation of mutants such as Δ*TolC*. There is however, the potential for this to have a significantly detrimental effect on the strain, potentially preventing expulsion of toxins from the cell. Testing of this mutant would permit determination of the function of these proteins within the context of power generation within an MFC and provide valuable information for the MFC and *Shewanella* community. iTRAQ still holds a lot of potential in its ability to help decipher metabolic bottlenecks and aid in forward engineering (272), when used in tandem with bioinformatic techniques such as flux balance analysis. The use of this technique on the plasmid based or preferentially the chromosomally based electrogenic *E. coli,* could help to illustrate ways in which current density could be increased. The use of the information generated within this iTRAQ study may also be used to help further engineer a more adapted, current

generation strain. The issues with the lack of identification of the Mtr proteins within the *Shewanella* iTRAQ samples, could potentially be due to the low abundance of the proteins within the samples. The detection of these could be attempted through the use of targeted protein analysis in the form of MRMs.

7.6.4 Future electrogenic targets

Analysis of the literature throughout this thesis has provided ideas of future targets for integration into engineered *E. coli*. This begs the question as to whether there is potential for the use of *Geobacter* cytochromes within *E. coli.* This has never been demonstrated before and the ability of the *Geobacter* system to be able to integrate and functionally link with the *E. coli* system is questionable. This is based upon the assumption that *Shewanella* proteins are more likely to be able to interact with *E. coli* host proteins, due to the fact that they are both Gammaproteobacteria and therefore share a closer evolutionary ancestor than *Geobacter* which is a Deltaproteobacterium.

Now that the Mtr system has been established within *E. coli*, it presents an opportunity for mediator based electron transfer. The UshA (316) and bfe (104) proteins that are touted as having a huge role within *Shewanella,* could potentially be carried across to *E. coli* to allow for greater power densities.

Closing statement

Throughout this thesis there has been an attempt to further the understanding the mechanisms and transferability of extracellular electron transfer in regard to current generation. Cloning of varying components of the Mtr pathway from *S. oneidensis* into *E. coli* demonstrated, not only that electrogenic activity can be transferred but that this can lead to 64% of *S. oneidensis* power output being generated.

Proteomic analysis of *S. oneidensis* under aerobic growth compared to cells grown within an MFC demonstrated the potentially important influence of proteins outside of the Mtr pathway.

The attempted chromosomal basing of the Mtr pathway onto the E. coli genome, although unsuccessful at this point has led to a greater understanding of methods that should not be employed. There are also numerous other molecular biology techniques and options detailed that may allow for this to be successful.

Determining the interacting partners of the recombinant Mtr pathway within *E. coli* presented an opportunity to elucidate an important part of the puzzle as to how recombinant electrogenicity functions. The continuation of this work may well yield the answer to this question.

The aims set out at the beginning of this thesis were achieved, through the engineering paradigm, with the transfer of electrogenic activity into an organism that was previously incapable of such activity. Proteomic analysis and attempts at chromosomal insertion of relevant genetic elements and their interaction with the native machinery present further challenges to go forward with. The demonstration of transferrable electrogenic activity most importantly showing the fact that this was possible now presents the opportunity to further increase the electrogenic activity of this recombinant system.

From the results obtained during the course of this thesis and the developments seen in the field over the course of this study, it is clear that electrogenic activity can be transferred through the use of the Mtr pathway from *S. oneidensis* MR-1. The

developments carried out by Goldbeck et al (124) showed that optimisation of promoter sequences, allowed for a balance of Mtr proteins produced and current generation whilst still yielding "healthy looking" cells. The results obtained from the transfer of activity into *E. coli* still yield relatively low levels when compared to those demonstrated by *S. oneidensis* MR-1 (661 W m^{-3}) (428) and mixed culture MFCs (3320 W m^{-3}) (429). In order for engineered organisms to become a feasible option within BES's this issue must be addressed. One way in which this may be possible to achieve is through the further enhancement of a well characterised organism such as *E. coli*. Transferring the initial Mtr pathway to the chromosome and upregulation of the native cytochrome maturation genes would present the option for use of other plasmid based elements. The identification and removal of unnecessary competing pathways (e.g. potentially the nitrate reductase pathway) could theoretically allow for more electrons to be transferred to the anode.

All the work carried out with the transfer of this activity is however, carried out within the Gammaproteobacteria, (the same as *S. oneidensis* MR-1) *E. coli*. These organisms have important proteins that are closely related to each other in the form of the inner membrane anchored tetrahaem *c*-type cytochromes NapC (*E. coli*) and CymA (*S. oneidensis)*. Both of these are involved with interaction with the quinone pool and then transfer of electrons into the periplasm. The ability to transfer electrogenic activity in to an organism that isn't as closely related would surely be a much greater challenge.

Due to the high desirable ability of BES's to degrade waste organic material and convert it directly to electricity (or hydrogen) this is likely how the system will be used if carried on to industrial level use. In this circumstance there will be a large range of organisms that will be transferred into the system alongside the feedstock. Any single strain of bacteria is, unless high modified, to be outcompeted by a mixture of naturally occurring microorganisms. The future of the microorganisms used within BES's may well lie with use of synthetic mixed cultures. This may either mean determining the ideal mixed culture for the conditions required or generating a collection of genetically

modified metabolically diverse organisms that are able to form a cohesive mutualistic relationship within the anode. Not all organisms need be DMRB or genetically modified to have electrogenic activity but they would as a whole need to be able to degrade all waste organic material whilst eventually transferring electrons (potentially through the transfer of by products to each other) to the anode with a high coulombic efficiency.

Considering the challenges that have been encountered during the course of this thesis the main differences I would want to make would be with the MFCs and BESs in general. It is these devices that have caused the most trouble throughout. I considered the project to be a strongly interdisciplinary study that could likely have benefitted from collaboration with a research group specialising in the technically challenging domain of MFCs.

As for what I consider the next direct steps that hold the most promise in regards to the continuation of this work, I think the experiments attempted within Chapter 6 (chromosomal insertion and interaction of Mtr components) have potential to yield interesting and useful information. Understanding what proteins the Mtr pathway is interacting with in the periplasmic space may provide opportunities for metabolic engineering and a greater understanding of how this recombinant pathway is working. As discussed previously, the basing of the Mtr pathway chromosomally provides an opportunity to free up space for plasmid based elements that may be able to enhance current generation. In order for the system to be able to achieve the levels seen within *Shewanella* there may be other components that need to be expressed. The use of a genetic library screen and a high throughput screening method may help to identify relevant targets.

As for the long term future of MFCs, I have a strong belief in their abilities as a renewable energy technology although I find it incredibly unlikely that they will ever be a sole source of power for a large community. I do think that given the energy and waste challenges we face from a growing and developing global population I think they stand a good chance of being able to provide an economically viable venture. They have gathered considerable media attention recently, especially with real world

application like that done by Dr Ioannis Ieropoulos and colleagues at UWE with the use of urine as a feedstock. There are still considerable challenges that must be overcome with the engineering of the devices and being able to generate a large scale system that can be integrated alongside the current infrastructure. They also face strong competition from other waste to energy technologies such as anaerobic digesters.

I've had some ups and downs throughout the course of my studies with this project but I'd like to think I've come out as a more knowledgeable person with an added appreciation for renewable technology and the important role that science plays in our lives.

References

1. Lutz W, K C S. Dimensions of global population projections: what do we know about future population trends and structures? Philos Trans R Soc Lond B Biol Sci. 2010;365(1554):2779–91.

2. Barrett CB. Measuring food insecurity. Science. 2010;327(5967):825–8.

3. Godfray HCJ, Beddington JR, Crute IR, Haddad L, Lawrence D, Muir JF, et al. Food security: the challenge of feeding 9 billion people. Science. 2010;327(5967):812–8.

4. Parfitt J, Barthel M, Macnaughton S. Food waste within food supply chains: quantification and potential for change to 2050. Philos Trans R Soc Lond B Biol Sci. 2010;365(1554):3065–81.

5. Onda K, LoBuglio J, Bartram J. Global access to safe water: accounting for water quality and the resulting impact on MDG progress. Int J Environ Res Public Health. 2012;9(3):880–94.

6. Courtland R. Enough water to go around? Nature. 2008;

7. Rabaey K, Verstraete W. Microbial fuel cells: novel biotechnology for energy generation. Trends Biotechnol. 2005;23(6):291–8.

8. Oh ST, Kim JR, Premier GC, Lee TH, Kim C, Sloan WT. Sustainable wastewater treatment: How might microbial fuel cells contribute. Biotechnol Adv.2010

9. Pant D, Van Bogaert G, Diels L, Vanbroekhoven K. A review of the substrates used in microbial fuel cells (MFCs) for sustainable energy production. Bioresour Technol.2010;101(6):1533–43.

10. Li W-W, Yu H-Q, He Z. Towards sustainable wastewater treatment by using microbial fuel cells-centered technologies. Energy Environ Sci. 2014;7(3):911.

11. Oliveira VB, Simões M, Melo LF, Pinto A. MFR. Overview on the developments of microbial fuel cells. Biochem Eng J..; 2013;73:53–64.

12. Ren L, Ahn Y, Logan BE. A Two-Stage Microbial Fuel Cell and Anaerobic Fluidized Bed Membrane Bioreactor (MFC-AFMBR) System for Effective Domestic Wastewater Treatment. Environ Sci Technol. 2014;48(7):4199–206.

13. Zhang F, Ge Z, Grimaud J, Hurst J, He Z. Long-term performance of liter-scale microbial fuel cells treating primary effluent installed in a municipal wastewater treatment facility. Environ Sci Technol. 2013;47(9):4941–8.

14. Dou X. Low Carbon-Economy Development: China's Pattern and Policy Selection. Energy Policy. Elsevier; 2013;63:1013–20.

15. Höök M, Tang X. Depletion of fossil fuels and anthropogenic climate change—A review. Energy Policy. 2013;52:797–809.

16. Keppel-Aleks G, Wennberg PO, O'Dell CW, Wunch D. Towards constraints on fossil fuel emissions from total column carbon dioxide. Atmos Chem Phys. 2013;13(8):4349–57.

17. Lucas PL, Shukla PR, Chen W, van Ruijven BJ, Dhar S, den Elzen MGJ, et al. Implications of the international reduction pledges on long-term energy system changes and costs in China and India. Energy Policy.2013;63:1032–41.

18. Bentley R. Global oil & gas depletion: an overview. Energy Policy. 2002;30(3):189–205.

19. Bentley R, Mannan S, Wheeler S. Assessing the date of the global oil peak: The need to use 2P reserves. Energy Policy. 2007;35(12):6364–82.

20. Corsetti M, Stomper A. Past, Present and Future Evolution of Oil Prices. MIT Master Sci Manag Stud. 2010;

21. DECC Fossil Fuel Price Projections. 2012

22. Fournier J, Koske I, Wanner I, Zipperer V. The Price of Oil–Will It Start Rising Again? 2013;(1031).

23. Tripati AK, Roberts CD, Eagle RA. Coupling of CO2 and ice sheet stability over major climate transitions of the last 20 million years. Science. 2009;326(5958):1394–7.

24. Kawase R, Matsuoka Y, Fujino J. Decomposition analysis of CO2 emission in long-term climate stabilization scenarios. Energy Policy. 2006;34(15):2113–22.

25. Cohen JE. Human population: the next half century. Science. 2003;302(5648):1172–5.

26. Battaglini A, Lilliestam J, Haas A, Patt A. Development of SuperSmart Grids for a more efficient utilisation of electricity from renewable sources. J Clean Prod. Elsevier Ltd; 2009;17(10):911–8.

27. Kerr RA. Nuclear Waste disposal. Science and policy clash at Yucca Mountain. Science. 2000;288(5466):602.

28. Gross C. Community perspectives of wind energy in Australia: The application of a justice and community fairness framework to increase social acceptance. Energy Policy. 2007;35(5):2727–36.

29. De Alwis HPNS, Mohamad AA, Mehrotra AK. Exergy Analysis of Direct and Indirect Combustion of Methanol by Utilizing Solar Energy or Waste Heat. Energy & Fuels. 2009;23(3):1723–33.

30. Klessmann C, Nabe C, Burges K. Pros and cons of exposing renewables to electricity market risks—A comparison of the market integration approaches in Germany, Spain, and the UK. Energy Policy. 2008;36(10):3646–61.

31. Khan M, Iqbal M, Quaicoe J. A Technology Review and Simulation Based Performance Analysis of River Current Turbine Systems. 2006 Can Conf Electr Comput Eng. Ieee; 2006:2288–93.

32. Patterson T, Dinsdale R, Esteves S. Review of Energy Balances and Emissions Associated with Biomass-Based Transport Fuels Relevant to the United Kingdom Context. Energy & Fuels. 2008;22(5):3506–12.

33. Field CB, Campbell JE, Lobell DB. Biomass energy: the scale of the potential resource. Trends Ecol Evol (Personal Ed. 2008;23(2):65–72.

34. Petrou EC, Pappis CP. Biofuels: A Survey on Pros and Cons. Energy & Fuels. 2009;23(2):1055–66.

35. D'Alessandro W, Brusca L, Kyriakopoulos K, Michas G, Papadakis G. Hydrogen sulphide as a natural air contaminant in volcanic/geothermal areas: the case of Sousaki, Corinthia (Greece). Environ Geol. 2008;57(8):1723–8.

36. Richter BD, Mathews R, Harrison DL, Wigington R. Ecologically Sustainable Water Management: Managing River Flows for Ecological Integrity. Ecol Appl. 2003;13(1):206–24.

37. Logan BE. Exoelectrogenic bacteria that power microbial fuel cells. Nat Rev Microbiol. 2009;7(5):375–81.

38. Nallathambigunaseelan V. Anaerobic digestion of biomass for methane production: A review. Biomass and Bioenergy. 1997;13(1-2):83–114.

39. Mata-Alvarez J. Anaerobic digestion of organic solid wastes. An overview of research achievements and perspectives. Bioresour Technol. 2000;74(1):3–16.

40. Murphy J, Mccarthy K. The optimal production of biogas for use as a transport fuel in Ireland. Renew Energy. 2005;30(14):2111–27.

41. Watanabe K. Recent developments in microbial fuel cell technologies for sustainable bioenergy. J Biosci Bioeng. The Society for Biotechnology, Japan; 2008;106(6):528–36.

42. Yue P, Lowther K. Enzymatic oxidation of C1 compounds in a biochemical fuel cell. Chem Eng J. 1986;33(3):B69–77.

43. Liu ZD, Du ZW, Lian J, Zhu XY, Li SH, Li HR. Improving energy accumulation of microbial fuel cells by metabolism regulation using Rhodoferax ferrireducens as biocatalyst. Lett Appl Microbiol. 2007;44(4):393–8.

44. Schröder U. Anodic electron transfer mechanisms in microbial fuel cells and their energy efficiency. Phys Chem Chem Phys. 2007;9(21):2619–29.

45. Lovley DR. Bug juice: harvesting electricity with microorganisms. Nat Rev Microbiol. 2006;4(7):497–508.

46. Lovley DR. The microbe electric: conversion of organic matter to electricity. Curr Opin Biotechnol. 2008;19(6):564–71.

47. Potter MC. Electrical effects accompanying the decomposition of organic compounds. Proc R Soc London Ser B. 1911;84:260–76.

48. Holmes DE, Chaudhuri SK, Nevin KP, Mehta T, Methé BA, Liu A, et al. Microarray and genetic analysis of electron transfer to electrodes in *Geobacter sulfurreducens*. Environ Microbiol. 2006;8(10):1805–15.

49. Pham TH, Jang JK, Chang IS, Kim BH. Improvement of cathode reaction of a mediatorless microbial fuel cell. J Microbiol Biotechnol. 2004;14(2):324–9.

50. Davis F, Higson SPJ. Biofuel cells--recent advances and applications. Biosens Bioelectron. 2007;22(7):1224–35.

51. Strik DPBTB, Terlouw H, Hamelers HVM, Buisman CJN. Renewable sustainable biocatalyzed electricity production in a photosynthetic algal microbial fuel cell (PAMFC). Appl Microbiol Biotechnol. 2008;81(4):659–68.

52. Chaudhuri SK, Lovley DR. Electricity generation by direct oxidation of glucose in mediatorless microbial fuel cells. Nat Biotechnol. 2003;21(10):1229–32.

53. Pham TH, Rabaey K, Aelterman P, Clauwaert P, De Schamphelaire L, Boon N, et al. Microbial Fuel Cells in Relation to Conventional Anaerobic Digestion Technology. Eng Life Sci. 2006;6(3):285–92.

54. Matsuzaki Y, Baba Y, Sakurai T. High electric conversion efficiency and electrochemical properties of anode-supported SOFCs. Solid State Ionics. 2004;174(1-4):81–6.

55. Rosenbaum M, Schröder U, Scholz F. Utilizing the green alga *Chlamydomonas reinhardtii* for microbial electricity generation: a living solar cell. Appl Microbiol Biotechnol. 2005;68(6):753–6.

56. Rosenbaum M, Schröder U, Scholz F. In situ electrooxidation of photobiological hydrogen in a photobioelectrochemical fuel cell based on *Rhodobacter sphaeroides*. Environ Sci Technol. 2005;39(16):6328–33.

57. Aelterman P, Rabaey K, Clauwaert P, Verstraete W. Microbial fuel cells for wastewater treatment. Water Sci Technol. 2006;54(8):9.

58. Fan Y, Hu H, Liu H. Comment on “Sustainable power generation in microbial fuel cells using bicarbonate buffer and proton transfer mechanisms”. Environ Sci Technol. 2008;42(16):6303–5; author reply 6306.

59. Liu H, Logan BE. Electricity generation using an air-cathode single chamber microbial fuel cell in the presence and absence of a proton exchange membrane. Environ Sci Technol. 2004;38(14):4040–6.

60. Kim JR, Min B, Logan BE. Evaluation of procedures to acclimate a microbial fuel cell for electricity production. Appl Microbiol Biotechnol. 2005;68(1):23–30.

61. Ieropoulos I, Greenman J, Melhuish C. Microbial fuel cells based on carbon veil electrodes:Stack configuration and scalability. Int J Energy Res. 2008:1228–40.

62. Du Z, Li H, Gu T. A state of the art review on microbial fuel cells: A promising technology for wastewater treatment and bioenergy. Biotechnol Adv. 2007;25(5):464–82.

63. Cheng S, Logan BE. Sustainable and efficient biohydrogen production via electrohydrogenesis SCIENCE. 2007;104(47):18871–3.

64. Park H, Mushtaq U, Perello D, Lee I, Cho SK, Star A, et al. Effective and low-cost platinum electrodes for microbial fuel cells deposited by electron beam evaporation. Energy & Fuels. 2007;(9):2984–90.

65. Kim BH, Chang IS, Gadd GM. Challenges in microbial fuel cell development and operation. Environ Sci Technol. 2007;485–94.

66. Oh S, Min B, Logan BE. Cathode performance as a factor in electricity generation in microbial fuel cells. Environ Sci Technol. 2004;38(18):4900–4.

67. Zimmerman WB, Hewakandamby BN, Tesař V, Bandulasena HCH, Omotowa O a. On the design and simulation of an airlift loop bioreactor with microbubble generation by fluidic oscillation. Food Bioprod Process. 2009;87(3):215–27.

68. Cheng S, Liu H, Logan BE. Increased power generation in a continuous flow MFC with advective flow through the porous anode and reduced electrode spacing. Environ Sci Technol. 2006;40(7):2426–32.

69. Gil GC, Chang IS, Kim BH, Kim M, Jang JK, Park HS, et al. Operational parameters affecting the performance of a mediator-less microbial fuel cell. Biosen Bioelectron. 2003;18:327–34.

70. Call D, Logan BE. Hydrogen production in a single chamber microbial electrolysis cell lacking a membrane. Environ Sci Technol. 2008;42(9):3401–6.

71. Jeremiasse AW, Hamelers HVM, Buisman CJN. Microbial electrolysis cell with a microbial biocathode. Bioelectrochemistry. Elsevier B.V.; 2010;78(1):39–43.

72. Kim Y, Logan BE. Microbial desalination cells for energy production and desalination. Desalination. Elsevier B.V.; 2013;308:122–30.

73. Cao X, Huang X, Liang P, Xiao K, Zhou Y, Zhang X, et al. A new method for water desalination using microbial desalination cells. Environ Sci Technol. 2009;43(18):7148–52.

74. Luo H, Jenkins PE, Ren Z. Concurrent desalination and hydrogen generation using microbial electrolysis and desalination cells. Environ Sci Technol. 2011;45(1):340–4.

75. Liu H, Grot S, Logan BE. Electrochemically assisted microbial production of hydrogen from acetate. Environ Sci Technol. 2005;39(11):4317–20.

76. Ieropoulos I, Greenman J, Melhuish C, Hart J. Comparative study of three types of microbial fuel cell. Enzym Microb Tech. 2005;37(2):238–45.

77. Melhuish C, Ieropoulos I, Greenman J, Horsfield I. Energetically autonomous robots: Food for thought. Auton Robots. 2006;21(3):187–98.

78. Velasquez-Orta SB, Head IM, Curtis TP, Scott K, Lloyd JR, von Canstein H. The effect of flavin electron shuttles in microbial fuel cells current production. Appl Microbiol Biotechnol. 2010;85(5):1373–81.

79. Venkata Mohan S, Mohanakrishna G, Srikanth S, Sarma PN. Harnessing of bioelectricity in microbial fuel cell (MFC) employing aerated cathode through anaerobic treatment of chemical wastewater using selectively enriched hydrogen producing mixed consortia. Fuel. 2008;87(12):2667–76.

80. Rabaey K, Lissens G, Siciliano SD, Verstraete W. A microbial fuel cell capable of converting glucose to electricity at high rate and efficiency. 2003;1531–5.

81. Watson VJ, Logan BE. Power production in MFCs inoculated with *Shewanella oneidensis* MR-1 or mixed cultures. Biotechnol Bioeng. 2010;105(3):489–98.

82. Lovley DR, Phillips EJ. Rapid assay for microbially reducible ferric iron in aquatic sediments. Appl Environ Microbiol. 1987;53(7):1536–40.

83. Lovley DR, Giovannoni SJ, White DC, Champine JE, Phillips EJ, Gorby YA, et al. *Geobacter metallireducens* gen. nov. sp. nov., a microorganism capable of coupling the complete oxidation of organic compounds to the reduction of iron and other metals. Archives of microbiology. 1993. p. 336–44.

84. Aklujkar M, Krushkal J, DiBartolo G, Lapidus A, Land ML, Lovley DR. The genome sequence of *Geobacter metallireducens*: features of metabolism, physiology and regulation common and dissimilar to *Geobacter sulfurreducens*. BMC Microbiol. 2009;9:109.

85. Heidelberg JF, Paulsen IT, Nelson KE, Gaidos EJ, Nelson WC, Read TD, et al. Genome sequence of the dissimilatory metal ion-reducing bacterium *Shewanella oneidensis*. Nat Biotechnol. 2002;20(11):1118–23.

86. Martín-Gil J, Ramos-Sánchez MC, Martín-Gil FJ. *Shewanella putrefaciens* in a fuel-in-water emulsion from the Prestige oil spill. Antonie Van Leeuwenhoek. 2004;86(3):283–5.

87. Tsai TT, Kao CM, Surampalli RY, Chien HY. Enhanced Bioremediation of Fuel-Oil Contaminated Soils: Laboratory Feasibility Study. J Environ Eng. 2009;135(9):845.

88. Löffler FE, Edwards E A. Harnessing microbial activities for environmental cleanup. Curr Opin Biotechnol. 2006;17(3):274–84.

89. Logan BE, Murano C, Scott K, Gray ND, Head IM. Electricity generation from cysteine in a microbial fuel cell. Water Res. 2005;39(5):942–52.

90. Lanthier M, Gregory KB, Lovley DR. Growth with high planktonic biomass in *Shewanella oneidensis* fuel cells. FEMS Microbiol Lett. 2008;278(1):29–35.

91. Rabaey K. Bioelectrochemical Systems - From extracellular electron transfer to biotechnological approach. IWA Publ. 2009;1st.

92. Trinh NT, Park JH, Kim SS, Lee J, Lee BY, Kim B. Generation behavior of elctricity in a microbial fuel cell. 2010;27(2):546–50.

93. Mitchell P. Coupling of phosphorylation to electron and hydrogen transfer by a chemi-osmotic type of mechanism. Nature. 1961. p. 144–8.

94. Kumar GG, Sarathi VGS, Nahm KS. Recent advances and challenges in the anode architecture and their modifications for the applications of microbial fuel cells. Biosens Bioelectron. Elsevier; 2013;43:461–75.

95. Logan BE, Hamelers B, Rozendal R, Schröder U, Keller J, Freguia S, et al. Microbial fuel cells: methodology and technology. Environ Sci Technol. 2006;40(17):5181–92.

96. Biffinger JC, Ray R, Little BJ, Fitzgerald LA, Ribbens M, Finkel SE, et al. Simultaneous analysis of physiological and electrical output changes in an operating microbial fuel cell with *Shewanella oneidensis*. Biotechnol Bioeng. 2009;103(3):524–31.

97. Verstraete W, Rabaey K. Critical Review Microbial Fuel Cells : Methodology and Technology †. Environ Sci Technol. 2006;40(17):5181–92.

98. Luchi S, Lin ECC. Adaptation of *Escherichia coii* Xo redox environments by gene expression. Mol Microbiol. 1993;9:9–15.

99. Fredrickson JK, Kostandarithes HM, Li SW, Plymale AE, Daly MJ. Reduction of Fe(III), Cr(VI), U(VI), and Tc(VII) by *Deinococcus radiodurans* R1. Appl Environ Microbiol. 2000;66(5):2006–11.

100. Gibson DG, Glass JI, Lartigue C, Noskov VN, Chuang R-Y, Algire MA, et al. Creation of a bacterial cell controlled by a chemically synthesized genome. Science. 2010;329(5987):52–6.

101. Reardon CL, Dohnalkova AC, Nachimuthu P, Kennedy DW, Saffarini DA, Arey BW, et al. Role of outer-membrane cytochromes MtrC and OmcA in the biomineralization of ferrihydrite by *Shewanella oneidensis* MR-1. Geobiology. 2010;8(1):56–68.

102. Shi L, Squier TC, Zachara JM, Fredrickson JK. Respiration of metal (hydr)oxides by *Shewanella* and *Geobacter*: a key role for multihaem c-type cytochromes. Mol Microbiol. 2007;65(1):12–20.

103. Gorby YA, Yanina S, McLean JS, Rosso KM, Moyles D, Dohnalkova A, et al. Electrically conductive bacterial nanowires produced by *Shewanella oneidensis* strain MR-1 and other microorganisms. Proc Natl Acad Sci USA. 2006;103(30):11358–63.

104. Kotloski N, Gralnick JA. Flavin electron shuttles dominate extracellular electron transfer by *Shewanella oneidensis*. MBio. 2013;4(1).

105. Pitts KE, Dobbin PS, Reyes-Ramirez F, Thomson AJ, Richardson DJ, Seward HE. Characterization of the *Shewanella oneidensis* MR-1 decaheme cytochrome MtrA: expression in *Escherichia coli* confers the ability to reduce soluble Fe(III) chelates. J Biol Chem. 2003;278(30):27758–65.

106. Beliaev AS, Klingeman DM, Klappenbach JA, Wu L, Romine MF, Tiedje JM, et al. Global Transcriptome Analysis of *Shewanella oneidensis* MR-1 Exposed to Different Terminal Electron Acceptors †. Omi A J Integr Biol. 2005;187(20):7138–45.

107. Gescher JS, Cordova CD, Spormann AM. Dissimilatory iron reduction in *Escherichia coli*: identification of CymA of *Shewanella oneidensis* and NapC of *E. coli* as ferric reductases. Mol Microbiol. 2008;68(3):706–19.

108. Fredrickson JK, Romine MF, Beliaev AS, Auchtung JM, Driscoll ME, Gardner TS, et al. Towards environmental systems biology of *Shewanella*. Nat Rev Microbiol. 2008;6(8):592–603.

109. Bretschger O, Obraztsova A, Sturm CA, Chang IS, Gorby YA, Reed SB, et al. Current production and metal oxide reduction by *Shewanella oneidensis* MR-1 wild type and mutants. Appl Environ Microbiol. 2007;73(21):7003–12.

110. Clarke TA, Edwards MJ, Gates AJ, Hall A, White GF, Bradley J, et al. Structure of a bacterial cell surface decaheme electron conduit. Proc Natl Acad Sci USA. 2011;1–6.

111. Richardson DJ, Butt JN, Fredrickson JK, Zachara JM, Shi L, Edwards MJ, et al. The “porin-cytochrome” model for microbe-to-mineral electron transfer. Mol Microbiol. 2012;85(2):201–12.

112. Myers CR, Myers JM. MtrB Is Required for Proper Incorporation of the Cytochromes OmcA and OmcB into the Outer Membrane of *Shewanella putrefaciens* MR-1. Appl Environ Microbiol. 2002;68(11):5585–94.

113. Bretschger O, Obraztsova A, Sturm CA, Chang IS, Gorby YA, Reed SB, et al. An exploration of current production and metal oxide reduction by *Shewanella oneidensis* MR-1 wild type and mutants. Microbiology. 2007.

114. Yi H, Nevin KP, Kim B-C, Franks AE, Klimes A, Tender LM, et al. Selection of a variant of *Geobacter sulfurreducens* with enhanced capacity for current production in microbial fuel cells. Biosens Bioelectron. 2009;24(12):3498–503.

115. Schicklberger M, Sturm G, Gescher JS. Genomic plasticity enables a secondary electron transport pathway in *Shewanella oneidensis*. Appl Environ Microbiol. 2012.

116. Myers JM, Myers CR. Role of the tetraheme cytochrome CymA in anaerobic electron transport in cells of *Shewanella putrefaciens* MR-1 with normal levels of menaquinone. J Bacteriol. 2000;182(1):67–75.

117. Ahuja U, Thöny-Meyer L. Dynamic features of a heme delivery system for cytochrome C maturation. J Biol Chem. 2003;278(52):52061–70.

118. Kranz RG, Richard-Fogal C, Taylor J-S, Frawley ER. Cytochrome c biogenesis: mechanisms for covalent modifications and trafficking of heme and for heme-iron redox control. Microbiol Mol Biol Rev. 2009;73(3):510–28.

119. Mcmillan DGG, Marritt SJ, Butt JN, Jeuken LJC. Menaquinone-7 Is Specific Cofactor in Tetraheme Quinol. 2012;287(17):14215–25.

120. Donald JW, Hicks MG, Richardson DJ, Palmer T. The c-type cytochrome OmcA localizes to the outer membrane upon heterologous expression in *Escherichia coli*. J Bacteriol. 2008;190(14):5127–31.

121. Shi L, Rosso KM, Clarke TA, Richardson DJ, Zachara JM, Fredrickson JK. Molecular Underpinnings of Fe(III) Oxide Reduction by *Shewanella Oneidensis* MR-1. Front Microbiol. 2012;3:50.

122. Richter H, Lanthier M, Nevin KP, Lovley DR. Lack of electricity production by *Pelobacter carbinolicus* indicates that the capacity for Fe(III) oxide reduction does not necessarily confer electron transfer ability to fuel cell anodes. Appl Environ Microbiol. 2007;73(16):5347–53.

123. White GF, Shi Z, Shi L, Wang Z, Dohnalkova AC, Marshall MJ, et al. Rapid electron exchange between surface-exposed bacterial cytochromes and Fe(III) minerals. Proc Natl Acad Sci. 2013;(Iii):1–6.

124. Goldbeck C, Jensen H, TerAvest M, Beedle N, Appling Y, Helper M, et al. Tuning Promoter Strengths for Improved Synthesis and Function of Electron Conduits in *Escherichia coli*. ACS Synth Biol. 2013;2:150–9.

125. Jensen HM, Albers AE, Malley KR, Londer YY, Cohen BE, Helms BA, et al. Engineering of a synthetic electron conduit in living cells. Proc Natl Acad Sci USA. 2010;107(45):19213–8.

126. Childers SE, Ciufo S, Lovley DR. *Geobacter metallireducens* accesses insoluble Fe(III) oxide by chemotaxis. Nature. 2002;416(6882):767–9.

127. Gorby YA, Yanina YS, Mclean JS, Rosso KM, Moyles D, Dohnalkova A, et al. Electrically conductive bacterial nanowires produced by *Shewanella oneidensis* strain MR-1 and other microorganisms. Proc Natl Acad Sci USA. 2006;103:11358–63.

128. Alfonta L. Genetically Engineered Microbial Fuel Cells. Electroanalysis. 2010;22(7-8):822–31.

129. Pugsley AP. The complete general secretory pathway in gram-negative bacteria. Microbiol Rev. 1993;57(1):50–108.

130. Pichel MG, Binsztein N, Qadri F, Girón JA. Type IV Longus Pilus of Enterotoxigenic *Escherichia coli*: Occurrence and Association with Toxin Types and Colonization Factors among Strains Isolated in Argentina. Society. 2002;40(2):694–7.

131. Francetić O, Lory S, Pugsley AP. A second prepilin peptidase gene in *Escherichia coli* K-12. Mol Microbiol. 1998;27(4):763–75.

132. Cianciotto NP. Type II secretion: a protein secretion system for all seasons. Trends Microbiol. 2005;13(12):581–8.

133. Richter H, McCarthy K, Nevin KP, Johnson JP, Rotello VM, Lovley DR. Electricity generation by *Geobacter sulfurreducens* attached to gold electrodes. Langmuir. 2008;24(8):4376–9.

134. Bouhenni RA, Vora GJ, Biffinger JC, Shirodkar S, Brockman K, Ray R, et al. The Role of *Shewanella oneidensis* MR-1 Outer Surface Structures in Extracellular Electron Transfer. Electroanalysis. 2010;(7):856–64.

135. Canstein H Von, Ogawa J, Shimizu S, Lloyd JR. Secretion of flavins by *Shewanella* species and their role in extracellular electron transfer. Appl Environ Microbiol. 2008;74(3):615–23.

136. Marsili E, Baron DB, Shikhare ID, Coursolle D, Gralnick JA, Bond DR. *Shewanella* secretes flavins that mediate extracellular electron transfer. Proc Natl Acad Sci USA. 2008;105(10):3968–73.

137. Okamoto A, Hashimoto K, Nealson KH, Nakamura R. Rate enhancement of bacterial extracellular electron transport involves bound flavin semiquinones. Proc Natl Acad Sci U S A. 2013;110(19):7856–61.

138. Biffinger JC, Pietron J, Ray R, Little B, Ringeisen BR. A biofilm enhanced miniature microbial fuel cell using *Shewanella oneidensis* DSP10 and oxygen reduction cathodes. Biosens Bioelectron. 2007;22(8):1672–9.

139. Cho EJ, Ellington AD. Optimization of the biological component of a bioelectrochemical cell. Engineering. 2007;70:165–72.

140. Ringeisen BR, Henderson E, Wu PK, Pietron J, Ray R, Little B, et al. High power density from a miniature microbial fuel cell using *Shewanella oneidensis* DSP10. Environ Sci Technol. 2006;40(8):2629–34.

141. Lovley DR, Coates JD, Blunt-Harries EL, Phillips EJP, Woodward JC. Humic substances as electron acceptors for microbial respiration. Nature. 1996;382:445–8.

142. Roden EE, Lovley DR. Dissimilatory Fe(III) Reduction by the Marine Microorganism Desulfuromonas acetoxidans. Appl Environ Microbiol. 1993;59(3):734–42.

143. Rabaey K, Boon N, Siciliano SD, Verhaege M, Verstraete W. Biofuel Cells Select for Microbial Consortia That Self-Mediate Electron Transfer. Society. 2004;70(9):5373–82.

144. Arnold RG, DiChristina TJ, Hoffmann MR. Inhibitor studies of dissimilative Fe(III) reduction by Pseudomonas sp. strain 200 ("*Pseudomonas ferrireductans*"). Appl Environ Microbiol. 1986;52(2):281–9.

145. Hou B, Hu Y, Sun J, Cao Y. Effect of anodic biofilm growth on the performance of the microbial fuel cell (MFC). Environ Sci Eng. 2010;(20977032):1–4.

146. Venkata Mohan S, Veer Raghavulu S, Sarma PN. Influence of anodic biofilm growth on bioelectricity production in single chambered mediatorless microbial fuel cell using mixed anaerobic consortia. Biosens Bioelectron. 2008;24(1):41–7.

147. Solano C, Echeverz M, Lasa I. Biofilm dispersion and quorum sensing. Curr Opin Microbiol. 2014;18(Figure 1):96–104.

148. Winkelman JT, Bree AC, Bate AR, Eichenberger P, Gourse RL, Kearns DB. RemA is a DNA-binding protein that activates biofilm matrix gene expression in *Bacillus subtilis*. Mol Microbiol. 2013;88(5):984–97.

149. Stoodley P, Sauer K, Davies DG, Costerton JW. Biofilms as complex differentiated communities. Annu Rev Microbiol. 2002;56:187–209.

150. Ghigo JM. Natural conjugative plasmids induce bacterial biofilm development. Nature. 2001;412(6845):442–5.

151. Goller CC, Romeo T. Environmental Influences on Biofilm Development. Curr Top Microbiol Immunol. 2008;322.

152. Wu B, Feng C, Huang L, Lv Z, Xie D, Wei C. Anode-biofilm electron transfer behavior and wastewater treatment under different operational modes of bioelectrochemical system. Bioresour Technol. Elsevier Ltd; 2014;157C:305–9.

153. Liu W-T, Jansson JK. Environmental Molecular Microbiology. Horiz Sci Press. 2010;

154. Surette MG, Miller MB, Bassler BL. Quorum sensing in *Escherichia coli*, *Salmonella typhimurium*, and *Vibrio harveyi*: a new family of genes responsible for autoinducer production. Proc Natl Acad Sci U S A. 1999;96(4):1639–44.

155. Prüß BM, Verma K, Samanta P, Sule P, Kumar S, Wu J, et al. Environmental and genetic factors that contribute to *Escherichia coli* K-12 biofilm formation. Arch Microbiol. 2010;715–28.

156. Murphy TF, Kirkham C. Biofilm formation by nontypeable *Haemophilus influenzae*: strain variability, outer membrane antigen expression and role of pili. BMC Microbiol. 2002;2:7.

157. Klausen M, Heydorn A, Ragas P, Lambertsen L, Aaes-Jorgensen A, Molin S, et al. Biofilm formation by *Pseudomonas aeruginosa* wild type, flagella and type IV pili mutants. Mol Microbiol. 2003;48(6):1511–24.

158. Davey ME, O'toole GA. Microbial biofilms: from ecology to molecular genetics. Microbiol Mol Biol Rev. 2000;64(4):847–67.

159. Heilmann C, Hussain M, Peters G, Götz F. Evidence for autolysin-mediated primary attachment of *Staphylococcus epidermidis* to a polystyrene surface. Mol Microbiol. 1997;24(5):1013–24.

160. Gooding JR, May AL, Hilliard KR, Campagna SR. Establishing a Quantitative Definition of Quorum Sensing Provides Insight into the Information Content of the Autoinducer Signals in *Vibrio harveyi* and *Escherichia coli*. Biochemistry. 2010;5621–3.

161. Padera RF. Infection in ventricular assist devices: the role of biofilm. Cardiovasc Pathol. 2006;15(5):264–70.

162. Beloin C, Ghigo J-M. Finding gene-expression patterns in bacterial biofilms. Trends Microbiol. 2005;13(1):16–9.

163. Sponza DT. Investigation of extracellular polymer substances (EPS) and physicochemical properties of different activated sludge flocs under steady-state conditions. Enzyme Microb Technol. 2003;32(3-4):375–85.

164. Mukherjee J, Ow SY, Noirel J, Biggs CA. Quantitative protein expression and cell surface characteristics of *Escherichia coli* MG1655 biofilms. Proteomics. 2011;11(3):339–51.

165. Wood TK. Insights on *Escherichia coli* biofilm formation and inhibition from whole-transcriptome profiling. Environ Microbiol. 2009;11(1):1–15.

166. Domka J, Lee J, Bansal T, Wood TK. Temporal gene-expression in *Escherichia coli* K-12 biofilms. Environ Microbiol. 2007;9(2):332–46.

167. Ren D, Bedzyk LA, Thomas SM, Ye RW, Wood TK. Gene expression in *Escherichia coli* biofilms. Appl Microbiol Biotechnol. 2004;64(4):515–24.

168. Jose J. Autodisplay: efficient bacterial surface display of recombinant proteins. Appl Microbiol Biotechnol. 2006;69(6):607–14.

169. Fishilevich S, Amir L, Fridman Y, Aharoni A, Alfonta L. Surface display of redox enzymes in microbial fuel cells. J Am Chem Soc. 2009;131(34):12052–3.

170. Zhang T, Cui C, Chen S, Ai X, Yang H, Shen P, et al. A novel mediatorless microbial fuel cell based on direct biocatalysis of Escherichia coli. Chem Commun. 2006;(21):2257.

171. Xing D, Zuo Y, Cheng S, Regan JM, Logan BE. Electricity generation by *Rhodopseudomonas palustris* DX-1. Environ Sci Technol. 2008;42(11):4146–51.

172. Yadav VG, Stephanopoulos G. Reevaluating synthesis by biology. Curr Opin Microbiol. Elsevier Ltd; 2010;13(3):371–6.

173. Bailey JE. Toward a science of metabolic engineering. Science. 1991;252(5013):1668–75.

174. Stephanopoulos G, Sinskey AJ. Metabolic engineering--methodologies and future prospects. Trends Biotechnol. 1993;11(9):392–6.

175. Windass JD, Worsey MJ, Pioli EM, Pioli D, Barth PT, Atherton KT, et al. Improved conversion of methanol to single-cell protein by *Methylophilus methylotrophus*. Nature. 1980;287.

176. Cameron DC, Tong I-T. Cellular and metabolic engineering. Appl Biochem Biotechnol. 1993;38.

177. Blattner F, Plunkett G, Bloch C, Perna N. The complete genome sequence of *Escherichia coli* K-12. Science (80). 1997;277:1453–74.

178. Lukjancenko O, Wassenaar TM, Ussery DW. Comparison of 61 sequenced *Escherichia coli* genomes. Microb Ecol. 2010;60(4):708–20.

179. ScarabGenomics. Rationally Designed *E . coli* Genome : A Platform for Improved DNA and Protein Production. 2010;

180. Kolisnychenko V, Iii GP, Herring CD, Fehér T, Pósfai J, Blattner FR, et al. Engineering a Reduced *Escherichia coli* Genome. Genome Res. 2002;640–7.

181. Dworkin M, Falkow S, Rosenberg E, Schleifer K-H. The Prokaryotes: Ecophysiology and biochemistry. Springer. 2006;Third Edit.

182. Zellner G, Neudorfer F, Diekmann H. Degradation of lactate by an anaerobic mixed culture in a fluidized-bed reactor. Water Res. 1994;28(6):1337–40.

183. Zhou Y, Nambou K, Wei L, Cao J, Imanaka T, Hua Q. Lycopene production in recombinant strains of *Escherichia coli* is improved by knockout of the central carbon metabolism gene coding for glucose-6-phosphate dehydrogenase. Biotechnol Lett. 2013;35(12):2137–45.

184. Chen Y-Y, Shen H-J, Cui Y-Y, Chen S-G, Weng Z-M, Zhao M, et al. Chromosomal evolution of *Escherichia coli* for the efficient production of lycopene. BMC Biotechnol. BMC Biotechnology; 2013;13(1):6.

185. Mao L, Verwoerd W. Selection of organisms for systems biology study of microbial electricity generation: a review. Int J Energy Environ Eng. 2013;4(17):1–18.

186. Mao L, Verwoerd WS. Model-driven elucidation of the inherent capacity of Geobacter sulfurreducens for electricity generation. J Biol Eng. Journal of Biological Engineering; 2013;7(1):14.

187. Pinchuk GE, Hill EA, Geydebrekht O V, De Ingeniis J, Zhang X, Osterman A, et al. Constraint-based model of *Shewanella oneidensis* MR-1 metabolism: a tool for data analysis and hypothesis generation. PLoS Comput Biol. 2010;6(6):e1000822.

188. Potter LC, Cole JA. periplasmic nitrate reduction by *Escherichia coli* K-12. Society. 1999;76:69–76.

189. Fonseca BM, Paquete CM, Neto SE, Pacheco I, Soares CM, Louro RO. Mind the gap: cytochrome interactions reveal electron pathways across the periplasm of *Shewanella oneidensis* MR-1. Biochem J. 2013;449(1):101–8.

190. Unden G, Bongaerts J. Alternative respiratory pathways of *Escherichia coli*: energetics and transcriptional regulation in response to electron acceptors. Biochim Biophys Acta. 1997;1320(3):217–34.

191. Sauer U, Heinemann M, Zamboni N. Getting Closer to the Whole Picture. Science (80). 2007;(5).

192. Bailey JE, Sburlati A, Hatzimanikatis V, Lee K, Renner WA, Tsai PS. Inverse metabolic engineering: a strategy for directed genetic engineering of useful phenotypes. Biotechnol Bioeng. 1996;79(5):568–79.

193. Gill RT, Dodge T. Special issue on inverse metabolic engineering. Metab Eng. 2004;6(3):175–6.

194. Gill RT, Wildt S, Yang YT, Ziesman S, Stephanopoulos G. Genome-wide screening for trait conferring genes using DNA microarrays. Proc Natl Acad Sci U S A. 2002;99(10):7033–8.

195. Gill RT. Enabling inverse metabolic engineering through genomics. Curr Opin Biotechnol. 2003;14(5):484–90.

196. Saerens SMG, Duong CT, Nevoigt E. Genetic improvement of brewer's yeast: current state, perspectives and limits. Appl Microbiol Biotechnol. 2010;86(5):1195–212.

197. Borden JR, Papoutsakis ET. Dynamics of genomic-library enrichment and identification of solvent tolerance genes for *Clostridium acetobutylicum*. Appl Environ Microbiol. 2007;73(9):3061–8.

198. Welch M, Villalobos A, Gustafsson C, Minshull J. You're one in a googol: optimizing genes for protein expression. J R Soc Interface. 2009 Aug 6;6 Suppl 4:S467–76.

199. Welch M, Govindarajan S, Ness JE, Villalobos A, Gurney A, Minshull J, et al. Design parameters to control synthetic gene expression in *Escherichia coli*. PLoS One. 2009;4(9):e7002.

200. Dubnau D, Losick R. Bistability in bacteria. Mol Microbiol. 2006;61(3):564–72.

201. Tirumalai RS, Chan KC, Prieto DA, Issaq HJ, Conrads TP, Veenstra TD. Characterization of the low molecular weight human serum proteome. Mol Cell Proteomics. 2003;2(10):1096–103.

202. Ong S-E, Blagoev B, Kratchmarova I, Kristensen DB, Steen H, Pandey A, et al. Stable Isotope Labeling by Amino Acids in Cell Culture, SILAC, as a Simple and Accurate Approach to Expression Proteomics. Mol Cell Proteomics. 2002;1(5):376–86.

203. Ross PL, Huang YN, Marchese JN, Williamson B, Parker K, Hattan S, et al. Multiplexed protein quantitation in *Saccharomyces cerevisiae* using amine-reactive isobaric tagging reagents. Mol Cell Proteomics. 2004;3(12):1154–69.

204. Chong P, Gan C. Isobaric tags for relative and absolute quantitation (iTRAQ) reproducibility: Implication of multiple injections. Journal of proteome Res. 2006;1232–40.

205. Zieske LR. A perspective on the use of iTRAQ reagent technology for protein complex and profiling studies. J Exp Bot. 2006;57(7):1501–8.

206. Allen JW, Leach N, Ferguson SJ. The histidine of the c-type cytochrome CXXCH haem-binding motif is essential for haem attachment by the *Escherichia coli* cytochrome c maturation (Ccm) apparatus. Biochem J. 2005;389(Pt 2):587–92.

207. Wagner S, Baars L, Ytterberg AJ, Klussmeier A, Wagner CS, Nord O, et al. Consequences of membrane protein overexpression in *Escherichia coli.* Mol Cell Proteomics. 2007;6(9):1527–50.

208. Babu M, Kagan O, Guo H, Greenblatt J, Emili A. Identification of protein complexes in *Escherichia coli* using sequential peptide affinity purification in combination with tandem mass spectrometry. J Vis Exp. 2012;(69):3–9.

209. Bryksin A V, Matsumura I. Overlap extension PCR cloning: a simple and reliable way to create recombinant plasmids. Biotechniques. 2010;48(6):463–5.

210. Datsenko KA, Wanner BL. One-step inactivation of chromosomal genes in *Escherichia coli* K-12 using PCR products. Proc Natl Acad Sci USA. 2000;97(12):6640–5.

211. Greenman J, Spencer PS, C M. In vitro biofilm model to study hydrogen sulphide production. J Dent Res. 2002;81.

212. Ledezma P, Greenman J, Ieropoulos I. Maximising electricity production by controlling the biofilm specific growth rate in microbial fuel cells. Bioresour Technol; 2012;118:615–8.

213. Pham TK, Roy S, Noirel J, Douglas I, Wright PC, Stafford GP. A quantitative proteomic analysis of biofilm adaptation by the periodontal pathogen *Tannerella forsythia*. Proteomics. 2010;10(17):3130–41.

214. Pham TK, Sierocinski P, van der Oost J, Wright PC. Quantitative proteomic analysis of *Sulfolobus solfataricus* membrane proteins. J Proteome Res. 2010;9(2):1165–72.

215. Pereira-Medrano AG, Knighton M, Fowler GJS, Ler ZY, Pham TK, Ow SY, et al. Quantitative proteomic analysis of the exoelectrogenic bacterium *Arcobacter butzleri* ED-1 reveals increased abundance of a flagellin protein under anaerobic growth on an insoluble electrode. J Proteomics; 2012;

216. Fischer F, Wolters D, Rögner M, Poetsch A. Toward the complete membrane proteome: high coverage of integral membrane proteins through transmembrane peptide detection. Mol Cell Proteomics. 2006;5(3):444–53.

217. Mckenzie GJ, Craig NL. Fast , easy and efficient : site-specific insertion of transgenes into Enterobacterial chromosomes using Tn7 without need for selection of the insertion event. BMC Microbiol. 2006;7:1–7.

218. Jittawuttipoka T. Mini Tn7 vectors as genetic tools for gene cloning at a single copy number in an industrially important and phytopathogenic bacteria, Xanthomonas spp. FEMS Microbiol Lett. 2009;298(1):111–7.

219. Sibley MH, Raleigh EA. A versatile element for gene addition in bacterial chromosomes. Nucleic Acids Res. 2012 Feb;40(3).

220. Zeghouf M, Li J, Butland G. Sequential Peptide Affinity (SPA) system for the identification of mammalian and bacterial protein complexes. J Proteome Res. 2004;3:463–8.

221. Finehout EJ, Cantor JR, Lee KH. Kinetic characterization of sequencing grade modified trypsin. Proteomics.2005;5(9):2319–21.

222. Anderson L, Hunter CL. Quantitative mass spectrometric multiple reaction monitoring assays for major plasma proteins. Mol Cell Proteomics. 2006;5(4):573–88.

223. Ow SY, Noirel J, Salim M, Evans C, Watson R, Wright PC. Balancing robust quantification and identification for iTRAQ: application of UHR-ToF MS. Proteomics. 2010;10(11):2205–13.

224. Colinge J, Masselot A, Giron M, Dessingy T, Magnin J. OLAV: towards high-throughput tandem mass spectrometry data identification. Proteomics. 2003;3(8):1454–63.

225. Elias JE, Gygi SP. Target-decoy search strategy for increased confidence in large-scale protein identifications by mass spectrometry. Nat Methods. 2007;4.

226. Elias JE, Haas W, Faherty BK, Gygi SP. Comparative evaluation of mass spectrometry platforms used in large-scale proteomics investigations. Nat Methods. 2005;2(9):667–75.

227. Moser DP, Nealson KH. Growth of the facultative anaerobe *Shewanella putrefaciens* by elemental sulfur reduction. Appl Environ Microbiol. 1996;62(6):2100–5.

228. Ieropoulos I, Winfield J, Greenman J, Melhuish C. Small scale microbial fuel cells and different ways of reporting output. ECS Trans. 2010;28(9):1–9.

229. Carmona-Martínez AA, Harnisch F, Kuhlicke U, Neu TR, Schröder U. Electron transfer and biofilm formation of *Shewanella putrefaciens* as function of anode potential. Bioelectrochemistry.2012.

230. Pereira-Medrano AG, Knighton M, Fowler GJS, Ler ZY, Pham TK, Ow SY, et al. Quantitative proteomic analysis of the exoelectrogenic bacterium *Arcobacter butzleri* ED-1 reveals increased abundance of a flagellin protein under anaerobic growth on an insoluble electrode. J Proteomics.2013;78:197–210.

231. Sambrook J, Russell DW. Molecular Cloning: A Laboratory Manual. Cold Spring Harbor Laboratory Press;

232. Park DH, Zeikus JG. Electricity generation in microbial fuel cells using neutral red as an electronophore. Appl Environ Microbiol. 2000;66(4):1292–7.

233. Rabaey I, Ossieur W, Verhaege M, Verstraete W. Continuous microbial fuel cells convert carbohydrates to electricity. Water Sci Technol. 2005;52(1-2):515–23.

234. Kiely PD, Cusick R, Call DF, Selembo PA, Regan JM, Logan BE. Anode microbial communities produced by changing from microbial fuel cell to microbial electrolysis cell operation using two different wastewaters. Bioresour Technol.; 2011;102(1):388–94.

235. Kim BH, Park HS, Kim HJ, Kim GT, Chang IS, Lee J, et al. Enrichment of microbial community generating electricity using a fuel-cell-type electrochemical cell. Appl Microbiol Biotechnol. 2004;63(6):672–81.

236. Izallalen M, Mahadevan R, Burgard A, Postier B, Didonato R, Sun J, et al. *Geobacter sulfurreducens* strain engineered for increased rates of respiration. Metab Eng. 2008;10(5):267–75.

237. Ross DE, Ruebush SS, Brantley SL, Hartshorne RS, Clarke TA, Richardson DJ, et al. Characterization of protein-protein interactions involved in iron reduction by *Shewanella oneidensis* MR-1. Appl Environ Microbiol. 2007;73(18):5797–808.

238. Cordova CD, Schicklberger MFR, Yu Y, Spormann AM. Partial functional replacement of CymA by SirCD in *Shewanella oneidensis* MR-1. J Bacteriol. 2011;193(9):2312–21.

239. Coursolle D, Gralnick JA. Modularity of the Mtr respiratory pathway of *Shewanella oneidensis* strain MR-1. Mol Microbiol. 2010;77:995–1008.

240. Malvankar NS, Vargas M, Nevin KP, Franks AE, Leang C, Kim B-C, et al. Tunable metallic-like conductivity in microbial nanowire networks. Nat Nanotech. 2011;6:573–9.

241. Leang C, Qian X, Mester T, Lovley DR. Alignment of the c-type cytochrome OmcS along pili of *Geobacter sulfurreducens*. Appl Environ Microbiol. 2010;76(12):4080–4.

242. Shi L, Richardson DJ, Wang Z, Kerisit SN, Rosso KM, Zachara JM, et al. The roles of outer membrane cytochromes of *Shewanella* and *Geobacter* in extracellular electron transfer. Environ Microbiol Rep. 2009;1(4):220–7.

243. Shi L, Deng S, Marshall MJ, Wang Z, Kennedy DW, Dohnalkova AC, et al. Direct involvement of type II secretion system in extracellular translocation of *Shewanella oneidensis* outer membrane cytochromes MtrC and OmcA. J Bacteriol. 2008;190(15):5512–6.

244. Durfee T, Nelson R, Baldwin S, Plunkett G, Burland V, Mau B, et al. The complete genome sequence of *Escherichia coli* DH10B: insights into the biology of a laboratory workhorse. J Bacteriol. 2008;190(7):2597–606.

245. Joyce AR, Palsson BØ. The model organism as a system: integrating “omics” data sets. Nat Rev Mol Cell Bio. 2006;7(3):198–210.

246. Vannelli T, Wei Qi W, Sweigard J, Gatenby AA, Sariaslani FS. Production of p-hydroxycinnamic acid from glucose in *Saccharomyces cerevisiae* and *Escherichia coli* by expression of heterologous genes from plants and fungi. Metab Eng. 2007;9(2):142–51.

247. Zhu J, Sánchez A, Bennett GN, San K-Y. Manipulating respiratory levels in *Escherichia coli* for aerobic formation of reduced chemical products. Metab Eng. 2011;13(6):704–12.

248. Pitts K, Dobbin P, Reyes-Ramirez F, AJ. Characterization of the *Shewanella oneidensis* MR-1 decaheme cytochrome MtrA. J Biol Chem. 2003;278(30):27758–65.

249. Donald JW, Hicks MG, Richardson DJ, Palmer T. The *c*-type cytochrome OmcA localizes to the outer membrane upon heterologous expression in *Escherichia coli*. J Bacteriol. 2008;190(14):5127–31.

250. Madden D. The microbial fuel cell : electricity from yeast. Read Univ. 2010;

251. Dyrløv Bendtsen J, Nielsen H, von Heijne G, Brunak S. Improved Prediction of Signal Peptides: SignalP 3.0. J Mol Biol. 2004;340(4):783–95.

252. Thöny-Meyer L, Fischer F, Künzler P, Ritz D, Hennecke H. *Escherichia coli* genes required for cytochrome c maturation. J Bacteriol. 1995;177(15):4321–6.

253. Ringeisen BR, Henderson E, Wu PK, Pietron J, Ray R, Little B, et al. High Power Density from a Miniature Microbial Fuel Cell Using *Shewanella oneidensis* DSP10. Environ Sci Technol. 2006;40(8):2629–34.

254. Kulp A, Kuehn MJ. Biological functions and biogenesis of secreted bacterial outer membrane vesicles. Annu Rev Microbiol. 2010;64:163–84.

255. Johs A, Shi L, Droubay TC, Ankner JF, Liang L. Characterization of the decaheme c-type cytochrome OmcA in solution and on hematite surfaces by small angle x-ray scattering and neutron reflectometry. Biophys J. Biophysical Society; 2010;98(12):3035–43.

256. Baneyx F. Recombinant protein expression in *Escherichia coli*. MBio. Am Soc Microbiol; 2010;1(5).

257. Tabor S, Richardson C. A bacteriophage T7 RNA polymerase/promoter system for controlled exclusive expression of specific genes. Proc Natl Acad Sci. 1985;82:1074–8.

258. Studier FW, Moffatt BA. Use of bacteriophage T7 RNA polymerase to direct selective high-level expression of cloned genes. J Mol Biol. 1986 May 5;189(1):113–30.

259. Kesik-Brodacka M, Romanik A, Mikiewicz-Sygula D, Plucienniczak G, Plucienniczak A. A novel system for stable, high-level expression from the T7 promoter. Microb Cell Fact. Microbial Cell Factories; 2012;11(1):109.

260. Rodionov DA, Novichkov PS, Stavrovskaya ED, Rodionova IA, Li X, Kazanov MD, et al. Comparative genomic reconstruction of transcriptional networks controlling central metabolism in the *Shewanella* genus. BMC Genomics. BioMed Central Ltd; 2011;12 Suppl 1(Suppl 1):S3.

261. Biffinger JC, Pietron J, Bretschger O, Nadeau LJ, Johnson GR, Williams CC, et al. The influence of acidity on microbial fuel cells containing *Shewanella oneidensis*. Biosens Bioelectron. 2008;24(4):906–11.

262. Harris HW, El-Naggar MY, Nealson KH. *Shewanella oneidensis* MR-1 chemotaxis proteins and electron-transport chain components essential for congregation near insoluble electron acceptors. Biochem Soc Trans. 2012;40(6):1167–77.

263. Watson VJ, Logan BE. Power production in MFCs inoculated with *Shewanella oneidensis* MR-1 or mixed cultures. Biotechnol Bioeng. 2010;105(3):489–98.

264. Wu D, Xing D, Lu L, Wei M, Liu B, Ren N. Ferric iron enhances electricity generation by *Shewanella oneidensis* MR-1 in MFCs. Bioresour Technol. 2012;1–5.

265. Richardson DJ, Edwards MJ, White GF, Baiden N, Hartshorne RS, Fredrickson JK, et al. Exploring the biochemistry at the extracellular redox frontier of bacterial mineral Fe(III) respiration. Biochem Soc Trans. 2012;40(3):493–500.

266. Lovley DR. Electromicrobiology. Annu Rev Microbiol. 2012;66:391–409.

267. Coursolle D, Gralnick JA. Reconstruction of Extracellular Respiratory Pathways for Iron(III) Reduction in *Shewanella Oneidensis* Strain MR-1. Front Microbiol. 2012;3:56.

268. Shi L, Rosso KM, Clarke TA, Richardson DJ, Zachara JM, Fredrickson JK. Molecular Underpinnings of Fe(III) Oxide Reduction by *Shewanella Oneidensis* MR-1. Front Microbiol. 2012;3:50.

269. Habermann W, Pommer E-H. Biological fuel cells with sulphide storage capacity. Appl Microbiol Biotechnol. 1991;35:128–33.

270. Fitzgerald LA, Petersen ER, Ray RI, Little BJ, Cooper CJ, Howard EC, et al. *Shewanella oneidensis* MR-1 Msh pilin proteins are involved in extracellular electron transfer in microbial fuel cells. Process Biochem; 2012;47(1):170–4.

271. Rabaey K, Boon N, Höfte M, Verstraete W. Microbial phenazine production enhances electron transfer in biofuel cells. Environ Sci Technol. 2005;39(9):3401–8.

272. Pandhal J, Ow SY, Noirel J, Wright PC. Improving N-glycosylation efficiency in *Escherichia coli* using shotgun proteomics, metabolic network analysis, and selective reaction monitoring. Biotechnol Bioeng. 2011;108(4):902–12.

273. Brown SD, Thompson MR, Verberkmoes NC, Chourey K, Shah M, Zhou J, et al. Molecular dynamics of the *Shewanella oneidensis* response to chromate stress. Mol Cell Proteomics. 2006;5(6):1054–71.

274. Thompson MR, Verberkmoes NC, Chourey K, Shah M, Thompson DK, Hettich RL. Dosage-Dependent Proteome Response of *Shewanella oneidensis* MR-1 to Acute Chromate Challenge research articles. J Proteome Res. 2007;6:1745–57.

275. Wan X, Verberkmoes NC, Mccue LA, Stanek D, Connelly H, Hauser LJ, et al. Transcriptomic and Proteomic Characterization of the Fur Modulon in the Metal-Reducing Bacterium *Shewanella oneidensis*. J Bacteriol. 2004;186(24):8385–400.

276. Yang Y, Harris DP, Luo F, Wu L, Parsons AB, Palumbo A V, et al. Characterization of the *Shewanella oneidensis* Fur gene: roles in iron and acid tolerance response. BMC Genomics. 2008;9 Suppl 1:S11.

277. Brown RN, Romine MF, Schepmoes AA, Smith RD, Lipton MS. Mapping the Subcellular Proteome of *Shewanella oneidensis* MR-1 using Sarkosyl-Based Fractionation and LC-MS / MS Protein Identification research articles. 2010;4454–63.

278. Tang X, Yi W, Munske GR, Adhikari DP, Zakharova NL, Bruce JE. Profiling the membrane proteome of *Shewanella oneidensis* MR-1 with new affinity labeling probes. J Proteome Res. 2007;6(2):724–34.

279. Gao H, Wang X, Yang ZK, Palzkill T, Zhou J. Probing regulon of ArcA in *Shewanella oneidensis* MR-1 by integrated genomic analyses. BMC Genomics. 2008;9(Iii):42.

280. Cao B, Shi L, Brown RN, Xiong Y, Fredrickson JK, Romine MF, et al. Extracellular polymeric substances from *Shewanella* sp. HRCR-1 biofilms: characterization by infrared spectroscopy and proteomics. Environ Microbiol. 2011;13(4):1018–31.

281. Rosenbaum M, Bar HY, Beg QK, Segrè D, Booth J, Cotta M a, et al. Transcriptional Analysis of *Shewanella oneidensis* MR-1 with an Electrode Compared to Fe(III)Citrate or Oxygen as Terminal Electron Acceptor. PLoS One. 2012;7(2):e30827.

282. Hartshorne RS, Reardon CL, Ross DE, Nuester J, Clarke TA, Gates AJ, et al. Characterization of an electron conduit between bacteria and the extracellular environment. Proc Natl Acad Sci U S A. 2009;106(52):22169–74.

283. Ow SY, Salim M, Noirel J, Evans C, Rehman I, Wright PC. iTRAQ Underestimation in Simple and Complex Mixtures : " The Good , the Bad and the Ugly ." J Proteome Res. 2009;5347–55.

284. Coursolle D, Baron DB, Bond DR, Gralnick JA. The Mtr Respiratory Pathway is Essential for Reducing Flavins and Electrodes in *Shewanella oneidensis*. Microbiology. 2009:612–26.

285. Keshamouni VG, Michailidis G, Grasso CS, Anthwal S, Strahler JR, Walker A, et al. Differential Protein Expression Profiling by iTRAQ-2DLC-MS / MS of Lung Cancer Cells Undergoing Epithelial-Mesenchymal Transition Reveals a Migratory / Invasive Phenotype. J Proteome Res. 2006;1143–54.

286. Glen A, Gan CS, Hamdy FC, Eaton CL, Cross SS, Catto JWF, et al. iTRAQ-Facilitated Proteomic Analysis of Human Prostate Cancer Cells Identifies Proteins Associated with Progression. J Proteome Res. 2008;7:897–907.

287. Bantscheff M, Boesche M, Eberhard D, Matthieson T, Sweetman G, Kuster B. Robust and sensitive iTRAQ quantification on an LTQ Orbitrap mass spectrometer. Mol Cell Proteomics. 2008;7(9):1702–13.

288. Karp N, Huber W, Sadowski P, Charles PD, Hester S V, Lilley KS. Addressing accuracy and precision issues in iTRAQ quantitation. Mol Cell Proteomics.2010;1885–97.

289. Evans C, Noirel J, Ow SY, Salim M, Pereira-Medrano AG, Couto N, et al. An insight into iTRAQ: where do we stand now? Anal Bioanal Chem. 2012.

290. Ring G, Eichler J. In the Archaea *Haloferax volcanii*, membrane protein biogenesis and protein synthesis rates are affected by decreased ribosomal binding to the translocon. J Biol Chem. 2004;279(51):53160–6.

291. Zhang Y. I-TASSER server for protein 3D structure prediction. BMC Bioinformatics. 2008;9:40.

292. Shyu JBH, Lies DP, Newman DK. Protective Role of tolC in Efflux of the Electron Shuttle Protective Role of tolC in Efflux of the Electron Shuttle. J Bacteriol. 2002;184(6):1806–10.

293. Vega DE, Young KD. Accumulation of periplasmic enterobactin impairs the growth and morphology of *Escherichia coli* tolC mutants. Mol Microbiol. 2014;91(3):508–21.

294. Bleuel C, Große C, Taudte N, Scherer J, Wesenberg D, Krauß GJ, et al. TolC Is Involved in Enterobactin Efflux across the Outer Membrane of *Escherichia coli*. J Bacteriol. 2005;187(19):6701–7.

295. Kim B-C, Postier BL, Didonato RJ, Chaudhuri SK, Nevin KP, Lovley DR. Insights into genes involved in electricity generation in *Geobacter sulfurreducens* via whole genome microarray analysis of the OmcF-deficient mutant. Bioelectrochemistry. 2008;73(1):70–5.

296. Zhao Q, Poole K. A second tonB gene in *Pseudomonas aeruginosa* is linked to the exbB and exbD genes. FEMS Microbiol Lett. 2000;184(1):127–32.

297. Seliger SS, Mey AR, Valle AM, Payne SM. The two TonB systems of *Vibrio cholerae*: redundant and specific functions. Mol Microbiol. 2001;39(3):801–12.

298. Stork M, Lorenzo M Di, Mourin S, Osorio CR, Lemos ML, Crosa JH. Two tonB Systems Function in Iron Transport in *Vibrio anguillarum*, but Only One Is Essential for Virulence. Infect Immun. 2004;72(12):7326–9.

299. Wang Q, Liu Q, Cao X, Yang M, Zhang Y. Characterization of two TonB systems in marine fish pathogen *Vibrio alginolyticus*: their roles in iron utilization and virulence. Arch Microbiol. 2008;190(5):595–603.

300. Kustusch RJ, Kuehl CJ, Crosa JH. The ttpC gene is contained in two of three TonB systems in the human pathogen *Vibrio vulnificus*, but only one is active in iron transport and virulence. J Bacteriol. 2012;194(12):3250–9.

301. Stork M, Otto BR, Crosa JH. A novel protein, TtpC, is a required component of the TonB2 complex for specific iron transport in the pathogens *Vibrio anguillarum* and *Vibrio cholerae*. J Bacteriol. 2007;189(5):1803–15.

302. Lopez C, Peacock R, Crosa J, Vogel H. Molecular characterization of the TonB2 protein from the fish pathogen *Vibrio anguillarum*. Biochem J. 2009;418(1):49–59.

303. Hider RC, Kong X. Chemistry and biology of siderophores. Nat Prod Rep. 2010;27(5):637–57.

304. Neilands JB. Siderophores: Structure and Function of Microbial Iron Transport Compounds. J Biol Chem. 1995;270(45):26723–6.

305. Kuehl CJ, Crosa JH. Molecular and genetic characterization of the TonB2-cluster TtpC protein in pathogenic *vibrios*. Biometals. 2009;22(1):109–15.

306. Shi L, Chen B, Wang Z, Elias DA, Mayer MU, Gorby YA, et al. Isolation of a high-affinity functional protein complex between OmcA and MtrC: Two outer membrane decaheme c-type cytochromes of *Shewanella oneidensis* MR-1. J Bacteriol. 2006;188(13):4705–14.

307. Cascales E, Lloubès R, Sturgis JN. The TolQ-TolR proteins energize TolA and share homologies with the flagellar motor proteins MotA-MotB. Mol Microbiol. 2001;42(3):795–807.

308. Roy A, Kucukural A, Zhang Y. I-TASSER: a unified platform for automated protein structure and function prediction. Nat Protoc. Nature Publishing Group; 2010;5(4):725–38.

309. Orme R, Douglas CWI, Rimmer S, Webb M. Proteomic analysis of *Escherichia coli* biofilms reveals the overexpression of the outer membrane protein OmpA. Proteomics. 2006;6(15):4269–77.

310. Song T, Mika F, Lindmark B, Liu Z, Schild S, Bishop A, et al. A new *Vibrio cholerae* sRNA modulates colonization and affects release of outer membrane vesicles. Mol Microbiol. 2008;70(1):100–11.

311. Sonntag I, Schwarz H, Hirota Y, Henning U. Cell Envelope and Shape of *Escherichia coli*: Multiple Mutants Missing the Outer Membrane Lipoprotein and Other Major Outer Membrane Proteins Lpp-. J Bacteriol. 1978;136(1):280–5.

312. Hirashima A, Wang S, Inouye M. Cell-free synthesis of a specific lipoprotein of the *Escherichia coli* outer membrane directed by purified messenger RNA. Proc Natl Acad Sci U S A. 1974;71(10):4149–53.

313. Cowles C, Li Y, Semmelhack MF, Cristea IM, Silhavy TJ. The free and bound forms of Lpp occupy distinct subcellular locations in *Escherichia coli*. Mol Microbiol. 2011;79(5):1168–81.

314. Patil SA, Gorecki K, Hagerhall C, Gorton L. Cisplatin-induced elongation of *Shewanella oneidensis* MR-1 cells improves microbe-electrode interactions for use in microbial fuel cells. Energy Environ Sci. The Royal Society of Chemistry; 2013;6(9):2626–30.

315. Coursolle D, Baron DB, Bond DR, Gralnick JA. The Mtr respiratory pathway is essential for reducing flavins and electrodes in *Shewanella oneidensis*. J Bacteriol. 2010;192(2):467–74.

316. Covington ED, Gelbmann CB, Kotloski NJ, Gralnick JA. An essential role for UshA in processing of extracellular flavin electron shuttles by *Shewanella oneidensis*. Mol Microbiol. 2010 Oct;78(2):519–32.

317. Beliaev A, Thompson D. Gene and protein expression profiles of *Shewanella oneidensis* during anaerobic growth with different electron acceptors. Omi A J Integr Biol. 2002;6(1).

318. Beliaev A, Thompson D, Fields M. Microarray transcription profiling of a *Shewanella oneidensis* etrA mutant. J Bacteriol. 2002;184(16):4612–6.

319. Myers CR, Myers JM. Ferric reductase is associated with the membranes of anaerobically grown *Shewanella putrefaciens* MR-1. FEMS Microbiol Lett; 1993;108(1):15–22.

320. Chourey K, Thompson MR, Morrell-Falvey J, Verberkmoes NC, Brown SD, Shah M, et al. Global molecular and morphological effects of 24-hour chromium(VI) exposure on *Shewanella oneidensis* MR-1. Appl Environ Microbiol. 2006;72(9):6331–44.

321. Cruz-Garcia C, Murray AE, Rodrigues JLM, Gralnick JA, McCue LA, Romine MF, et al. Fnr (EtrA) acts as a fine-tuning regulator of anaerobic metabolism in *Shewanella oneidensis* MR-1. BMC Microbiol. 2011;11(1):64.

322. De Vriendt K, Theunissen S, Carpentier W, De Smet L, Devreese B, Van Beeumen J. Proteomics of *Shewanella oneidensis* MR-1 biofilm reveals differentially expressed proteins, including AggA and RibB. Proteomics. 2005;5(5):1308–16.

323. De Windt W, Gao H, Krömer W, Van Damme P, Dick J, Mast J, et al. AggA is required for aggregation and increased biofilm formation of a hyper-aggregating mutant of *Shewanella oneidensis* MR-1. Microbiology. 2006;152(Pt 3):721–9.

324. Elias DA, Tollaksen SL, Kennedy DW, Mottaz HM, Giometti CS, McLean JS, et al. The influence of cultivation methods on *Shewanella oneidensis* physiology and proteome expression. Arch Microbiol. 2008;189(4):313–24.

325. Fang R, Elias DA, Monroe ME, Shen Y, McIntosh M, Wang P, et al. Differential label-free quantitative proteomic analysis of *Shewanella oneidensis* cultured under aerobic and suboxic conditions by accurate mass and time tag approach. Mol Cell Proteomics. 2006;5(4):714–25.

326. Gao H, Yang ZK, Wu L, Thompson DK, Zhou J. Global transcriptome analysis of the cold shock response of *Shewanella oneidensis* MR-1 and mutational analysis of its classical cold shock proteins. J Bacteriol. 2006;188(12):4560–9.

327. Gödeke J, Binnenkade L, Thormann KM. Transcriptome analysis of early surface-associated growth of *Shewanella oneidensis* MR-1. PLoS One. 2012;7(7):e42160.

328. Leaphart A, Thompson D, Huang K. Transcriptome profiling of *Shewanella oneidensis* gene expression following exposure to acidic and alkaline pH. J Bacteriol. 2006;188(4):1633–42.

329. Liang Y, Gao H, Guo X, Chen J, Qiu G, He Z, et al. Transcriptome analysis of pellicle formation of *Shewanella oneidensis*. Arch Microbiol. 2012

330. Liu Y, Gao W, Wang Y, Wu L, Liu X, Yan T, et al. Transcriptome Analysis of *Shewanella oneidensis* MR-1 in Response to Elevated Salt Conditions. Society. 2005;187(7):2501–7.

331. McLean JS, Pinchuk GE, Geydebrekht O V, Bilskis CL, Zakrajsek B a, Hill E a, et al. Oxygen-dependent autoaggregation in *Shewanella oneidensis* MR-1. Environ Microbiol. 2008;10(7):1861–76.

332. Ruebush S, Brantley S, Tien M. Reduction of soluble and insoluble iron forms by membrane fractions of *Shewanella oneidensis* grown under aerobic and anaerobic conditions. Appl Environ Microbiol. 2006;72(4):2925–35.

333. Thompson M. Dosage-dependent proteome response of *Shewanella oneidensis* MR-1 to acute chromate challenge. J Proteome Res. 2007;1745–57.

334. Vanrobaeys F, Devreese B, Lecocq E, Rychlewski L, De Smet L, Van Beeumen J. Proteomics of the dissimilatory iron-reducing bacterium *Shewanella oneidensis* MR-1, using a matrix-assisted laser desorption/ionization-tandem-time of flight mass spectrometer. Proteomics. 2003;3(11):2249–57.

335. Wang B, Xu M, Sun G. Comparative analysis of membranous proteomics of *Shewanella decolorationis* S12 grown with azo compound or Fe (III) citrate as sole terminal electron acceptor. Appl Microbiol Biotechnol. 2010;86(5):1513–23.

336. Rosenbaum M, Bar HY, Beg QK, Segrè D, Booth J, Cotta M a, et al. Transcriptional analysis of *Shewanella oneidensis* MR-1 with an electrode compared to Fe(III)citrate or oxygen as terminal electron acceptor. PLoS One. 2012;7(2):e30827.

337. Nie L, Wu G, Zhang W. Correlation of mRNA expression and protein abundance affected by multiple sequence features related to translational efficiency in *Desulfovibrio vulgaris*: a quantitative analysis. Genetics. 2006;174(4):2229–43.

338. Guo Y, Xiao P, Lei S, Deng F, Xiao GG, Liu Y, et al. How is mRNA expression predictive for protein expression? A correlation study on human circulating monocytes. Acta Biochim Biophys Sin (Shanghai). 2008;40(5):426–36.

339. Ross DE, Brantley SL, Tien M. Kinetic characterization of OmcA and MtrC, terminal reductases involved in respiratory electron transfer for dissimilatory iron reduction in *Shewanella oneidensis* MR-1. Appl Environ Microbiol. 2009;75(16):5218–26.

340. Higgs PI, Myers PS, Postle K. Interactions in the TonB-dependent energy transduction complex: ExbB and ExbD form homomultimers. J Bacteriol. 1998;180(22):6031–8.

341. Bücking C, Piepenbrock A, Kappler A, Gescher JS. Outer-membrane cytochrome-independent reduction of extracellular electron acceptors in *Shewanella oneidensis*. Microbiology. 2012;158(Pt 8):2144–57.

342. Qian Y, Shi L, Tien M. SO2907, a putative TonB-dependent receptor, is involved in dissimilatory iron reduction by *Shewanella oneidensis* strain MR-1. J Biol Chem. 2011;286(39):33973–80.

343. Rozkov A, Avignone-Rossa CA, Ertl PF, Jones P, O'Kennedy RD, Smith JJ, et al. Characterization of the metabolic burden on *Escherichia coli* DH1 cells imposed by the presence of a plasmid containing a gene therapy sequence. Biotechnol Bioeng. 2004;88(7):909–15.

344. Yadav VG, De Mey M, Giaw Lim C, Kumaran Ajikumar P, Stephanopoulos G. The future of metabolic engineering and synthetic biology: Towards a systematic practice. Metab Eng. Elsevier; 2012;14(3):233–41.

345. Ow D, Nissom P, Philp R, Oh S, Yap M. Global transcriptional analysis of metabolic burden due to plasmid maintenance in *Escherichia coli* DH5α during batch fermentation. Enzyme Microb Technol. 2006;39(3):391–8.

346. Bentley WE, Mirjalili N, Andersen DC, Davis RH, Kompala DS. Plasmid-encoded protein: the principal factor in the "metabolic burden" associated with recombinant bacteria. Biotechnology Bioengineering, 1990. Biotechnol Bioeng. 2009;102(5):1284–97; discussion 1283.

347. Jones KL, Kim SW, Keasling JD. Low-copy plasmids can perform as well as or better than high-copy plasmids for metabolic engineering of bacteria. Metab Eng. 2000;2(4):328–38.

348. Olson P, Zhang Y, Olsen D, Owens A, Cohen P, Nguyen K, et al. High-level expression of eukaryotic polypeptides from bacterial chromosomes. Protein Expr Purif. 1998;14(2):160–6.

349. Keseler IM, Collado-Vides J, Santos-Zavaleta A, Peralta-Gil M, Gama-Castro S, Muñiz-Rascado L, et al. EcoCyc: a comprehensive database of *Escherichia coli* biology. Nucleic Acids Res. 2011;39:D583–90.

350. Keseler IM, Mackie A, Peralta-Gil M, Santos-Zavaleta A, Gama-Castro S, Bonavides-Martínez C, et al. EcoCyc: fusing model organism databases with systems biology. Nucleic Acids Res. 2013;41(Database issue):D605–12.

351. Fields S, Sciences G. The paradox of model organisms. EMBO Rep. 2008;9(8):717–20.

352. Wang Y, Pfeifer BA. 6-deoxyerythronolide B production through chromosomal localization of the deoxyerythronolide B synthase genes in *E. coli*. Metab Eng. 2008;10(1):33–8.

353. York D, Welch K, Goryshin IY, Reznikoff WS. Simple and efficient generation in vitro of nested deletions and inversions: Tn5 intramolecular transposition. Nucleic Acids Res. 1998;26(8):1927–33.

354. De Lorenzo V, Herrero M, Jakubzik U, Timmis KN. Mini-Tn5 transposon derivatives for insertion mutagenesis, promoter probing, and chromosomal insertion of cloned DNA in gram-negative eubacteria. J Bacteriol. 1990;172(11):6568–72.

355. Mosberg JA, Lajoie MJ, Church GM. Lambda red recombineering in *Escherichia coli* occurs through a fully single-stranded intermediate. Genetics. 2010;186(3):791–9.

356. Sharan S, Thomason L, Kuznetsov S, Court D. Recombineering: a homologous recombination-based method of genetic engineering. Nat Protoc. 2009;4(2):206–23.

357. Baba T, Ara T, Hasegawa M, Takai Y, Okumura Y, Baba M, et al. Construction of *Escherichia coli* K-12 in-frame, single-gene knockout mutants: the Keio collection. Mol Syst Biol. 2006;2:2006.0008.

358. Cherepanov PP, Wackernagel W. Gene disruption in *Escherichia coli*: TcR and KmR cassettes with the option of Flp-catalyzed excision of the antibiotic-resistance determinant. Gene. 1995;158(1):9–14.

359. Murphy KC. Use of bacteriophage lambda recombination functions to promote gene replacement in *Escherichia coli*. J Bacteriol. 1998;180(8):2063–71.

360. Parks A, Peters J. Tn7 elements: engendering diversity from chromosomes to episomes. Plasmid. 2009;61(1):1–14.

361. Damron FH, McKenney ES, Barbier M, Liechti GW, Schweizer HP, Goldberg JB. Construction of mobilizable mini-Tn7 vectors for bioluminescent detection of gram-negative bacteria and single-copy promoter lux reporter analysis. Appl Environ Microbiol. 2013;79(13):4149–53.

362. Bao Y, Lies D, Fu H, Roberts G. An improved Tn7-based system for the single-copy insertion of cloned genes into chromosomes of gram-negative bacteria. Gene. 1991;109:167–8.

363. Lambertsen L, Sternberg C, Molin S. Mini-Tn7 transposons for site-specific tagging of bacteria with fluorescent proteins. Environ Microbiol. 2004;6(7):726–32.

364. Koch B, Jensen LE, Nybroe O. A panel of Tn7-based vectors for insertion of the gfp marker gene or for delivery of cloned DNA into Gram-negative bacteria at a neutral chromosomal site. J Microbiol Methods. 2001;45(3):187–95.

365. Wada M, Kano Y. Promoters and Autogenous Control of the *Escherichia coli* hupA and hupB Genes. 1990;27–36.

366. Claret L, Rouviere-yaniv J. Regulation of HUa and HUb by CRP and FIS in *Escherichia coli.* Control. 1996;126–39.

367. Price MN, Dehal PS, Arkin AP. Orthologous transcription factors in bacteria have different functions and regulate different genes. PLoS Comput Biol. 2007;3(9):1739–50.

368. Wei Y, Lee J, Richmond C, Frederick R, Rafalski JA, Larossa RA, et al. High-Density Microarray-Mediated Gene Expression Profiling of *Escherichia coli*. J Bacteriol. 2001; 545-56.

369. Guzman LM, Belin D, Carson MJ, Beckwith J. Tight regulation, modulation, and high-level expression by vectors containing the arabinose PBAD promoter. J Bacteriol. 1995;177(14):4121–30.

370. Taylor R, Walker D, McInnes R. *E. coli* host strains significantly affect the quality of small scale plasmid DNA preparations used for sequencing. Nucleic Acids Res. 1993;21(7):1677–8.

371. Copeland MF, Politz MC, Pfleger BF. Application of TALEs, CRISPR/Cas and sRNAs as trans-acting regulators in prokaryotes. Curr Opin Biotechnol. 2014;29C:46–54.

372. Cong L, Ran F, Cox D, Lin S, Barretto R. Multiplex genome engineering using CRISPR/Cas systems. Science (80). 2013;339(6121):819–23.

373. Sander JD, Joung JK. CRISPR-Cas systems for editing, regulating and targeting genomes. Nat Biotechnol.; 2014.

374. Enyeart PJ, Chirieleison SM, Dao MN, Perutka J, Quandt EM, Yao J, et al. Generalized bacterial genome editing using mobile group II introns and Cre-lox. Mol Syst Biol.2013;9(685):685.

375. Nagy A. Cre recombinase: the universal reagent for genome tailoring. Genesis. 2000;26(2):99–109.

376. St-Pierre F, Cui L, Priest D, Endy D, Dodd I, Shearwin K. One-step cloning and chromosomal integration of DNA. ACS Synth Biol. 2013;2:537–41.

377. Wright PC, Jaffe S, Noirel J, Zou X. Opportunities for protein interaction network guided cellular engineering. IUBMB Life. 2013;65(1):17–27.

378. Fields S, Song O. A novel genetic system to detect protein–protein interactions. Nature. 1989;340(6230):245–6.

379. Chien CT, Bartel PL, Sternglanz R, Fields S. The two-hybrid system: a method to identify and clone genes for proteins that interact with a protein of interest. Proc Natl Acad Sci U S A. 1991;88(21):9578–82.

380. Gavin A-C, Aloy P, Grandi P, Krause R, Boesche M, Marzioch M, et al. Proteome survey reveals modularity of the yeast cell machinery. Nature. 2006;440(7084):631–6.

381. Krogan NJ, Cagney G, Yu H, Zhong G, Guo X, Ignatchenko A, et al. Global landscape of protein complexes in the yeast *Saccharomyces cerevisiae*. Nature. 2006;440(7084):637–43.

382. Hurt JA Thibodeau S A, Hirsh AS, Pabo CO, Joung JK. Highly specific zinc finger proteins obtained by directed domain shuffling and cell-based selection. Proc Natl Acad Sci U S A. 2003;100(21):12271–6.

383. Karimova G, Pidoux J, Ullmann A, Ladant D. A bacterial two-hybrid system based on a reconstituted signal transduction pathway. Proc Natl Acad Sci U S A. 1998;95(10):5752–6.

384. Causier B. Studying the interactome with the yeast two-hybrid system and mass spectrometry. Mass Spectrom Rev. 2004;23(5):350–67.

385. Uetz P, Giot L, Cagney G, Mansfield TA, Judson RS, Knight JR, et al. A comprehensive analysis of protein-protein interactions in S*accharomyces cerevisiae*. Nature. 2000;403(6770):623–7.

386. Yu H, Braun P, Yildirim MA, Lemmens I, Venkatesan K, Sahalie J, et al. High-quality binary protein interaction map of the yeast interactome network. Science. 2008;322(5898):104–10.

387. Giot L, Bader JS, Brouwer C, Chaudhuri A, Kuang B, Li Y, et al. A protein interaction map of *Drosophila melanogaster*. Science. 2003;302(5651):1727–36.

388. Rual J-F, Venkatesan K, Hao T, Hirozane-Kishikawa T, Dricot A, Li N, et al. Towards a proteome-scale map of the human protein-protein interaction network. Nature. 2005;437(7062):1173–8.

389. Deane CM, Salwinski L, Xenarios I, Eisenberg D. Protein Interactions: Two Methods for Assessment of the Reliability of High Throughput Observations. Mol Cell Proteomics. 2002;1(5):349–56.

390. Snider J, Kittanakom S, Curak J, Stagljar I. Split-ubiquitin based membrane yeast two-hybrid (MYTH) system: a powerful tool for identifying protein-protein interactions. J Vis Exp. 2010;(36):1–7.

391. Puig O, Caspary F, Rigaut G, Rutz B, Bouveret E, Bragado-Nilsson E, et al. The tandem affinity purification (TAP) method: a general procedure of protein complex purification. Methods. 2001;24(3):218–29.

392. Rigaut G, Shevchenko A, Rutz B, Wilm M. A generic protein purification method for protein complex characterization and proteome exploration. Nat Biotechnol. 1999;17:7–9.

393. Xu X, Song Y, Li Y, Chang J, Zhang H, An L. The tandem affinity purification method: an efficient system for protein complex purification and protein interaction identification. Protein Expr Purif. Elsevier Inc.; 2010;72(2):149–56.

394. Butland G, Li J, Yang W. Interaction network containing conserved and essential protein complexes in *Escherichia coli*. Nature. 2005;433:531–7.

395. Gavin A-C, Bösche M, Krause R, Grandi P, Marzioch M, Bauer A, et al. Functional organization of the yeast proteome by systematic analysis of protein complexes. Nature. 2002;415(6868):141–7.

396. Kiemer L, Cesareni G. Comparative interactomics: comparing apples and pears? Trends Biotechnol. 2007;25(10):448–54.

397. Söderberg O, Gullberg M, Jarvius M, Ridderstrale K, Leuchowius K-J, Jarvius J, et al. Direct observation of individual endogenous protein complexes in situ by proximity ligation. Nat Methods. 2006;3(12):995–1000.

398. Banér J, Nilsson M, Mendel-Hartvig M, Landegren U. Signal amplification of padlock probes by rolling circle replication. Nucleic Acids Res. 1998;26(22):5073–8.

399. Clegg C, Hayes D. Identification of neighbouring proteins in the ribosomes of *Escherichia coli*. A topographical study with the cross-linking reagent dimethyl suberimidate. Eur J Biochem. 1974;42(1):21–8.

400. Suchanek M, Radzikowska A, Thiele C. Photo-leucine and photo-methionine allow identification of protein-protein interactions in living cells. 2005;1–7.

401. Rappsilber J. The beginning of a beautiful friendship: cross-linking/mass spectrometry and modelling of proteins and multi-protein complexes. J Struct Biol. Elsevier Inc.; 2011;173(3):530–40.

402. Stengel F, Aebersold R, Robinson C V. Joining forces: integrating proteomics and cross-linking with the mass spectrometry of intact complexes. Mol Cell Proteomics. 2012;11(3):R111.014027.

403. Sinz A. Investigation of protein-protein interactions in living cells by chemical crosslinking and mass spectrometry. Anal Bioanal Chem. 2010;397(8):3433–40.

404. Müller M, Mentel M, van Hellemond JJ, Henze K, Woehle C, Gould SB, et al. Biochemistry and evolution of anaerobic energy metabolism in eukaryotes. Microbiol Mol Biol Rev. 2012;76(2):444–95.

405. Dudev T, Lim C. Metal binding affinity and selectivity in metalloproteins: insights from computational studies. Annu Rev Biophys. 2008;37(c):97–116.

406. Martínez-Fábregas J, Rubio S, Díaz-Quintana A, Díaz-Moreno I, De la Rosa MÁ. Proteomic tools for the analysis of transient interactions between metalloproteins. FEBS J. 2011;278(9):1401–10.

407. Waldron KJ, Robinson NJ. How do bacterial cells ensure that metalloproteins get the correct metal? Nat Rev Microbiol. 2009;7(1):25–35.

408. Díaz-Moreno I, De la Rosa MÁ. Transient interactions in metalloproteins. FEBS J. 2011;278(9):1381.

409. Bashir Q, Scanu S, Ubbink M. Dynamics in electron transfer protein complexes. FEBS J. 2011;278(9):1391–400.

410. Forner F, Foster LJ, Toppo S. Mass Spectrometry Data Analysis in the Proteomics Era. Current Bioinformatics. 2007. p. 63–93.

411. Heck AJR. Native mass spectrometry: a bridge between interactomics and structural biology. Nat Meth;2008;5(11):927–33.

412. Oeljeklaus S, Meyer HE, Warscheid B. New dimensions in the study of protein complexes using quantitative mass spectrometry. FEBS Lett. Federation of European Biochemical Societies; 2009;583(11):1674–83.

413. Goh WWB, Lee YH, Chung M, Wong L. How advancement in biological network analysis methods empowers proteomics. Proteomics. 2012;12(4-5):550–63.

414. Thelen JJ, Miernyk JA. The proteomic future: where mass spectrometry should be taking us. Biochem J. 2012;444(2):169–81.

415. Hyung S-J, Ruotolo BT. Integrating mass spectrometry of intact protein complexes into structural proteomics. Proteomics. 2012;12(10):1547–64.

416. Zhang H, Tang X, Munske GR, Tolic N, Anderson GA, Bruce JE. Identification of protein-protein interactions and topologies in living cells with chemical cross-linking and mass spectrometry. Mol Cell Proteomics. 2009;8(3):409–20.

417. Zeghouf M, Li J, Butland G. Sequential Peptide Affinity (SPA) system for the identification of mammalian and bacterial protein complexes. J Proteome Res. 2004;463–8.

418. Gibson DG, Young L, Chuang R, Venter JC, Iii CAH, Smith HO. Enzymatic assembly of DNA molecules up to several hundred kilobases. Nat Methods. 2009;6(5):12–6.

419. Lichty JJ, Malecki JL, Agnew HD, Michelson-Horowitz DJ, Tan S. Comparison of affinity tags for protein purification. Protein Expr Purif. 2005;41(1):98–105.

420. Hengen P. Purification of His-Tag fusion proteins from *Escherichia coli*. Trends Biochem Sci. 1995;8–9.

421. Waugh DS. Making the most of affinity tags. Trends Biotechnol. 2005;23(6):316–20.

422. Annaluru N, Muller H, Mitchell LA, Ramalingam S, Stracquadanio G, Richardson SM, et al. Total Synthesis of a Functional Designer Eukaryotic Chromosome. Sci . 2014;

423. Brutinel ED, Gralnick JA. Shuttling happens: soluble flavin mediators of extracellular electron transfer in *Shewanella*. Appl Microbiol Biotechnol. 2012;93(1):41–8.

424. Nevin KP, Lovley DR. Lack of production of electron-shuttling compounds or solubilization of Fe(III) during reduction of insoluble Fe(III) oxide by *Geobacter metallireducens*. Appl Environ Microbiol. 2000;66(5):2248–51.

425. Seoane J, Sin G, Lardon L, Gernaey K V, Smets BF. A new extant respirometric assay to estimate intrinsic growth parameters applied to study plasmid metabolic burden. Biotechnol Bioeng. 2010;105(1):141–9.

426. Heyland J, Blank LM, Schmid A. Quantification of metabolic limitations during recombinant protein production in *Escherichia coli*. J Biotechnol; 2011;155(2):178–84.

427. Tyo KEJ, Ajikumar PK, Stephanopoulos G. Stabilized gene duplication enables long-term selection-free heterologous pathway expression. Nat Biotechnol. 2009;27(8):760–5.

428. Wang H, Wang G, Ling Y, Qian F, Song Y et al. High power density microbial fuel cells with flexible 3D graphene-nickel foam as anode. Nanoscale. 2013. 5. 10283-10290.

429. Hao R, Pyo S, Lee JI, Park TJ, Gittleson FS et al. A high power density miniaturised microbial fuel cell having carbon nanotube anodes. J. Power Sources. 2015. 273. 823-830.

Chapter 8: Appendix

8.1 – Plasmids

8.1.1 – Cytochrome maturation genes

pRGK333

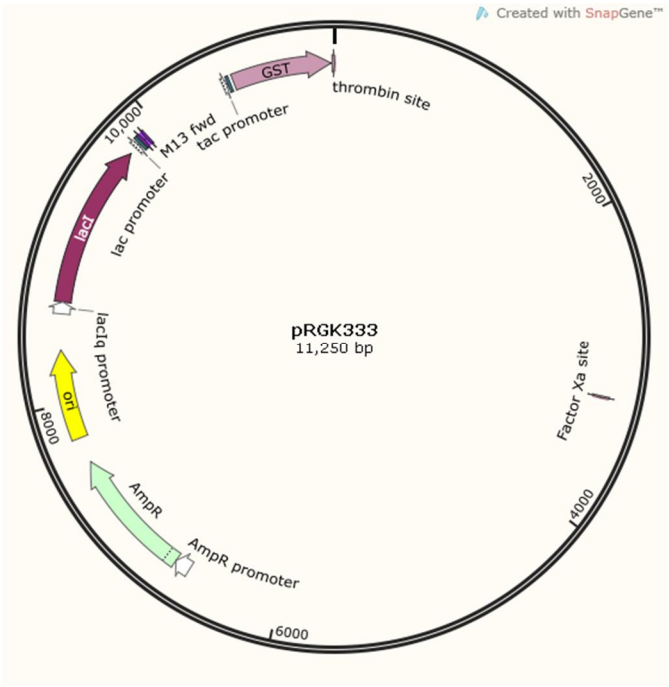

8.1.2 – Mtr plasmids

pACYCDuet-1

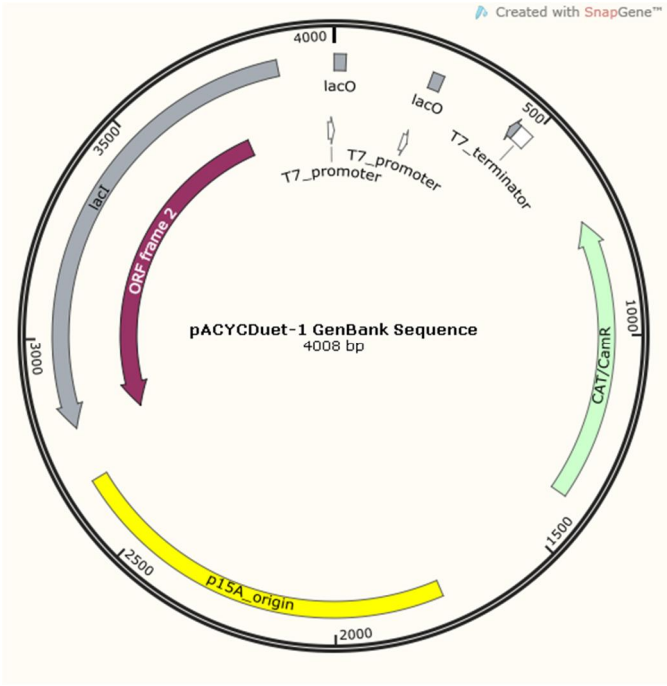

pACYCOmcA

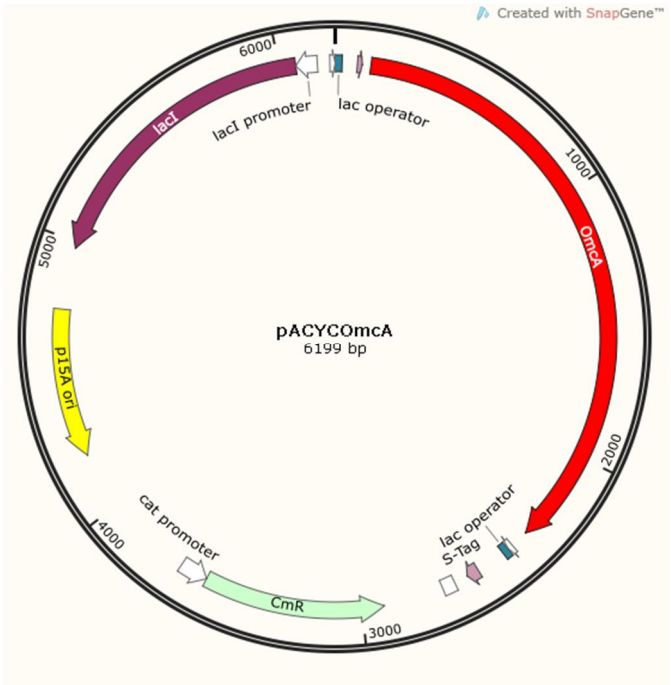

pACYCMtrABO

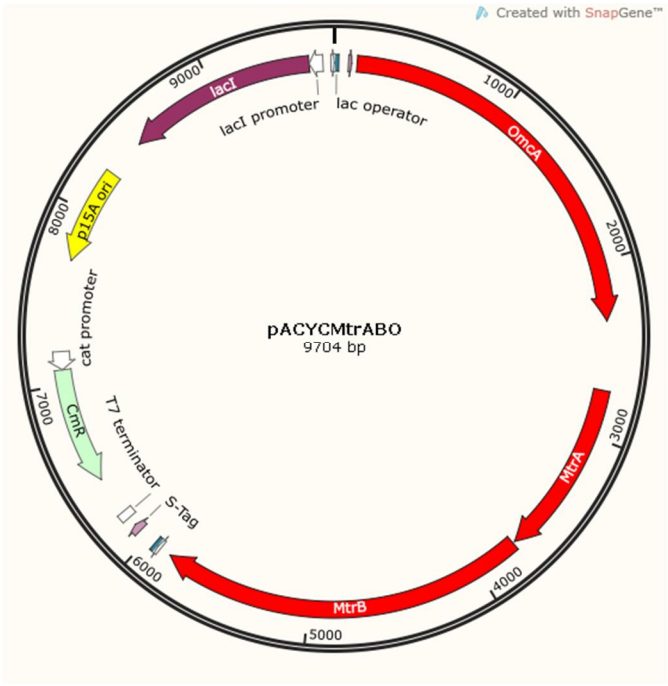

pACYCMtrCAB

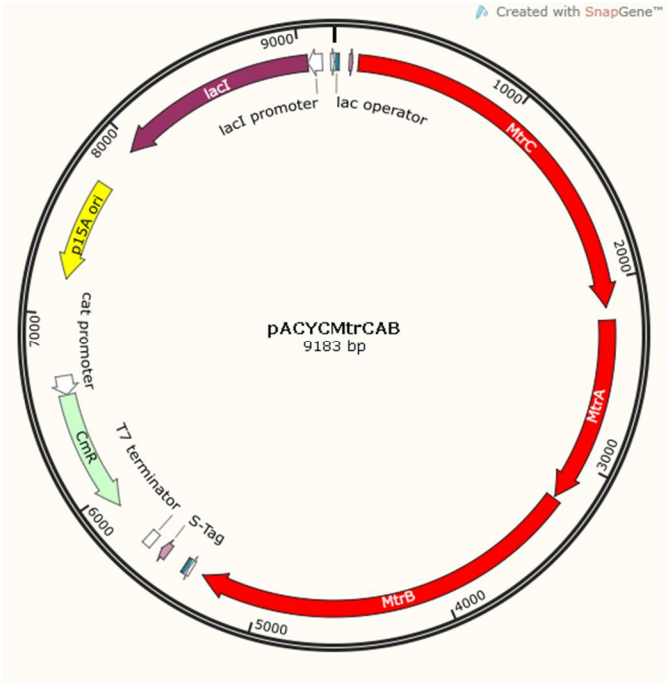

pACYCMtrCABO

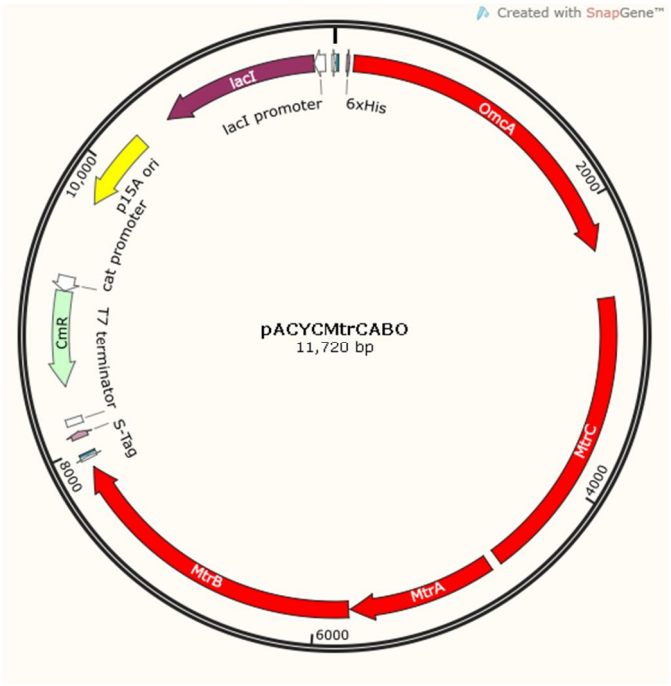

pACYCMR-1

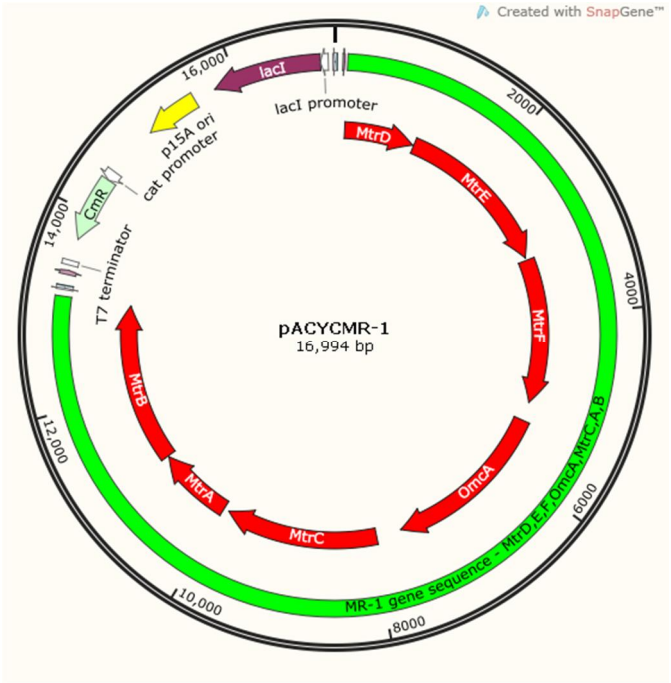

8.1.3 Recombination plasmids:

pKD46

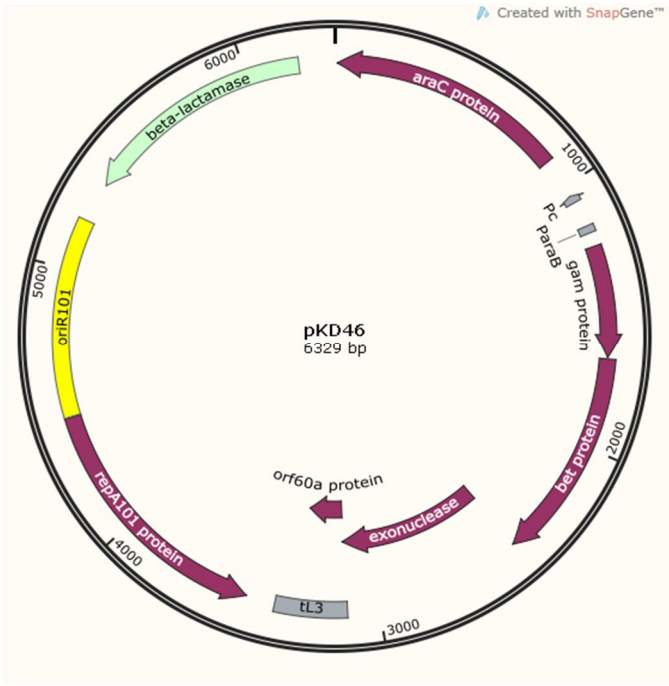

pKD13

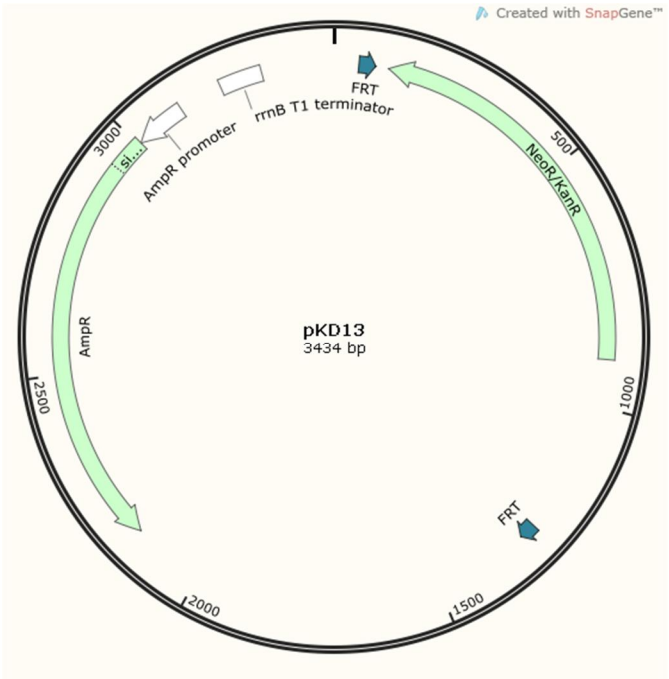

8.1.4 Transposon plasmids:

pGRG36

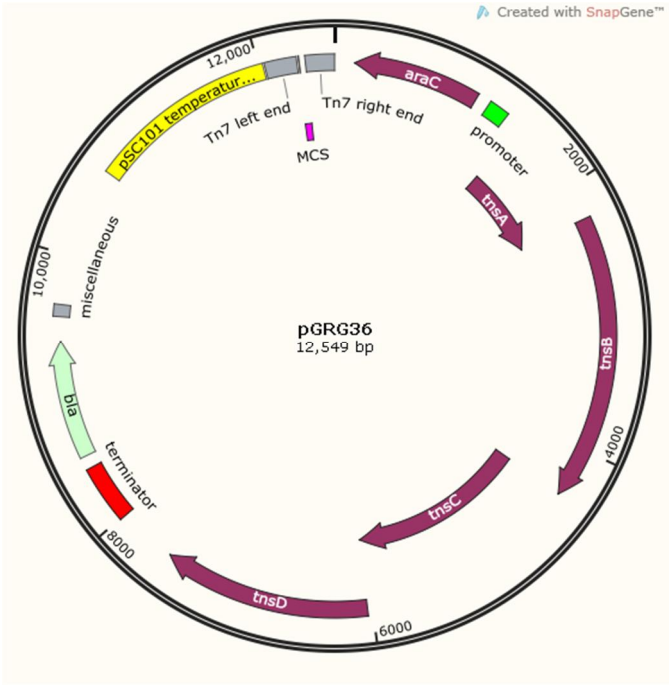

pUC19

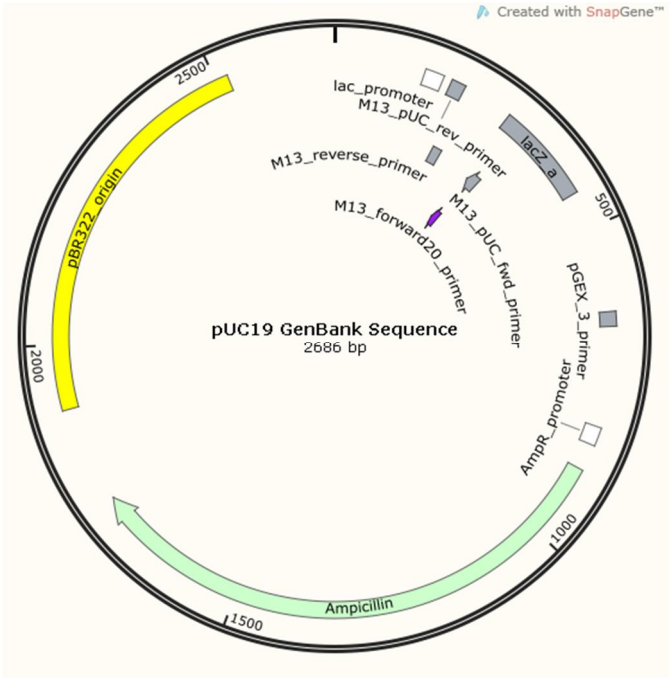

pUC19 Cm

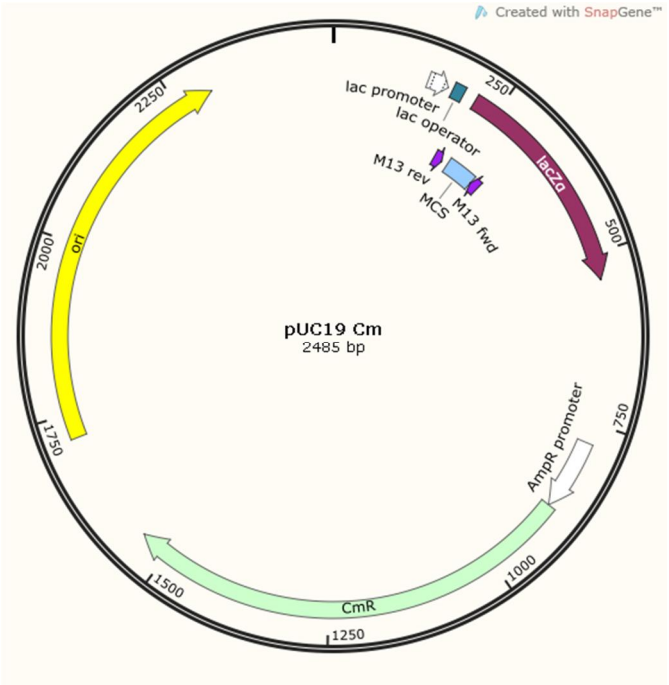

pUC19Cm-Tn7

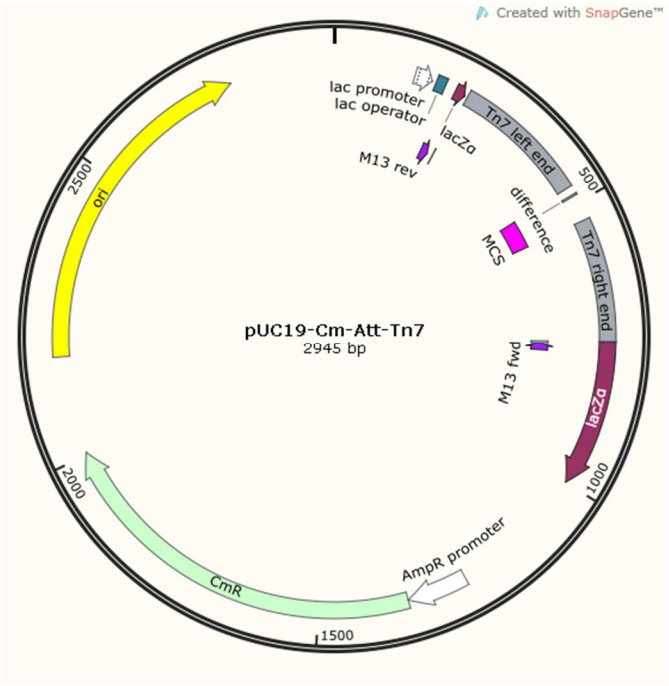

Bioelectrochemical system pictures

University of West England (UWE) MFC – MK1

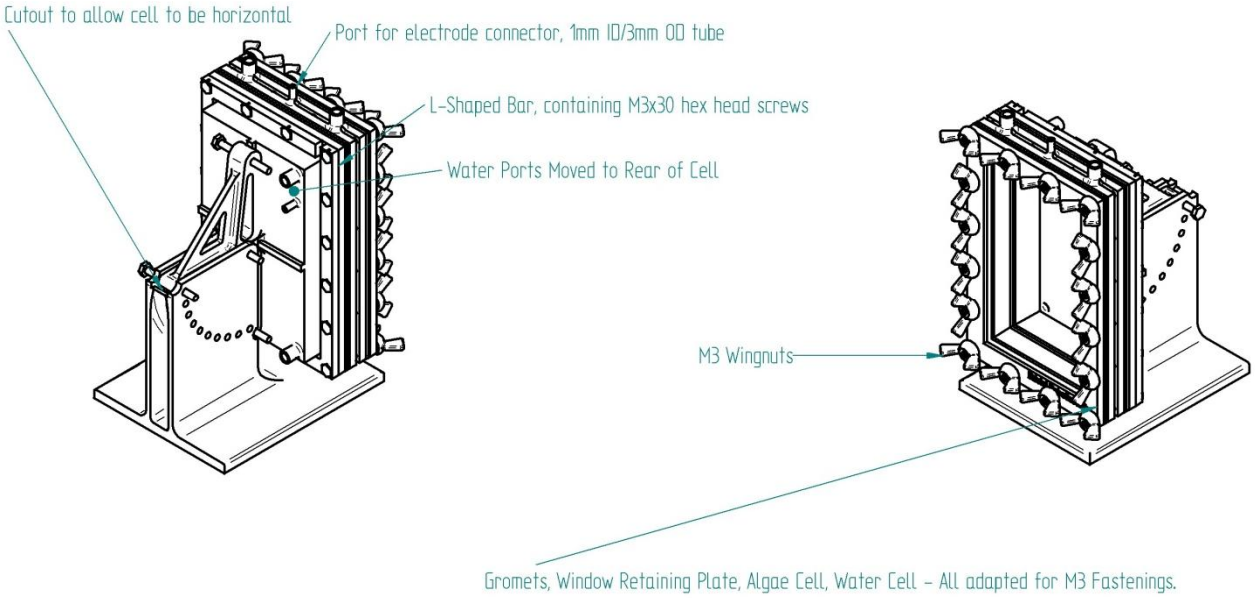

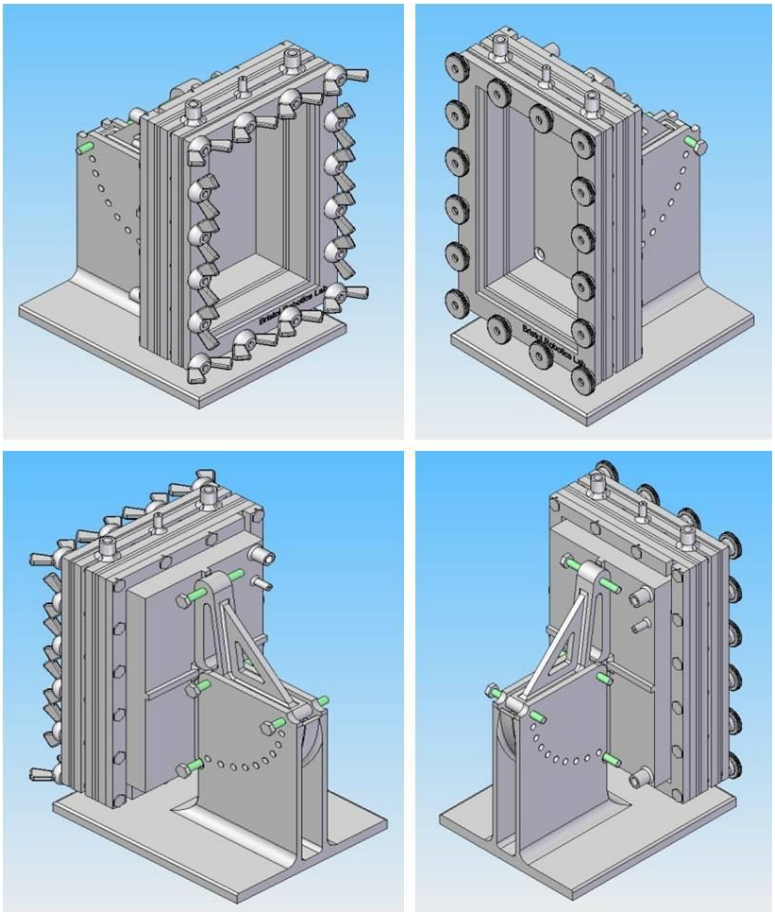

Bioinformatics for Chapter 4

MS results:

MtrA

Identified peptides:

FAEGNYSPK

GGNEPMITFGK

QKADMNK

These peptides map onto the target protein as follows:

>gi|24347597|gb|AAN54830.1|AE015621_8 decahaem cytochrome c MtrA [Shewanella oneidensis MR-1]

MKNCLKMKNLLPALTITMAMSAVMALVVTPNAYASKWDEKMTPEQVEATLDKK**FAEGNYSPK**GADSCLMCHKKSEKVMDLFKGVHGAIDSSKSPMAGLQCEACHGPLGQHNK**GGNEPMITFGK**QSTLSADKQNSVCMSCHQDDKRMSWNGGHHDNADVACASCHQVHVAKDPVLSKNTEMEVCTSCHTK**QKADMNK**RSSHPLKWAQMTCSDCHNPHGSMTDSDLNKPSVNDTCYSCHAEKRGPKLWEHAPVTENCVTCHNPHGSVNDGMLKTRAPQLCQQCHASDGHASNAYLGNTGLGSNVGDNAFTGGRSCLNCHSQVHGSNHPSGKLLQR

MtrB

Identified peptides:

VDLLGMNLK

YANQLNTDAVDAK

This peptide maps onto the target protein as follows:

>gi|24347596|gb|AAN54829.1|AE015621_7 outer membrane protein precursor MtrB [Shewanella oneidensis MR-1]

MKFKLNLITLALLANTGLAVAADGYGLANANTEKVKLSAWSCKGCVVETGTSGTVGVGVGYNSEE
DIRSANAFGTSNEVAGKFDADLNFKGEKGYRASVDAYQLGMDGGRLDVNAGKQGQYNVNVNY
RQIATYDSNSALSPYAGIGGNNLTLPDNWITAGSSNQMPLLMDSLNALELSLKRERTGLGFEYQGE
SLWSTYVNYMREEKTGLKQASGSFFNQSMMLAEPVDYTTDTIEAGVKLKGDRWFTALSYNGSIFK
NEYNQLDFENAFNPTFGAQTQGTMALDPDNQSHTVSLMGQYNDGSNALSGRILTGQMSQDQA
LVTDNYR**YANQLNTDAVDAKVDLLGMNLK**VVSKVSNDLRLTGSYDYYDRDNNTQVEEWTQISI
NNVNGKVAYNTPYDNRTQRFKVAADYRITRDIKLDGGYDFKRDQRDYQDRETTDENTVWARLR
VNSFDTWDMWVKGSYGNRDGSQYQASEWTSSETNSLLRKYNLADRDRTQVEARITHSPLESLTI
DVGARYALDDYTDTVIGLTESKDTSYDANISYMITADLLATAFYNYQTIESEQAGSSNYSTPTWTGF
IEDQVDVVGAGISYNNLLENKLRLGLDYTYSNSDSNTQVRQGITGDYGDYFAKVHNINLYAQYQAT
EKLALRFDYKIENYKDNDAANDIAVDGIWNVVGFGSNSHDYTAQMLMLSMSYKL

MtrC

Identified peptides:

ADLAFATLSGK

VFNAQLTQR

ETLESFGAVVDGTK

GALNTAAAADK

FDAFDSNK

These peptides map onto the target protein as follows:

>gi|24347598|gb|AAN54831.1|AE015621_9 decahaem cytochrome c [Shewanella oneidensis MR-1]

MMNAQKSKIALLLAASAVTMALTGCGGSDGNNGNDGSDGGEPAGSIQTLNLDITKVSYENGA
PMVTVFATNEADMPVIGLANLEIKKALQLIPEGATGPGNSANWQGLGSSKSYVDNKNGSYTFK
FDAFDSNKVFNAQLTQRFNVVSAAGKLADGTTVPVAEMVEDFDGQGNAPQYTKNIVSHEVC
ASCHVEGEKIYHQATEVETCISCHTQEFADGRGKPHVAFSHLIHNVHNANKAWGKDNKIPTVA
QNIVQDNCQVCHVESDMLTEAKNWSRIPTMEVCSSCHVDIDFAAGKGHSQQLDNSNCIACH
NSDWTAELHTAKTTATKNLINQYGIETTSTINTETKAATISVQVVDANGTAVDLKTILPKVQRLEII

TNVGPNNATLGYSGKDSIFAIKNGALDPKATINDAGKLVYTTTKDLKLGQNGADSDTAFSFVG
WSMCSSEGKFVDCADPAFDGVDVTKYTGMK**ADLAFATLSGK**APSTRHVDSVNMTACANCHT
AEFEIHKGKQHAGFVMTEQLSHTQDANGKAIVGLDACVTCHTPDGTYSFANRGALELKLHKKH
VEDAYGLIGGNCASCHSDFNLESFKKK**GALNTAAAADK**TGLYSTPITATCTTCHTVGSQYMVHT
K**ETLESFGAVVDGTK**DDATSAAQSETCFYCHTPTVADHTKVKM

MtrD

No identified peptides

>gi|410519705|gb|AAN54835.2| extracellular respiratory system periplasmic decahaem cytochrome c component MtrD [Shewanella oneidensis MR-1]

MDMDIGLKFNSITQIMLTLMLSILSLSTLATPWDDKSSEEVVATLDKKFAEGKYSAKGADTCLMCH
KKSAVVMAIFDGVHGNPNIKDSPMADLQCEACHGPLGNHNKGGKEPMITFGQNSPVPAQKQN
SVCMSCHNDDQRIAWKGNHHDNADIPCSSCHQVHVAKDPISDKANEVAICTQCHSQQKADMH
KRSSHPLQWQQMVCSDCHNPHGSLNDASLKQMTVNENCYSCHAEKRGPKLWEHAPVTDNCA
NCHNPHGSVNESMLISKPPQLCQQCHASDGHSSNAYFGNQTNAFTSGNSCMNCHGQVHGSNH
PSGKLLQR

MtrE

Identified peptide:

DSDQAGSNR

>gi|24347604|gb|AAN54834.1| extracellular respiratory system outer membrane component MtrE [Shewanella oneidensis MR-1]

MQIVNISTPKVCFSLTLLAWTMSGVLNTAHAEGYEIQKANRSGVKNEAWSCKQCQPQTGRQGN
VSATLAHNDGDDSRFGNRTGIDKDGLVGAIGADMKYKAESGYQTSLMADKLGFDTGSAKLSTGQ
LGHYQINLGYKGLANYQYNQLKSPYIAENDKMLLPDNWVAGATTQSMPLLQSSLAEQDLSLKRD
RFNLGGYYAGHISSTNRYKASINYQHENRSGAKKTSANILTNSVMLAQPIDDSTDEIDARIYFGGIG
WQAGINSQISQYKNDHQALLWQSAYTPTFGAAYYGQNAVEPDNKAYRIAAEASGGQNGHNVL
MHAGISQMSQDEAFLPATINGPAPTLPADNLDGQVDILEMLLKYSGRITQDLSIQANYHYQDKDN

KTTQLDFPQVVTDSVYQGTAQNSLYDKRSNKLELKGKYRLTPSAYAEAGYSLDANDYSALDRQSV
DESGVFAKLSYRYSPSWSTWLKGEALTRDGSEYDPVSTTQSPSNPWLRKSYLADRKRQKVTLHTD
YQSDIGLSVGASLHNVDDDYNHTSVGLTHVSYLGYDVSAQYLIADNLSLNAYLNQDWR**DSDQAG**
SNRFSTPDWYSTAEEKSTLIGTGVVYQNLLDNHLDLGLDYSYSDGQSDTEVTYGITSPYGDYYNRK
HNINAYAKYKLADSMSLRFDWLFEKYQDASWQNQNTTWDTIPNVLSFGDISRDYNAHYLGLTLSY
QM

MtrF

No identified peptides

>gi|24347603|gb|AAN54833.1| extracellular respiratory system surface decahaem cytochrome c component MtrF [Shewanella oneidensis MR-1]

MNKFASFTTQYSLMLLIATLLSACGGSDGDDGSPGEPGKPPAMTISSLNISVDKVAISDGIAQVDY
QVSNQENQAVVGIPSATFIAAQLLPQGATGAGNSSEWQHFTSETCAASCPGTFVDHKNGHYSYR
FSATFNGMNGVTFLSDATQRLVIKIGGDALADGTVLPITNQHYDWQSSGNMLAYTRNLVSIDTCN
SCHSNLAFHGGRYNQVETCVTCHNSKKVSNAADIFPQMIHSKHLTGFPQSISNCQTCHADNPDLA
DRQNWYRVPTMEACGACHTQINFPAGQGHPAQTDNSNCVACHNADWTANVHSNAAQTSAL
AQFNASISSASMDANGTITVAVSLTNPTTGTAYADSADKLKFISDLRIYANWGTSFDYSSRSARSIRL
PESTPIAGSNGTYSYNISGLTVPAGTESDRGGLAIQGRVCAKDSVLVDCSTELAEVLVIKSSHSYFNM
SALTTTGRREVISNAKCASCHGDQQLNIHGARNDLAGQCQLCHNPNMLADATATNPSMTSFDFK
QLIHGLHSSQFAGFEDLNYPGNIGNCAQCHINDSTGISTVALPLNAAVQPLALNNGTFTSPIAAVCS
NCHSSDATQNHMRQQGAVFAGTKADATAGTETCAFCHGQGTVADVLKVHPIN

TMHMM

OmcA

Sequence Length: 735
Sequence Number of predicted TMHs: 0
Sequence Exp number of AAs in TMHs: 1.9354
Sequence Exp number, first 60 AAs: 1.92918

Sequence Total prob of N-in: 0.09716

Sequence TMHMM2.0 outside 1 735

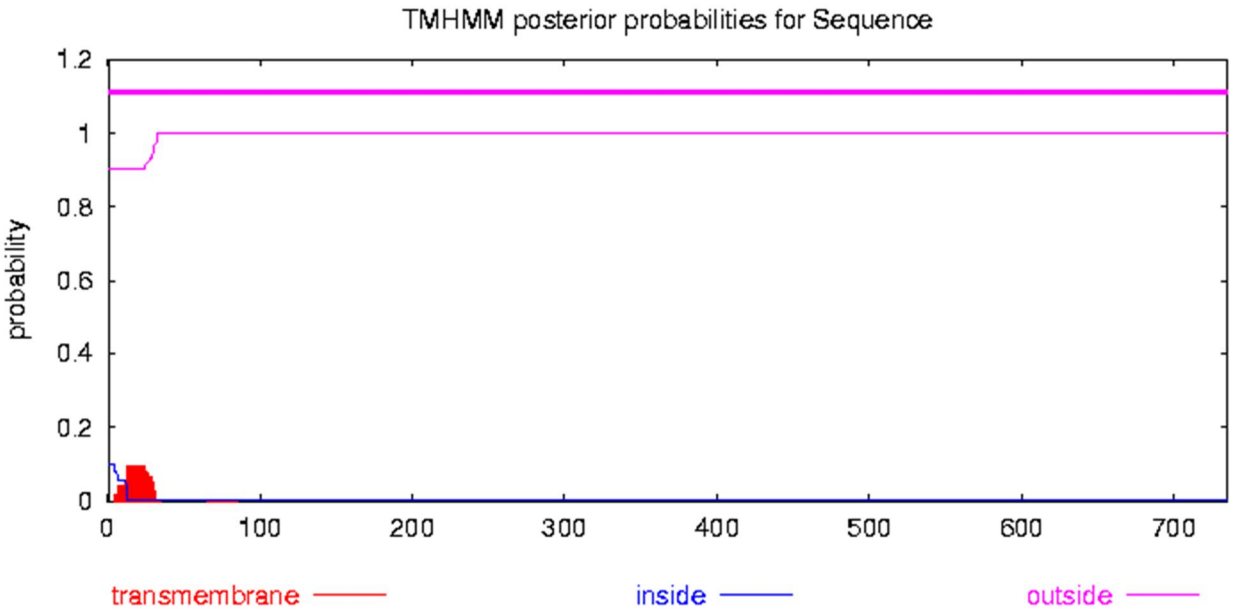

MtrA

Sequence Length: 333

Sequence Number of predicted TMHs: 1

Sequence Exp number of AAs in TMHs: 20.26577

Sequence Exp number, first 60 AAs: 20.26558

Sequence Total prob of N-in: 0.75587

Sequence POSSIBLE N-term signal sequence

Sequence TMHMM2.0 inside 1 11

Sequence TMHMM2.0 TMhelix 12 34

Sequence TMHMM2.0 outside 35 333

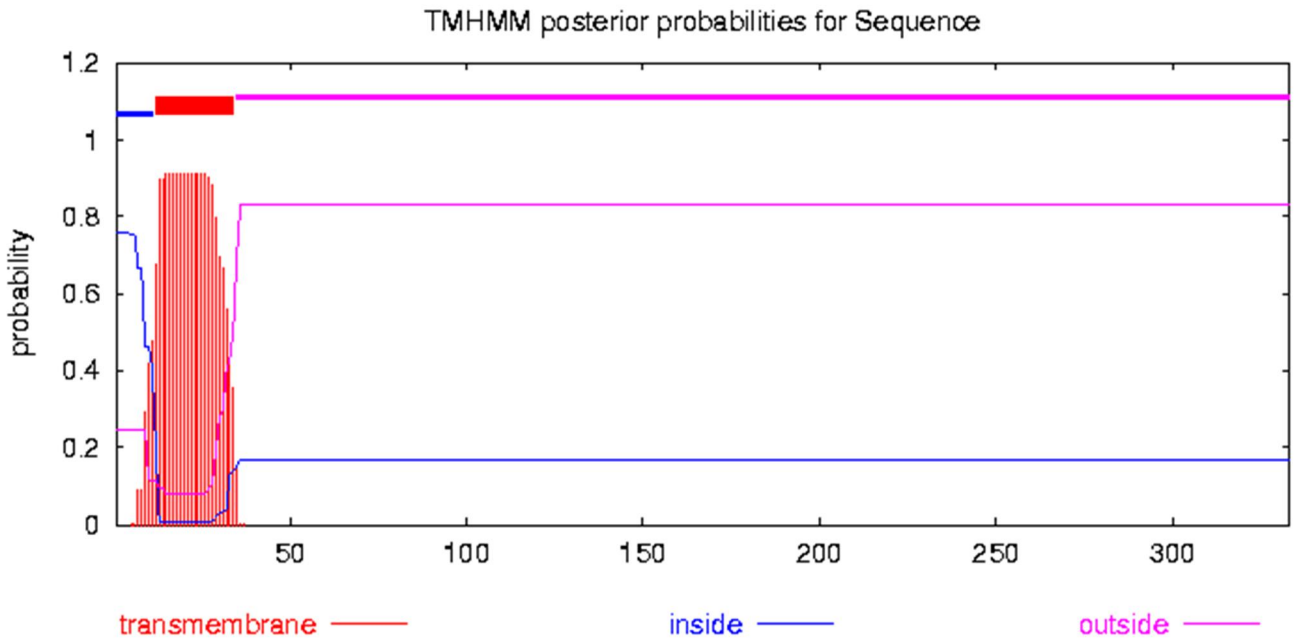

MtrF

Sequence Length: 639

Sequence Number of predicted TMHs: 0

Sequence Exp number of AAs in TMHs: 0.69532

Sequence Exp number, first 60 AAs: 0.65633

Sequence Total prob of N-in: 0.03427

Sequence TMHMM2.0 outside 1 639

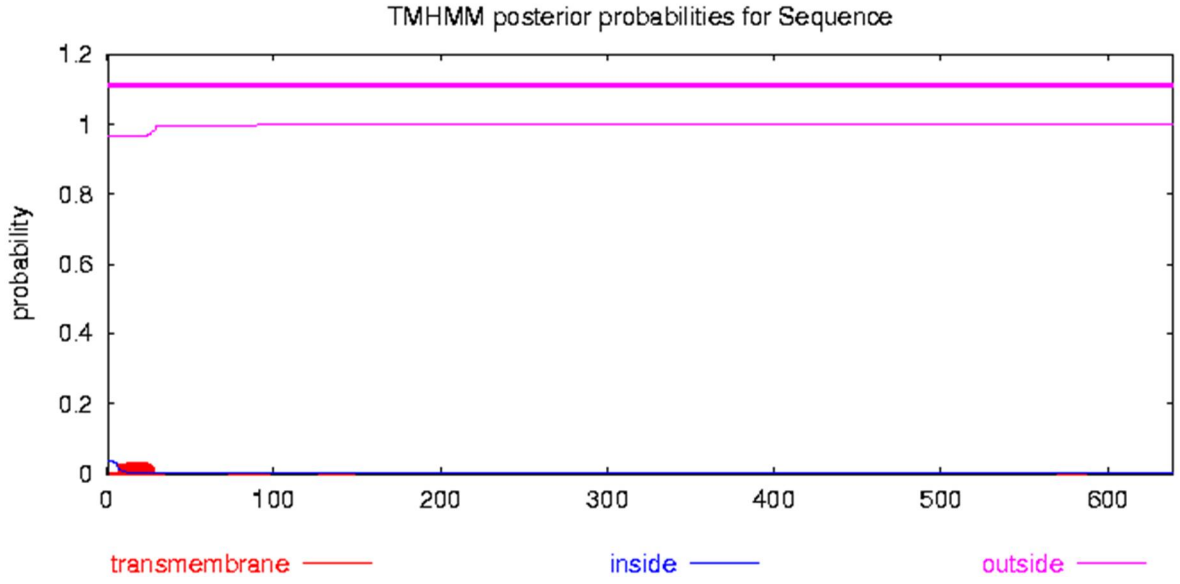

MtrD

Sequence Length: 306

Sequence Number of predicted TMHs: 0

Sequence Exp number of AAs in TMHs: 0.00018

Sequence Exp number, first 60 AAs: 0.00018

Sequence Total prob of N-in: 0.00321

Sequence TMHMM2.0 outside 1 306

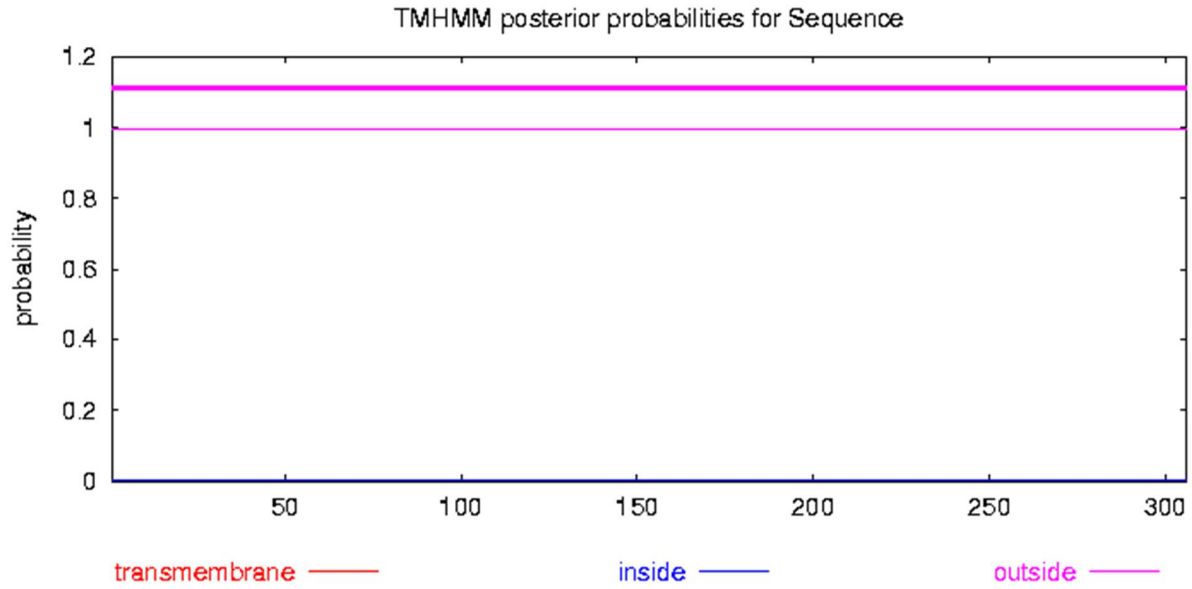

MtrB

Sequence Length: 697

Sequence Number of predicted TMHs: 0

Sequence Exp number of AAs in TMHs: 7.1145

Sequence Exp number, first 60 AAs: 7.10972

Sequence Total prob of N-in: 0.32241

Sequence TMHMM2.0 outside 1 697

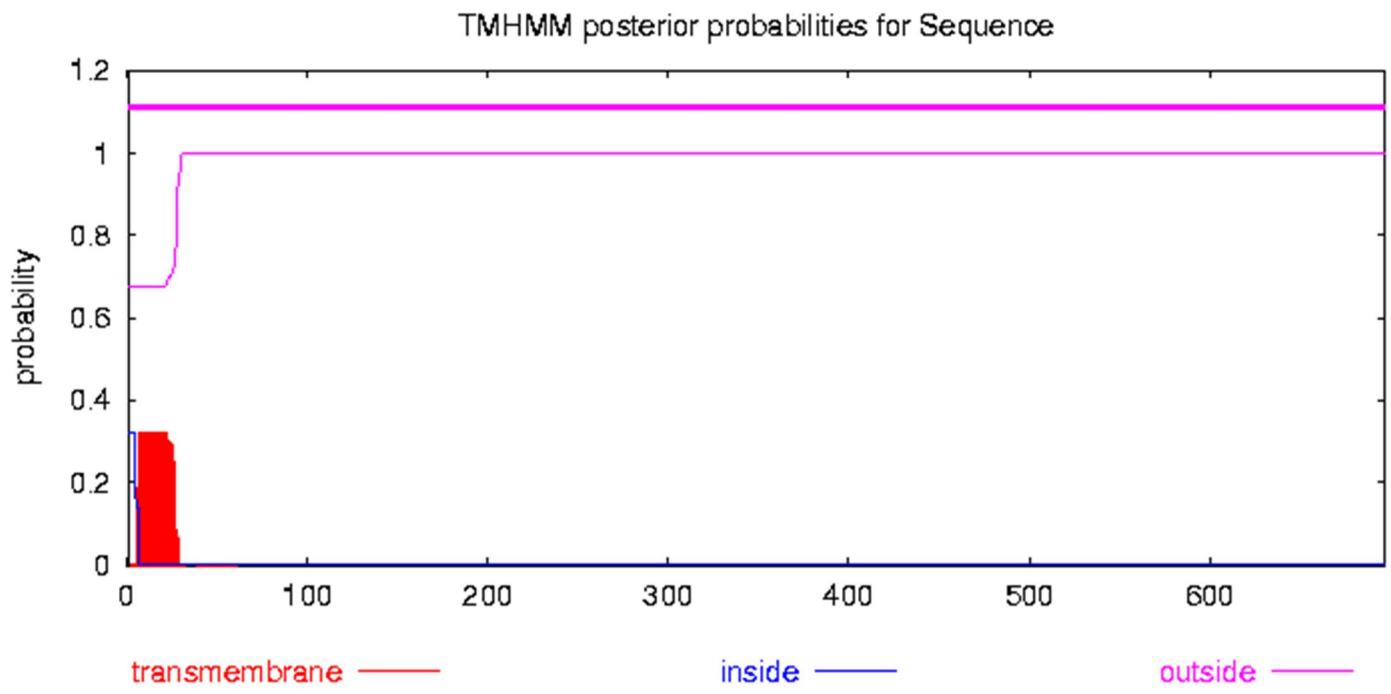

MtrE

Sequence Length: 712

Sequence Number of predicted TMHs: 0

Sequence Exp number of AAs in TMHs: 2.021

Sequence Exp number, first 60 AAs: 2.01926

Sequence Total prob of N-in: 0.09838

Sequence TMHMM2.0 outside 1 712

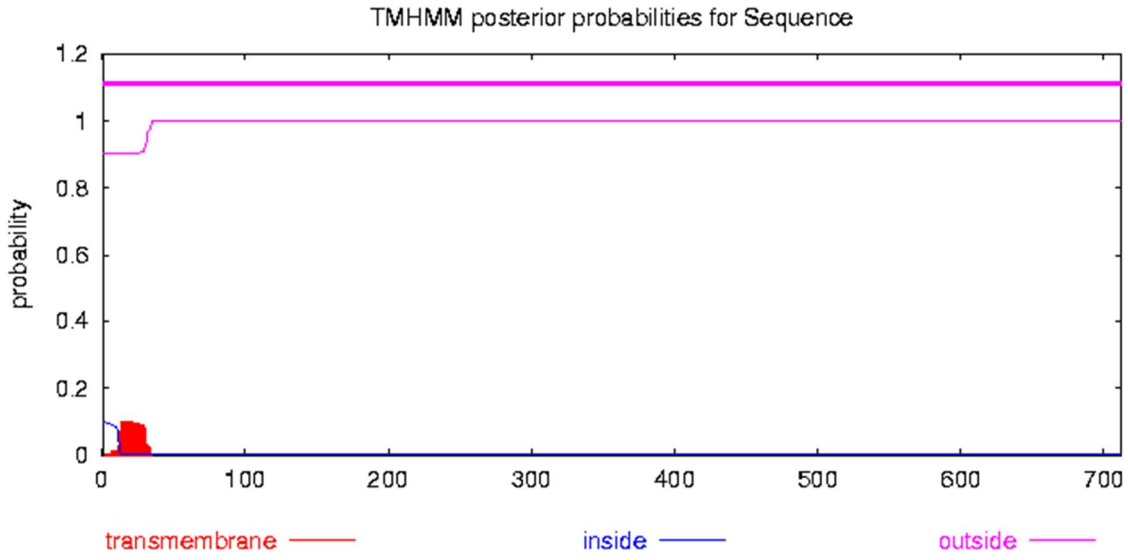

MtrC

Sequence Length: 671

Sequence Number of predicted TMHs: 0

Sequence Exp number of AAs in TMHs: 2.93629

Sequence Exp number, first 60 AAs: 2.92742

Sequence Total prob of N-in: 0.15213

Sequence TMHMM2.0 outside 1 671

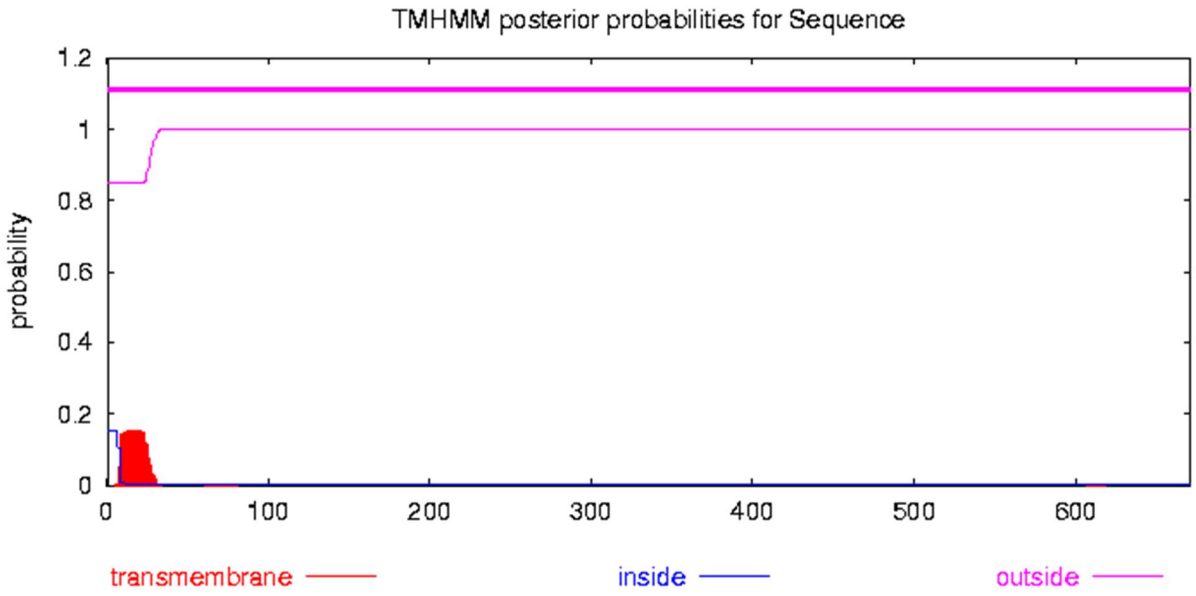

Signal Peptide

OmcA

Prediction: Signal peptide

Signal peptide probability: 1.000

Max cleavage site probability: 0.908 between pos. 32 and 33

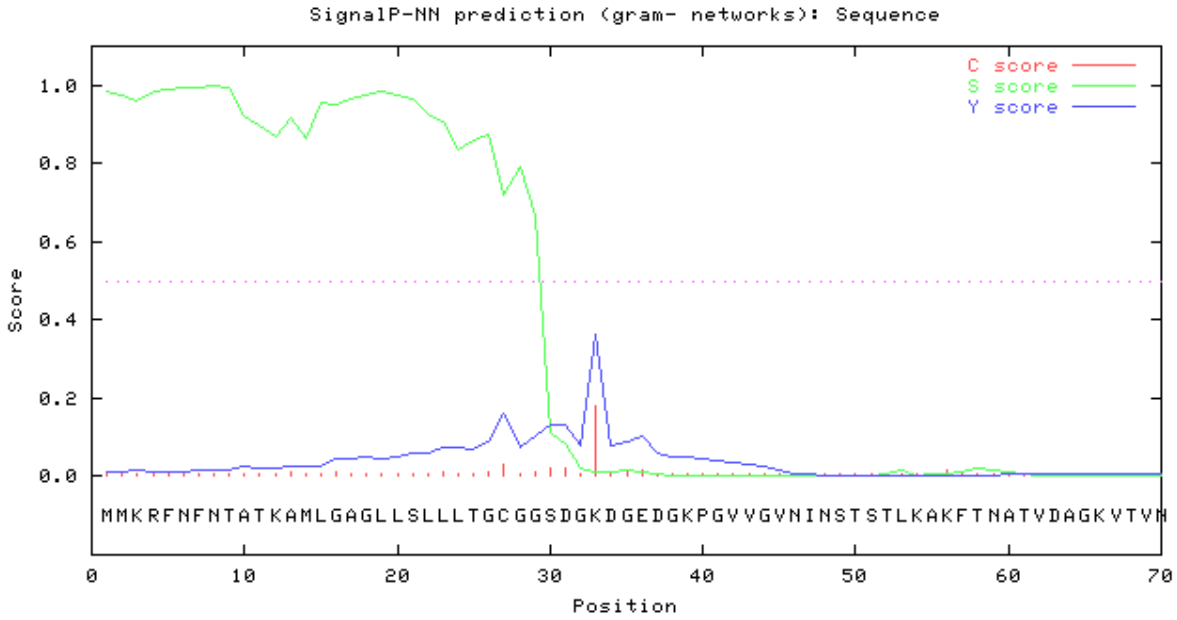

MtrA

Prediction: Signal peptide

Signal peptide probability: 1.000

Max cleavage site probability: 0.506 between pos. 25 and 26

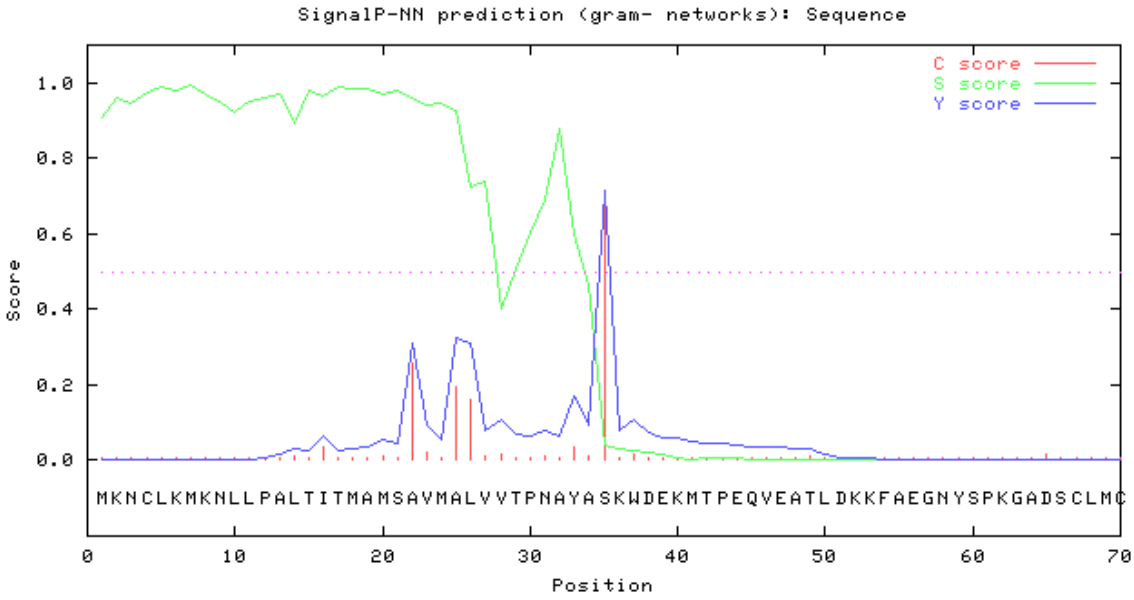

MtrF

Prediction: Signal peptide

Signal peptide probability: 0.998

Max cleavage site probability: 0.949 between pos. 29 and 30

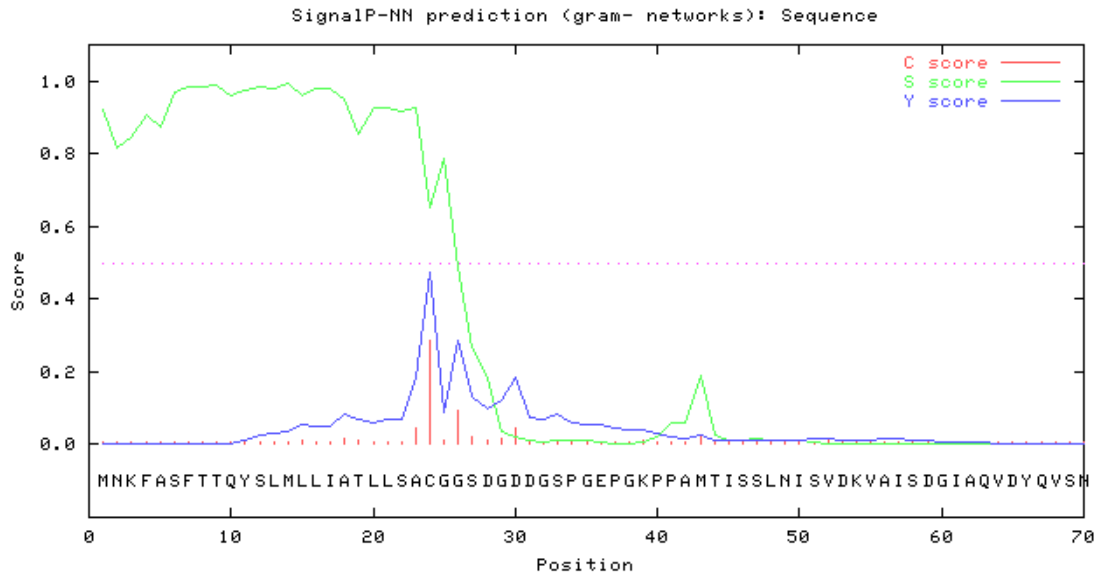

MtrD

Prediction: Signal peptide

Signal peptide probability: 0.681

Max cleavage site probability: 0.674 between pos. 15 and 16

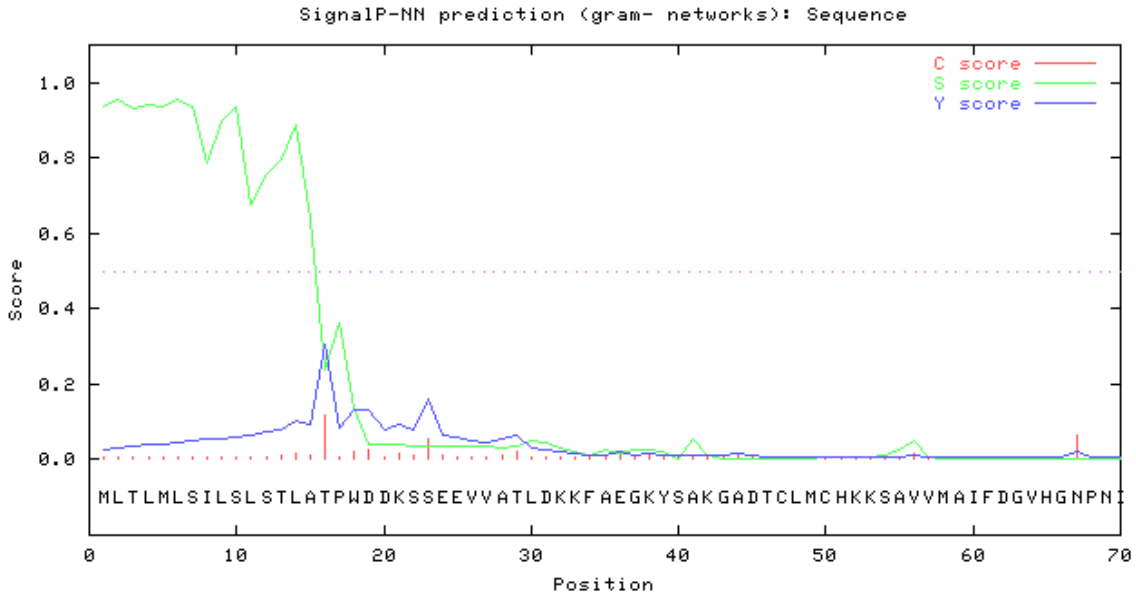

MtrE

Prediction: Signal peptide

Signal peptide probability: 0.996

Max cleavage site probability: 0.952 between pos. 31 and 32

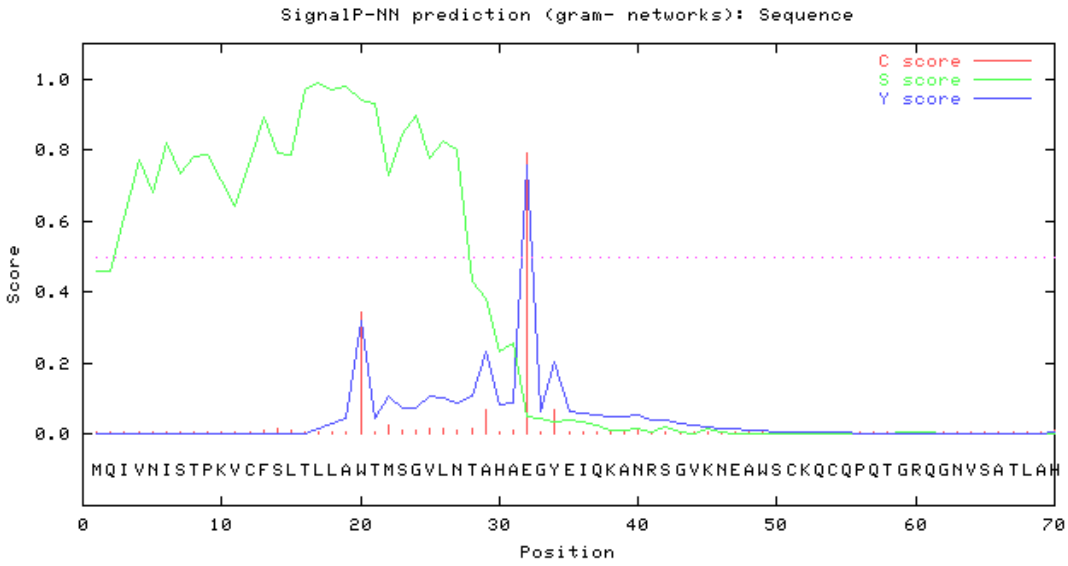

MtrC

Prediction: Signal peptide

Signal peptide probability: 0.999

Max cleavage site probability: 0.420 between pos. 30 and 31

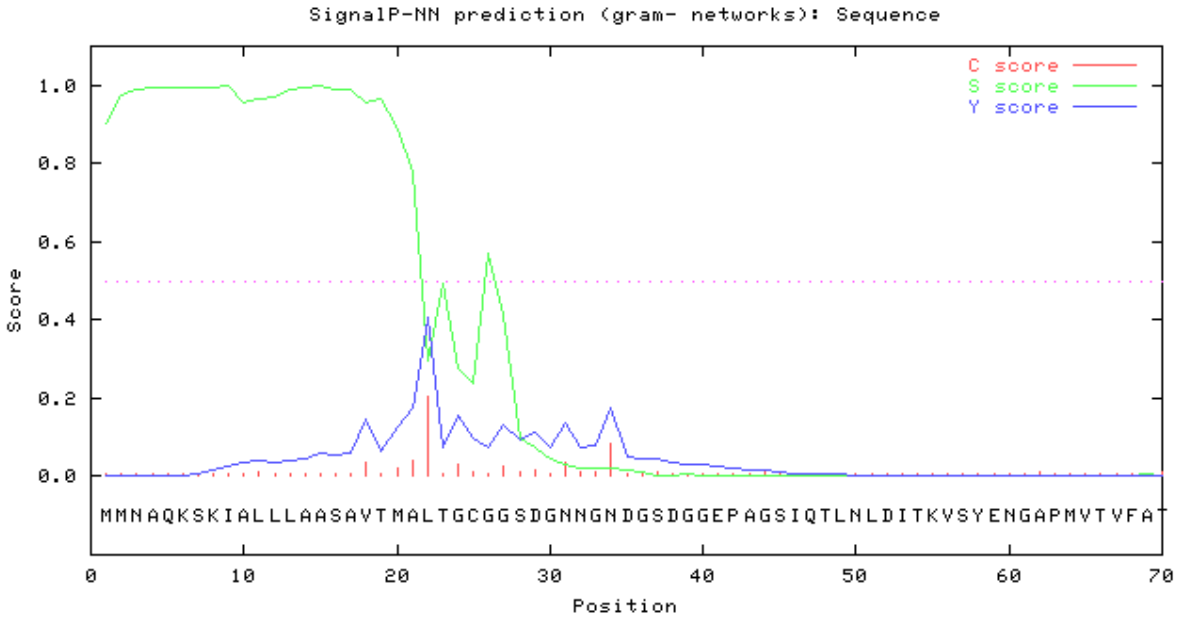

MtrB

Prediction: Signal peptide

Signal peptide probability: 1.000

Max cleavage site probability: 0.977 between pos. 21 and 22

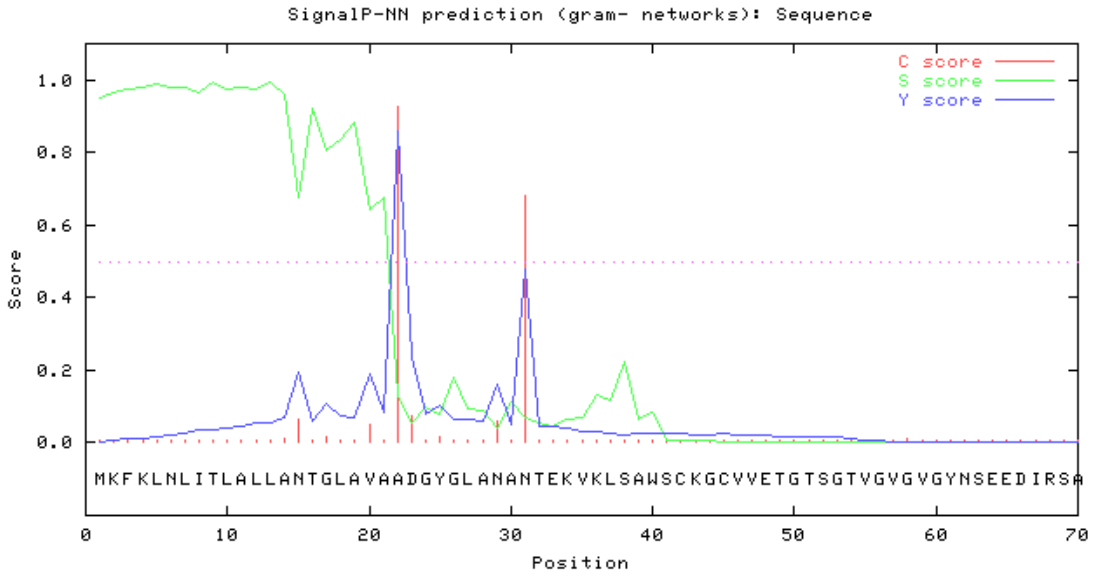

Chapter 5 – regulated proteins from iTRAQ 1 and 2

iTRAQ 1 - Aerobic Planktonic vs Semi-Anaerobic Anodic Biofilm cells - Soluble sub-proteome

UniProt ident.	gi Number	Name	# pept ides	119/115 (log difference)	119/116 (log difference)	121/115 (log difference)	121/116 (log difference)	119/115 (p-value)	119/116 (p-value)	121/115 (p-value)	121/116 (p-value)	Fold change (Anode associated cells/aerobic planktonic)	P-value (Anode associated cells/aerobic planktonic)
Q8EK77 (RL1_SHEON) SO0221	gi|24345624|gb|AAN53306.1|AE015471_11	AE015471_11 ribosomal protein L1	26	-0.39241	-0.94195	-0.32151	-0.87105	0.01580	4.6E-06	0.03217	1.32E-05	-1.88086	0.00042
Q8EK74 (RPOB_SHEON) SO0224	gi|24345631|gb|AAN53309.1|AE015472_1	AE015472_1 DNA-directed RNA polymerase, beta subunit	11	0.877683	0.933698	0.874364	0.930379	1.06E-05	1.49E-05	0.000104	5.38E-05	2.469537	3.07E-05
Q8EK73 (RPOC_SHEON) SO0225	gi|24345632|gb|AAN53310.1|AE015472_2	AE015472_2 DNA-directed RNA polymerase, beta' subunit	47	0.495379	0.579 96	0.446223	0.530804	0.00037	3.51E-05	0.00226	6.89E-06	1.670448	6.71E-05
Q8EK65 (RL2_SHEON) SO0234	gi|24345645|gb|AAN53319.1|	AE015473_6 ribosomal protein L2	17	0.938404	1.107135	0.698667	0.867397	3.06E-05	5.41E-06	4.61E-07	4.29E-08	2.466748	1.34E-06

Q8EK62 (RL16_SHEON) SO0238	AE015473_6 gi|24345649|gb|AAN53323.1|AE015473_10	AE015473_10 ribosomal protein L16	5	0.516184	0.989637	0.618082	1.091535	0.00523 6	0.00072 9	0.01012 4	0.00036 9	2.234147	0.001943
Q8EK58 (RL24_SHEON)SO0242	gi|24345653|gb|AAN53327.1|AE015473_14	AE015473_14 ribosomal protein L24	14	-0.51843	-1.02567	-0.58148	-1.08872	0.04950 4	0.00642 3	0.02052 4	0.00316	-2.23351	0.011983
Q8EK57 (RL5_SHEON) SO0243	gi|24345654|gb|AAN53328.1|AE015473_15	AE015473_15 ribosomal protein L5	55	-0.64604	-0.74927	-0.81984	-0.92307	6.61E-11	5.22E-14	3.46E-11	2.86E-13	-2.19143	2.42E-12
Q8EIM3 (Q8EIM3_SHEON) SO0815	gi|24346370|gb|AAN53891.1|AE015526_2	AE015526_2 TonB-dependent receptor C-terminal domain protein	7	0.531 59	0.750 497	0.496 669	0.715 575	0.01036 1	0.00092 7	0.00046 2	0.00098 9	1.8656	0.001447
Q8EHS3 (Q8EHS3_SHEON) SO1144	gi|24346793|gb|AAN54214.1|AE015558_8	AE015558_8 methyl-accepting chemotaxis protein	27	0.881679	1.049178	0.378562	0.546 06	2.04E-13	1.38E-14	0.00049 4	4.05E-07	2.041877	8.66E-10
Q8EHM2 (Q8EHM2_SHEO	gi|24346861|gb|AAN54267.1|	AE015563_7 cell division protein FtsH	3	0.851 71	0.707 735	0.847 712	0.703 737	0.03605 4	0.01032 8	0.01162 9	0.00300 2	2.176511	0.010678

N) SO1197	AE015563_7												
Q8EGV9 (Q8EGV9_SHEON) SO1482	gi|243472 32|gb|AAN54543.1| AE015593_2	AE015593_2 TonB-dependent receptor, putative	4	-0.66429	-0.43225	-0.68013	-0.44809	0.01287	0.03239	0.01446	0.03419	-1.74402	0.021315
Q8EFZ0 (Q8EFZ0_SHEON) SO1824	gi|243476 58|gb|AAN54876.1| AE015626_5	AE015626_5 conserved hypothetical protein	206	-0.47697	-0.42533	-0.45207	-0.40043	1.78E-12	1.76E-10	5.17E-12	3.94E-10	-1.55069	2.83E-11
Q8EFY9 (Q8EFY9_SHEON) SO1825	gi|243476 59|gb|AAN54877.1| AE015626_6	AE015626_6 MotA/TolQ/ExbB proton channel family protein [Shewanella oneidensis MR-1]	88	-0.48388	-0.52931	-0.48641	-0.53184	1.18E-08	6.73E-10	8.78E-08	8.69E-10	-1.66173	4.97E-09
Q8EFY7 (Q8EFY7_SHEON) SO1827	gi|243476 61|gb|AAN54879.1| AE015626_8	AE015626_8 TonB system transport protein ExbD2 [Shewanella oneidensis MR-1]	3	-0.76023	-0.76548	-0.70563	-0.71089	0.01292	0.00766	0.00302	0.00888	-2.08664	0.007185
Q8EFY6 (Q8EFY6_SHEON) SO1828	gi|243476 62|gb|AAN54880.1| AE015626_9	AE015626_9 TonB2 protein [Shewanella oneidensis MR-1]	9	-1.04933	-1.12482	-1.14069	-1.21618	0.00206	0.00150	0.00034	0.00021	-3.1042	0.00069
Q8EFP4 (Q8EFP4	gi|243477 90|gb|AAN54977.1|	AE015636_1 citrate synthase [Shewanella oneidensis MR-1]	6	-0.57317	-1.12705	-0.28703	-0.84091	0.00793	4.41E-05	0.04513	0.00134	-2.02798	0.001206

_SHEON) SO1926	AE015636_1												
Q8EEF5 (Q8EEF5_SHEON) SO2427	gi|243484 20|gb|AAN55461.1| AE015683_8	AE015683_8 TonB-dependent receptor, putative [Shewanella oneidensis MR-1]	43	- 0.729 82	- 0.719 6	- 0.796 91	- 0.786 7	3.42 E-11	9.86 E-12	3.02 E-11	3.81 E-12	-2.13455	1.4E-11
Q8EEB8 (Q8EEB8_SHEON) SO2469	gi|243484 76|gb|AAN55500.1| AE015688_6	AE015688_6 conserved hypothetical protein [Shewanella oneidensis MR-1]	14	- 0.767 55	- 0.770 81	- 0.966 19	- 0.969 45	0.00 028 9	0.00 019 1	4.75 E-06	2.16 E-06	-2.38333	2.74E-05
Q8ED60 (Q8ED60_SHEON) SO2907	gi|243490 09|gb|AAN55923.1| AE015729_7	AE015729_7 TonB-dependent receptor domain protein [Shewanella oneidensis MR-1]	13	- 0.947 72	- 0.711 98	- 0.938 74	- 0.703	0.00 066 6	0.00 395 4	0.00 190 7	0.00 960 7	-2.2827	0.002635
Q8EBN8 (GLYA_SHEON) SO3471	gi|243497 03|gb|AAN56464.1| AE015783_7	AE015783_7 serine hydroxymethyltransferase [Shewanella oneidensis MR-1]	8	- 0.813 37	- 0.563 04	- 0.542 01	- 0.291 68	0.00 028 4	0.00 265 4	5.55 E-05	0.00 406 7	-1.73763	0.000643
Q8EBE6 (CLPB_SHEON) SO3577	gi|243498 35|gb|AAN56566.1| AE015794_4	AE015794_4 clpB protein [Shewanella oneidensis MR-1]	4	2.677 645	2.519 805	1.942 581	1.784 742	0.00 047 8	1.37 E-05	0.00 124 8	0.00 018 4	9.310971	0.000197
Q8EB65 (Q8EB65	gi|243499 44|gb|AAN56654.1| AE015801_12	AE015801_12 heme transport protein	17	- 0.408 52	- 0.266 58	- 0.449 77	- 0.307 83	0.00 963 6	0.04 785 3	0.00 842 5	0.03 603 8	-1.43072	0.019344

_SHEON) SO3669	AE015801_12 gi|243502	[Shewanella oneidensis MR-1]											
Q8EAH2 (RS6_SHEON) SO3930	59|gb|AAN56905.1|AE015825_4 gi|243502	AE015825_4 ribosomal protein S6 [Shewanella oneidensis MR-1]	13	0.664783	0.499885	0.781645	0.616747	4.35E-05	0.01390 7	0.00038 2	0.01412 8	1.897932	0.001344
Q8EAG0 (Q8EAG0_SHEON) SO3942	74|gb|AAN56917.1|AE015826_2 gi|243512	AE015826_2 serine protease, HtrA/DegQ/DegS family [Shewanella oneidensis MR-1]	18	0.599505	0.767732	0.614649	0.782876	0.00070 9	0.00010 8	0.00168 7	0.00022 6	1.99609	0.000414
Q8E8C0 (ATPB_SHEON) SO4747	79|gb|AAN57706.1|AE015907_4 gi|243512	AE015907_4 ATP synthase F1, beta subunit [Shewanella oneidensis MR-1]	47	1.223955	1.189632	1.042367	1.008044	3.62E-16	2.69E-15	2.5E-13	1.23E-13	3.052618	1.32E-14
Q8E8B6 (ATPF_SHEON) SO4751	83|gb|AAN57710.1|AE015907_8 gi|243512	AE015907_8 ATP synthase F0, B subunit [Shewanella oneidensis MR-1]	3	-0.748 63	-0.804 94	-1.184 62	-1.240 92	0.02911 9	0.02320 5	0.00098 9	0.00080 1	-2.70412	0.004809

iTRAQ 2 - Aerobic Planktonic vs Semi-Anaerobic Anodic Biofilm cells - insoluble sub-proteome

	gi Number	Name	# peptides	119/115 (log difference)	119/116 (log difference)	121/115 (log difference)	121/116 (log difference)	119/115 (p-value)	119/116 (p-value)	121/115 (p-value)	121/116 (p-value)	Fold change (Anode associated cells/aerobic planktonic)	P-value (Anode associated cells/aerobic planktonic)
Q8EK81 (EFTU1_SHEON) SO0217	gi|24345620|gb|AAN53302.1|AE015471_7	AE015471_7 translation elongation factor Tu [Shewanella oneidensis MR-1]	347	-0.31254	-0.14525	-0.43472	-0.26742	4.09E-13	0.000401	6.19E-24	8.27E-11	-1.3364	5.38E-13
Q8EK76 (RL10_SHEON) SO0222	gi|24345625|gb|AAN53307.1|AE015471_12	AE015471_12 ribosomal protein L10 [Shewanella oneidensis MR-1]	27	-0.58495	-0.57742	-0.35371	-0.34619	0.00218	0.00170	0.03862	0.04751	-1.59291	0.009091
Q8EK74 (RPOB_SHEON) SO0224	gi|24345631|gb|AAN53309.1|AE015472_1	AE015472_1 DNA-directed RNA polymerase, beta subunit [Shewanella oneidensis MR-1]	43	0.545155	0.505266	0.507134	0.467245	5.86E-09	5.24E-08	1.92E-08	2.57E-07	1.658975	3.51E-08
Q8EK73 (RPOC_SHEON) SO0225	gi|24345632|gb|AAN53310.1|AE015472_2	AE015472_2 DNA-directed RNA polymerase, beta' subunit [Shewanella oneidensis MR-1]	54	0.513397	0.627565	0.314363	0.42853	1.95E-09	1.08E-10	2.68E-05	6.32E-07	1.601537	4.35E-08

P59166 (RS12_SHEON) SO0226	gi|24345633|gb|AAN53311.1|AE015472_3	AE015472_3 ribosomal protein S12 [Shewanella oneidensis MR-1]	7	-0.4044	-0.34698	-0.60919	-0.55176	0.02410	0.04106	0.00498	0.00952	-1.61298	0.014723
Q8EK65 (RL2_SHEON) SO0234	gi|24345645|gb|AAN53319.1|AE015473_6	AE015473_6 ribosomal protein L2 [Shewanella oneidensis MR-1]	30	-0.369058	-0.503319	-0.468274	-0.602535	5.62E-06	3.93E-08	3.26E-05	9.64E-08	1.62547	9.13E-07
Q8EK57 (RL5_SHEON) SO0243	gi|24345654|gb|AAN53328.1|AE015473_15	AE015473_15 ribosomal protein L5 [Shewanella oneidensis MR-1]	88	-0.58272	-0.55422	-0.73035	-0.70185	1.32E-13	1.11E-11	6.56E-12	2.64E-11	-1.90082	3.99E-12
P59124 (RS5_SHEON) SO0248	gi|24345659|gb|AAN53333.1|AE015473_20	AE015473_20 ribosomal protein S5 [Shewanella oneidensis MR-1]	60	-0.42163	-0.31408	-0.57219	-0.46465	6.92E-07	1.42E-05	1.34E-09	4.65E-07	-1.55759	2.8E-07
P59131 (RS4_SHEON) SO0255	gi|24345670|gb|AAN53340.1|AE015474_3	AE015474_3 ribosomal protein S4 [Shewanella oneidensis MR-1]	17	-0.44859	-0.49225	-0.43408	-0.47774	0.01469	0.00789	0.00828	0.00492	-1.5891	0.008292
Q8EIJ7 (EFG2_SHEON) SO0842	gi|24346408|gb|AAN53918.1|AE015529_2	AE015529_2 translation elongation factor G [Shewanella oneidensis MR-1]	47	-0.70283	-0.4932	-0.68535	-0.47573	2.49E-10	2.31E-07	3.41E-08	8.54E-06	-1.80268	6.4E-08

Q8EHS3 (Q8EHS3_SHEON) SO1144	gi|24346793|gb|AAN54214.1|AE015558_8	AE015558_8 methyl-accepting chemotaxis protein [Shewanella oneidensis MR-1]	30	0.886152	0.877048	0.9313	0.922196	1.43E-17	7.54E-15	4.15E-16	3.46E-18	2.469891	1.12E-16
Q8EHL1 (PNP_SHEON) SO1209	gi|24346879|gb|AAN54278.1|AE015565_1	AE015565_1 polyribonucleotide nucleotidyltransferase [Shewanella oneidensis MR-1]	9	0.680209	0.46701	0.664506	0.451307	0.01413 7	0.00626 7	0.01821 8	0.01632 2	1.760781	0.01274
Q8EHD1 (Q8EHD1_SHEON) SO1295	gi|24346990|gb|AAN54362.1|AE015573_9	AE015573_9 major outer membrane lipoprotein, putative [Shewanella oneidensis MR-1]	75	-0.91704	-0.8183	-0.82509	-0.72635	2.97E-13	6.55E-13	2.12E-10	7.35E-10	-2.27435	1.32E-11
Q8EGV9 (Q8EGV9_SHEON) SO1482	gi|24347232|gb|AAN54543.1|AE015593_2	AE015593_2 TonB-dependent receptor, putative [Shewanella oneidensis MR-1]	7	0.8114	0.852664	0.660667	0.701931	0.00781 1	0.00926 8	0.03949 4	0.04002 5	2.131158	0.018392
Q8EGH5 (RS2_SHEON) SO1629	gi|24347418|gb|AAN54684.1|AE015609_3	AE015609_3 ribosomal protein S2 [Shewanella oneidensis MR-1]	5	0.507834	0.594903	0.384601	0.471671	0.01201 2	0.00256 2	0.03065 4	0.02606 8	1.631912	0.012522
Q8EG20 (TIG_SHEON) S)1793	gi|24347619|gb|AAN54846.1|AE015623_8	AE015623_8 trigger factor [Shewanella oneidensis MR-1]	6	-0.7278	-0.71777	-0.81871	-0.80869	0.02324 5	0.02383 1	0.01185 7	0.01106 3	-2.15597	0.016418

Q8EFZ0 (Q8EFZ0_SHEON) SO1824	gi|243476 58|gb|AA N54876.1| AE015626 _5	AE015626_5 conserved hypothetical protein [Shewanella oneidensis MR-1]	19	- 0.980 92	- 0.923 76	- 1.067 4	- 1.010 25	5.47 E-07	3.1E -06	4.42 E-06	2.56 E-05	-2.7063	3.72E-06
Q8EFY9 (Q8EFY9_SHEON) SO1825	gi|243476 59|gb|AA N54877.1| AE015626 _6	AE015626_6 MotA/TolQ/ExbB proton channel family protein [Shewanella oneidensis MR-1]	10 6	- 0.326 28	- 0.517 41	- 0.341 16	- 0.532 28	1.71 E-07	2.64 E-14	2.94 E-06	1.14 E-12	-1.53616	3.51E-10
Q8EFY6 (Q8EFY6_SHEON) SO1828	gi|243476 62|gb|AA N54880.1| AE015626 _9	AE015626_9 TonB2 protein [Shewanella oneidensis MR-1]	7	- 0.536 47	- 0.623 94	- 0.627 28	- 0.714 75	0.04 093 8	0.01 988 4	0.01 080 1	0.00 423 5	-1.86939	0.013891
Q8EFY5 (Q8EFY5_SHEON) SO1829	gi|243476 63|gb|AA N54881.1| AE015626 _10	AE015626_10 TPR domain protein [Shewanella oneidensis MR-1]	5	0.466 007	0.405 748	0.426 822	0.366 563	0.00 437 5	0.00 733 8	0.02 417 4	0.04 419 1	1.516318	0.013609
Q8EEF5 (Q8EEF5_SHEON) SO2427	gi|243484 20|gb|AA N55461.1| AE015683 _8	AE015683_8 TonB-dependent receptor, putative [Shewanella oneidensis MR-1]	10	- 0.337 55	- 0.386 33	- 0.459 32	- 0.508 1	0.02 788 2	0.00 901 4	0.03 009 2	0.01 198 6	-1.52626	0.017352
Q8ED64 (Q8ED64_SHEON) SO2903	gi|243490 05|gb|AA N55919.1| AE015729 _3	AE015729_3 cysteine synthase A [Shewanella oneidensis MR-1]	49	- 0.650 46	- 0.621 66	- 0.570 09	- 0.541 29	2.35 E-06	4.36 E-06	5.6E -05	5.96 E-05	-1.81462	1.36E-05

Q8EBH9 (RS20_SHEON) SO3537	gi|24349784|gb|AAN56528.1|AE015789_15	AE015789_15 ribosomal protein S20 [Shewanella oneidensis MR-1]	18	0.511237	0.928064	0.852405	1.269232	0.00108 6	2.18E-06	0.00013 4	8.75E-08	2.435701	1.29E-05
Q8EBH3 (Q8EBH3_SHEON) SO3545	gi|24349795|gb|AAN56536.1|AE015790_7	AE015790_7 OmpA family protein [Shewanella oneidensis MR-1]	33	-0.45222	-0.46852	-0.43561	-0.45191	0.00106 7	0.0007	0.00189 2	0.00141 4	-1.57156	0.001189
Q8EB65 (Q8EB65_SHEON) SO3669	gi|24349944|gb|AAN56654.1|AE015801_12	AE015801_12 heme transport protein [Shewanella oneidensis MR-1]	11	0.60397	0.57888	0.467277	0.442187	0.00117 1	0.00124	0.00830 6	0.00697 1	1.687214	0.003028
Q8EAJ8 (Q8EAJ8_SHEON) SO3904	gi|24350226|gb|AAN56879.1|AE015823_1	AE015823_1 outer membrane protein TolC [Shewanella oneidensis MR-1]	6	1.079354	1.1656	0.761545	0.847791	0.00056 2	0.00067 6	0.00221 5	0.00039 3	2.621044	0.000758
Q8EAG3 (RS9_SHEON) SO3939	gi|24350268|gb|AAN56914.1|AE015825_13	AE015825_13 ribosomal protein S9 [Shewanella oneidensis MR-1]	15	-0.76814	-0.74667	-0.43022	-0.40875	4.7E-06	7.61E-06	0.00194 7	0.00372 8	-1.80119	0.000127
Q8EAG0 (Q8EAG0_SHEON) SO3942	gi|24350274|gb|AAN56917.1|AE015826_2	AE015826_2 serine protease, HtrA/DegQ/DegS family [Shewanella oneidensis MR-1]	14	0.74334	0.83260 1	0.782237	0.871498	0.00032 4	0.00022 1	9.27E-06	0.00010 2	2.242114	9.06E-05

Q8E8C0 (ATPB_SHEON) SO4747	gi|24351279|gb|AAN57706.1|AE015907_4	AE015907_4 ATP synthase F1, beta subunit [Shewanella oneidensis MR-1]	85	0.997501	1.002962	0.975493	0.980954	1.34E-31	1.06E-28	3.14E-30	1.54E-26	2.689157	2.88E-29

Media

M1 minimal media

M1 media for *Shewanella oneidensis* MR-1

The M1 media prepared had the following variations:

- 18 mM Lactate
- 50 mM PIPES
- 100 mM sodium chloride (NaCl)

(a) Vitamin Supplement 100x

0.01 g	Pyridoxine hydrochloride
0.005 g	Thiamine-HCl
0.005 g	Riboflavin
0.005 g	Nicotinic acid
0.005 g	Calcium D-(+)-pantothenate
0.005 g	p-Aminobenzoic acid
0.005 g	Thioctic acid
0.002 g	Biotin
0.002 g	Folic Acid
0.0001 g	Vitamin B12
1000ml	Water

Filter sterilize with 0.22 um pore diameter filter.

(b) Mineral Supplement 100x based on Wolfe's Vitamin Solution (pH 7.0)

1. Add 1.5 g nitrilotriacetic acid to approximately 500 ml of water and adjust to pH 7.0 with sodium hydroxide (NaOH) to dissolve.
2. Add the following:

3.0 g	$MgSO_4$-$7H_2O$

0.5 g	$MnSO_4$-H_2O
1.0 g	NaCl
0.1 g	$FeSO_4$-$7H_2O$
0.1 g	$CoCl_2$-$6H_2O$
0.1 g	$CaCl_2$-$2H_2O$
0.13 g	$ZnCl_2$
0.01 g	$CuSO_4$-$5H_2O$
0.01 g	$AlK(SO_4)_2$-$12H_2O$
0.01 g	H_3BO_3
0.025 g	Na_2MoO_4-$2H_2O$
0.024 g	$NiCl_2$-$6H_2O$
0.025 g	Na_2WO_4-$2H_2O$
1000ml	Water

3. Filter sterilize with 0.22 um pore diameter filter.

(c) Amino Acid Supplement 100x (pH 7.0)

1. Dissolve (or add appropriate concentrations solutions) for the following into 900ml of distilled water:

2.0 g	L-glutamic acid
2.0 g	L-arginine
2.0 g	DL-Serine

2. Adjust to pH 7.0 with sodium hydroxide (NaOH)
3. Make up to 1000ml water
4. Filter sterilize with 0.22 um pore diameter filter.

(d) PIPES buffer 1 L pH 7.0

1. Dissolve for the following into 700ml of distilled water:

15.12 g	PIPES

0.3 g sodium hydroxide (NaOH)

2. Adjust to pH 7.0 with sodium hydroxide (NaOH)
3. Make up to 1000ml water
4. Filter sterilize with 0.22 um pore diameter filter.

M1 MINIMAL MEDIA

1. Dissolve (or add appropriate concentrations solutions) for the following into 700ml of distilled water:

15.12 g	PIPES buffer (see above)
0.3 g	NaOH
1.5 g	NH_4Cl
0.1 g	KCl
0.6 g	$NaH_2PO_4.H_2O$
5.844 g	NaCl

2. Adjust to pH 7.0 with sodium hydroxide (NaOH)
3. Add the following solutions:

9.0 mL	sodium lactate 2M pH7.0
10.0 mL	mineral supplement (see above)
10.0 mL	vitamin supplement (see above)
10.0 mL	amino acid supplement (see above)

4. Make up to 1000ml water
5. Filter sterilize with 0.22 um pore diameter filter.